UNIVERSITEIT VAN PRETORIA
UNIVERSITY OF PRETORIA
YUNIBESITHI YA PRETORIA

The subcellular localization of *Eucalyptus grandis* sucrose synthase 1 (EgSUSY1) fusion proteins expressed in *Arabidopsis thaliana*

by

JAMIE-LEE SAUER

Submitted in partial fulfilment of the requirements for the degree

Magister Scientiae

In the Faculty of Natural and Agricultural Sciences

Department of Genetics

University of Pretoria

Pretoria

November 2011

Supervisor: Prof. Alexander A. Myburg

Co-supervisors: Dr. Sanushka Naidoo, Prof. Dave Berger

UNIVERSITEIT VAN PRETORIA
UNIVERSITY OF PRETORIA
YUNIBESITHI YA PRETORIA

DECLARATION

I, Jamie-Lee Sauer the undersigned, hereby declare that the thesis/dissertation submitted herewith for the degree ***Magister Scientiae*** to the University of Pretoria, contains my own independent work and has not been submitted previously for any degree at any other tertiary institution.

Signature: _____

Date:_____

PREFACE

The ever-growing demand for wood and wood derived cellulose products coupled with the public concern about the clearance of natural flora or agricultural land to make way for the forest tree plantations has sparked a renewed interest in the genetic improvement of forest tree species. Conventional breeding of forest trees is time-consuming due to the long generation times of most forest trees and the expression of selective traits such as wood quality only at harvesting age. Two approaches have been considered to accelerate the domestication of forest trees. The first is through the genetic modification of trees by introducing new genes into existing genotypes to confer advantageous phenotypes and the second is through marker-assisted breeding of new variants. Both of these processes require an extensive knowledge of the cellular toolkit and the regulation thereof that forest trees utilize to generate the diversity prevalent in natural populations. With the onset of the post-genomic era researchers are overwhelmed by the plethora of newly identified genes. Yet the successful application of this knowledge to facilitate genetic improvement of forest trees requires the comprehensive analysis of the functions of these identified proteins.

Sucrose synthase (SuSy) was recently identified as a promising target for genetic engineering in forest tree species. SuSy genes have been identified in many plant species including *Arabidopsis thaliana* and *Eucalyptus grandis*. Sucrose synthase is responsible for the formation of activated glucose which can be channeled into sink processes such as cellulose biosynthesis. Cellulose is the most abundant biopolymer on earth and is an important commodity for the timber, pulp and paper industry. Cellulose is a cell wall polymer of chains of β- 1,4-linked glucose molecules that crystallize to form cellulose microfibrils in plant cell walls. Biosynthesis of cellulose in plants occurs at the plasma membrane through the action of rosette-shaped cellulose synthase (CESA) protein complexes.

Various models have been proposed for the regulation of carbon allocation to cellulose biosynthesis. One of these models suggests that the allocation of activated carbon generated by SuSy is regulated by the subcellular distribution of this protein. Contradicting evidence has accumulated on the regulation of SuSy localization. One model suggests that phosphorylation status at a conserved

SuSy amino acid residue determines its cellular distribution. In order to elucidate the role of SuSy in cellulose biosynthesis a number of questions surrounding the function and regulation of SuSy need to be addressed. These questions include: What is the nature of the association between SuSy and CESA? What cellular mechanism underlies the temporal and spatial regulation SuSy localization? How does the cellular distribution of SuSy does effects its functionality?

Two general scientific questions were addressed in this study: (1) What is the predominant subcellular localization of Eucalyptus sucrose synthase 1 (EgSUSY1)? (2) Does the phosphorylation affect the membrane localization of *Eucalyptus* sucrose synthase? The effect of phosphorylation on the functionality EgSUSY1 were investigated in a parallel M.Sc. study by Mr. M. M. Mphahlele (University of Pretoria, Pretoria). The **aim of this M.Sc study** was to determine the effect of site directed modification of the conserved N-terminal serine residue on the subcellular localization of *Eucalyptus grandis* sucrose synthase 1 (EgSUSY1) fusion proteins expressed in *Arabidopsis thaliana* plants.

Literature pertaining to the functional regulation of sucrose synthase is reviewed in **Chapter 1**. Sucrose biosynthesis and degradation are discussed and the factors affecting sucrose synthase functional regulation is reviewed. Thereafter, the review is focused on the available methodologies that could be used to elucidate the subcellular localization of proteins *in planta* with special attention to confocal microscopy and intrinsically fluorescent reporter proteins.

In **Chapter 2** of this dissertation, questions regarding the subcellular localization of ectopically expressed GFP-EgSUSY1 fusions in *Arabidopsis* plants are addressed. Three proteins will be explored in parallel: unmodified *Eucalyptus* EgSUSY1 and modified S11A and S11E versions of this protein, where the eleventh serine residue has been respectively converted to an alanine and a glutamate residue through site directed mutagenesis.

Questions addressing the experimental design include: Are GFP-EgSUSY1 fusions expressed as intact proteins in transgenic *Arabidopsis* plants? Will the fusion of GFP to the N-terminus or C-terminus of EgSUSY1 affect the localization of the protein? Questions addressing the research

outcomes of this study include: Will the GFP-EgSUSY1 proteins associate with specific subcellular compartments such as the cytosol, plasma membrane, extracellular matrix and cell wall? Is there an observable difference in the localization patterns of modified GFP-EgSUSY1 proteins compared to each other and unmodified GFP-EgSUSY1 proteins? General findings, conclusions and implications of this M.Sc study are summarized in the final section of this dissertation entitled **Concluding Remarks**.

Outcomes from a study undertaken during August 2008 to August 2011 in the Department of Genetics, University of Pretoria, under the supervision of Prof. A.A. Myburg are presented in this dissertation. Laser Scanning Confocal Microscopy analysis, described in Chapter 2, were carried out at the Centre of Electron Microscopy, University of Kwa-Zulu Natal, Pietermaritzburg, South Africa by the author under the supervision of Mrs. S. Mackellar. Preliminary results generated during this M.Sc study were presented at the following national conference:

Sauer, J. and Myburg, A.A. 2009. The subcellular localization of *Eucalyptus grandis* sucrose synthase 1 (EgSUSY1) fusion proteins expressed in *Arabidopsis thaliana*. South African Genetics Society (SAGS) Congress, April 8-11, Bloemfontein, South Africa.

ACKNOWLEDGEMENTS

This ***Magister Scientiae*** study would not have been possible without the support, mentorship and encouragement of many others. I take this opportunity to express my gratitude to the institutions, organizations and persons who have been instrumental in the successful completion of this project.

- First and foremost I would like to thank my Supervisor, Prof. A.A. Myburg for his invaluable leadership, support, encouragement and commitment to this project. It has been a pleasure to work with Professor Myburg and his research team.
- Deepest gratitude is also due to the members of my supervisory committee, Prof. D. Berger and Dr. S. Naidoo; without whose knowledge and assistance this study would not have been successful.
- Mr. E. Mizrachi for numerous stimulating discussions, assistance with experimental setup and general advice.
- I am grateful to all my FMG colleagues: Adrene Laubscher, Elna Cowley, Luke Solomon, Martin Ranik, Nicky Creux, Marja O' Neill, Janine Silberbauer, Grant McNair, Eshchar Mizrachi, Mmoledi Mmphalele, Anand Kullan, Melissa Reynolds, Minique De Castro, Therese De Castro, Steven Hussey and Jonathan Botha for their continued moral support and willingness to assist in all situations. I will miss our candid moments together.
- Mrs. Soné Louise Ungerer and Dr.Vida van Staden for their assistance and guidance during SDS-PAGE and Western blot analyses.
- Mr Alan Hall at the microscopy unit for all his assistance on the technical aspects of confocal microscopy.
- Mrs. Shirley Mackellar at the UKZN Centre of Electron Microscopy for her comradeship and many hours spent collecting confocal images.
- Dr. Celia Snyman for allowing me to exploit her extensive technical knowhow.
- An honorable mention goes to my family for their unwavering understanding, endless patience and support during the completion of this project.

- Sappi and Mondi for funding of the project.
- The National Research Foundation of South Africa (NRF) for funding of the project and the awarded scholarship.
- The Human Resources and Technology for Industry Programme (THRIP) for financial contributions to the Wood and Fibre Molecular Genetics Programme (WFMG).
- The Department of Genetics of the University of Pretoria and the Forestry and Agricultural Biotechnology Institute (FABI) for providing facilities and stimulating an academic environment
- Finally I would like to thank all who were involved in the reviewing of this dissertation; your constructive criticism is greatly appreciated.

THESIS SUMMARY

The subcellular localization of *Eucalyptus grandis* sucrose synthase 1 (EgSUSY1) fusion proteins expressed in *Arabidopsis thaliana*

Jamie-Lee Sauer

Supervised by Prof. A.A. Myburg

Co-supervised by Dr. S. Naidoo and Prof D. Berger

Submitted in partial fulfilment of the requirements for the degree Magister Scientiae

Department of Genetics

University of Pretoria

Sucrose is the major transported photoassimilate in plants and is degraded concurrently by two enzymes: invertases and sucrose synthase. Sucrose synthase catalyzes the reversible conversion of UDP and sucrose to form fructose and UDP-glucose, the latter being the activated substrate for many metabolic processes including cellulose biosynthesis. There is evidence that sucrose synthase is phosphorylated as a regulatory mechanism of carbon allocation at a conserved N-terminal serine residue. The phosphorylation or dephosphorylation at this specific site has also been found to shift the protein localization in a tissue and species specific manner.

A literature study of the functional regulation of sucrose synthase in plants has highlighted several scientific questions: Is sucrose synthase cellular localization regulated by phosphorylation of an N-terminal conserved serine residue? What are the regulatory mechanisms underlying within and between species variation in sucrose synthase localization? Does sucrose synthase associate with the cellulose synthase enzyme complex? Can cellulose biosynthesis be increased by over-expression of the membrane-associated form of sucrose synthase? The aim of this M.Sc study was to determine the subcellular localization of *Eucalyptus grandis* sucrose synthase 1 (EgSUSY1) fusion proteins expressed in *Arabidopsis thaliana* plants.

This was investigated through modifying the 11th serine residue of EgSUSY1 into either a non-polar alanine residue that cannot be phosphorylated (S11A), or into a negatively charged glutamic acid residue which may mimic phosphorylation at this site (S11E). The modified proteins were translationally fused to green fluorescent protein (GFP) and expressed in transgenic *Arabidopsis thaliana*. The proteins' subcellular localization were analysed *in planta* using laser scanning confocal microscopy (LSCM).

Findings in this study point to the peripheral localization of modified and unmodified GFP-EgSUSY1 proteins with a prominent cytoplasmic component. No evidence was found for the localization of modified or unmodified GFP-EgSUSY1 proteins within the extracellular matrix. The current study did not establish nor negate plasma membrane association of any of the GFP-EgSUSY1 fusion proteins. It was concluded that alternative methodologies need to be explored to further address issues surrounding subcellular localization of sucrose synthase. These studies will not only aid in defining the role of this enzyme in carbon allocation, but also add to our expanding knowledge of cellulose biosynthesis and cell wall formation.

TABLE OF CONTENTS

LIST OF FIGURES

LIST OF TABLES

LIST OF ABBREVIATIONS

cDNA	Complementary deoxyribonucleic acid
CDS	Coding sequence
CESA	Cellulose synthase
CaMV	Cauliflower mosaic virus
Col-0	Columbia ecotype 0
DIC	Differential Interference Contrast
dNTP	Deoxyribonucleotide-triphosphate
EtBr	Ethidium bromide
GFP	Green Fluorescent Protein
LB	Luria-Bertani
LSCM	Laser Scanning Confocal Microscopy
NCBI	National Center for Biotechnology Information
PAGE	Polyacrylamide gel electrophoresis
PBS	Phosphate buffered saline
PCR	Polymerase chain reaction
RT-PCR	Reverse transcriptase polymerase chain reaction
SDS	Sodium dodecyl sulphate
SPP	Sucrose-phosphate phosphatase
SPS	Sucrose-phosphate synthase
SuSy	Sucrose synthase
T-DNA	Transferred DNA

UBQ	Ubiquitin
YEP	Yeast extract peptone

CHAPTER 1

Literature Review:

Functional regulation of sucrose synthase *in planta* with reference to cell wall formation

1.1. Introduction

Sucrose is the principal product of carbon fixation during photosynthesis. It is the major transport form of fixed organic carbon which is translocated from photosynthetic source tissues such as leaves to non-photosynthetic sink tissues such as roots, fruits and stems. In sink tissues, sucrose can be devoted to a number of metabolic destinations including storage in the form of starch, incorporation into structural polymers such as cellulose and hemi-cellulose or directed towards glycolysis for the generation of energy in the form of ATP (Déjardin et al., 1997).

The enzyme sucrose synthase (SUSY) is central not only to the synthesis of sucrose in the cell, but also to the metabolism of this molecule in sink tissues. It has been found that the spatial and temporal regulation of SUSY expression and activity determines sink strength and governs allocation of carbon to various metabolic processes such as starch and cellulose biosynthesis (Zrenner et al., 1995). Sucrose synthase also plays a role in stress response, where it has been shown to be up-regulated during osmotic stress and down-regulated during wounding (Springer et al., 1986; Salanoubat and Belliard, 1989; Maranã et al., 1990; Ricard et al., 1991; Hesse and Willmitzer, 1996; Kleines et al., 1999; Baud et al., 2004; Fernandes et al., 2004).

Sucrose synthase is highly regulated at both the transcriptional and post-translational levels (Winter and Huber, 2000; Wienkoop et al., 2008). At the protein level it can be found as two different isoforms within the cell, either as a soluble enzyme (S-SUSY) within the cytoplasm, or associated with the plasma membrane as a particulate form (P-SUSY) (Winter et al., 1997; Zhang et al., 1999; Winter and Huber, 2000). The allocation of SUSY to these cellular sites has been proposed to be regulated by several factors such as phosphorylation, sucrose concentration, proximal pH, multimeric form (dimers or tetramers) of the protein, or

even region of the leaf or stem (Huber et al., 1996; Hardin et al., 2003; Hardin et al., 2004; Hardin et al., 2006; Duncan and Huber, 2007). This partitioning of SuSy may allow for added functional plasticity where it is postulated that S-SUSY is responsible for general metabolic functions such as glycolysis and P-SUSY directs carbon assimilation to secondary processes such as cellulose biosynthesis (Ruan et al., 1997).

1.2. Sucrose metabolism and transport in the plant cell

1.2.1. Sucrose synthesis

Sucrose is the major photoassimilate in plants and forms the source of carbon and energy for many metabolic processes. It has been found to be a major storage reserve in fruits and the storage organs of sugarcane (*Saccharum officinarum*) and sugarbeets (*Beta vulgaris*) (Lunn and MacRaey, 2003). Sucrose is also assumed to play a role in stress tolerance following exposure to drought and low temperatures (Yang et al., 2001; Strand et al., 2003). The accumulated sucrose in stressed plant cells is thought to act as a protein stabilizer and also forms an energy reserve to assist in the survival of the plant until the return of favourable conditions (Lunn and MacRaey, 2003). Sucrose has also been found to play a role in the regulation of the expression of numerous genes encoding enzymes, transporter proteins and storage proteins (Ciereszko et al., 2001; Stitt et al., 2002; Vaughn et al., 2002; Zourelidou et al., 2002).

Sucrose is produced in autotrophic organs (leaves) during photosynthesis. Sucrose synthesis is restricted to the cytosol and synthesized sucrose is either stored in the cell vacuole or transported to various sink organs via the phloem. This biopolymer is synthesized through a two step synthesis reaction (Figure 1.1), whereby UDP-glucose (UDP-Glc) and fructose-6-phosphate (Fru6P) are converted to sucrose-6-phosphate (Suc6P) and uridine diphosphate

(UDP) by the enzyme sucrose phosphate synthase (SPS; EC 2.4.1.14). Suc6P is then dephosphorylated under the action of sucrose-6-phosphate phosphatase (SPP; EC 3.1.3.24) to form sucrose (Lunn and MacRaey, 2003).

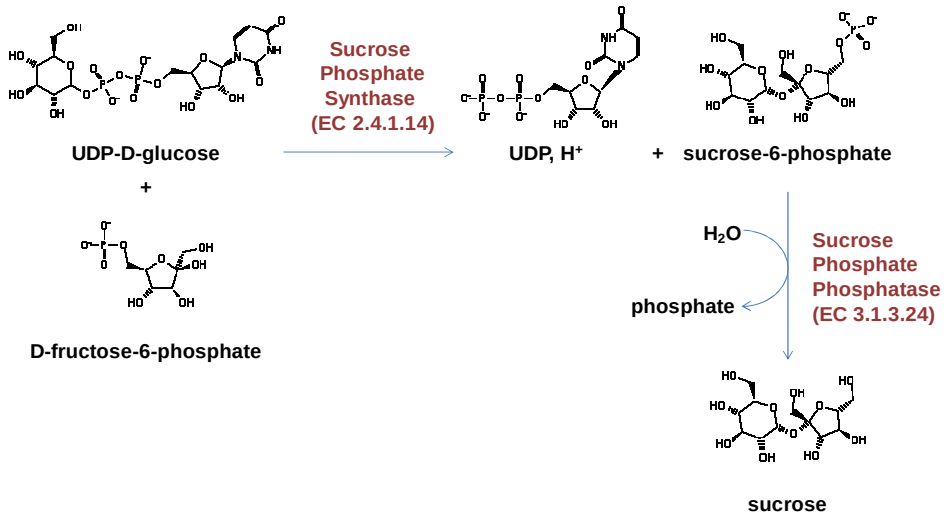

Figure 1.1. Committed pathway of sucrose synthesis based on PlantCyc (http://plantcyc.org/) and Lunn and MacRaey (2003).

The UDP-Glc precursor of sucrose biosynthesis can be provided by two alternative pathways. UDP-Glc can either be derived from glucose-1-phosphate and uridine triphosphate (UTP) via the enzyme UDP-glucose pyrophosphorylase (UGPase; EC 2.7.7.9, Figure 1.2) or from UDP and sucrose by the enzyme sucrose synthase (UDP-glucose: D-fructose 2-glucosyltransferase, SUSY; EC 2.4.1.13, Figure 1.3). UGPase is responsible for the supply of UDP-Glc in source organs (leaves), whilst SuSy actively produces UDP-Glc in sink organs (Zrenner et al., 1995; Tang and Sturm, 1999). Both these reactions are reversible and therefore these enzymes play a central role in both sucrose synthesis and sucrose hydrolysis. It is believed that the hydrolysis of sucrose by SUSY is important for the formation of complex polysaccharides such as cellulose that make up cell walls of sink tissues (Schlüpmann et al., 1994; Amor et al., 1995; Gibeaut, 2000; Johansson et al., 2002; Seifert, 2004). The metabolism of UDP-Glc by UGPase on the other hand is assumed to be essential for sucrose biosynthesis in photosynthetic source tissues (Huber and Akazawa, 1986).

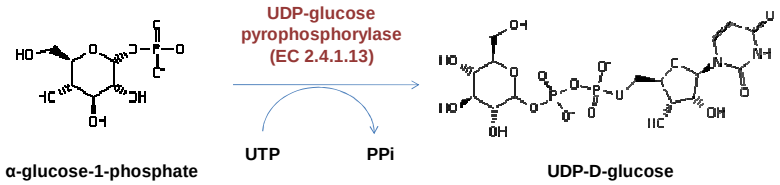

Figure 1.2. Formation of UDP-D-glucose from α-glucose-1-phosphate and UTP precursors under the catalytic action of UDP-glucose pyrophosphorylase in plant cells. This reaction is freely reversible and the production of UDP-D-glucose as depicted above is usually associated with the biosynthesis of sucrose in photosynthetic source tissues. Image based on PlantCyc (http://plantcyc.org/) and Kleczkowski (1994).

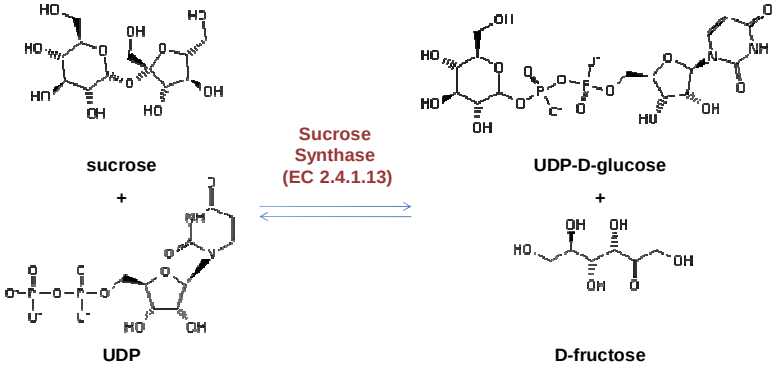

Figure 1.3. Freely reversible reaction performed by sucrose synthase in plant cells. Image based on PlantCyc (http://plantcyc.org/) and Römer et al. (2004).

1.2.2. Sucrose transport and phloem unloading

Sucrose is the ubiquitous source of carbon and energy in plants. This photoassimilate is synthesized in photosynthetically active source organs (leaves) characterized by the net export of carbohydrates. Sucrose is then transported to photosynthetically less active sink organs, such as roots, stems, tubers, flowers and fruits via the phloem (Godt and Roitsch, 2006). These sink organs are characterized by the net import of sucrose which is channeled into a number of metabolic processes essential to plant cell growth, differentiation and integrity (Figure 1.4, Wobus and Weber, 1999; Godt and Roitsch, 2006).

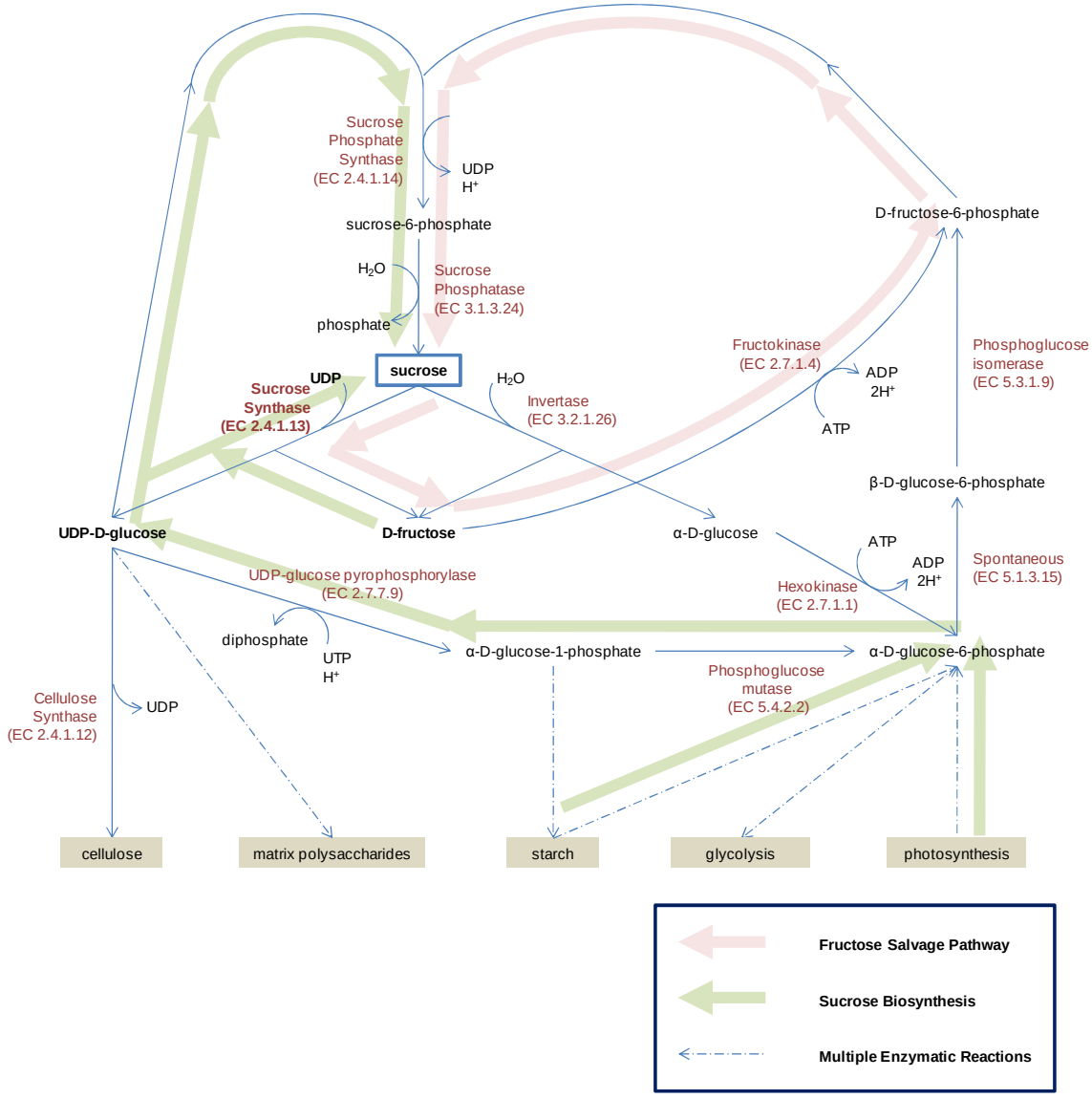

Figure 1.4. Enzymes involved in sucrose biosynthesis and carbon allocation to various metabolic destinations in planta. Enzymatic reactions leading to sucrose biosynthesis are indicated in green and those devoted to the recycling of fructose through the fructose salvage pathway are indicated in pink. Solid line (single enzyme reaction), dashed line (multiple enzyme reactions). Pathway based on PlantCyc (http://plantcyc.org/) and Andersson-Gunneras et al. (2006).

Sucrose transport by the phloem is driven by solute concentration and osmotic potential (Evert, 1982; DeWald et al., 1994). The import of sucrose into sink organs via phloem unloading is governed by the immediate hydrolysis of sucrose by SUSY and invertases (Inv; EC 3.2.1.26). SUSY catalyzes the reversible conversion of sucrose and UDP to UDP-glucose and fructose; whilst invertases are responsible for the irreversible cleavage of sucrose to glucose and fructose (Figure 1.4 and Figure 1.5). The removal of sucrose by these enzymes in sink organs is essential to ensure the flow of sucrose towards sink organs by maintaining a favourable sucrose gradient (Godt and Roitsch, 2006). The choice of enzyme (SUSY or Inv) defines the mechanism of phloem unloading where SUSY is involved in symplasmic phloem unloading of sucrose via the plasmodesmata and extranuclear invertases provide carbohydrates to sink organs via an apoplasmic pathway (the movement of water and dissolved solutes through the cell walls, Godt and Roitsch, 2006).

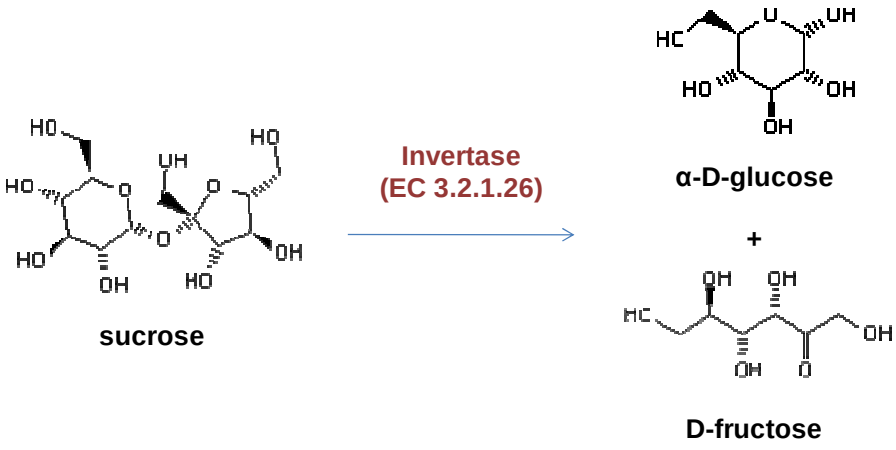

Figure 1.5. A schematic illustration of the cleavage of sucrose to α-D-glucose and D-fructose under the catalytic activity of the enzyme invertase. Image based on PlantCyc (http://plantcyc.org/) and Lunn and MacRaey (2003).

The fructose formed from the hydrolysis of sucrose can either be utilised for glycolysis or can be channelled into the fructose salvage pathway (Figure 1.4). The fructose salvage pathway recycles fructose and UDP-glucose back to sucrose, UDP and inorganic phosphate (Pi) under the action of SPS and SPP (Geigenberger and Stitt, 1991; Geigenberger et al., 1997). This recycling of fructose after sucrose catabolism is thought to allow the cell to respond to variations in sucrose supply as well as the demand for carbon utilized by metabolic processes such as cell wall polysaccharide synthesis (Fernie et al., 2002). It is evident that sucrose metabolism and transport is highly regulated to ensure the balance between produced photosynthates and metabolic carbon demands. Sink strengths are thus not only determined by the importing capabilities of sink cells, but also by the rate of photoassimilate transport and the means of phloem unloading (Farrar, 1982; Junghans and Metzlaff, 1990; Balibrea Lara et al., 2004).

1.2.3. Invertases

Plants contain three different types of invertases defined by their subcellular localization, pH optima and isoelectric points (Tymowska-Lalanne and Kreis, 1998; Roitsch and Gonzalez, 2004). Vacuolar invertases have an acidic pH-optimum and a low isoelectric point. These invertases are located in the vacuole where they function to regulate the level of sucrose stored in this compartment (Leigh et al., 1979; Lingle and Dunlap, 1987). Very little is known about cytoplasmic invertases other than that they commonly have neutral to alkaline pH-optima and are proposed to be of prokaryotic origin (Godt and Roitsch, 2006). Extracellular invertases form one of the key enzymes responsible for supplying carbohydrates to sink tissues. These invertases are characterised by highly acidic pH-optimum and very high isoelectric points (Roitsch and Gonzalez, 2004).

A study by Godt and Roitsch (2006) demonstrated the inverse regulation of invertase and sucrose synthase activity during tap root development in sugar beet (*Beta vulgaris*). Extracellular invertases were found to be predominantly active in the early stages of root development with sucrose synthase only becoming active at later stages. This supports the postulate that extracellular invertases are responsible for channelling carbohydrates into general cellular metabolism to support cell growth and division (Hubbard et al., 1989; Yelle et al., 1991; Weber et al., 2005), whilst SUSY is responsible for channelling sucrose into starch and cell wall polymer biosynthesis (Winter and Huber, 2000).

Invertases also play an important role in the regulation of gene expression through sugar sensing systems. A number of genes, forming part of diverse metabolic activities such as stress responses and nitrogen metabolism, have been found to be up and down-regulated based on the sucrose and hexose status of the cell (Koch, 1996; Rolland et al., 2002). Invertases typically play a greater role in sugar signalling than sucrose synthase as they produce two hexoses for every hydrolysed sucrose molecule, whilst SUSY only generates one (Figure 1.3 and Figure 1.5, Kingston-Smith et al., 1999; Sturm and Tang, 1999). The allocation of sucrose to various metabolic processes is thus governed by the developmental stage of the cell, the choice of hydrolysis by either invertases or SUSY and finally the carbohydrate status of the cell. This complex spatial and temporal regulation of sucrose metabolism makes it a very interesting field of study.

1.3. Cellulose biosynthesis

Cellulose is present universally in the cell walls of plants. It accounts for about 20% (by weight) of the primary cell walls and about 50% of the secondary cell walls. (Aspeborg et al., 2005; Zhou et al., 2005). This biopolymer is deposited in secondary cell walls of tracheary elements where it allows for the physical reinforcement of the cells. This is especially

important in xylem vessels, which have to withstand the tremendous turgor pressure enforced by the transport of water up the plant. Therefore it is vital that cellulose should be deposited in a correct and orderly manner to ensure that the plant cell can function (Taylor, 2008). Cellulose is a polymer composed of linear, unbranched β-1,4-linked glucan chains of repeating cellobiose units. Cellobiose is a disaccharide composed of two glucose molecules rotated at a 180° angle to each other. Insoluble, crystalline cellulose is formed when these β-1,4-linked glucan chains bind together through extensive intra- and inter-molecular hydrogen bonding forming a cable-like microfibril (Taylor, 2008).

Cellulose is catalysed by the membrane bound enzyme, cellulose synthase (CesA; EC 2.4.1.12), from the monomer UDP-glucose (Figure 1.6). Freeze fracture studies have shown that the cellulose synthase enzyme complex is found in a hexameric rossete structure approximately 25 to 30 nm in diameter (Delmer, 1999). Based on the dimensions of produced microfibrils it is hypothesised that each of the six subunits of the cellulose synthase complex is composed of six CesA proteins, each of which produces a single 1, 4-β-D-glucan chain (Herth, 1983). Three distinct CesA family members must be present to correctly form a functional rosette, and different family members make up rosettes in primary and secondary cell walls. The arrangement of these individual CesA proteins is still unknown and a number of postulated arrangements have been considered (Taylor, 2008).

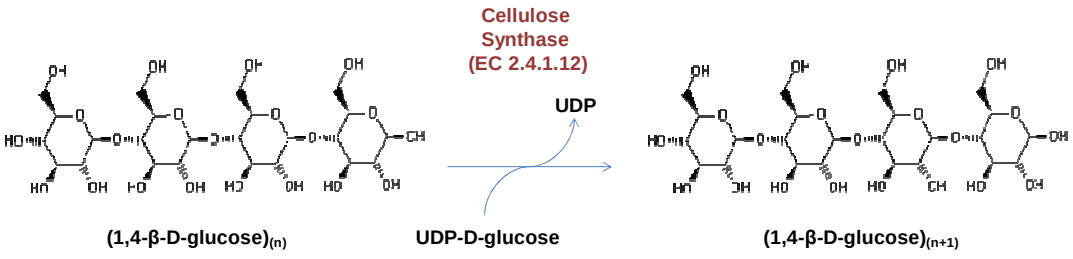

Figure 1.6. Incorporation of UDP-D-glucose monomers into a growing linear glucan chain of cellulose catalytic action of the enzyme cellulose synthase. Image based on PlantCyc (http://plantcyc.org/).

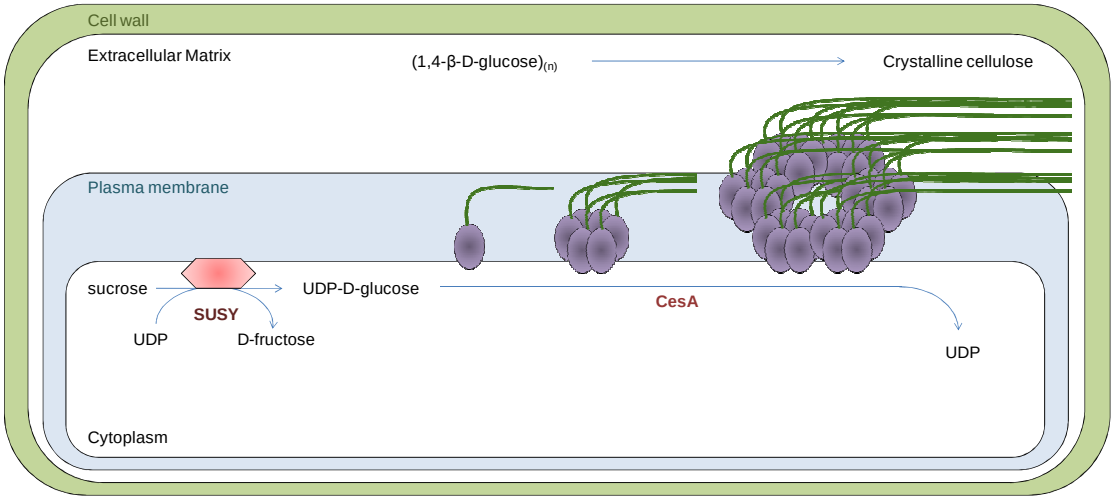

Figure 1.7. Model of the hexameric cellulose synthase complex found traversing the plant cell membrane. The active sites of the cellulose synthase enzymes are cytosolic. UDP-glucose is recruited from the cytoplasm and is then incorporated into the growing 1, 4-β-D-glucan chain found within the periplasmic space. Crystalline cellulose is deposited on the inner surface of the cell wall in the form of compact microfibrils. Illustration adapted from Doblin et al. (2002) and Taylor (2008).

Cellulose synthase has glycosyl transferase activity, enabling this enzyme to catalyse the irreversible formation of β-1, 4 bonds between the glucose monomers to form unbranched cellulose molecules called 1, 4-β-D-glucans. The cellulose precursor UDP-glucose can be provided by two alternative pathways. UDP-glucose can be generated through the phosphorylation of glucose-1-phosphate by UDP-glucose pyrophosphorylase (UGPase) or provided through the reversible conversion of UDP and sucrose to UDP-glucose and fructose under the catalytic action of the enzyme sucrose synthase. Both these pathways can be potentially modified to result in the shifting of carbon flux to cellulose synthesis. For other aspects of cellulose synthesis, including biochemistry, structure, and microfibril orientation readers are referred to several recent reviews (Somerville, 2006; Lloyd and Chan, 2008; Taylor, 2008).

1.4. Sucrose synthase

Sucrose synthase was first identified in 1953 in wheat germ (Leloir and Cardini, 1953). This enzyme can form homodimers or homotetramers composed of SUSY protein subunits each with a molecular mass between 80 and 94 kDa (Nguyen-Quoc et al., 1990; Sebková et al., 1995; Tanase and Yamaki, 2000; Duncan and Huber, 2007). The UDP-glucose generated by SUSY forms the substrate for a number of physiological processes including the production of storage polymers (Chourey and Nelson, 1976), structural polymers (Amor et al., 1995) and as a source of energy for general metabolic activity (Figure 1.4)(Xu et al., 1989; Amor et al., 1995; Zhou et al., 2005). Sucrose synthase is the only enzyme capable of both sucrose catabolism and anabolism. In addition, this enzyme is capable of conserving the high-energy glycosidic bond of sucrose following hydrolysis in the form of UDP-glucose (Römer et al., 2004).

Although sucrose synthase is found in all plant organs, it predominantly occurs within sink organs where it is mainly involved in the breakdown of the sucrose disaccharide (Sung et al., 1989; Kruger, 1990). SUSY has been found to be involved in a number of diverse pathways in sink tissues (Avigad, 1990). A considerable amount of evidence exists for the role of SUSY in carbon partitioning, sink-source relations and phloem loading and unloading in various carbohydrate storage organs and sink tissues (Sung et al., 1989; Zrenner et al., 1995; D'Aoust et al., 1999). Case studies for the role of SUSY in sink activities include studies on potato tubers (Zrenner et al., 1995), sunflower hypocotyls (Pfeiffer and Kutschera, 1995) and pea embryos (De´jardin et al., 1997). SUSY has also been found to be involved in the process of nitrogen fixation in legume nodules (Gordon et al., 1999; Horst et al., 2007).

SUSY gene expression has been found to be differentially regulated in response to various abiotic stresses. Hypoxia, anoxia and osmotic stress have all been shown to trigger an increase in SUSY expression (Springer et al., 1986; Maran˜a et al., 1990; Maranã et al., 1990;

Ricard et al., 1991; Hesse and Willmitzer, 1996; Kleines et al., 1999; Baud et al., 2004; Fernandes et al., 2004). This response could be due to the energy conserving nature of sucrose hydrolysis by SUSY. SUSY conserves energy by saving ATP produced during alcoholic fermentation and also provides for the increased energy demands of stressed cells (Perata et al., 1998; Ricard et al., 1998). Increase of SUSY expression is not the trend as it has been noted that SuSy transcript levels decline following wounding (Salanoubat and Belliard, 1989; Hesse and Willmitzer, 1996; Baud et al., 2004). It is thus important to note that the response of SUSY to various stresses is a function of the stress type, tissue type as well as the species in which the response is being tested as documented by Klotz and Haagenson (2008).

1.4.1. SUSY multigene family

To accommodate for the diverse roles SUSY has to perform, at least two sucrose synthase genes are encoded by the genomes of monocotyledon (Carlson et al., 2002) and dicotyledon plants (Sturm and Tang, 1999; Barratt et al., 2001). Some plant species have numerous *SuSy* gene loci with *Arabidopsis thaliana* having six *SuSy* genes (Baud et al., 2004) and poplar having 11 identified *SuSy* gene loci each with a distinct role in carbohydrate metabolism (Geisler-Lee et al., 2006). Amino acid alignments of SUSY sequences within and between species has shown that there is less homology between different SUSY proteins from the same species than SUSY proteins derived from different species. This trend is due to the numerous highly conserved amino acid regions between species such as a 55 residue conserved region found starting at residue 643 in rice, maize, wheat, and potato SUSYs. The highest amino acid sequence variation is found at the N and C-terminals of the SUSY protein (Wang et al., 1993).

Although the pH optima and substrate affinities of the different SUSY family members within a species are similar, these SUSY family members exhibit distinct expression patterns,

some of which can overlap due to the partial redundancy of these enzymes (Nguyen-Quoc et al., 1990; Buczynski et al., 1993; Huang et al., 1996; De´jardin et al., 1997; Sturm and Tang, 1999; Baud et al., 2004). For example, the maize (*Zea mays*) genome encodes three different *SuSy* genes, *Sus1*, *Sh1*, and *Sus3* (Carlson et al., 2002). All three of these genes are expressed in developing maize kernels, yet *Sh1* is thought to play an important role in cell wall synthesis, whilst *Sus1* channels sucrose into starch biosynthesis (Chourey et al., 1998). Matic et al. (2004) derived a simplified model to account for the observed differences in cellular roles of these two encoded SUSY enzymes. In this model the two SUSY enzymes SuSy1 and SuSy2 show a preference for different metabolic pathways, where SuSy1 plays a role in channelling sucrose into ATP production during periods of high energy demand and SuSy2 is involved in cell wall synthesis during low energy demanding conditions (Matic et al., 2004). The abundance and activity of these SUSY isoforms are thus dependent on environmental conditions experienced by various tissues and organs of the plant (De´jardin et al., 1997; Baud et al., 2004).

1.4.2. Regulation of sucrose synthase by posttranslational modification and subcellular localization

SUSY is regulated at the transcriptional level (reviewed in Winter and Huber 2000) and the posttranslational level (Winter and Huber, 2000; Hardin and Huber, 2004; Marino et al., 2008). Posttranslational modification of SUSY, for example phosphorylation, may assist SUSY in performing multiple cellular functions by changing the intracellular localization or the kinetics of this enzyme (Hardin et al., 2004). Sucrose synthase is a known phosphoserine (SerP)-containing enzyme and can be phosphorylated at either the major serine-15 (S15) or the minor serine-170 (S170) phosphorylation sites in maize (*Zea mays* L.) sucrose synthase by calcium-dependent protein kinases (Huber et al., 1996; Hardin et al., 2003).

Phosphorylation of S170 in maize is thought to regulate protein stability of SUSY by promoting ubiquitination of SUSY to produce a high molecular mass form (HMM) of SuSy. This HMM is then recognized by 26S-proteasomes for proteolysis (Hardin and Huber, 2004). A study by Röhrig et al. (2004) on early stages of soybean root nodule organogenesis during Rhizobium–legume interactions provided evidence that a 12 amino acid, cysteine containing peptide encoded by the *ENOD40* gene binds to sucrose synthase by means of a disulphide bond formation. S-thiolation of SUSY by this peptide activates the sucrose cleaving activity of SUSY, whilst the synthetic activity of SUSY remains unchanged. This increase in enzyme activity can either be contributed to a change in the conformation of SUSY or by the protection of SUSY against oxidation through the S-thiolation of the enzyme. Binding of peptide A to SUSY has also been shown to enhance the protein stability of SuSy by preventing the phosphorylation of SuSy at S170. Thus the non-enzymatic posttranslational modification of SuSy by S-thiolation through ENOD40 peptide A not only represents a novel means of regulating the enzyme activity of SuSy, but also acts as a protective mechanism against proteasomal cleavage of SUSY (Röhrig et al., 2004).

Phosphorylation of maize SUSY at the major S15 residue at the N-terminal region is proposed to have effects on enzyme activity and subcellular localization. The corresponding dephosphorylated form of mung bean SUSY showed a lower affinity for sucrose, yet after *in vitro* phosphorylation of this enzyme, sucrose affinity increased (Nakai, 1998, 1999). These findings were supported by an independent study done on SUSY2 purified from maize leaves (Huber et al., 1996). A study performed by Zhang et al. (1999) revealed an opposite trend, where *in vitro* phosphorylation of soybean nodule SUSY altered the protein's hydrophobicity rather than its substrate affinity. Phosphorylation of the enzyme increased hydrophylicity preventing the enzyme from associating with the plasma membrane and thus confining the enzyme to the cytosol. This subsequently stimulated further *in vivo* studies which revealed that

the phosphorylation and dephosphorylation of SUSY was responsible for the partitioning of SUSY to various regions within the cell. One isoform was found to be soluble in the cytoplasm, S-SUSY (soluble-SUSY) whilst the other isoform was associated with cellular membranes, P-SUSY (particulate-SUSY, Winter et al., 1997; Zhang et al., 1999; Winter and Huber, 2000). Posttranslational modification by seryl-phosphorylation of SUSY have also been observed in tomato fruits (*Lycopersicon esculentum*, Anguenot et al., 1999) and elongating cotton fibers (*Gossypium hirsutum*, Haigler et al., 2001).

A study by Haigler et al. (2001) disputed the proposal made by Winter et al. (1997) and Winter and Huber (2000) which assumed that the reversible phosphorylation of SUSY was like a simple "on-off switch" which controlled the intracellular partitioning of this enzyme. Haigler et al. (2001) reported no major differences in the phosphorylation status of P-SUSY and S-SUSY isoforms isolated from cotton fibres radiolabeled *in situ* with 32P-orthophosphate. Therefore the exact physiological role of SUSY phosphorylation at the conserved N-terminal seryl-residue remains unknown. Hardin et al. (2006) performed truncation and alanine substitution mutational analysis of SUS1 in maize to define the membrane binding domains within the protein and *in vitro* microsome binding assays to determine the microenvironment needed for membrane association. Based on their findings they proposed that the amino-terminal noncatalytic domain (residues 1–362) and a region showing similarity to the C-terminal pleckstrin homology domain of human pleckstrin contributed to SUS1's membrane affinity (residues 360–457). Environmental factors that promote the binding of SUS1 to cellular membranes include the presence of sucrose and a low cytosolic pH. The exact physiological mechanism of membrane association still needs to be determined. Many questions remain unanswered such as does SUSY bind directly to cellular membranes or is membrane association facilitated by the formation of a protein complex. If binding to the membrane requires the interaction with additional proteins, what are these

proteins and how do they interact and facilitate the association of SUSY to cellular membranes (Hardin et al., 2006).

The partitioning of sucrose synthase into various cellular compartments allows for the added functional plasticity of this enzyme (Figure 1.8, Ruan et al., 1997). It has been suggested that membrane bound P-SUSY is responsible for allocating activated glucose to the production of storage polymers such as cellulose and callose, whilst S-SUSY which interacts with the actin cytoskeleton in the cytosol channels UDP-glucose into the production of storage polymers like starch and as a source of energy for general metabolism (Amor et al., 1995; Haigler et al., 2001).

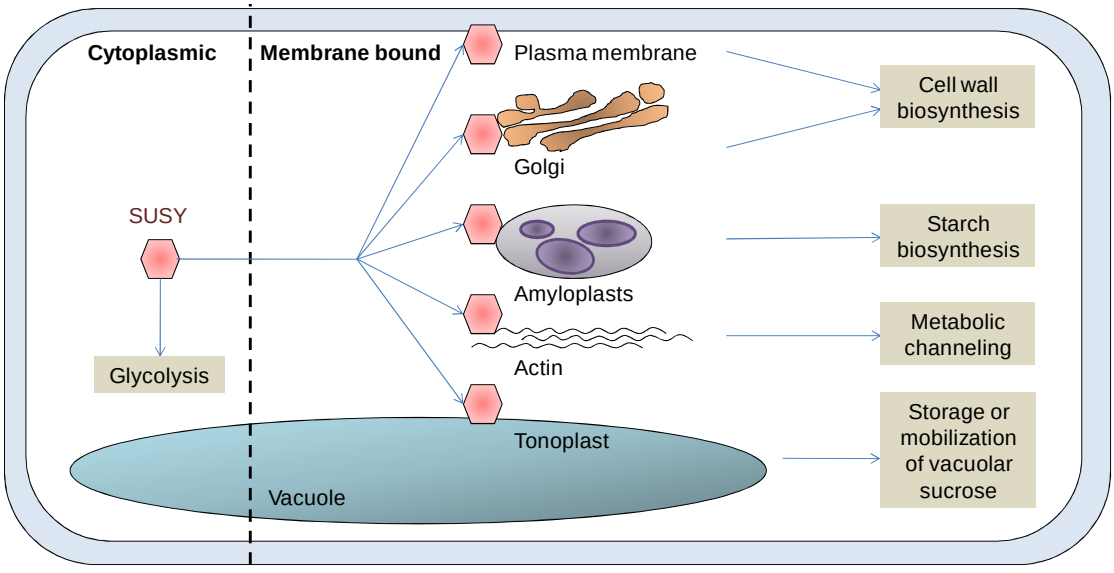

Figure 1.8. Regulation of sucrose synthase (SUSY) activity by subcellular localization. The transient association of SUSY with various membranes, organelles and actin allows for the channeling of sucrose into special functions such as cellulose biosynthesis and xylan biosynthesis (in the plasma membrane and golgi bodies), starch biosynthesis (in amyloplasts), metabolic channeling of stored sucrose in the vacuole to cytosolic processes (involving the tonoplast). Diagram adapted from Koch (2004).

Coleman (2006) tried to target carbon assimilation to cellulose biosynthesis through the overexpression of sucrose synthase in tobacco plants. Instead of getting increased cellulose content, plants were observed to have an overall increase in plant biomass. This finding could be attributed to an increase in the physiological concentrations of both P-SUSY and S-SUSY and thus an increase in the amount of UDP-glucose for cellulose synthesis and general metabolism. A subsequent study by Coleman et al. (2009) took an alternative approach to channel UDP-glucose assimilation from general metabolism to cellulose synthesis. In this study the same cotton SUSY was overexpressed in the model tree *Populus*. Transformants were found to have elevated levels of cell wall associated cellulose and thicker secondary cell walls in vascular cells. Thus Coleman et al. (2009) identified SUSY as a target for the manipulation of carbon allocation by successfully displaying directed the uptake of UDP-glucose to cellulose synthesis.

Alternatively Nakai et al. (1998) attempted to mimic the N-terminal seryl phosphorylation by replacing the serine residue with a charged glutamic acid residue. They hypothesized that the acidic side chain of glutamic acid at position 11 of the mung bean sucrose synthase would activate the enzyme to cooperate with the membrane-bound cellulose synthase. Contrary to the findings by Zhang et al. (1999) this mutant mung bean SUSY was found to associate with the cell membrane. Following expression in the bacterial species *Acetobacter xylinum* it was noticed that there was an overall increase in cellulose content. Further expression of this modified mung bean SUSY in cotton and poplar by Konishi et al. (2004) further supported the findings by Nakai et al. (1998). It is evident that the exact mechanism determining the subcellular localization of SUSY remains elusive with contrasting regulatory mechanisms identified in different species. Attempts to engineer the P-SUSY form for controlled channeling of carbon from sucrose into cellulose biosynthesis will require

further species specific studies of the posttranslational regulation of SUSY activity and localization.

1.5. Confocal microscopy as a tool for functional gene studies *in planta*

The cellular localization of enzymes, substrates and their associated regulatory factors plays an important role in the temporal and spatial regulation of biological reactions. Subcellular localization assays involve the detection of target proteins within a cell to deduce the location, function and interactions of proteins. Proteins can be viewed indirectly using technologies such as subcellular fractionation and Western blotting or can be viewed directly using a number of advanced methods of microscopy.

There has been a strong movement away from the use of epifluorescence scanning microscopy (ESM) towards confocal laser microscopy as a tool for subcellular localization of proteins. This shift is due to the limitations associated with ESM including its poor resolution and requirement for tedious sample fractioning during preparation. Confocal microscopy is a powerful alternative to ESM and allows for the visualization of a fluorescent signal within a narrow plane of focus (Paddock, 1999). This technique can exclude background noise and allows for the three-dimensional reconstruction of protein and cellular structures through analysis of a collection of optical sections (Paddock, 1999). Its deep tissue penetration allows for the use of live whole mounts, which expands the applications of this technology to the visualization of real-time protein dynamics within the cell.

1.5.1. Reporter genes

Reporter genes express chromogenic or fluorescent proteins that can be fused to target genes or proteins at the transcriptional or translational level, respectively. These genes have

numerous uses in functional genetic studies such as assisting in the cellular and subcellular localization of proteins, screening for mutants and protein-protein interaction studies. Traditionally, antibodies were used to visualize specific proteins via an immunoprecipitation assay. These antibodies have been replaced by chromogenic proteins such as GUS (Jefferson et al., 1987) and intrinsically fluorescent proteins such as GFP (Prasher et al., 1992).

GUS (β-3-glucuronidase) was isolated from the bacterial species *Escherichia coli* (Jefferson et al., 1987). GUS is typically used for organ and tissue-specific expression analysis of plant transgenes and an assay for nuclear localization due its inability to passively diffuse into the nucleus. Its large molecular mass of 68kDa confers a higher risk of protein folding artefacts. GUS is visualized through a histochemical assay that requires sample fixation and staining. This procedure is not only tedious but could also result in the development of structural and functional protein artefacts that could confound study findings (Weigel and Glazebrook, 2002).

1.5.2. Intrinsically fluorescent proteins (IFP's)

An alternative to GUS is the green fluorescent protein (GFP) isolated from the illuminescent jellyfish *Aequorea victoria* (Prasher et al., 1992). This small protein, consisting of only 238 amino acids, fluoresces bright green when visualized under UV and blue light (Shimomura et al., 1962). In 2008 Professors Osamu Shimomura, Martin Chalfie and Roger Y. Tsien were awarded Nobel prize in Chemistry for their contributions towards the development of GFP as a reporter protein. GFP diffuses readily between the cytosol and nucleus making it capable of providing spatial and temporal information about the distribution of proteins within the cell. GFP is autoilluminescent circumventing the need for destructive staining techniques associated with GUS visualization (Chalfie, 2006). This reporter gene has undergone numerous modifications to make it applicable in a plant system. It was found that GFP had a cryptic

intron, which was recognised by plant spliceosomes and spliced out of the mRNA prior to translation. To prevent the incorrect splicing of GFP and subsequent loss of fluorescent activity, Haselhoff et al. (1997) removed this cryptic intron by changing the codon usage.

GFP has been used in many applications from the simple screening of segregants for reporter gene expression to high-resolution subcellular localization imaging (DeBlasio et al., 2010). The visualization of GFP in live whole mounts expands the applications of this reporter system to the visualization of real-time protein dynamics in the cell. Some scepticism exists over the applicability of amino-terminal GFP fusion proteins as it has been found that the N-terminus is essential for proper membrane-protein associations. A study by Hampton (1996) focused on assessing the affect of N-terminal GFP fusions on the localization of the yeast membrane protein hydroxymethylglutaryl-CoA reductase. It was found that this fusion protein showed characteristics that were consistent with that of the native protein suggesting that both C-terminal and N-terminal GFP fusion proteins can be utilized for subcellular localization studies.

A number of GFP variants have been designed for optimisation of reporter gene activity (Table 1.1). These variants called intrinsically fluorescent proteins (IFPs) either fluoresce more brightly or emit light at a different spectral quality such as yellow fluorescent protein (YFP), cyan fluorescent proteins (CFP) and a red fluorescent protein (DsRED) isolated from corals. Newcomers to the ever growing spectral fluorescent variant list include “superfolder” GFP (Pédelacq et al., 2006), mRuby (Kredel et al., 2009) and mCherry (Shaner et al., 2004). Superfolder GFP as the name suggests was designed to fold even when fused to insoluble proteins. Superfolder GFP is also brighter and more acid resistant than EGFP and even the esteemed Emerald GFP (Pédelacq et al., 2006). mRuby has the potential to become very useful in the field of fluorescent reporters as it has a large Stokes shift (the difference between the excitation and emission maximums) of 47 nm, is resistant to denaturation at pH

extremes and has been found to be ten-fold brighter than enhanced GFP (EGFP, Kredel et al., 2009). The bright red fluorescent protein, mCherry, has a short maturation time and much longer excitation and emission wavelengths. These features reduce the amount of autofluorescence and cellular damage produced during fluorescence imaging (Fan et al., 2008). For a comprehensive review of the developments in IFPs and the properties of specific spectral variants please refer to Day and Davidson (2009).

Table 1.1. Fluorescent protein variants with their associated excitation and emission wavelengths. Table based on Held et al. (2008), Dixit et al. (2006) and Shaner et al. (2004).

Colour	IFP	Excitation maximum (nm)	Emission maximum (nm)	Reference
Blue	EBFP	380	440	(Patterson et al., 1997)
Cyan	ECFP	433/452	475/505	(Rizzo et al., 2004)
	Cerulean CFP	433	475	(Rizzo et al., 2004)
Green	mGFP4	395/475	509	(Haselhoff et al., 1997)
	EGFP	488	507	(Cormack et al., 1996)
Lime	EYFP	515	528	(Nagai et al., 2002)
	Citrine YFP	516	529	(Griesbeck et al., 2001)
Yellow	Venus YFP	515	528	(Nagai et al., 2002)
	mHoneydew	487/504	537/562	(Shaner et al., 2004)
	mBanana	540	553	(Shaner et al., 2004)
Orange	mOrange	548	562	(Shaner et al., 2004)
Red	dsRed	558	583	(Dixit et al., 2006)
	mTangerine	568	585	(Shaner et al., 2004)
	mStrawberry	574	596	(Shaner et al., 2004)
	mRFP1	584	607	(Merzlyak et al., 2007)
	mRuby	558	605	
	mCherry	587	610	(Shaner et al., 2004)
Far Red	mRaspberry	596	625	(Shaner et al., 2004)
	mPlum	590	648	(Shaner et al., 2004)

The availability of numerous spectral variants allows for the simultaneous imaging of several reporter genes and facilitates *in vivo* studies of protein interactions by methodologies such as fluorescence resonance energy transfer (FRET) microscopy (Sekar and Periasamy,

2003) and bimolecular fluorescence complementation (BiFC, Bracha-Drori et al., 2004). For an in depth review on the various molecular and cellular techniques used to detect protein-protein interactions refer to Lalonde et al. (2008).

The choice of IFP is dependent on the experimental scenario. There are however some general requirements for the efficient use of fluorescent proteins in bioimaging. Firstly you would want an IFP that expresses efficiently such that the fluorescence signal is detectable. The chosen IFP should not be toxic to the organism in which it is expressed. It is suggested that the IFP should be bright enough to provide enough signal above autofluorescence especially when working *in planta*. The IFP should display sufficient photostability to be used for the duration of the imaging and should not oligomerize. It is recommended that the fluorescent protein should be insensitive to environmental effects such as acidity. In multi-labelling where more than one fluorescent protein is imaged there should be minimal cross talk (overlap) in the emission and excitation channels (Shaner et al., 2005).

The extensive use of GFP as a reporter protein has lead to a toolkit of markers specific to tissue-type, cell-type and subcellular localization. A marker is typically a fusion construct in which the transgene is fully characterized as being localized to a particular physiological niche. A repertoire of subcellular markers have been engineered for studies in plants specifically the model plant *Arabidopsis thaliana* (Table 1.2). Subcellular markers have also been engineered from fusions with different spectral variants and for different biological backgrounds such as mammalian cells (Day and Davidson, 2009; DeBlasio et al., 2010). These molecular markers can be used to study the temporal and spatial dynamics of their associated cellular structure or can be utilized in colocalization studies to determine the localization of proteins *in vivo*. The principles underlying colocalization and the recent advances in this innovative field are reviewed in Bolte and Cordelieres (2006), French et al. (2008), Waters (2009) and Zinchuk and Grossenbacher-Zinchuk (2009).

Table 1.2. Fluorescent protein fusion constructs targeting subcellular locations *in planta.* Table based on Cutler et al. (2000) and Dixit et al. (2006).

Subcellular structure	Marker used	References
Actin	fimbrin1-GFP	(Sheahan et al., 2004)
	GFP-mouse talin	(Wang et al., 2004)
Cell membrane	PIP1b-GFP	(Cutler et al., 2000)
	PIP2a-GFP	(Cutler et al., 2000)
Centromere	Histone 3-GFP	(Fang and Spector, 2005)
Chloroplast/Plastid	Stroma signal peptide-GFP	(Kohler et al., 1997)
	Rubisco-GFP	(Kwok and Hanson, 2004)
Chromosomes	Cry2-GFP	(Cutler et al., 2000)
Endoplasmic reticulum	ER retention signal-GFP	(Haselhoff et al., 1997)
Golgi	N-acetylglucosaminyl transferase 1-GFP	(Lu et al., 2005)
Microtubules	GFP-beta-tubulin 6	(Nakamura et al., 2004)
	GFP-mouse MAP4	(Granger and Cyr, 2001)
Mitochondria	Mitochondrial signal peptide-GFP	(Logan and Leaver, 2000)
Nucleus	Histone 2B-GFP	(Boisnard-Lorig et al., 2001)
	Ankyrin-like protein-GFP	(Cutler et al., 2000)
	Ribosomal Protein S31-GFP	(Cutler et al., 2000)
Nuclear envelope	RanGAP-GFP	(Pay et al., 2002)
Peroxisome	Peroxisomal targeting signal-GFP	(Mathur et al., 2002)
Vacuole	Vacuolar syntaxin-GFP	(Uemura et al., 2002)
Vacuolar membrane	DIP aquaporin homolog-GFP	(Cutler et al., 2000)
	Delta TIP-GFP	(Cutler et al., 2000)

1.6. Conclusion

Due to the rise in fuel costs and detrimental environmental effects of consuming fossil fuels there has been a shift of interest towards the use of renewable fuel resources. Cellulose is one of these fuel resources considered due to its abundance in woody plants. Therefore much research is focused on getting a better understanding of the spatial and temporal complexities of cellulose biosynthesis, to facilitate purification of cellulose as well as simplify the fermentation process required to produce cellulosic ethanol. Studies are also underway to identify and molecularly modify existing crops for use as bioethanol crops.

Sucrose synthase plays an important role in the regulation of carbon allocation to general metabolism or to the synthesis of structural polysaccharides such as cellulose (Kleczkowski, 1994). It is evident that this enzyme is greatly regulated at both the transcriptional and posttranslational levels. The subcellular localization of SUSY is thought to channel the activated glucose produced by this enzyme into different sink metabolic processes. Drawing from literature one can hypothesize that through the up-regulation of the membrane-bound P-SUSY form of sucrose synthase one can cause a corresponding increase in cellulose biosynthesis by channelling carbon allocation towards cell membrane associated processes (Konishi et al., 2004; Coleman et al., 2006). This is of particular interest to the pulp and paper industry as this engineered P-SUSY form can be utilized to genetically engineer a crop of forest trees capable of producing higher cellulose content. The effect of this shift in carbon allocation towards cellulose synthesis *in vivo* is still to be determined. Future studies need to determine whether genetically modified plants remain physiologically indistinctive or show increased biomass or severely disrupted cellular homeostasis resulting in reduced viability. A better understanding of the regulation of sucrose synthase activity and source-sink relations *in vivo* is thus essential to making this hypothesis a reality.

References

Amor Y, Haigler CH, Johnson S, Wainscott M, Delmar DP (1995) A membrane-associated form of sucrose synthase and its potential role in synthesis of cellulose and callose in plants. Plant Biology **92:** 9353-9357

Andersson-Gunneras S, Mellerowicz EJ, Love J, Segerman B, Ohmiya Y, Coutinho PM, Nilsson P, Henrissat B, Moritz T, Sundberg B (2006) Biosynthesis of cellulose-enriched tension wood in Populus: global analysis of transcripts and metabolites identifies biochemical and developmental regulators in secondary wall biosynthesis. The Plant Journal **45:** 144–165

Anguenot R, Yelle S, Nguyen-Quoc B (1999) Purification of tomato sucrose synthase phosphorylated isoforms by Fe(III)-immobilized metal affinity chromatography. Archives Biochemistry and Biophysics **365:** 163–169

Aspeborg H, Schrader J, Coutinho PM, Stam M, Kallas A, Djerbi S, Nilsson P, Denman S, Amini B, Sterky F, Master E, Sandberg G, Mellerowicz E, Sundberg B, Henrissat B, Teeri TT (2005) Carbohydrate-Active Enzymes Involved in the Secondary Cell Wall Biogenesis in Hybrid Aspen. Plant Physiology **137:** 983–997

Avigad G (1990) Sucrose and disaccharides. Springer Verlag, Berlin

Balibrea Lara ME, Gonzalez Garcia MC, Fatima T, Ehneß R, Lee TK, Proels R, Tanner W, Roitsch T (2004) Extracellular invertase is an essential component of cytokinin-mediated delay of senescence. Plant Cell **16:** 1276–1287

Barratt DHP, Barber L, Kruger NJ, Smith AM, Wang TL, Martin C (2001) Multiple, distinct sioforms of sucrose synthase in pea. Plant Physiology **127:** 655-664

Baud S, Vaultier MN, Rochat C (2004) Structure and expression profile of sucrose synthase multigene family in Arabidopsis. Journal of Experimental Botany **55:** 396-409

Boisnard-Lorig C, Colon-Carmona A, Bauch M, Hodge S, Doerner P, Bancharel E, Dumas C, Haseloff J, Berger F (2001) Dynamic Analyses of the Expression of the HISTONE::YFP Fusion Protein in Arabidopsis Show That Syncytial Endosperm Is Divided in Mitotic Domains. The Plant Cell **13:** 495–509

Bolte S, Cordelieres FP (2006) A guided tour into subcellular colocalization analysis in light microscopy. Journal of Microscopy **224:** 213–232

Bracha-Drori K, Shichrur K, Katz A, Oliva M, Angelovici R, Yalovsky S, Ohad N (2004) Detection of protein–protein interactions in plants using bimolecular fluorescence complementation. The Plant Journal **40:** 419-427

Buczynski SR, Thom M, Chourey P, Maretzki A (1993) Tissue distribution and characterisation of sucrose synthase isozymes in sugarcane. Journal of Plant Physiology **142:** 641–646

Carlson SJ, Chourey PS, Helentjaris T, Datta R (2002) Gene expression studies on developing kernels of maize sucrose synthase (SUSY) mutants show evidence for a third SUSY gene. Plant Molecular Biology **49:** 15-29

Chalfie MK, S. (2006) Green fluorescent protein: properties, applications, and protocols, Ed 2nd. Wiley-Interscience, Hoboken, NY

Chourey PS, Nelson OE (1976) The enzymatic deficiency conditioned by theshrunken-1 mutation in maize. Biochemistry and Genetics **14:** 1041–1055

Chourey PS, Taliercio EW, Carlson SJ, Ruan YL (1998) Genetic evidence that the two isozymes of sucrose synthase present in developing maize endosperm are critical, one for cell wall integrity and the other for starch biosynthesis. Molecular Genomes and Genetics **259:** 88-96

Ciereszko I, Johansson H, Kleczkowski LA (2001) Sucrose and light regulation of a cold-inducible UDP-glucose pyrophosphorylase gene via a hexokinase-independent and abscisic acid-insensitive pathway in Arabidopsis. Biochemistry Journal **354:** 67-72

Coleman HD, Ellis DD, Gilbert M, Mansfield SD (2006) Up-regulation of sucrose synthase and UDP-glucose pyrophosphorylase impacts plant growth and metabolism. Plant Biotechnology Journal **4:** 87–101

Coleman HD, Yan J, Mansfield SD (2009) Sucrose synthase affects carbon partitioning to increase cellulose production and altered cell wall ultrastructure. Proceedings of the National Academy of Sciences, USA. **106:** 13118

Cormack BP, Valdivia RH, Falkow S (1996) FACS-optimized mutants of the green fluorescent protein (GFP). Gene **173:** 33-38

Cutler SR, Ehrhardt DW, Griffitts JS, Somerville CR (2000) Random GFP::cDNA fusions enable visualization of subcellular structures in cells of *Arabidopsis* at a high frequency. Proceedings of the National Academy of Sciences, USA. **97:** 3718–3723

D'Aoust MA, Yelle S, Nguyen QB (1999) Antisense inhibition of tomato fruit sucrose synthase decreases fruit setting and the sucrose unloading capacity of young fruit. Plant Cell **11:** 2407–2418

Day RN, Davidson MW (2009) The fluorescent protein palette: tools for cellular imaging. Chemistry Society Review **38:** 2887-2921

De´jardin A, Rochat C, Wuille`m S, Boutin J-P (1997) Contribution of sucrose synthase, ADP-glucose pyrophosphorylase and starch synthase to starch synthesis in developing pea seeds. Plant Cell Environment **20:** 1421–1430

DeBlasio SL, Sylvester AW, Jackson D (2010) Illuminating plant biology: using fluorescent proteins for high-throughput analysis of protein localization and function in plants. Briefings in functional genomics **9:** 129-138

Déjardin A, Rochat C, Wuillèm S, Boutin J-P (1997) Contribution of sucrose synthase, ADP-glucose pyrophosphorylase and starch synthase to starch synthesis in developing pea seeds. Plant Cell Environment **20:** 1421–1430

Delmer DP (1999) CELLULOSE BIOSYNTHESIS: Exciting Times for A Difficult Field of Study. Annual Review in Plant Physiology and Plant Molecular Biology **50:** 245–276

DeWald DB, Sadka A, Mullet JE (1994) Sucrose modulation of soybean Vsp gene expression is inhibited by auxin. Plant Physiology **104:** 439–444

Dixit R, Cyr R, Gilroy S (2006) Using intrinsically fluorescent proteins for plant cell imaging. The Plant Journal **45:** 599–615

Doblin MS, Kurek I, Jacob-Wilk D, Delmer DP (2002) Cellulose Biosynthesis in Plants: from Genes to Rosettes. Plant Cell Physiology **43:** 1407–1420

Duncan KA, Huber SC (2007) Sucrose Synthase Oligomerization and F-actin Association are Regulated by Sucrose Concentration and Phosphorylation. Plant Cell Physiology **48:** 1612–1623

Duncan KA, Huber SC (2007) Sucrose synthase oligomerization and F-actin association regulated by sucrose concentration and phosphorylation. Plant and Cell Physiology **48:** 1612-1623

Evert RF (1982) Sieve-tube structure in relation to function. Bioscience **32:** 789–795

Fan J-Y, Cui Z-Q, Wei H-P, Zhang Z-P, Zhou Y-F, Wang Y-P, Zhang X-E (2008) Split mCherry as a new red bimolecular fluorescence complementation system for visualizing protein–protein interactions in living cells. Biochemical and Biophysical Research Communications **367:** 47–53

Fang Y, Spector DL (2005) Centromere positioning and dynamics in living *Arabidopsis* plants. Molecular Biology of the Cell **16:** 5710–5718

Farrar J (1982) Regulation of shoot–root ratio is mediated by sucrose. Plant Soil **185:** 13–19

Fernandes FM, Arrabaca MC, Carvalho LMM (2004) Sucrose metabolism in *Lupinus albus* L. under salt stress. Biological Plant **48:** 317–319

Fernie AR, Willmitzer L, Trethewey RN (2002) Sucrose to starch: a transition in molecular plant physiology. Trends in Plant Science **7:** 35–41

French AP, Mills S, Swarup R, Bennett MJ, Pridmore TP (2008) Colocalization of fluorescent markers in confocal microscope images of plant cells. Nature Protocols **3:** 619-628

Geigenberger P, Reimholz R, Geiger M, Merlo L, Canale V, Stitt M (1997) Regulation of sucrose and starch metabolism in potato tubers in response to short-term water deficit. Planta **201:** 502–518

Geigenberger P, Stitt M (1991) A 'futile' cycle of sucrose synthesis and degradation is involved in regulating partitioning between sucrose, starch and respiration in cotyledons of germinating *Ricinus communis* L. seedlings when phloem transport is inhibited. Planta **185:** 81–90

Geisler-Lee J, Geisler M, Coutinho PM, Segerman B, Nishikubo N, Takahashi J, Aspeborg H, Djerbi S, Master E, Andersson-Gunnera°s S, Sundberg B, Karpinski S, Teeri TT, Kleczkowski LA, Henrissat B, Mellerowicz EJ (2006) Poplar carbohydrate active enzymes (CAZymes).Gene identification and expression analyses. Plant Physiology **140:** 946–962

Gibeaut DM (2000) Nucleotide sugars and glucosyltransferases for synthesis of cell wall matrix polysaccharides. Plant Physiology and Biochemistry **38:** 69–80

Godt D, Roitsch T (2006) The developmental and organ specific expression of sucrose cleaving enzymes in sugar beet suggests a transition between apoplasmic and symplasmic phloem unloading in the tap roots. Plant Physiology and Biochemistry **44:** 656–665

Gordon AJ, Minchin FR, James CL, Komina O (1999) Sucrose synthase in legume nodules is essential for nitrogen fixation. Plant Physiology **120:** 867-887

Granger CL, Cyr RJ (2001) Spatiotemporal relationships between growth and microtubule orientation as revealed in living root cells of *Arabidopsis thaliana* transformed with green-fluorescent-protein gene construct *GFP-MBD*. Protoplasma **216:** 201-214

Griesbeck O, Baird GS, Campbell RE, Zacharias DA, Tsien RY (2001) Reducing the environmental sensitivity of yellow fluorescent protein. Mechanism and applications. Journal of Bioliogical Chemistry **276:** 29188-29194

Haigler CH, Ivanova-Datcheva M, Hogan PS, Salnikov VV, Hwang S, Martin K, Delmer DP (2001) Carbon partitioning to cellulose synthesis. Plant Molecular Biology **47:** 29–51

Hampton RY, Koning A, Wright R, Rine J (1996) In vivo examination of membrane protein localization and degradation with green fluorescent protein. Cell Biology **93:** 828-833

Hardin SC, Duncan KA, Huber SC (2006) Determination of structural requirements and probable regulatory effectors for membrane association of maize sucrose synthase. Plant physiology **141:** 1106–1119

Hardin SC, Huber SC (2004) Proteasome activity and the post-translational control of sucrose synthase stability in maize leaves. Plant Physiology and Biochemistry **42:** 197–208

Hardin SC, Tang G-Q, Scholz A, Holtgraewe D, Winter H, Huber SC (2003) Phosphorylation of sucrose synthase at serine 170: occurrence and possible role as a signal for proteolysis. Plant Journal **35:** 588–603

Hardin SC, Winter H, Huber SC (2004) Phosphorylation of the Amino Terminus of Maize Sucrose Synthase in Relation to Membrane Association and Enzyme Activity. Plant physiology **134:** 1427–1438

Haselhoff J, Siemering KR, Prasher DC, Hodge S (1997) Removal of a cryptic intron and subcellular localization of green fluorescent protein are required to mark transgenic Arabidopsis plants brightly. Applied Biological Sciences **94:** 2122–2127

Held MA, Boulaflous A, Brandizzi F (2008) Advances in fluorescent protein-based imaging for the analysis of plant endomembranes. Plant Physiology **147:** 1469-1481

Herth W (1983) Arrays of plasma-membrane 'rosettes' involved in cellulose microfibril formation in spirogyra. Planta **159:** 347–356

Hesse H, Willmitzer L (1996) Expression analysis of a sucrose synthase gene from sugar beet (*Beta vulgaris* L.). Plant Molecular Biology **30:** 863–872

Horst I, Welham T, Kelly S, Kanoko T, Sato S, Tabata S, Parniske M, Wang TL (2007) TILLING mutants of *Lotus japonicus* reveal that nitrogen assimilation and fixation can occur in the absence of nodule-enhanced sucrose synthase. Plant Physiology **144:** 806 - 820

Huang JW, Chen JT, Yu WP, Shyur LF, Wang AY, Sung HY, Lee PD, Su JC (1996) Complete structures of three rice sucrose synthase isogenes and differential regulation of their expressions. Bioscience Biotechnology Biochemistry **60:** 233-239

Hubbard N, Huber S, Pharr D (1989) Sucrose phosphate synthase and acid invertase as determinants of sucrose concentration in developing muskmelon (*Cucumis melo* L.) fruits. Plant Physiology **91:** 1527–1534

Huber SC, Akazawa T (1986) A Novel Sucrose Synthase Pathway for Sucrose Degradation in Cultured Sycamore Cells. Plant Physiology **81:** 1008-1013

Huber SC, Huber JL, Liao P-C, Gage DA, McMichael JRW, Chourey PS, Hannah LC (1996) Phosphorylation of Serine-15 of maize leaf sucrose synthase. Plant Physiology **112:** 793-802

Jefferson RA, Kavanagh TA, Bevan MW (1987) GUS fusions: β-glucoronidase as a sensitive and versatile gene fusion marker in higher plants. The EMBO Journal **6:** 3901 -3907

Johansson H, Sterky F, Amini B, Lundeberg J, Kleczkowski LA (2002) Molecular cloning and characterization of a cDNA encoding poplar UDP-glucose dehydrogenase, a key enzyme of hemicellulose/pectin formation. Biochimica Biophysica Acta **1576:** 53–58

Junghans H, Metzlaff M (1990) A simple and rapid method for the preparation of total plant DNA. Biotechniques **8:** 176

Kleczkowski LA (1994) Glucose activation and metabolism through UDP-glucose pyrophosphorylase in plants. Phytochemistry **37:** 1507-1515

Kleines M, Elster R-C, Rodrigo M-J, Blervacq A-S, Salamini F, Bartels D (1999) Isolation and expression analysis of two stress-responsive sucrose-synthase genes from the resurrection plant *Craterostigma plantagineum* (Hochst.). Planta **209:** 13–24

Klotz KL, Haagenson DM (2008) Wounding, anoxia and cold induce sugarbeet sucrose synthase transcriptional changes that are unrelated to protein expression and activity. Journal of Plant Physiology **165:** 423—434

Koch KE (1996) Carbohydrate-modulated gene expression in plants. Annual Review in Plant Physiology and Plant Molecular Biology **47:** 509–540

Koch KE (2004) Sucrose metabolism: regulatory mechanisms and pivotal roles in sugar sensing and plant development. Current Opinion in Plant Biology **7:** 235–246

Kohler RH, Cao J, Zipfel WR, Webb WW, Hanson MR (1997) Exchange of protein molecules through connections between higher plant plastids. Science **276:** 2039–2042

Konishi T, Ohmiya Y, Hayashi T (2004) Evidence That Sucrose Loaded into the Phloem of a Poplar Leaf Is Used Directly by Sucrose Synthase Associated with Various β-Glucan Synthases in the Stem. Plant Physiology **134:** 1146–1152

Kost B, Spielhofer P, Chua NH (1998) A GFP-mouse talin fusion protein labels plant actin filaments *in vivo* and visualizes the actin cytoskeleton in growing pollen tubes. Plant Journal **16:** 393–401

Kredel S, Oswald F, Nienhaus K, Deuschle K, Röcker C, Wolff M, Heilker RG, Nienhaus U, Wiedenmann J (2009) mRuby, a bright monomeric red fluorescent protein for labeling of subcellular structures. PLoS ONE **4:** e4391

Kruger NJ (1990) Carbohydrate synthesis and degradation. Longman Scientific and Technical, Essex

Kwok EY, Hanson MR (2004) GFP-labelled Rubisco and aspartate aminotransferase are present in plastid stromules and traffic between plastids. Journal of Experimental Botany **55:** 595–604

Lalonde S, Ehrhardt DW, Loqué D, Chen J, Rhee SY, Frommer WB (2008) Molecular and cellular approaches for the detection of protein-protein interactions: latest techniques and current limitations. The Plant Journal **53:** 610-635

Leigh RA, Rees T, Fuller WA, Banfield J (1979) The location of invertase activity and sucrose in the vacuoles of storage roots of beetroot (*Beta vulgaris*). Biochemistry Journal **178:** 539–547

Leloir LF, Cardini CE (1953) Journal of the American Chemistry Society **75:** 6084

Lingle SE, Dunlap JR (1987) Sucrose metabolism in netted musk-melon fruit during development. Plant Physiology **84:** 386–389

Lloyd C, Chan J (2008) The parallel lives of microtubules and cellulose microfibrils. Current Opinion in Plant Biology **11:** 641-646

Logan DC, Leaver CJ (2000) Mitochondria-targeted GFP highlights the heterogeneity of mitochondrial shape, size and movement within living plant cells. Journal of Experimental Botany **51:** 865-871

Lu L, Lee YR, Pan R, Maloof JN, Liu B (2005) An internal motor kinesin is associated with the Golgi apparatus and plays a role in trichome morphogenesis in *Arabidopsis*. Molecular Biology of the Cell **16:** 811–823

Lunn JE, MacRaey E (2003) New complexities in the synthesis of sucrose. Current Opinion in Plant Biology **6:** 208–214

Mano S, Nakamori C, Hayashi M, Kato A, Kondo M, Nishimura M (2002) Distribution and characterization of peroxisomes in Arabidopsis by visualization with GFP: dynamic morphology and actin-dependent movement. Plant Cell Physiology **43:** 331–341

Maran˜a C, Garcı´a-Olmedo F, Carbonero P (1990) Differential expression of two types of sucrose synthase-encoding genes in wheat in response to anaerobiosis, cold shock and light. Gene **88:** 167–172

Marino D, Hohnjec N, Küster H, Moran JF, González EM, Arrese-Igor C (2008) Evidence for transcriptional and post-translational regulation of sucrose synthase in pea nodules by the cellular redox state. Molecular Plant-Microbe Interactions **21:** 622-630

Mathur J, Mathur N, Hűlskamp M (2002) Simultaneous visualization of peroxisomes and cytoskeletal elements reveals actin and not microtubule-based peroxisome motility in plants. Plant Physiology **128:** 1031–1045

Matic S, Åkerlund H-E, Everitt E, Widell S (2004) Sucrose synthase isoforms in cultured tobacco cells. Plant Physiology and Biochemistry **42:** 299–306

Merzlyak EM, Goedhart J, Shcherbo D, Bulina ME, Shcheglov AS, Fradkov AF, Gaintzeva A, Lukyanov KA, Lukyanov S, Gadella TW, al. e (2007) Bright monomeric red fluorescent protein with an extended fluorescence lifetime. Nature Methods **4:** 555-557

Nagai T, Ibata K, Park ES, Kubota M, Mikoshiba K, Miyawaki A (2002) A variant of yellow fluorescent protein with fast and efficient maturation for cell-biological applications. Nature Biotechnology **20:** 87-90

Nakai T, Konishi T, Zhang X, Chollet R, Tonouchi N, Tsuchida T, Yoshinaga F, Mori H, Sakai F, Hayashi T (1998) An Increase in apparent affinity for sucrose of mung bean sucrose synthase is caused by in vitro phosphorylation or directed mutagenesis of Ser^{11}. Plant Cell Physiology **39:** 1337-1341

Nakai T, Tonouchi, N., Konishi, T., Kojima, Y., Tsuchida, T., Yoshinaga, F., Sakai, F., and Hayashi, T. (1999) Enhancement of cellulose production by expression of sucrose synthase in *Acetobacter xylinum*. PNAS USA **96:** 14-18

Nakamura M, Naoi K, Shoji T, Hashimoto T (2004) Low concentrations of propyzamide and oryzalin alter microtubule dynamics in *Arabidopsis* epidermal cells. Plant Cell Physiology **45:** 1330–1334

Nguyen-Quoc B, Krivitzky M, Huber SC, Lecharny A (1990) Sucrose synthase in developing maize leaves. Plant Physiology **94:** 516–523

Paddock SW (1999) Confocal laser scanning microscopy. BioTechniques **27:** 992-1004

Patterson GH, Knobel SM, Sharif WD, Kain SR, Piston DW (1997) Use of the green fluorescent protein and its mutants in quantitative fluorescence microscopy. Biophysics Journal **73:** 2782–2790

Pay A, Resch K, Frohnmeyer H, Fejes E, Nagy F, Nick P (2002) Plant RanGAPs are localized at the nuclear envelope in interphase and associated with microtubules in mitotic cells. Plant Journal **30:** 699–709

Pédelacq JD, Cabantous S, Tran T, Terwilliger TC, Waldo GS (2006) Engineering and characterization of a superfolder green fluorescent protein. Nature Biotechnology **24:** 79-88

Perata P, Loreti E, Gugulielminetti L, Alpi A (1998) Carbohydrate metabolism and anoxia tolerance in cereal grains. Acta Botanical Neel **47:** 269-283

Pfeiffer I, Kutschera U (1995) Sucrose metabolism and cell elongation in developing sunflower hypocotyls. Journal Of Experimantal Botany **46:** 631-638

Prasher DC, Eckenrode VK, Ward WW, Prendergast FG, Cormier MJ (1992) Primary structure of the *Aequorea victoria* green-fluorescent protein. Gene **111:** 229

Ricard B, Rivoal J, Spiteri A, Pradet A (1991) Anaerobic stress induces the transcription and translation of sucrose synthase in rice. Plant Physiology **95:** 669-674

Ricard B, VanToai T, Chourey P, Saglio P (1998) Evidence for the critical role of sucrose synthase for anoxic tolerance of maize roots using a double mutant. Plant Physiology **116:** 1323–1331

Ridge RW, Uozumi Y, Plazinski J, Hurley UAaW, R.E. (1999) Developmental transitions and dynamics of the cortical ER of *Arabidopsis* cells seen with green fluorescent protein. Plant Cell Physiology **40:** 1253–1261

Rizzo MA, Springer GH, Granada B, Piston DW (2004) An improved cyan fluorescent protein variant useful for FRET. Nature Biotechnology **22:** 445–449

Röhrig H, John M, Schmidt J (2004) Modification of soybean sucrose synthase by S-thiolation with ENOD40 peptide A. Biochemical and Biophysical Research Communications **325:** 864–870

Roitsch T, Gonzalez MC (2004) Function and regulation of plant invertases:sweet sensations. Trends in Plant Science **9:** 606–613

Rolland F, Moore B, Sheen J (2002) Sugar sensing and signaling in plants. Plant Cell **14:** 185–205

Römer U, Schrader H, Günther N, Nettelstroth N, Frommer WB, Elling L (2004) Expression, purification and characterization of recombinant sucrose synthase 1 from *Solanum tuberosum* L. for carbohydrate engineering. Journal of Biotechnology **107:** 135–149

Ruan Y, Chourey PS, Delmer DP, Perez-Grau L (1997) The differential expression of sucrose synthase in relation to diverse patterns of carbon partitioning in developing cotton seed. Plant Physiology **115:** 375-385

Salanoubat M, Belliard G (1989) The steady-state level of potato sucrose synthase mRNA is dependent on wounding, anaerobiosis and sucrose concentration. Gene **84:** 181–185

Schlüpmann H, Bacic A, Read SM (1994) Uridine-diphosphate glucose metabolism and callose synthases in cultured pollen tubes of *Nicotiana alata*. Plant Physiology **105:** 659–670

Sebková V, Unger C, Hardegger M, Sturm A (1995) Biochemical, physiological and molecular characterization of sucrose synthase from *Daucus carota*. Plant Physiology **108:** 75–83

Seifert GJ (2004) Nucleotide sugar interconversions and cell wall biosynthesis: how to bring the inside to the outside. Current Opinion in Plant Biology **7:** 1–8

Sekar RB, Periasamy A (2003) Fluorescence resonance energy transfer (FRET) microscopy imaging of live cell protein localizations. The Journal of Cell Biology **160:** 629-633

Shaner NC, Campbell RE, Steinbach PA, Giepmans BNG, Palmer AE, Tsien RY (2004) Improved monomeric red, orange and yellow fluorescent proteins derived from *Discosoma* sp. red fluorescent protein. Nature Biotechnology **22**

Shaner NC, Steinbach PA, Tsien RY (2005) A guide to choosing fluorescent proteins. Nature **12:** 905-909

Sheahan MB, Staiger CJ, Rose RJ, McCurdy DW (2004) A green fluorescent protein fusion to actin-binding domain 2 of *Arabidopsis* fimbrin highlights new features of a dynamic actin cytoskeleton in live plant cells. Plant Physiology **136**

Shimomura O, Johnson FH, Saiga YJ (1962) Extraction, purification and properties of aequorin, a bioluminescent protein from the luminous hydromedusan, Aequorea. Journal of Cellular and Comparitive Physiology **59:** 223-239

Somerville C (2006) Cellulose Synthesis in Higher Plants. Annual Review in Cell Developmental Biology **22:** 53-78.

Springer B, Werr W, Starlinger P, Bennett DC, Zololica M, Freeling M (1986) The Shrunken gene on chromosome 9 of *Zea mays* L. is expressed in various plant tissues and encodes an anaerobic protein. Molecular Genomes and Genetics **205:** 461–468

Stitt M, Muller C, Matt P, Gibon Y, Carillo P, Morcuende R, Scheible WR, Krapp A (2002) Steps towards an integrated view of nitrogen metabolism. Journal of Experimental Botany **53:** 959-970

Strand A, Foyer CH, Gustafsson P, Gardestrom P, Hurry V (2003) Altering flux through the sucrose biosynthesis pathway in transgenic *Arabidopsis thaliana* modifies photosynthetic acclimation at low temperatures and the development of freezing tolerance. Plant Cell Environment

Sturm A (1999) Invertases. Primary structures, functions, and roles in plant development and sucrose partitioning. Plant physiology **121** 1–7

Sturm A, and Tang, G-Q. (1999) The sucrose-cleaving enzymes of plants are crucial for development, growth and carbon partitioning. Trends in Plant Science **4:** 401-407

Sturm A, Tang G-Q (1999) The sucrose-cleaving enzymes of plants are crucial for development, growth and carbon partitioning. Trends Plant Sci **4:** 401–407

Sung S-J, Xu D-P, Black CC (1989) Identification of actively filling sucrose sinks. Plant Physiology **89:** 1117–1121

Tanase K, Yamaki S (2000) Purification and characterization of two sucrose synthase isoforms from Japanese pear fruit. Plant Cell Physiology **41:** 408–414

Tang GQ, Sturm A (1999) Antisense repression of sucrose synthase in carrot (*Daucus carota* L.) affects growth rather than sucrose partitioning. Plant Molecular Biology **41:** 465–479

Taylor NG (2008) Cellulose biosynthesis and deposition in higher plants. New Phytologist **178:** 239–252

Tymowska-Lalanne Z, Kreis M (1998) The plant invertases: physiology, biochemistry and molecular biology. Adv Botanical Research **28:** 71–117

Uemura T, Yoshimura SH, Takeyasu K, Sato MH (2002) Vacuolar membrane dynamics revealed by GFP-AtVam3 fusion protein. Genes Cells **7:** 743–753

Vaughn MW, Harrington GN, Bush DR (2002) Sucrose-mediated transcriptional regulation of sucrose symporter activity in the phloem. Proceedings of the National Academy of Sciences, USA **99:** 10876-10880

Wang F, Sanz A, Brenner M, Smith A (1993) Sucrose Synthase, Starch Accumulation, and Tomato Fruit Sink Strength. Plant Physiology **101:** 321-327

Wang YS, Motes CM, Mohamalawari DR, Blancaflor EB (2004) Green fluorescent protein fusions to *Arabidopsis* fimbrin 1 for spatio-temporal imaging of F-actin dynamics in roots. Cell Motility and Cytoskeleton **59:** 79–93

Waters JC (2009) Accuracy and precision in quantitative fluorescence microscopy. The Journal of Cell Biology **185:** 1135-1148

Weber H, Borisjuk L, Wobus U (2005) Molecular physiology of legume seed development. Annual Review in Plant Biology **56:** 253–279

Weber H, Buchner P, Borisjuk L, Wobus U (1996) Sucrose metabolism during cotyledon development of *Vicia faba* L. is controlled by the concerted action of both sucrose-phosphate synthase and sucrose synthase: expression pattern, metabolic regulation and implications for seed development. Plant Journal **9:** 841–850

Weigel D, Glazebrook J (2002) *Arabidopsis*, A Laboratory Manual. Cold Spring Harbor Laboratory Press

Wienkoop S, Larrainzar E, Glinski M, González EM, Arrese-Igor C, Weckwerth W (2008) Absolute quantification of Medicago truncatula sucrose synthase isoforms and N-metabolism enzymes in symbiotic root nodules and the detection of novel nodule phosphoproteins by mass spectrometry. Journal of Experimental Botany **59:** 3307–3315

Winter H, Huber JL, Huber SC (1997) Membrane association of sucrose synthase: changes during the graviresponse and possible control by protein phosphorylation. FEBS Letters **420:** 151-155

Winter H, Huber SC (2000) Regulation of Sucrose Metabolism in Higher Plants: Localization and Regulation of Activity of Key Enzymes. Critical Reviews in Plant Sciences **19:** 31–67

Winter H, Huber SC (2000) Sucrose metabolism and the actin cytoskeleton: SUSY as actin-binding protein. Kluwer Academic Publishe, The Netherlands

Xu DP, Sung SJ, Loboda T, Kormanik PP, Black CC (1989) Plant Physiology **90:** 635–642

Yang J, Zhang J, Wang Z, Zhu Q (2001) Activities of starch hydrolytic enzymes and sucrose-phosphate synthase in the stems of rice subjected to water stress during grain filling. Journal of Experimental Botany **52:** 2169-2179

Yelle S, Chetelat RT, Dorais M, DeVerna JW, Bennett AB (1991) Sink metabolism in tomato fruit IV. Genetic and biochemical analysis of sucrose accumulation. Plant Physiology **95:** 1026–1035

Zhang XQ, Lund AA, Sarath G, Cerny RL, Roberts DM, Chollet R (1999) Soybean nodule sucrose synthase (Nodulin-100): Further analysis of its phosphorylation using recombinant and authentic root-nodule enzymes. Archives Biochemistry and Biophysics **371:** 70–82

Zhou H, Myburg AA, Berger DK (2005) Isolation and functional genetic analysis of Eucalyptus wood formation genes. University of Pretoria, Pretoria

Zinchuk V, Grossenbacher-Zinchuk O (2009) Recent advances in quantitative colocalization analysis: Focus on neuroscience. Progress in Histochemistry and Cytochemistry **44:** 125–172

Zourelidou M, de Torres-Zabala M, Smith C, Bevan MW (2002) Storekeeper defines a new class of plant-specific DNA-binding proteins and is a putative regulator of patatin expression. Plant Journal **30:** 489-497

Zrenner R, Salanoubat M, Willmitzer L, Sonnewald U (1995) Evidence of the crucial role of sucrose synthase for sink strength using transgenic potato plants (*Solanum tuberosum* L.). Plant Journal **7:** 97–107

CHAPTER 2

The subcellular localization of *Eucalyptus grandis* sucrose synthase 1 (EgSUSY1) fusion proteins expressed in *Arabidopsis thaliana*

Jamie-Lee Sauer, Sanushka Naidoo, Alexander A. Myburg

Department of Genetics, Forestry and Agricultural Biotechnology Institute (FABI), University of Pretoria, Pretoria, 0002, South Africa

---

This chapter has been prepared in the format of a manuscript for a peer-reviewed research journal. I performed all laboratory work and all analyses. Prof. A.A. Myburg provided funding, facilities and infrastructure at the University of Pretoria, Pretoria, South Africa. I wrote the manuscript with extensive suggestions on organization and content from Dr. S. Naidoo, Prof. D. Berger and Prof. A.A. Myburg.

2.1. Abstract

The temporal and spatial distribution of sucrose synthase in the cellular milieu has been found to influence the channelling of sucrose into specific sink processes such as cellulose biosynthesis and subsequently sink strength. Sucrose synthase catalyzes the formation UDP-glucose, the activated substrate for cellulose biosynthesis. In this study, we investigated the subcellular localization of a *Eucalyptus* sucrose synthase 1 (EgSUSY1) protein. We generated transgenic *Arabidopsis* plants that constitutively expressed unmodified and translationally modified *Eucalyptus* sucrose synthase (EgSUSY1) proteins fused to green fluorescent protein (GFP). Contradicting evidence has accumulated on the role of phosphorylation in the regulation of sucrose synthase subcellular localization and carbon allocation. Two modified EgSUSY1 transgenes (S11A and S11E) were engineered to investigate the effects of phosphorylation as a post-translational regulator of EgSUSY1 localization. The proteins' subcellular localization were analysed *in planta* using laser scanning confocal microscopy (LSCM). Findings in this study point to the peripheral localization of modified and unmodified EgSUSY1 proteins with a prominent cytoplasmic component. No evidence was found for the localization of modified or unmodified GFP-EgSUSY1 proteins within the extracellular matrix. Although there was qualitative colocalization evidence of EgSUSY1 association with the plasma membrane quantitative colocalization analysis could not establish nor negate plasma membrane association of any of the EgSUSY1 proteins.

2.2. Introduction

Plants are autotrophic organisms capable of synthesizing their own organic energy from inorganic resources via photosynthesis. This energy is typically transported through the phloem in the form of sucrose which is utilized in a number of metabolic processes throughout the plant. One of the sinks that sucrose is channeled into is cellulose biosynthesis (2004). Cellulose is an organic polymer that prominently occurs within the cell wall especially in the thick secondary cell walls found in vascular cells. This polymer aids to strengthen and support the cell wall and facilitates the movement of water in the plant to various organs such as the leaves, stems and flowers (Plomion et al., 2001). Cellulose is also widely exploited by humans in the form of wood, which forms the raw material for textiles, furniture, pulp and paper (Plomion et al., 2001). Recent fossil fuel shortages have triggered a renewed interest in wood as a possible form of renewable energy where the cellulose within wood can be broken down to form cellulosic ethanol. Wood is an attractive energy resource as it does not impede on food resources.

Sucrose synthase (SUSY) catalyzes the reversible conversion of UDP and sucrose to form fructose and UDP-glucose. This reaction allows sucrose via UDP-glucose and fructose to enter multiple cellular metabolic pathways (Winter and Huber, 2000). Furthermore SUSY gene family members may divert sucrose carbon to different sink tissues (Fu, 1995; Barratt, 2001; Matic, 2004). SUSY has been identified as a key enzyme associated with cell wall biosynthesis (Ruan, 1997; Chourey, 1998; Nakai, 1999; Salnikov, 2003; Curatti, 2008; Coleman et al., 2009), starch synthesis (De´jardin et al., 1997), and overall sink strength (Zrenner et al., 1995; Tang and Sturm, 1999). A recent study by Coleman and colleagues found that hybrid poplar trees overexpressing cotton SUSY presented with increased levels of

crystalline cellulose production. Thus identifying SUSY as a key candidate to alter sucrose carbon allocation into secondary metabolic processes such as cellulose biosynthesis.

SUSY was traditionally thought to occupy the cytosol, but Amor et al. (Amor et al., 1995) demonstrated that SUSY associates with the membrane fraction in cotton fibre cells. This association of SUSY with the cell membrane is proposed to reduce competition for activated glucose between cytosolic and cell wall related biosynthetic pathways (Haigler, 2001; Konishi, 2001; Salnikov, 2001) and also to ensure rapid turnover of UDP, which is known to be an feedback inhibitor of this process (Ross, 1991). The presence of two functional sucrose synthase isoforms, soluble SUSY (S-SUSY) and particulate SUSY (P-SUSY) has been postulated to play a regulatory role in the allocation of activated carbon to specific metabolic processes. S-SUSY is found soluble in the cytosol whilst the particulate isoform, P-SUSY, is associated with the cell membrane (Carlson et al., 2002). Where S-SUSY is responsible for directing UDP-glucose into the assimilation of the glycosidic pathway and secondary metabolite synthesis and P-SUSY is thought to play a role in the channelling of UDP-glucose specifically towards cellulose and callose biosynthesis (Amor et al., 1995; Ruan et al., 1997; Haigler et al., 2001).

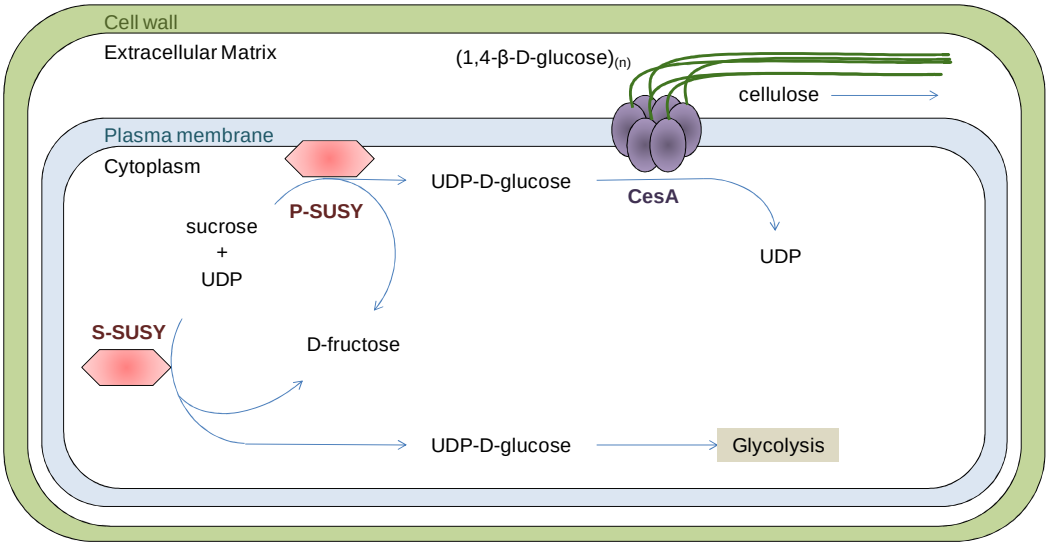

Figure 2.1. Schematic illustration of the functional regulation of sucrose synthase through subcellular compartmentation. Sucrose synthase predominantly occurs as a cytosol soluble S-SUSY where it can channel UDP-glucose towards glycolysis and other cytoplasmic processes. Plasma membrane bound P-SUSY has been proposed to direct UDP-glucose towards the hexameric cellulose synthase complex found traversing the plant cell membrane. UDP-glucose is then incorporated into the growing 1, 4-β-D-glucan chain found within the periplasmic space. Crystalline cellulose is deposited on the inner surface of the cell wall in the form of compact microfibrils. Illustration adapted from Haigler et al., 2001 and Salnikov et al., 2001.

The allocation of SUSY to these various subcellular sites is regulated by a number of processes including phosphorylation, sucrose concentration, oligomerization and tissue specificity (Hardin et al., 2004; Hardin et al., 2006; Duncan and Huber, 2007; Huber, 2007). Post translational regulation of sucrose synthase activity by phosphorylation occurs at numerous sites along the protein. The phosphorylation of SUSY at a non-catalytic N-terminal serine phosphorylation domain conserved among monocot and dicot species (Figure 2.9) has been proposed to be involved in the subcellular localization of this protein (Huber, 1996; Zhang et al., 1999). A number of studies have accumulated contradicting evidence alluding to the possible role of phosphorylation on the cellular distribution of SUSY. Anguenot et al. (2006) demonstrated that a protein kinase inhibitor increased the membrane activity of SUSY, whereas Winter et al. (1997) demonstrated decreased membrane activity of SUSY due the presence of a phosphatase inhibitor. A study Zhang et al. (1999) showed that phosphorylation of SUSY decreased its surface hydrophobicity resulting in a change in the conformation of the protein.

Studies involving the site-directed modification of this conserved serine phosphorylation site have resulted in altered properties of the SUSY protein. The modification of the N-terminal serine residue of the mung bean SUSY to a charged amino acid, glutamate (S11E, Nakai et al., 1998) was proposed to mimic the properties of the phosphorylated wild-type SUSY protein (Nakai, 1999; Konishi, 2004). Although S11E activity in transgenic poplar trees was demonstrated in both the membrane and the soluble fraction, there was a significant increase in activity in the soluble fraction of stem tissue

compared to the membrane fraction (Konishi, 2004). This is consistent with the suggestion that phosphorylation of SUSY specifically at the N-terminal serine residue may in part influence its sub-cellular localization by promoting cytosolic association.

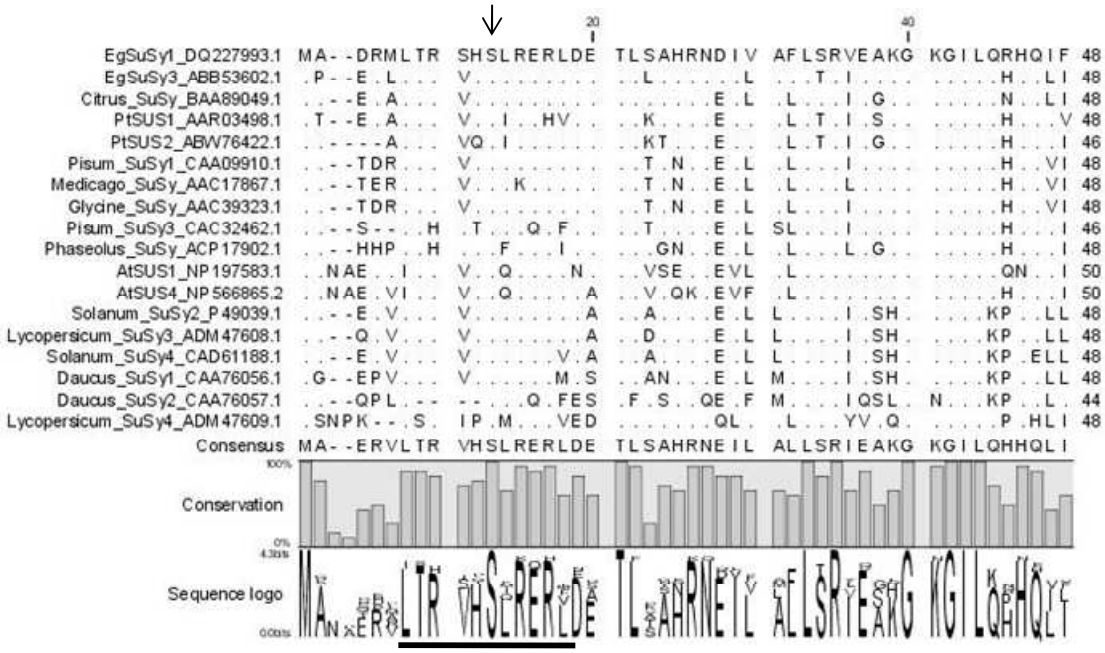

Figure 2.9. Amino acid alignment of 18 Dicot sucrose synthases, including EgSUSY1 (GenBank accession number DQ227993.1). All 18 sucrose synthases show a highly conserved N-terminal serine phosphorylation site (arrow) within the phosphorylation domain LTRVHSLRERL (Amor et al., 1995; Huber et al., 1996; Zhang et al., 1999; Komatsu et al., 2002). Alignment generated using CLC bio CLC Main Workbench 5.0.2. (·) indicates identical amino acid to EgSUSY1 and (–) a gap or the absence of an amino acid at this site.

The Myburg laboratory previously isolated two sucrose synthase genes, *EgSuSy1* and *EgSuSy3*, from immature xylem tissues of the forest tree species *Eucalyptus grandis*. Expression profiling of these genes revealed that both genes were predominantly expressed in xylem, immature xylem, mature flowers and young leaves. All of these tissues are characterized by high levels of primary cell wall deposition and, in mature xylem, secondary cell wall thickening. Quantitative real-time PCR showed that *EgSuSy1* had much higher expression levels than that of *EgSuSy3* (Zhou et al., 2005). Based on this evidence we hypothesised that *EgSuSy1* is the predominant gene responsible for the flux of sucrose

towards cellulose biosynthesis. The functional regulation of *EgSuSy1*, its cellular distribution and its involvement in cellulose biosynthesis is yet to be investigated.

This study characterized the cellular distribution of wild-type *Eucalyptus* sucrose synthase enzyme, EgSUSY1 and evaluated the role of its phosphorylation status on the subcellular localization of this enzyme when ectopically expressed in *Arabidopsis*. Two modified versions of this gene were examined EgSUSY1-S11A, with a phosphorylation insensitive alanine at the N-terminal serine residue, and EgSUSY1-S11E, with a positively charged glutamate at this site to mimic phosphorylation. These modified enzymes were translationally fused to green fluorescent protein (GFP) reporter gene and visualized *in vivo* using laser scanning confocal microscopy (LSCM). LSCM is a powerful tool for bioimaging proteins *in vivo* due to the availability of various spectral variants of fluorescent reporter proteins and subcellular markers. Confocal microscopy also allows for the direct real-time imaging of proteins *in vivo* without the need for destructive sample preparation steps (DeBlasio et al., 2010).

It was hypothesised that EgSUSY1-S11A would have putative increased cytosolic distribution towards the membrane fraction, due to the absence of a charged residue at S11. Whilst EgSUSY1-S11E would have increased association with the plasma membrane due to the negative charge of the glutamate residue. We showed that the *Arabidopsis* Col-0 plants overexpressing *wt-EgSuSy1, EgSuSy1-S11A and EgSuSy1-S11E* had recordable levels of GFP fluorescence. Wild-type EgSUSY1 was found to be associated with the cytoplasm with a strong concentration at the periphery of the cells suggesting either direct or indirect association with the plasma membrane. There were no quantitative differences in the cellular localizations of EgSUSY1-S11A and EgSUSY1-S11E and both were found to have similar localization patterns to that of wild-type EgSUSY1.

2.3. Materials and Methods

2.3.1. Biological Materials

Arabidopsis thaliana growth conditions

Arabidopsis thaliana L. Heynh. ecotype Columbia (Col-0 and Col-2) (Nottingham *Arabidopsis* Stock Centre) untransformed and transgenic lines were grown using standard *Arabidopsis* growth conditions. *Arabidopsis* Col-2 plants transformed with *PIP2a*-pEGAD were obtained from the ***Arabidopsis*** **Biological Resource Centre (**ABRC, Germplasm number CS84725) (Cutler et al., 2000). *Arabidopsis* Col-0 plants transformed with pCAMBIA1302 were kindly provided by Mr. M. Ranik (Table 2.3).

Table 2.3. Plant lines used during subcellular localization and immunoblotting studies.

Plant Line[a]	Description[b]
Col-0	Untransformed *Arabidopsis thaliana* Ecotype Col-0
GFP	*Arabidopsis* Col-0 transformed with pCAMBIA1302. Constitutive expression of mGFP6 under the action of a double cauliflower mosaic virus promoter
GFP-EgSUSY1	*Arabidopsis* Col-0 transformed with *EgSuSy1*-pMDC43. Constitutive expression of mGFP6-EgSUSY1 C-terminal[c] fusion under the action of a double cauliflower mosaic virus promoter
GFP-EgSUSY1-S11A (S11A)	*Arabidopsis* Col-0 transformed with *EgSuSy1-S11A*-pMDC43. Constitutive expression of mGFP6-EgSUSY1-S11A C-terminal[c] fusion under the action of a double cauliflower mosaic virus promoter
GFP-EgSUSY1-S11E (S11E)	*Arabidopsis* Col-0 transformed with *EgSuSy1-S11E*-pMDC43. Constitutive expression of mGFP6-EgSUSY1-S11E C-terminal[c] fusion under the action of a double cauliflower mosaic virus promoter
EgSUSY1-GFP	*Arabidopsis* Col-0 transformed with *EgSuSy1*-pMDC83. Constitutive expression of EgSUSY1-mGFP6 N-terminal[c] fusion under the action of a double cauliflower mosaic virus promoter
GFP-PIP2a (PIP2a)	*Arabidopsis* Col-2 transformed with *PIP2a*-pEGAD. Constitutive expression of PIP2a-eGFP C-terminal[c] fusion protein under the action of a double cauliflower mosaic virus promoter (Cutler et al., 2000)

a. The naming conventions of all wild-type, transgenic and marker *Arabidopsis* thaliana Columbia plant lines used during this research project

b. A brief description of each plant line indicating the genetic background of each plant line. The identity of the transgene and fluorophore as well as the orientation of the translational fusion.

c. Fusions were denoted as C-terminal or N-terminal based on the naming convention stipulated in (Cutler et al., 2000) where a C-terminal fusion is identified by the protein being translationally fused to the C-terminus of GFP and a N-terminal is identified by the protein being translationally fused to the N-terminus of GFP

Seeds were surface sterilized in 70% (v/v) ethanol for five minutes followed by 30 minute incubation in 10% (v/v) bleach solution containing 0.1% (v/v) tritonX. The seeds were then repeatedly washed followed by resuspension in 0.1% (w/v) bacteriological agar and plated on 90 mm plates containing a minimal plant growth media consisting of 0.7% (w/v) bacteriological agar and 1 mM potassium nitrate supplemented with 100 µg/ml cefotaxime. In addition 20 µg/ml hygromycin was added to the media for transgenic plants transformed with expression constructs. The seeds were incubated at 4°C for 48 hours and then at 22 to 25°C under a 16-hour day and 8-hour night cycle for ten to 12 days. *Arabidopsis* plants were fertilized weekly with multifeed-19:8:16 classic (http://www.plaaskem.co.za/). At the four leaf stage young seedlings were transferred to soil medium (http://www.jiffypot.com) and grown in a plant growth chamber at 22°C to 25°C with a 14-hour photoperiod (light exposure period).

Escherichia coli growth conditions

Two different *Escherichia coli* cell lines were used during the propagation of various vectors. *E.coli* DB3.1 cell lines were used to multiply empty pMDC43 and pMDC83 destination vectors (Curtis and Grossniklaus, 2003), whilst One Shot® chemically competent *E.coli* TOP10 cell lines (Invitrogen, Carisbad, California, USA) were used for the propagation of entry vectors and recombinant expression constructs. All cell lines were cultured in luria-bertani (LB) media [1% (w/v) tryptone, 0.5% (w/v) yeast extract, 1% (w/v) sodium chloride] for 48 hours at 37°C. For the propagation of recombinant entry vectors in TOP10 cells (Invitrogen), 100 µg/ml spectinomycin was supplemented in the culture media. *E.coli* DB3.1 cells containing destination vectors were propagated in LB-media supplemented with 20

µg/ml chloramphenicol. In addition 50 µg/ml kanamycin was added to the medium for propagation of *E.coli* TOP10 cell lines containing recombinant destination vectors.

Agrobacterium tumefaciens growth conditions

LBA4044 *Agrobacterium tumefaciens* strain was selected for floral dip transformation of *Arabidopsis* plants (Clough, 1998). Empty *A. tumefaciens* LBA4044 cells where propagated in preparation for transformation with recombinant destination vectors in yeast extract peptone (YEP) media [1% (w/v) yeast extract, 1% (w/v) bacto-peptone, 0.5% (w/v) sodium chloride] supplemented with 50 µg/ml rifampicin and 30 µg/ml streptomycin. Transformed cells were cultured prior to floral dipping in the same YEP-media with an additional 50 µg/ml kanamycin. All positive bacterial stocks were stored at -80°C in a 50% (v/v) glycerol stock.

2.3.2. Vector construction

Primer design and PCR amplification of full-length EgSuSy1

Primers were designed based on the cDNA sequence of the *Eucalyptus grandis* sucrose synthase 1 (*EgSuSy1)* gene (GenBank accession number DQ227993.1) identified and isolated by Zhou (2005). Three alternative primers were designed namely EgSUSY1_Stop, EgSUSY1_NoStop and EgSUSY1_Start (Table 2.4). The primers were used to amplify two 2 400 base-pair DNA fragments corresponding to the coding sequence (CDS) of *EgSuSy1*, with and without a stop codon, from *Eucalyptus grandis* x *urophylla* hybrid late tension wood cDNA samples (kindly provided by Mr. M. Ranik). The PCR reaction mixture included 0.8 units of ExSel *Taq* polymerase (Southern Cross Biotechnology Ltd.), 1X Reaction buffer (1X Exsel buffer, 20 mM $MgSO_4$), and 1200 ng of cDNA as template, 0.2 mM dNTPs and 0.4 µM of each primer in a 20 µl reaction volume. Touchdown PCR reactions were carried out using the following cycling parameters: one cycle of denaturing at 94°C for 5 min, ten cycles of

denaturing at 95°C for 30 sec, annealing at 65°C for 30 sec decreasing the temperature by 0.7°C with each cycle and extension at 72°C for two min, 30 cycles of denaturing at 95°C for 30 sec, annealing at 55°C for 30 sec and extension at 72°C for two min increasing the duration by one sec per cycle, followed by one cycle of extension at 72°C for 30 min. All PCR and RT-PCR reactions were carried out in a BioRad iCycler thermocycler (Bio-Rad, Hercules, California, USA). All PCR products were resolved on 1% (w/v) agarose gel stained with ethidium bromide via gel electrophoresis.

Table 2.4. Primers used during the cloning of *EgSuSy1* into GFP fusion binary vectors.

Primer Name	Gene	Primer Sequence (5' → 3')
EgSuSy1_Start[a,b]	*EgSuSy1*	ATGGCTGATCGCATGTTGAC
EgSuSy1_NoStop[a,b]	*EgSuSy1*	CTCGACAGCCGGAGGAACAG
EgSuSy1_Stop[a,b]	*EgSuSy1*	TTACTCGACAGCCGGAGGAA
EgSUSY1-138-R[b,c,d]	*EgSuSy1*	GTGTGGTTCATGGCGATGAG
EgSUSY1-396-F[b,c,d]	*EgSuSy1*	TGTGGCCAGCGCCTTGAGAA
SuSy_94R[b]	*EgSuSy1*	GAAGGCCACAATATCGTTGC
SUSY1SEQ1-486-F[b]	*EgSuSy1*	ATTGGCAATGGCGTCGAGTT
5'SUSY-GSP2-214[b,c,d]	*EgSuSy1*	GTCATGGAAGAGCTTAGCTTAGCGGAGAG
EuSUSY1-5'RACE209[b]	*EgSuSy1*	ATAGCCGGTTGAACGAAGAC
EgSuSy1_1813[b]	*EgSuSy1*	GTCGTGGTTGGAGGTGACAG
EgSuSy1_2283[b]	*EgSuSy1*	GAACCTGACTGCCGTGTATG
M13 F-Narrow[b]	Vector Backbone	CACGACGTTGTAAAACGAC
M13 R-Narrow[b]	Vector Backbone	GGAAACAGCTATGACCATG
mGFP5_36[c,d]	*mGFP6*	CACTGGAGTTGTCCCAATTC
mGFP5_322C[c,d]	*mGFP6*	CGTCGTCCTTGAAGAAGATG
eGFP_283[c,d]	*eGFP* and *mGFP6*	CAGGAGCGCACCATCTTCTT
eGFP_647C[c,d]	*eGFP*	CGCTTCTCGTTGGGGTCTTT
ACT2-48-F[d]	*AtActin2*	TCTCGTTGTCCTCCTCACTT
ACT2-289-R[d]	*AtActin2*	AATCCAGCCTTCACCATACC
UBQ-F[d]	*AtUbiquitin*	CCGGATCAGCAGAGGCTTAT
UBQ-R[d]	*AtUbiquitin*	CACGGAGCCTGAGAACAAGA

a. Oligonucleotide primers used for the amplification of *EgSuSy1* full-length gene fragments

b. Oligonucleotide primers used to screen and sequence recombinant entry vectors carrying full-length *EgSuSy1* gene fragments. Primer binding sites are indicated in Supplemental Figure S2.

c. Oligonucleotide primers used to screen and sequence recombinant destination vectors. Primer binding sites are indicated in Supplemental Figure S5.

d. Oligonucleotide primers used during PCR and RT-PCR screening of transgenic *Arabidopsis* plants

TA- cloning into TOPO donor vector and sequence analysis of entry clones

The amplified *EgSuSy1* CDS fragments (*EgSuSy1Stop* and *EgSuSy1NoStop*) were excised and purified from the 1% (w/v) agarose gel using the PCR Purification Kit (Qiagen, Hilden, Germany) following the manufacturer's instructions. The fragments were TA-cloned into the TOPO donor vector pCR®8/GW/TOPO® (Figure S1, Invitrogen) as per the manufacturer's instructions. The recombinant *EgSuSy1*-pCR®8/GW/TOPO® entry vectors were transformed into One Shot® TOP10 chemically competent *E. coli* cells (Invitrogen) as per the manufacturer's instructions.

Colony screening was performed on plates containing 1.5% (w/v) agar-LB medium supplemented with 100 µg/ml spectinomycin. Putative positive colonies were selected for colony PCR verification of inserted *EgSuSy1*-pCR®8/GW/TOPO® entry vectors. A 380 base-pair *EgSuSy1* fragment was amplified using primers EgSUSY1-138-R and EgSUSY1-396-F. The PCR reaction mixture included 0.8 units of ExSel *Taq* polymerase (Southern Cross Biotechnology Ltd.), 1X reaction buffer (1X Exsel buffer, 20 mM $MgSO_4$), 0.2 mM dNTPs, 0.4 µM of each primer and DNA as template in a 20 µl reaction volume. Standard PCR reactions were carried out using the following cycling parameters: 1 cycle of denaturing at 94°C for 1 min, 32 cycles of denaturing at 94°C for 30 sec, annealing at 55°C for 30 sec and extension at 72°C for 1 min, followed by one cycle of extension at 72°C for 5 min.

E. coli transformants containing recombinant plasmids were cultured in LB- medium supplemented with 100 µg/ml spectinomycin. Plasmid DNA was isolated using a GeneJet™ Plasmid Miniprep Kit (Fermentas). To determine the orientation of *EgSuSy1* transgenes, recombinant *EgSuSy1*-pCR®8/GW/TOPO® were double digested with *Eco*RV (Roche) and

*Sac*I (Roche) restriction endonucleases according to manufacturer's instructions. Recombinant plasmids were sequenced (Macrogen, USA) using the primers listed in Table 2.4 to ensure that the sequence integrity of inserted *EgSuSy1* transgenes. Sequences were aligned and analysed using CLC Bio and BioEdit Sequence Alignment Editor (Tom Hall) software.

LR-recombination of EgSuSy1 into Gateway compatible destination vectors and sequence analysis of expression clones.

The Gateway® compatible pMDC43 and pMDC83 (Figure S3) destination vectors, with double 35S cauliflower mosaic virus (CaMV) constitutive promoter driven expression of C-terminal and N-terminal Green Fluorescent protein (GFP) fusions were chosen for expression of transgenes in *Arabidopsis* plants (Curtis and Grossniklaus, 2003). A C-terminal fusion arises through the in-frame insertion of the transgene on the C-terminus of *mGFP6* in pMDC43. Similarly, an N-terminal fusion arises through the in frame insertion of the transgene on the N-terminus of mGFP6 in pMDC43. To generate *EgSuSy1*-GFP translational fusions, LR-recombination was performed between *EgSuSy1*-pCR®8/GW/TOPO® entry plasmids and the destination vectors pMDC43 and pMDC83 (Curtis and Grossniklaus, 2003). The LR-recombination reaction is schematically illustrated in Figure 2.2.3. LR-recombination was performed using the Gateway® LR Clonase™ Enzyme Mix (Invitrogen) and a 3:1 insert-to-vector molar ratio as per the kit manual. Vector maps of the resulting recombinant destination vectors are schematically represented in Supplemental Figure S4. The entire reaction mix was subsequently used to transform One Shot® TOP10 chemically competent *E. coli* cells (Invitrogen) as per manufacturer's instructions. Colony screening was performed on selective 1.5% (w/v) agar-LB medium supplemented with 50 µg/ml kanamycin.

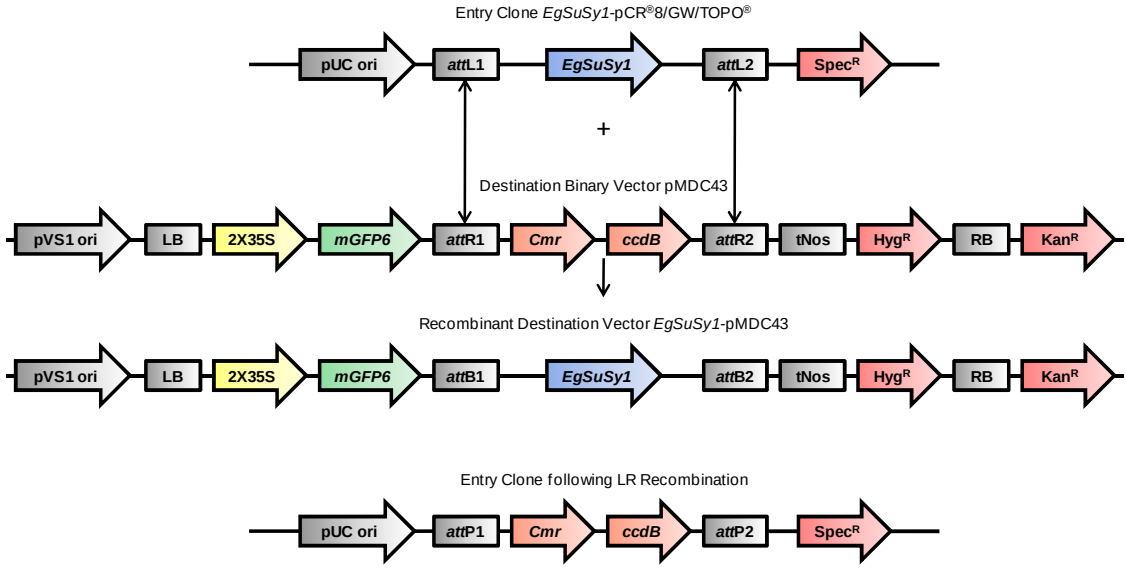

Figure 2.2.3. Schematic representation of the Gateway® cloning (Invitrogen Co.) reaction used to produce EgSUSY1-mGFP6 fusion expression constructs. Gateway® cloning involved a two-step process where the initial step was to insert the transgene (*EgSuSy1*) into an entry vector (pCR®8/GW/TOPO®) via TA-cloning. In the entry clone (*EgSuSy1*- pCR®8/GW/TOPO®) the transgene (*EgSuSy1*) is flanked by two recombination sites attL1 and attL2. The Gateway compatible destination vector (pMDC43) contains corresponding attR1 and attR2 sites flanking the ccdB and Cmr genes. The Cmr gene encodes for chloramphenicol resistance whilst the ccdB gene encodes a protein which interferes with *E. coli* DNA gyrase and inhibits growth of most *E. coli* strains, e.g. TOP10 and DH5α™ (Bernard and Couturier, 1992). The second step involves recombination between the attL and attR sites thus facilitating the exchange of DNA fragments between these sites in the presence of the enzyme LR clonase. During recombination new attB1 and attB2 as well as attP1 and attP2 are formed on the recombinant destination vector and entry vector respectively. pUC ori: Origin of replication for *E. coli*. pVS1 ori: Origin of replication for *Agrobacteria*. 2X35S: Double Cauliflower mosaic virus promoter. Spec^R: Spectinomycin resistance gene Kan^R: Kanamycin resistance gene. RB: T-DNA right border. LB: T-DNA left border. *att*L, *att*R, *att*B, *att*P: recombination sites. Schematic adapted from Xu and Quinn (2008)

E. coli transformants identified by screening were cultured and plasmid DNA isolated as described above. Plasmids were screened for the presence of the integrated *EgSuSy1* fragments by double digesting the recombinant plasmids with *Asc*I (New England Biolabs, NEB) and *Sac*I (NEB) restriction endonucleases as per manufacturer's instructions. Additional vector (*mGFP6*, Haseloff et al. , 1999) , *EgSuSy1* and linker-specific regions were PCR amplified to further screen destination vectors (Table 2.5). To verify the sequence integrity of the linker region between *EgSuSy1* and m*GF6P*, recombinant plasmids were sequenced (Macrogen USA) using primers 5'SUSY-GSP2-214 for *EgSuSy1*-pMDC43

expression constructs and mGFP5_322C for *EgSuSy1*-pMDC83 expression constructs (Table 2.4). Sequences were aligned and analysed as described above.

Table 2.5. Vector, *EgSuSy1* and linker-specific regions PCR amplified during screening of recombinant destination vectors and transgenic *Arabidopsis* plants.

Region[a]	Fragment Size (Base-pairs)[b]	Primers[c]
Vector (*mGFP6*)	287	mGFP5_36 mGFP5_322C
Transgene (*EgSuSy1*)	380	EgSUSY1-396-F EgSUSY1-138-R
pMDC43 Linker	1005	eGFP_283 5'SUSY-GSP2-214
pMDC83 Linker	1771	EgSUSY1-396-F mGFP5_322C

a. The identity of the region amplified by the respective primers.
b. The expected size of the amplified region of true transformants where the transgene is in the correct orientation.
c. The primers used to amplify the indicated region. Oligonucleotide primers sequences found in Table II and primer binding sites in Supplemental Figure S5.

2.3.3. *Agrobacterium* transformation of *Arabidopsis* plants

Chemically competent *Agrobacterium* cells were prepared by centrifuging 50 ml aliquots of mid-log phase cultures for 15 minutes at 3000 x *g* and resuspending the pellet in 1 ml ice-cold $CaCl_2$. The solution was aliquoted in 100 µl volumes and rapidly frozen in liquid nitrogen. Recombinant expression vectors were transformed into chemically competent LBA4404 *Agrobacterium tumefaciens* cells. This procedure included aliquoting 3 µg of vector DNA onto 100 µl of frozen competent LBA4404 cells. The DNA-bacteria mixture was then incubated in a 37°C waterbath for 5 minutes followed by resuspension and a further incubation at 28°C with shaking for 4 hours. Thereafter the culture was centrifuged at 12 000 x *g* for one minute and the resulting pellet was resuspended in 50 µl YEP medium. Colony screening was performed on 1.5 % (w/v) YEP-agar medium supplemented with 50 µg/ml

kanamycin, 50 µg/ml rifampicin and 30 µg/ml streptomycin. Putative positive *Agrobacterium* transformants were screened through colony PCR amplification of a 380 base-pair *EgSuSy1* fragment using the primers EgSUSY1-138-R and EgSUSY1-396-F (Table 2.4).

Positive *Agrobacterium* transformants were cultured as described above and the *EgSuSy1* specific screening PCR was repeated to ensure that *Agrobacterium* remained recombinant for expression constructs. Positive overnight cultures were used to inoculate four 250 ml flasks of YEP medium supplemented with antibiotics. The resulting cultures were incubated at 28°C for three days with shaking at 250 rpm until cultures reached a log growth phase after which cultures were centrifuged at 5000 ×*g* for 20 min. Pelleted cells were resuspended in a 5% (w/v) sucrose (Sigma) solution to an OD_{600} of 1.0 (NanoDrop® ND-1000 spectrophotometer). Prior to dipping *Arabidopsis* Col-0 inflorescence stems, 0.05% (v/v) of surfactant, Silwett L-77 (LETHEL, Round Rock, U.S.A.) was added.

Dipping was performed as per Clough and Bent (1998) and was repeated after seven days to increase the transformation efficiency. In brief: *Arabidopsis* seedlings were propagated for two weeks on soil Jiffy® pots (http://www.jiffypot.com). After two weeks all inflorescence stems were cut to synchronise flower development. Approximately one week later when all plants had immature flowers, dipping commenced. Dipping involved submersing *Arabidopsis* inflorescence stems in the *Agrobacteria* mixture for 30 seconds with gentle agitation. The plants were then placed horizontally in a humid, dark environment overnight. Hereafter plants were grown under standard conditions until maturation of siliques at which time T1 seeds were collected.

2.3.4. Analysis of transgenic plants

T1 seeds were dried at room temperature for one week followed by sieving and sterilization as described above. Seeds were selectively grown on 0.8% (w/v) agar plates containing 1 mM (w/v) KNO_3 and 20 µg/ml hygromycin. Putative positive seedlings were transplanted to Jiffy® pots (http://www.jiffypot.com) and propagated under controlled conditions. Plants were allowed to self-pollinate and T2 seed were collected once silique maturation had commenced. GFP-PIP2a transgenic plants were grown on nonselective minimal media and transplanted directly onto Jiffy® pots. Two weeks after transplanting, GFP-PIP2a plants were selectively screened by spraying leaf surfaces with 230 µM (v/v) BASTA (phosphinothricin-3-D-glufosinate ammonium in detergent) three times every 48 hours. Surviving plants that showed no wilting or chlorosis of the leaves were transplanted to Jiffy® pots and propagated under controlled conditions.

Putative positively transformed plants were screened for integration of the T-DNA into the plant genome through a series of PCRs. At two weeks post transplantation, leaf samples were collected for genomic DNA isolation. Genomic DNA was isolated from leaf samples by homogenizing samples in a FastPrep FP120 followed by extraction using the NucleoSpin III Plant DNA Extraction Kit (Machery-Nagel, Düren, Germany) as per manufacturer's instructions. Transgenic plant lines were screened with a multiplex PCR amplifying the *Arabidopsis Actin2* (GenBank accession number AT3G18780.1) internal control fragment of 700 base-pairs, using primers ACT2-48-F and ACT2-289-R, and a 286 base-pair *mGFP6* fragment, amplified by primers mGFP5_36 and mGFP5_322C (Table 2.4). Multiplex PCR reactions were carried out using the following cycling parameters: 1 cycle of denaturing at 94°C for 1 min, 32 cycles of denaturing at 94°C for 30 sec, annealing at 55°C for 30 sec and extension at 72°C for 2 min, followed by one cycle of extension at 72°C for 5

min. The PCR reaction mixture included 0.8 units of ExSel *Taq* polymerase (Southern Cross Biotechnology Ltd.), 1X reaction buffer (1X Exsel buffer, 20 mM $MgSO_4$), and 1200 ng of cDNA as template, 0.2 mM dNTPs and 0.4 µM of each primer in a 20 µl reaction volume. To ascertain wether plant lines were positive transformants for the EgSUSY1-GFP expression constructs an additional PCR was perfomed to amplify a 380 base-pair *EgSuSy1* fragment using primers EgSUSY1-396-F and EgSUSY1-138-R. PIP2a-GFP plants were screened for the presence of PIP2a-pEGAD expression constructs by the PCR amplification of a 365 base-pair *eGFP* (GenBank accession number 255710028) fragment using primers eGFP_283 and eGFP_647C (Table 2.4). T1 plants confirmed to contain the T-DNA insert with an intact *EgSuSy1* transgene were advanced to T2. The above mentioned PCR screens were repeated on subsequent T2 to Tn generations to ensure integrity of the inserted T-DNA in the plant genome.

2.3.5. Reverse transcription PCR analysis

Plants were propagated for six weeks prior to tissue sampling for RNA isolation. At six weeks the above ground organs of four plants per line were collected and immediately ground in liquid nitrogen and stored at -80°C. Total RNA was isolated using the NucleoSpin® RNA Plant extraction kit (Machery-Nagel, Düren, Germany) as per manufacturer's instructions. This kit has an incorporated DNase digestion step to ensure that RNA samples are DNA free.

Isolated total RNA was used to synthesise first strand cDNA using Improm-II™ Reverse Transcriptase (Invitrogen) according to the manufacturer's guidelines. The resulting cDNA was screened for contaminating DNA through the amplification of an intron spanning *UBIQUITIN 10* (GenBank accession number AT4G05320.1) gene fragment. Amplification of a single 580bp fragment indicated pure cDNA. Genomic DNA contamination would be

indicated by an additional larger fragment of 920 base-pairs. Samples contaminated with genomic DNA were passed through a second DNase digestion step and rescreened prior to RT-PCR.

To ensure that transgenic plant lines contain an integrated fully transcribed expression construct, vector, *EgSuSy1* and linker specific RT-PCRs were performed (Table 2.5). The following cycling parameters were used for RT-PCRs: 1 cycle of denaturing at 94°C for 1 min, 32 cycles of denaturing at 94°C for 30 sec, annealing at 55°C for 30 sec and extension at 72°C for 2 min, followed by one cycle of extension at 72°C for 5 min. To verify the sequence integrity of the linker region between *EgSuSy1* and *GFP*, positive transformants were sequenced (Macrogen USA) using primers 5'SUSY-GSP2-214 for GFP-*EgSuSy1* (C-terminal fusions) transgenic plant lines and mGFP5_322C for *EgSuSy1*-GFP (N-terminal fusions) transgenic plant lines.

2.3.6. Confocal microscopy analysis and imaging

Live plant specimens were imaged using an inverted LSM710 META Laser Scanning Confocal Microscope (CLSM, Zeiss) equipped with an LCl Plan-Neofluar 63x/1.3 Imm Korr DIC (Zeiss) water immersion objective and an Argon ion laser source (Zeiss). *Arabidopsis* seedlings were grown on minimal growth agar plates for 6 days prior to imaging. Intact plants or sectioned plant organs were placed on glass slides, immersed in distilled water and gently covered with a coverslip. Coverslips were secured in place using non-reactive dental wax (Cavex® set up modelling wax, Dental Wax). Membrane staining was done prior to slide preparation and involved suspending seedlings in 8.2 µM FM4-64 (SynaptoRed™, Sigma) solution for 15 minutes (Speth et al., 2009). Seedlings were then rinsed with distilled water and prepared for imaging. Preparation of plasmolysed cells involved incubating seedlings in

1M KNO_3 for 5 min. Plasmolysed seedlings were then placed on slides immersed in a 1M KNO_3 solution and imaged immediately.

Three plant lines were obtained for use as imaging controls (Table 2.3). Untransformed *Arabidopsis thaliana* Col-0 was used as a negative control for GFP fluorescence and for determining the range of autofluorescence. GFP-PIP2a plant line (ABRC: Q8, Germplasm stock CS84723, Cutler et al., 2000) was used as a membrane localisation positive control. The 35S::GFP line (Col-0 transformed with pCAMBIA 1302), kindly donated by Mr. M. Ranik was used as a free GFP control.

For GFP fluorescence and autofluorescence analysis, the 488 nm excitation line of the argon ion laser was used with a 505 nm to 530 nm band-pass emission filter. FM4-64 and chloroplast autofluorescence imaging was performed by exciting samples with a 488 nm excitation line and capturing fluorescence signals with a 601 nm to 757 nm band-pass emission filters. Colocalization of FM4-64 membrane staining and GFP fusions was performed through the sequential scanning of FM4-64 stained leaf epidermal cells excited by a 488 nm Argon laser line and capturing a z-stack of GFP fluorescence, collected with a 505- to 530-nm band-pass filter, and FM4-64 fluorescence, collected with a 615-nm long-pass filter (Supplemental Figure SP4). Image stacks were passed through a Manders Coefficients Plugin (Manders et al., 1993) in the ImageJ public domain image processing software (http://rsbinfo.nih.gov.ij/) to calculate colocalization coefficients and create scatter plots. Time series were taken of single focal planes subtending hypocotyl stems over a period of 11 seconds at 0.3 second intervals.

Digital images were captured and prepared as graphics using Zeiss LSM Image Browser version 4.2.0.121 software and ImageJ public domain image processing software (http://rsbinfo.nih.gov.ij/). Computational prediction of the subcellular localization of

EgSUSY1-GFP fusions based on amino acid sequence was determined using YLoc, an interpretable web server for predicting subcellular localization (www.multiloc.org/YLoc, Briesemeister at al., 2010, 2010).

2.3.7. Protein extraction and subcellular fractionation

Total proteins were extracted by grinding approximately 500 mg (fresh weight) of fresh or frozen *Arabidopsis* leaf tissue with a pestle and mortar in the presence of 1 ml of Hypotonic Buffer [0.1 M Tris- HCl, 10mM $MgCl_2$, pH8.0 and Protease Inhibitor Cocktail (Roche)]. Samples were incubated on ice for 15 minutes and centrifuged for 10 min at 1000xg at 4°C to remove debris. To separate soluble and membrane fractions the resultant supernatant was centrifuged (Beckman Ultracentrifuge) at 100 000xg for one hour at 4°C in a SW55Ti rotor (Beckman). The resultant supernatant constituting the soluble fraction was acetone precipitated by incubating in four volumes of ice cold acetone at -70°C for an hour and centrifuging at 15 000xg for 20 minutes at 4°C. The soluble fraction pellet and the 100 000xg pellet constituting the membrane fraction where resupended in 1X protein buffered saline (PBS, 137 mM NaCl, 2.7 mM KCl, 4.3 mM Na2HPO4.7H2O, 1.4 mM KH2PO4; pH 7.3) prior to analysis via sodium dodecyl sulphate (SDS) polyacrylamide gel electrophoresis (PAGE).

2.3.8. SDS polyacrylamide gel electrophoresis

Proteins were visualised by SDS-PAGE under denaturing conditions as described by Sambrook and Russel (2001). This method separates the proteins based on their molecular size. The sizes of the heterologously expressed proteins were determined by depositing amino acid sequence data for the proteins into the ProtParam tool of the ExPASy Proteomics Server, Swiss Institute of Bioinformatics (http://au.expasy.org, Gasteiger at al., 2005). Protein

samples were denatured prior to gel electrophoresis by mixing samples (v/v) in 2X protein solvent buffer (PSB, 4% (v/v) SDS, 20% (v/v) Glycerol, 10% (v/v) 2-mercaptoethanol, 0.005% (w/v) Bromophenol Blue, 0.125% (w/v) Tris-HCl, pH 6.8) and heating at 95°C for 5 min. Equal volumes of each sample were resolved using SDS-PAGE on a 12% separating gel [12% (v/v) polyacrylamide, 0.375M Tris-HCl, pH8.8, 0.1% SDS, 0.01% (v/v) TEMED, 0.1% (v/v) ammonium persulphate] and a 5% stacking gel [5% (v/v) polyacrylamide, 0.125M Tris-HCl, pH8.8, 0.1% SDS, 0.01% (v/v) TEMED, 0.1% (v/v) ammonium persulphate]. PageRulerTM prestained protein ladder (Fermentas, Catalog No. SM0671) was used as a protein molecular weight standard. Gels were run in 1X TGS buffer (0.3% tris; 1.44% glycine, 0.1% SDS) in the Hoefer^{TM} II SE 250 mini-vertical gel electrophoresis unit (Amersham Biosciences) at 130V for three hours. Protein gels were either used in immunoblots or immediately stained with coomassie blue staining solution [0.125% (w/v) coomassie blue, 50% (v/v) methanol, 10% (v/v) acetic acid] followed by destaining overnight in destain solution [5% (v/v) methanol, 5% (v/v) acetic acid].

2.3.9. Immunoblotting

For immunoblotting, proteins were transferred from polyacrylamide gels to Hybond-C Extra nitrocellulose membranes (Amersham Biosciences, Cat no. RPN303E) in semi-dry transfer buffer [0.025 M Tris, 0.15 M Glycine, 20% (v/v) Methanol, pH 8.3]. Blots were rinsed with 1X PBS and incubated with blocking solution [1% (w/v) non-fat milk powder, 1X PBS] for one hour to block any non-specific binding sites. The membranes were then incubated in Ant-GFP N-terminal primary antibody (Sigma, Cat no. G1544 100UG, raised in rabbit, diluted to 1 in 4000 in blocking solution) at room temperature overnight. Blots were rinsed repeatedly with wash buffer [0.05% (v/v) tween in 1X PBS] and reacted with protein A peroxidase conjugated anti-rabbit IgG secondary antibody (Calbiochem, Cat no. 539 253,

diluted to 1 in 10 000 in blocking solution) for an hour. Blots were rinsed repeatedly with wash buffer and finally with 1X PBS for five minutes each. Localization of the immune complex was achieved by incubating the blot in horseradish peroxidise substrate (60 mg 4-chloro-1-naphthol, BIO-RAD, Cat no. 170-6534 in 20 ml ice-cold methanol mixed just prior to use with 60 µl hydrogen peroxide in 100 ml 1X PBS). The membrane was then washed with distilled water and allowed to air dry. A mammalian SF9 protein sample containing constitutively expressed free eGFP (Gift of Miss S. L. Ungerer) was used as a positive control for immunoblotting.

2.4. Results

2.4.1. Genetic engineering of transgenic *Arabidopsis* plants

Cloning EgSuSy1 into entry vector and screening of recombinant clones

Two *EgSuSy1* fragments were successfully amplified from *Eucalyptus grandis x urophylla* immature xylem cDNA. The first fragment, *EgSuSy1-Stop*, included the complete 2418bp *EgSuSy1* CDS ending in a 3' stop codon. The second fragment *EgSuSy1-NoStop* lacked the 3' stop codon and was thus 2415bp in size. These *EgSuSy1* PCR fragments were resolved on an agarose gel, excised and purified (Figure 2.10). Purified *EgSuSy1* fragments were then TA-cloned into pCR®8/GW/TOPO® (Invitrogen) entry vectors and recombinant entry vectors (*EgSuSy1-Stop*-pCR®8/GW/TOPO® and *EgSuSy1-NoStop*-pCR®8/GW/TOPO®) were transformed into competent TOP10 *E.coli* cells (Invitrogen). Two recombinant entry clones containing modified *EgSuSy1* transgenes, *EgSuSy1-S11A* and *EgSuSy1-S11E*, were provided by Mr. M. M. Mphahlele (MSc. Study, University of Pretoria). *EgSuSy1-S11A* is a 2418bp *EgSuSy1* CDS fragment with a codon specific modification of the 11th serine codon to an alanine codon (Figure 2.11). EgSuSy*1-S11E* is a 2418bp *EgSuSy1*

CDS fragment with a codon specific modification of the 11th serine codon to a glutamate codon (Figure 2.11). The presence of the full-length modified *EgSuSy1* transgenes in recombinant entry vectors was established through amplification of a 2418bp fragment corresponding to the full-length *EgSuSy1* CDS (Figure 2.12).

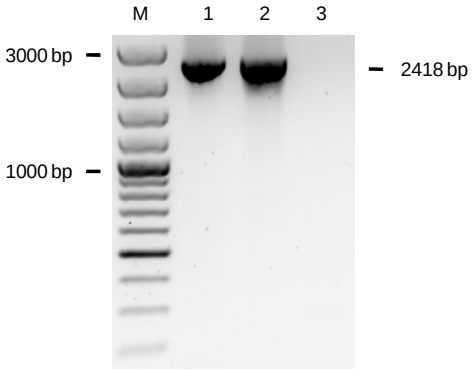

Figure 2.10. *EgSuSy1* gene fragments amplified from *Eucalyptus* cDNA. Lane 1 contains the 2415bp *EgSuSy1* gene fragment lacking a stop codon (*EgSuSy1-NoStop*) amplified using primers EgSuSy1_Start and EgSuSy1_NoStop. Lane 2 contains the 2418bp *EgSuSy1* gene fragment with a stop codon (*EgSuSy1-Stop)* amplified using the EgSuSy1_Start and EgSuSy1_Stop primer pair. Lane 3 contains a distilled water negative control for the PCR. M is a 100 bp DNA size standard (Fermentas).

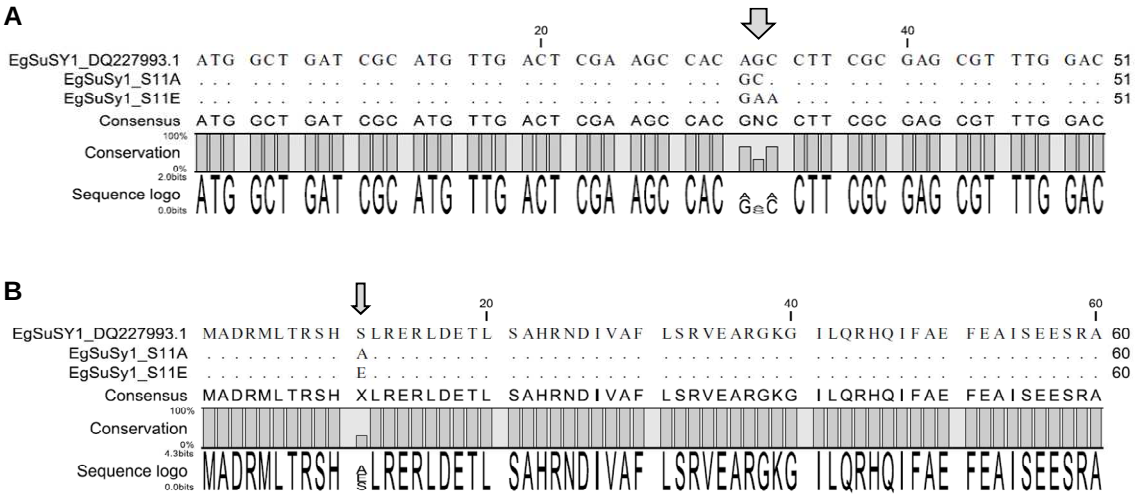

Figure 2.11. The 5' DNA and protein sequence corresponding to N-terminal phosphorylation domain of *EgSuSy1*, *EgSuSy1-S11A* and *EgSuSy1-S11E*. Indicated by an arrow is the eleventh serine modification site showing the conversion to an alanine residue in EgSUSY1-S11A and a glutamine

residue in EgSUSY1-S11E. Alignment A shows the nucleotide modifications, while alignment B shows the corresponding amino acid modifications.

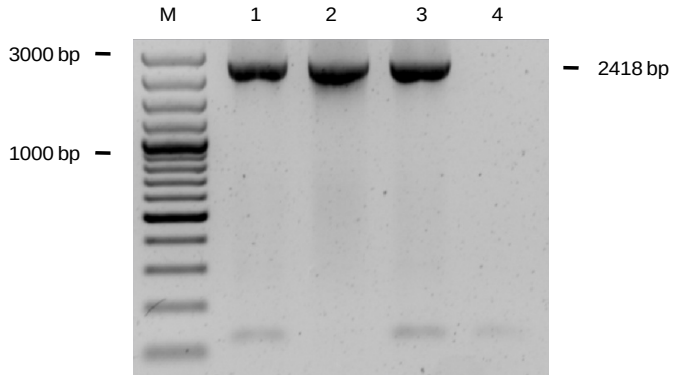

Figure 2.12. PCR amplification of full length *EgSuSy1* gene fragments to confirm the presence of modified *EgSuSy1* fragments in recombinant *EgSuSy1*-pCR®8/GW/TOPO® entry vectors kindly received from Mr. M. M. Mphahlele. Lane 1 contains *EgSuSy1-S11A* gene fragment. Lane 2 contains *EgSuSy1-S11E* gene fragment. Lane M is a 100bp DNA size standard (Fermentas). Lane 3 is the amplification of unmodified *EgSuSy1* from *Eucalyptus* cDNA as a positive size control. Lane 4 contains a distilled water negative control for the PCR.

Recombinant *EgSuSy1*-pCR®8/GW/TOPO® clones were screened through colony PCR amplification of a 380bp *EgSuSy1* fragment (Figure 2.14.). To determine the orientation of the inserted *EgSuSy1* transgene, recombinant entry clones were double digested with restriction endonucleases *Eco*RV and *Sac*I and excised fragments were resolved on an agarose gel (Figure 2.15.). A 584bp excised fragment was expected if the *EgSuSy1* transgene was in the sense orientation and a 2094bp excised fragment in the antisense orientation. Two *EgSuSy1-NoStop*- pCR®8/GW/TOPO® clones (N22 and N28) and three *EgSuSy1-Stop*- pCR®8/GW/TOPO® clones (S2, S4 and S6) were found to contain the *EgSuSy1* transgene in the correct sense orientation.

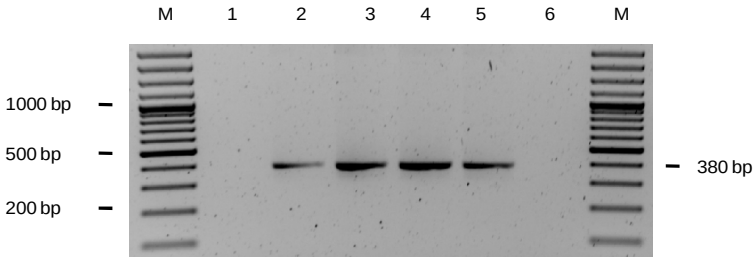

Figure 2.13. Colony PCR products amplified from *EgSuSy1*- pCR®8/GW/TOPO® modified and unmodified entry vectors. A 380bp *EgSuSy1* fragment was amplified as evidence of successful insertion of *EgSuSy1* coding sequences (CDS) into the pCR8/GW/TOPO entry vector using primers EgSUSY1-138-R and EgSUSY1-396-F. Lane 1 shows the absence of a 380bp amplified product from empty pCR8/GW/TOPO. Lane 2 to 5 shows successful amplification of the gene fragment from *EgSuSy1-NoStop*- pCR®8/GW/TOPO® (Lane 2), *EgSuSy1-Stop*-pCR®8/GW/TOPO® (Lane 3), *EgSuSy1-S11A*-pCR®8/GW/TOPO® (Lane 4) and *EgSuSy1-S11E*-pCR®8/GW/TOPO® (Lane 5). Lane 6 contains a distilled water negative control for the PCR. Lane M is a 100bp DNA size standard (Fermentas)

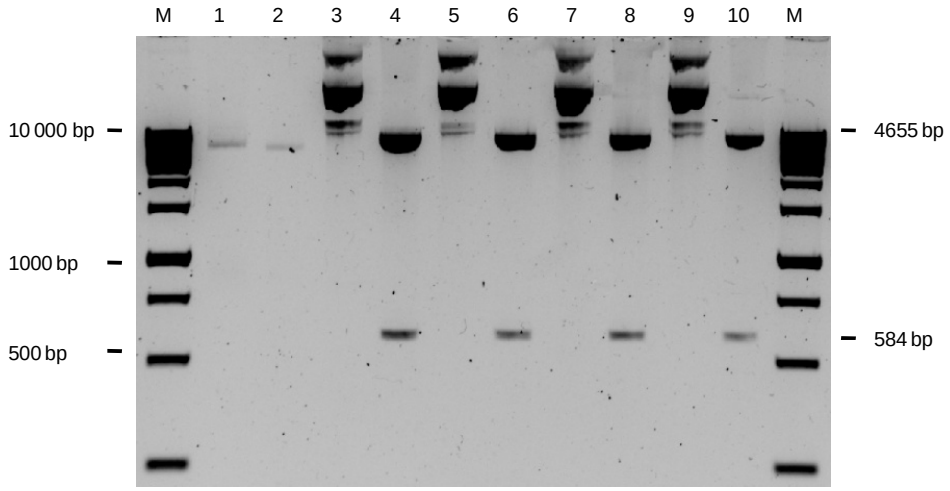

Figure 2.14. *Sac*I and *Eco*RV restriction endonuclease digestion of recombinant entry vectors to confirm insertion and orientation of *EgSuSy1* CDS in pCR8/GW/TOPO. A 584bp excised fragment was expected if the *EgSuSy1* transgene was in the sense orientation and a 2094bp excised fragment in the antisense orientation. Odd lanes represent undigested products whilst even lanes represent the corresponding double digested products. Lane 1 and 2 contains empty pCR8/GW/TOPO while Lanes 3 to 10 show successful excision of the 584bp fragment from *EgSuSy1-NoStop*-pCR®8/GW/TOPO® (Lane 3 and 4), *EgSuSy1-Stop*-pCR®8/GW/TOPO® (Lane 5 and 6), *EgSuSy1-S11A*-pCR®8/GW/TOPO® (Lane 7 and 8) and *EgSuSy1-S11E*-pCR®8/GW/TOPO® (Lane 9 and 10). Lane M is a 1kbp DNA size standard (Fermentas).

Full-length sequence analysis of the positive EgSuSy1- pCR®8/GW/TOPO® clones including the modified EgSuSy1- S11A and EgSuSy1- S11E entry clones confirmed the integrity of the serine codon modifications but also revealed several background PCR induced bp changes (Supplemental Figure S6). Translation of the consensus sequences of the entry clones identified a number of nonsynonymous mutations. None of these were nonsense mutations (Supplemental Figure S7). Nonsynonymous mutations were analyzed for physiochemical differences compared to the original protein (Supplemental Figure S8), conservation (Supplemental Figure S9 and S10) and effect on in silico secondary structure predictions (Supplemental Figure S11 and Table S1). Based on these findings, EgSuSy1-NoStop-pCR®8/GW/TOPO® clone N22, EgSuSy1-Stop- pCR®8/GW/TOPO® clone S6 and modified EgSuSy1- S11A and EgSuSy1- S11E entry clones were chosen for recombination into destination vectors (Supplemental Table S2).Gateway cloning into GFP fusion binary vector

Gateway enabled binary vectors pMDC43 and pMDC83 (Curtis and Grossniklaus, 2003) were chosen to construct EgSUSY1-GFP expression constructs. *EgSuSy1-Stop* and modified *EgSuSy1-S11A* and *EgSuSy1-S11E* transgenes were successfully recombined into pMDC43 to form C-terminal GFP-EgSUSY1 expression constructs. The *EgSuSy1-NoStop* transgene was LR-recombined into pMDC83 to form an N-terminal EgSUSY1-GFP expression construct. Recombinant destination vectors were successfully transformed into competent TOP10 *E. coli* cells (Invitrogen). Positive recombinants were identified through double digestion of the destination vector by *Asc*I and *Pac*I restriction endonucleases (Figure 2.15). A 2526bp excised fragment was expected if the *EgSuSy1* transgene was incorporated in the destination vector and a 1730bp excised fragment in empty destination vectors. In addition to restriction endonuclease digestion, positive recombinant destination clones were confirmed to contain the *EgSuSy1* transgenes in the correct orientation, as well as intact linker regions

through PCR amplification of *EgSuSy1*, *mGFP6* and linker specific fragments (Figure 2.16). Sequence analysis of the linker region between *EgSuSy1* and *mGFP6* concluded that the linker regions remained intact and in frame with no missense or nonsense induced mutations (Data not shown). The positive recombinant EgSUSY1-GFP expression constructs were isolated and successfully transformed into competent *Agrobacterium* LBA4404 cells for use in plant transformation and confirmed by colony and culture PCR amplification of an *EgSuSy1* specific fragment (Figure 2.17).

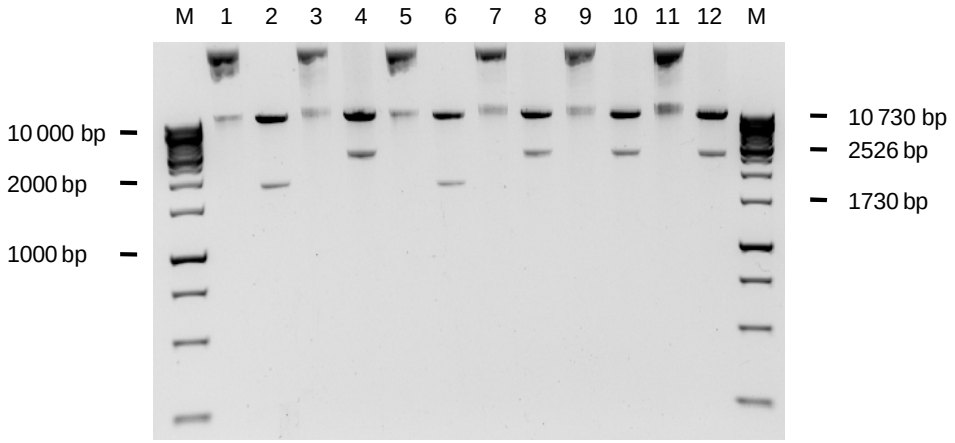

Figure 2.15. *Asc*I and *Pac*I restriction endonuclease digestion of recombinant entry vectors to confirm LR recombination of *EgSuSy1* CDS in pMDC43 and pMDC83. Indicated are the final positive destination vectors used for transformation into competent *Agrobacterium*. Odd lanes represent undigested products while even lanes represent the corresponding double digested products. Lane 1 and 2 represent empty pMDC83 while Lanes 5 and 6 represent empty pMDC43. Lanes 3 and 4 as well as lanes 7 to 12 show successful excision of the 2526bp fragment from *EgSuSy1*-pMDC83 (Lane 3 and 4), *EgSuSy1*- pMDC43 (Lane 7 and 8), *EgSuSy1-S11A*-pMDC43 (Lane 9 and 10) and *EgSuSy1-S11E*-pMDC43 (Lane 11 and 12). Lane M is a 1kbp DNA size standard (Fermentas).

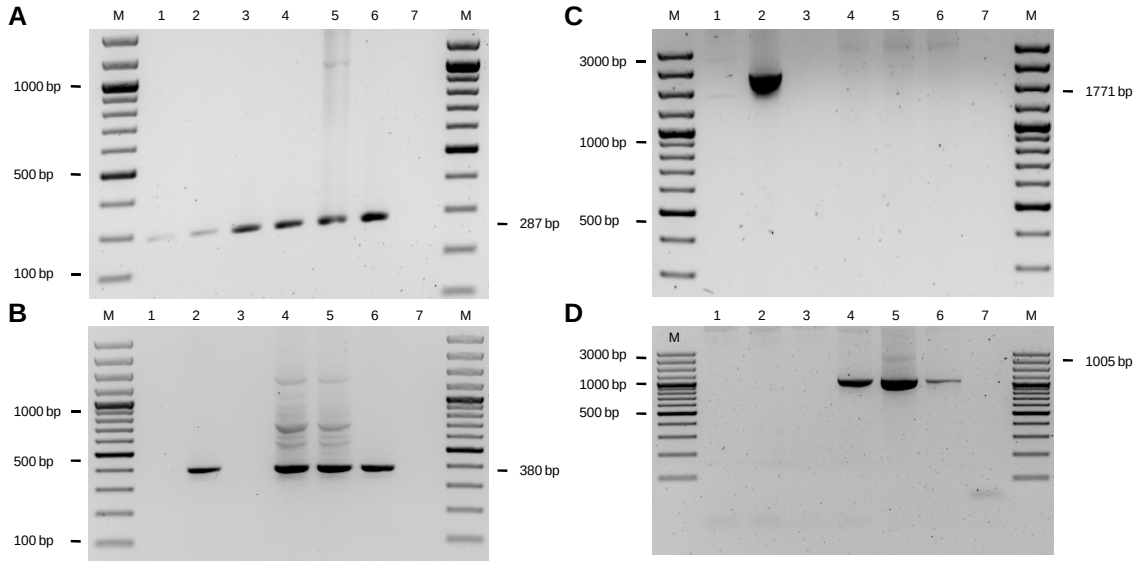

Figure 2.16. PCR screening of recombinant destination vector colonies. Gel A shows the amplification of a 287bp vector-specific *mGFP6* fragment using primers mGFP5_36 and mGFP5_322C. In gel B a 380bp *EgSuSy1* fragment was amplified as evidence of successful recombination of *EgSuSy1* CDS into either pMDC43 or pMDC83 destination vectors using primers EgSUSY1-396-F or EgSUSY1-138-R. Gel C shows the amplification of a 1771bp fragment spanning the linker region between *EgSuSy1* and *mGFP6* in pMDC83 using primers EgSUSY1-396-F x mGFP5_322C. To confirm the integrity of the linker region between *EgSuSy1* and *mGFP6* in pMDC43 a 1005bp fragment was PCR amplified as seen in Gel D using primers 5'SUSY-GSP2-214 and eGFP_283. Lane 1 and 3 represent empty pMDC83 and pMDC43 destination vectors respectively. Lanes 2 and 4 to 6 contains the final positive recombinant destination vectors *EgSuSy1*- pMDC83 (Lane2), *EgSuSy1*- pMDC43 (Lane 4), *EgSuSy1-S11A*- pMDC43 (Lane 5) and *EgSuSy1-S11E*- pMDC43 (Lane 6). Lane 7 contains a distilled water negative control for the above PCRs. Lane M is a 100bp DNA size standard (Fermentas).

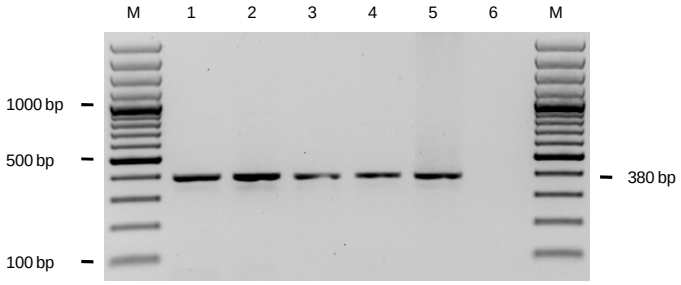

Figure 2.17. PCR confirmation of the presence of the *EgSuSy1* transgene in LBA4404 *Agrobacterium* cells prior to floral dipping of *Arabidopsis* plants. A 380bp *EgSuSy1* fragment was amplified as evidence of successful transformation of LBA4404 *Agrobacterium* cells with *EgSuSy1-mGFP6* expression constructs using primers EgSUSY1-138-R and EgSUSY1-396-F. Lanes 1 to 4 contains the final positive Agrobacteria cultures transformed with *EgSuSy1-mGFP6* expression constructs *EgSuSy1*-pMDC83 (Lane 1), *EgSuSy1*- pMDC43 (Lane 2), *EgSuSy1-S11A*- pMDC43 (Lane 3) and *EgSuSy1-S11E*- pMDC43 (Lane 4). Lane 5 contains a recombinant entry clone positive control and Lane 6 contains a distilled water negative control for the above PCRs. Lane M is a 100bp DNA size standard (Fermentas).

Transformation and screening of Arabidopsis plants

T1 generation *A. thaliana* Col-0 plants transformed with EgSUSY1-GFP expression constructs were selectively screened on Hygromycin supplemented media (Figure 2.18.A.). Positive transformants were transplanted to Jiffy® pots for propagation until maturation under controlled growth conditions (Figure 2.18.B.). Genomic DNA was isolated from leaf samples and the integration of T-DNA into the plant genome was established through mulitplex PCR amplification of a *mGFP6* (expression construct specific) and genomic DNA positive control an *Actin2* (*Arabidopsis*) fragment (Figure 2.19). The presence of an intact expression construct was successfully established in T2 and subsequent generation transgenic plants through leaf PCR amplification of an *mGFP6, Actin2* and *EgSuSy1* specific fragments (Figure 2.20). Positive PIP2a-GFP transgenic plants were identified through the amplification of a 365bp *eGFP* fragment in PIP2a-GFP plants using primers eGFP_283 and eGFP_647C. There was evidence of non-specific amplification of a similar sized fragment from EgSUSY1-GFP plants due to the nucleotide similarities between *eGFP* and *mGFP6* (Figure 2.20.C lane 3). The final positive transgenic plant lines used for RT-PCR and subcellular localization analysis included EgSUSY1-GFP line 1-5.7, GFP-EgSUSY1 line 3-1, GFP-EgSUSY1-S11A line 5-5, GFP-EgSUSY1-S11E line 7-2, GFP lines 6-1 and 7-1, GFP-PIP2a lines Q8-2 and Q8-8 and untransformed *Arabidopsis* Col-0 plants as a negative control.

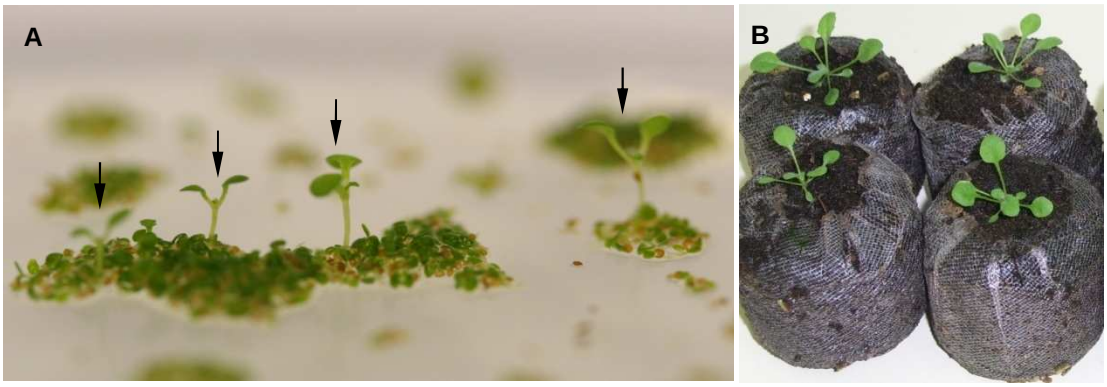

Figure 2.18. Selective screening of T1 transgenic seeds based on Hygromycin resistance. (A) Putative positive transgenic seedlings show enhanced growth and root development (arrow) compared to adjacent non-transgenic seedlings when plated on a hygromycin selective agar plate. (B) Putative positive seedlings were transplanted to Jiffy® pots for propagation until maturation under controlled growth conditions.

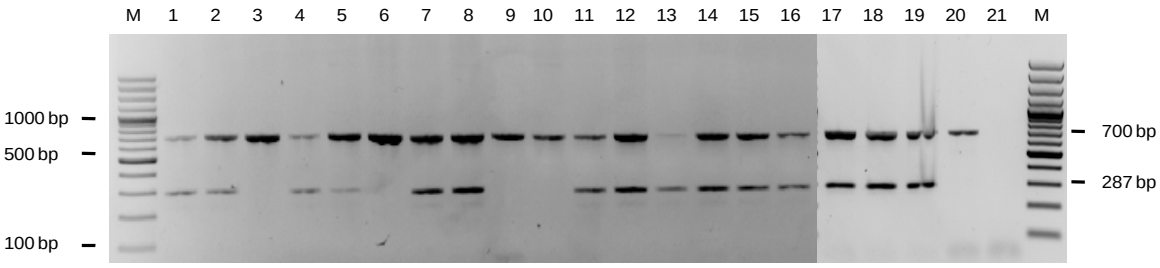

Figure 2.19. Screening of putative positive T1 lines via leaf multiplex PCR. To ascertain whether T1 plant lines were positive transformants for the EgSUSY1-GFP expression constructs two DNA fragments were amplified. A 700bp *Arabidopsis Actin2* fragment was amplified using primers ACT2-48-F and ACT2-289-R to test for the succesful isolation of genomic DNA from *Arabidopsis* leaf samples. To confirm transformation of T1 lines an additional 287 bp Expression construct specific *mGFP6* fragment was amplified using primers mGFP5_36 and mGFP5_322C. Lanes 1 to 19 contains the putative positive T1 plant lines where lanes 3, 6, 9, and 10 are false positives and do not contain the expression constructs. The presence of a 287 bp band in lanes 1, 2, 4, 5, 7, 8, 11, 12, 13, 14, 15, 16, 17, 18, and 19 confirm that these lines are true transformants and have integrated the expression construct into their genomic DNA. Lane 20 contains an untransformed *Arabidopsis* Col-0 negative control and lane 21 is a water control for the above PCR. Lane M is a 100 bp DNA size standard (Fermentas).

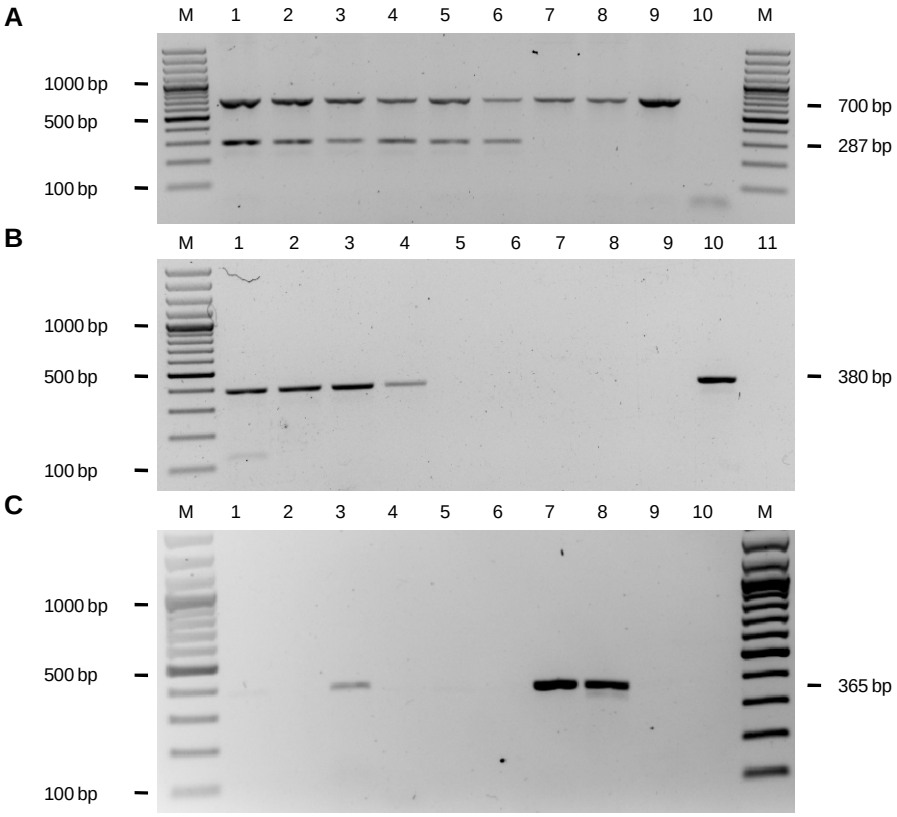

Figure 2.20. Screening of final positive plant lines used for subcellular localization. To ascertain wether plant lines were positive transformants for the EgSUSY1-GFP expression constructs two PCRs were perfomed on isolated genomic DNA from T2 generation plants. (A) First a multiplex PCR was perfomed to amplify a 700bp *Arabidopsis Actin2* fragment using primers ACT2-48-F and ACT2-289-R and an additional 287bp expression construct specific *mGFP6* fragment was amplified using primers mGFP5_36 and mGFP5_322C. (B) The second PCR involved the amplification of a 380bp *EgSuSy1* fragment using primers EgSUSY1-396-F and EgSUSY1-138-R. (C) An additional PCR was performed to test for the presence of 365bp *eGFP* fragment in PIP2a-GFP plants using primers eGFP_283 and eGFP_647C. Lanes 1 to 8 contains the final positive transgenic plant lines EgSUSY1-GFP line 1-5.7 (Lane 1), GFP-EgSUSY1 line 3-1 (Lane 2), GFP-EgSUSY1-S11A line 5-5 (Lane 3) and GFP-EgSUSY1-S11E line 7-2 (Lane 4), GFP lines 6-1 (Lane 5) and 7-1 (Lane 6) and GFP-PIP2a lines Q8-2 (Lane 7) and Q8-8 (Lane 8) . Lane 9 contains an untransformed *Arabidopsis* Col-0 negative control, lane 10 in gel B is a plasmid DNA positive control and the last lane in each gel is a water control for the above PCRs. Lane M is a 100bp DNA size standard (Fermentas).

Reverse transcriptase (RT)-PCR analysis of transgenic lines

Total RNA was successfully isolated from six week-old transgenic plant samples and resolved on an ethidium bromide agarose gel (Figure 2.21 A). RNA isolates ranged from 0.3 µg/µl and 0.7 µg/µl in concentration and the presence of prominent intact 28S and 18S rRNA bands confirmed RNA quality. Synthesized cDNA was tested for the presence of contaminating genomic DNA through the amplification of an intron spanning *UBIQUITIN 10* gene fragment. Analysis of PCR products found that all samples showed the amplification of a single 580bp fragment indicative of pure cDNA (Figure 2.21 B).

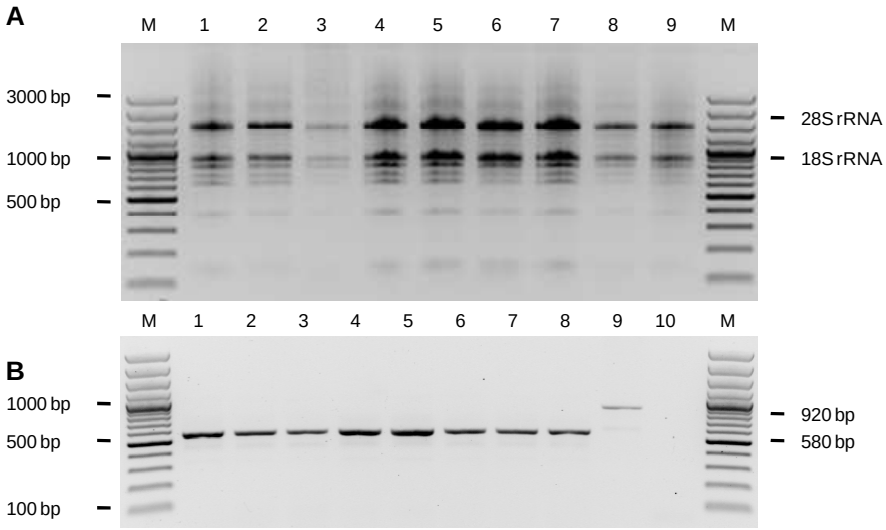

Figure 2.21. Gel electrophoresis analysis of extracted RNA followed by cDNA screening from final positive plant lines used for subcellular localization. (**A**) RNA isolated from plant lines was separated using gel electrophoresis to determine concentration and integrity. Optimal RNA will separate into a multiple bands with two prominent bands corresponding to the 28S rRNA and 18S rRNA. Synthesised cDNA was screened for integrity and the presence of contaminating genomic DNA by amplifying an *Arabidopsis AtUbiquitin10* fragment spanning an intron region using primers UBQ-F and UBQ-R. Pure cDNA will show only the amplification of a 580bp fragment lacking the intron region. Should there be any genomic DNA contamination an additional larger fragment of 920 base-pairs will be amplified. Lanes 1 to 8 contains the final positive transgenic plant lines EgSUSY1-GFP line 1-5.7 (Lane 1), GFP-EgSUSY1 line 3-1 (Lane 2), GFP-EgSUSY1-S11A line 5-5 (Lane 3) and GFP-EgSUSY1-S11E line 7-2 (Lane 4), GFP lines 6-1 (Lane 5) and 7-1 (Lane 6) and GFP-PIP2a lines Q8-2 (Lane 7) and Q8-8 (Lane 8) . Lane 9 in Gel A contains an untransformed Arabidopsis Col-0 control and in Gel B a genomic DNA negative control. Lane 10 is a water control for the above PCRs. Lane M is a 100bp DNA size standard (Fermentas).

To ensure that transgenic plant lines contain a fully transcribed expression construct; vector, *EgSuSy1* and linker-specific RT-PCR analyses were performed. RT-PCR products were analyzed using ethidium bromide agarose gel electrophoresis (Figure 2.22). An *mGFP6* specific fragment was successfully amplified from EgSUSY1-GFP line 1-5.7, GFP-EgSUSY1 line 3-1, GFP-EgSUSY1-S11A line 5-5, GFP-EgSUSY1-S11E line 7-2 and GFP lines 6-1 and 7-1 supporting the transcription of *mGFP6* from these lines. GFP-PIP2a lines Q8-2 and Q8-8 showed the absence of an amplified mGFP6 fragment as they contained an enhanced GFP variant (*eGFP*) (Figure 2.22 A). Amplification of a 380bp *EgSuSy1* fragment from cDNA samples of EgSUSY1-GFP line 1-5.7, GFP-EgSUSY1 line 3-1, GFP-EgSUSY1-S11A line 5-5 and GFP-EgSUSY1-S11E line 7-2 provided evidence of the successfully transcription of *EgSuSy1* from T-DNA inserts (Figure 2.22 B). The amplification of a 1005bp fragment spanning the linker region between *EgSuSy1* and *mGFP6* showed that *GFP-EgSuSy1* was transcribed as an intact fusion in GFP-EgSUSY1 line 3-1, GFP-EgSUSY1-S11A line 5-5 and GFP-EgSUSY1-S11E line 7-2 (Figure 2.22 C). Sequence analysis of this linker region confirmed the sequence integrity of the linker region and also confirmed the modification status of GFP-EgSUSY1-S11A line 5-5 and GFP-EgSUSY1-S11E line 7-2 (Data not shown).

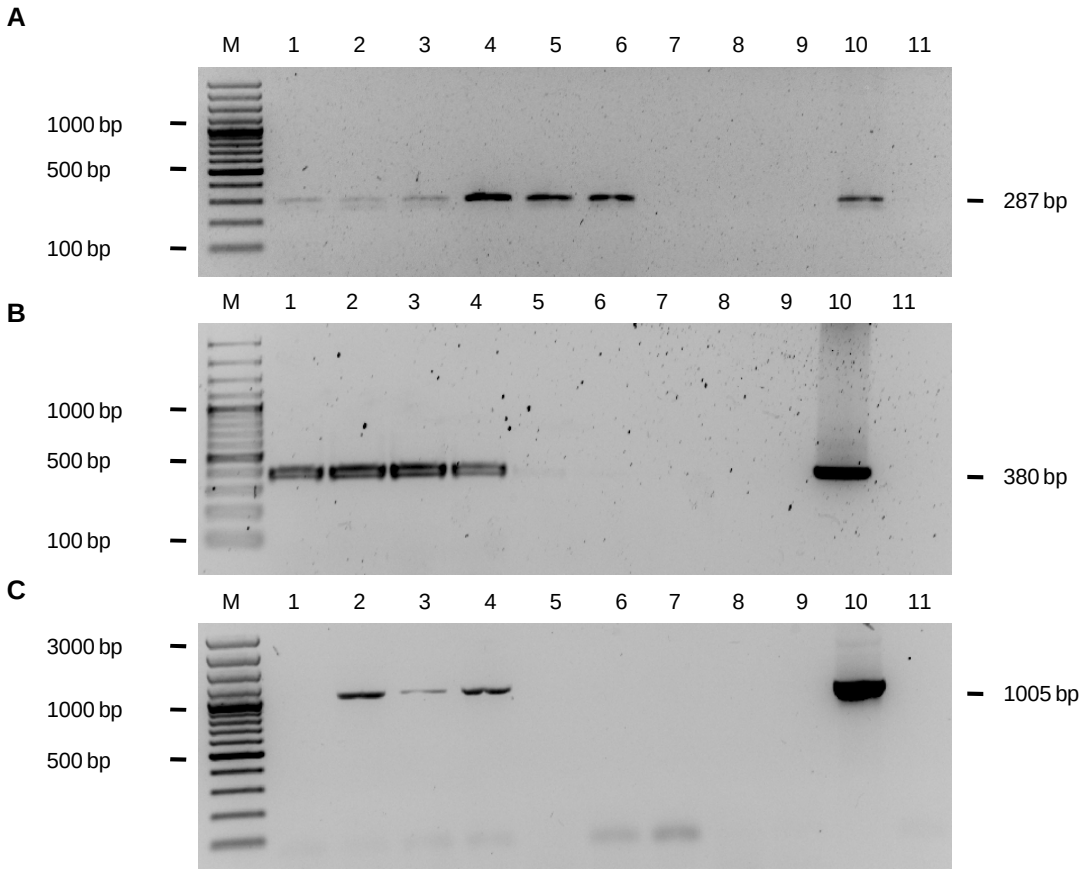

Figure 2.22. RT-PCR screening of final positive plant lines used for subcellular localization. (A) To test for the transcription of the inserted expression constructs a 287bp vector specific *mGFP6* fragment was amplified using primers mGFP5_36 and mGFP5_322C. (B) To test for the transcription of *EgSuSy1* from EgSUSY1-GFP expression constructs a 380bp *EgSuSy1* fragment was amplified using primers EgSUSY1-396-F and EgSUSY1-138-R. (C) A 1005bp fragment spanning the linker region between *EgSuSy1* and *mGFP6* in C-terminal GFP fusion expression constructs was amplified to determine the integrity of the linker region using primers 5'SUSY-GSP2-214 and eGFP_283. Lanes 1 to 8 contains the final positive transgenic plant lines EgSUSY1-GFP line 1-5.7 (Lane 1), GFP-EgSUSY1 line 3-1 (Lane 2), GFP-EgSUSY1-S11A line 5-5 (Lane 3) and GFP-EgSUSY1-S11E line 7-2 (Lane 4), GFP lines 6-1 (Lane 5) and 7-1 (Lane 6) and GFP-PIP2a lines Q8-2 (Lane 7) and Q8-8 (Lane 8) . Lane 9 contains an untransformed *Arabidopsis* Col-0 control, Lane 10 a plasmid DNA positive control and Lane 11 a water control for the above PCRs. Lane M is a 100bp DNA size standard (Fermentas).

2.4.2. Microscopy and image analysis of transgenic lines

To determine the subcellular localization and distribution of GFP-EgSUSY1 fusions; various transgenic and reference plant lines (Figure 2.23) were imaged using an inverted

LSM710 META Laser Scanning Confocal Microscope (CLSM, Zeiss) equipped with an LCl Plan-Neofluar 63x/1.3 Imm Korr DIC (Zeiss) water immersion objective and an Argon ion laser source (Zeiss). Plant cell plasma membranes were stained prior to slide preparation by suspending seedlings in FM4-64 solution. Confocal images of live plant tissues were captured by preparing live whole or sectioned plant samples for CLSM imaging. Three different *Arabidopsis* plant tissues were imaged concurrently namely roots, leaf epidermal cells and hypocotyls (Supplemental Figure SP2).

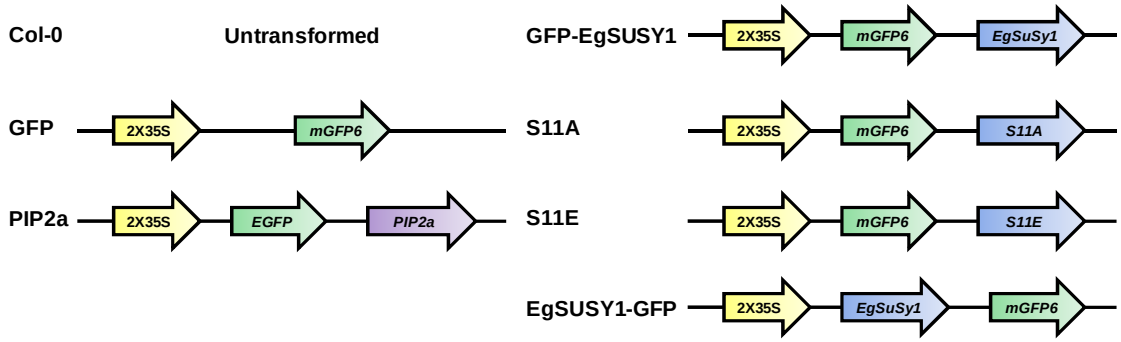

Figure 2.23. Expression cassettes for Col-0, GFP, PIP2a, GFP-EgSUSY1, S11A, S11E and EgSUSY1-GFP Arabidopsis plant lines. 2X35S: Double cauliflower mosaic virus promoter, mGFP6: modified Green Flourescent Protein version 6, EGFP: Enhanced Green Fluorescent Protein.

Localization of GFP-EgSUSY1 in root tissues of transgenic plants

Confocal live cell images of root cells of *Arabidopsis* Col-0 untransformed plants showed the presence of FM4-64 stain associated with the plasma membrane, but the absence of GFP signal in the GFP emission spectrum (Figure 2.24 A). Confocal live cell images of root cells of *Arabidopsis* plants, stably expressing GFP, show the presence of FM4-64 stain associated with the plasma membrane and GFP fluorescence in the cytoplasmic regions of root cells (Figure 2.24 B). These results provide evidence that the CLSM imaging setup selectively detected GFP fluorescence signal whilst excluding plant autofluorescence (Supplemental Figure SP3).

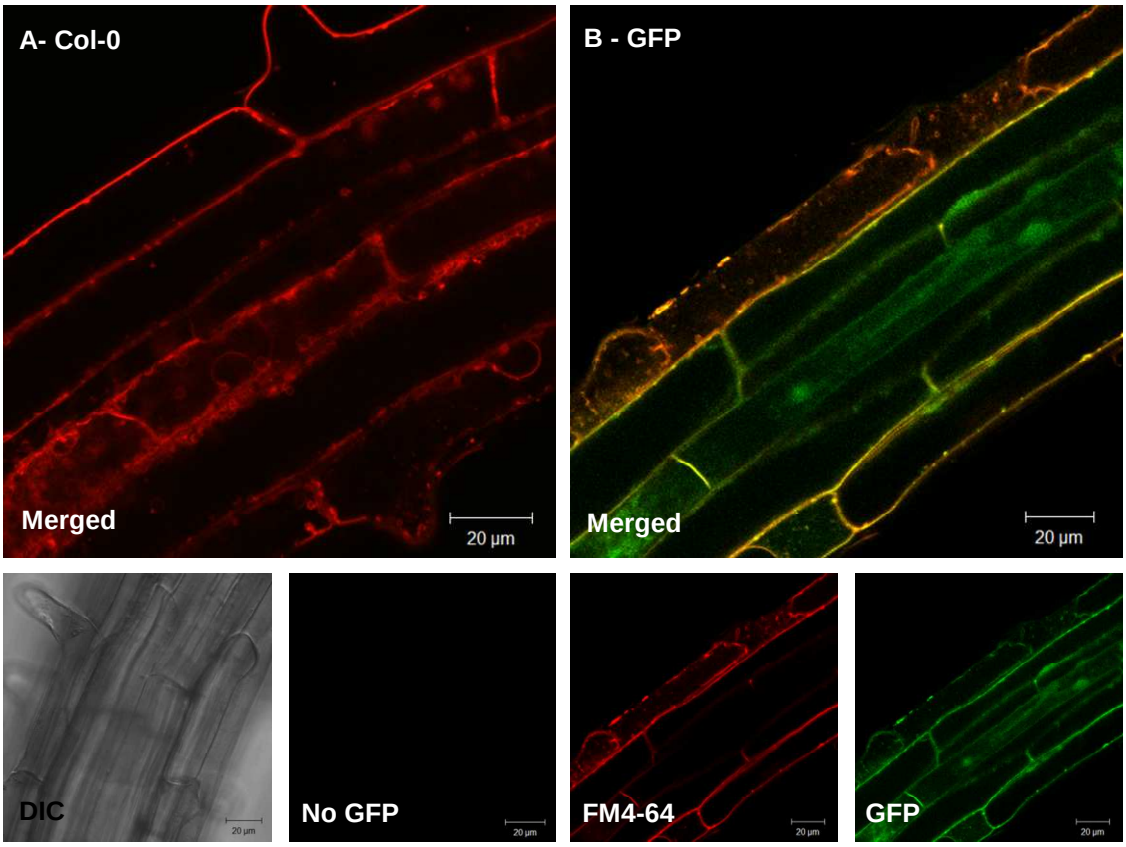

Figure 2.24. Verification of confocal imaging in root cells of Arabidopsis plants. (A) Confocal live cell images of root cells of Arabidopsis Col-0 untransformed plants show the presence of FM4-64 stain associated with the plasma membrane and the absence of GFP signal in the GFP emission spectrum. Differential Interference Contrast (DIC) image of the morphology of Arabidopsis Col-0 root cells. (B) Confocal live cell images of root cells of Arabidopsis Col-0 stably expressing GFP. Images show the presence of FM4-64 stain associated with the plasma membrane and GFP in the cytoplasmic regions of root cells. All images are of single focal planes. Scale bars 20 µm.

Confocal images of root sections from all GFP-EgSUSY1 fusion lines showed recordable levels of GFP fluorescence and partial colocalization of GFP-EgSUSY1 fusion proteins and FM4-64 membrane stain in merged images (Figure 2.25). This is evidence of cytosolic localization of the fusion protein found preferentially within the vascular bundles of root sections (Figure 2.25, indicated by arrows). A similar pattern of cytoplasmic localization was observed when viewing animations through a z-stack of the confocal optical sections of S11A root samples (Supplemental Figure SP5 and SP6).

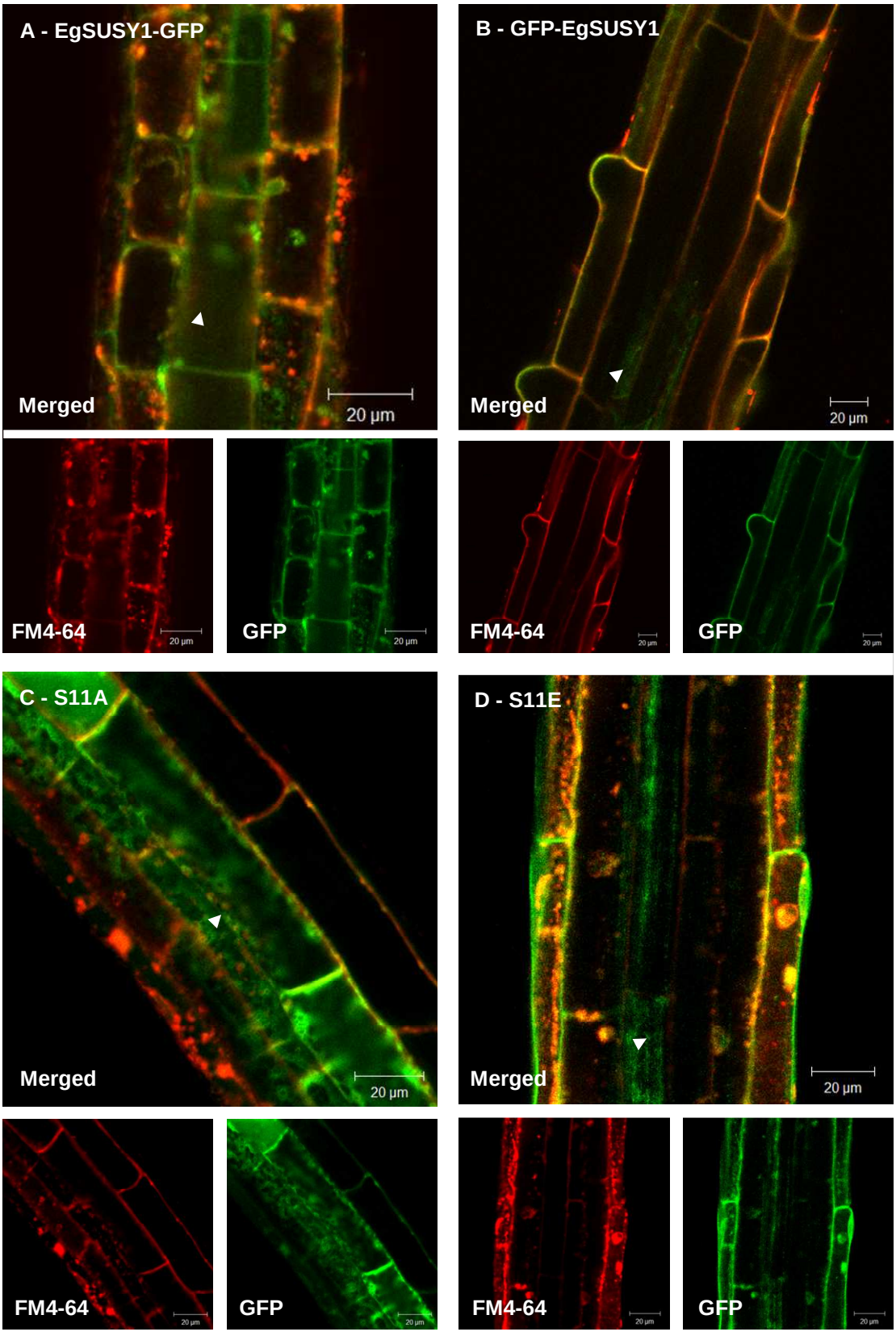
A - EgSUSY1-GFP
Merged
20 µm
B - GFP-EgSUSY1
Merged
20 µm
FM4-64
GFP
FM4-64
GFP
C - S11A
Merged
20 µm
D - S11E
Merged
20 µm
FM4-64
GFP
FM4-64
GFP

Figure 2.25. The subcellular localization and distribution of GFP-EgSUSY1 fusion proteins in *Arabidopsis* root tissues. (A) Confocal live cell images of root cells of *Arabidopsis* plants stably expressing EgSUSY1-GFP (A), GFP-EgSUSY1 (B), S11A (C), S11E (D). All fusion lines showed partial colocalization (yellow pixels) of GFP-EgSUSY1 fusion proteins and FM4-64 membrane stain in merged images. This is evidence of cytosolic localization of the fusion protein found preferentially within the vascular bundle (indicated by arrows). All images are of single focal planes. Scale bars 20µm.

Localization of GFP-EgSUSY1 in epidermal tissues of transgenic plants

The second *Arabidopsis* plant tissue to be imaged was leaf epidermal cells. Leaf epidermal cells have a unique cellular architecture which makes them informative in terms of subcellular localization. There exists two main types of cells namely thin epidermal plate cells and kidney shaped guard cells which surround the stomatal pores (Figure 2.26).

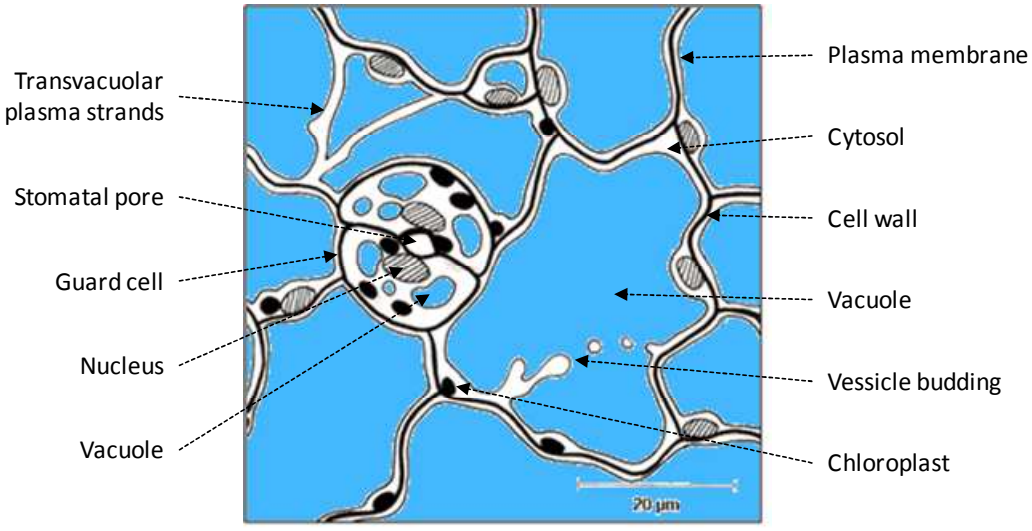

Figure 2.26 Schematic representation of the subcellular architecture of *Arabidopsis* leaf epidermal tissues. Illustration based on Confocal live cell images of *Arabidopsis* leaf epidermal cells. Scale bar 20 µm.

Transgenic GFP and PIP2a marker lines were imaged as references for cytoplasmic and plasma membrane fluorescence localization respectively. Confocal images of GFP lines revealed the presence of GFP signal in the green channel within nuclear (indicated by red arrows) and cytoplasmic (indicated by white arrows) regions of leaf epidermal cells (Figure

2.27 A). On the other hand, confocal images of PIP2a leaf epidermal cells showed a distinct association of GFP-PIP2a proteins with the plasma membrane, indicated by a high level of colocalization with membrane stain FM4-64 in merged images (Figure 2.27 B).

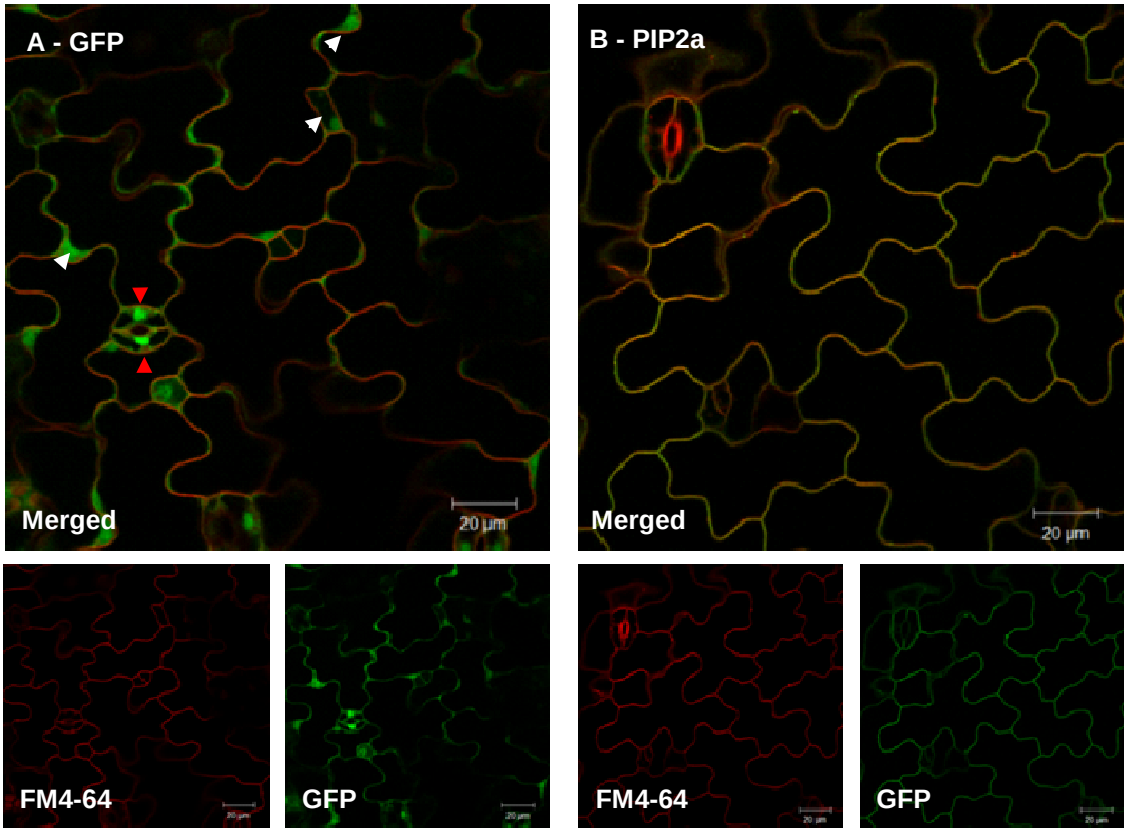

Figure 2.27. Live cell imaging of the cytosolic and plasma membrane specific subcellular markers in *Arabidopsis* Col-0 leaf epidermal cells. (A) Confocal live cell images of leaf epidermal cells of *Arabidopsis* plants stably expressing GFP showed a typical cytosolic (indicated by white arrows) and nuclear distribution (indicated by red arrows). (B) Whereas confocal live cell images of leaf epidermal cells of *Arabidopsis* plants stably expressing PIP2a showed plasma membrane localization supported by colocalization (yellow pixels) with membrane stain FM4-64 in merged images. All images are of single focal planes. Scale bars 20 µm.

Confocal images of leaf epidermal sections from all GFP-EgSUSY1 fusion lines showed recordable levels of GFP fluorescence and varying degrees colocalization of GFP-EgSUSY1 fusion proteins and FM4-64 membrane stain in merged images (Figure 2.28). There was evidence of cytosolic localization of the fusion proteins seen preferentially within the guard cells of leaf epidermal sections (Figure 2.28, indicated by arrows).

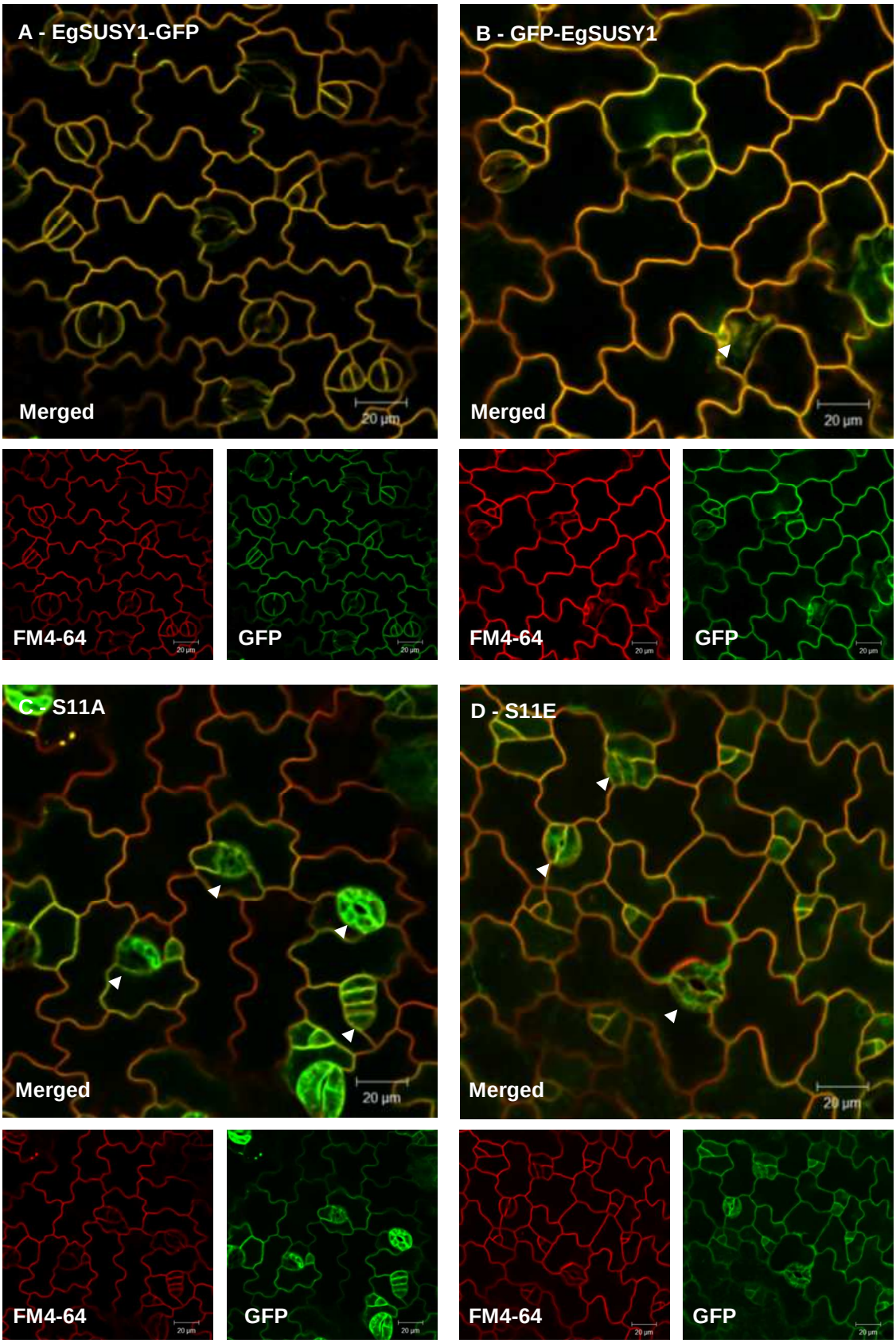
A - EgSUSY1-GFP
Merged
20 µm
B - GFP-EgSUSY1
Merged
20 µm
FM4-64
GFP
FM4-64
GFP
C - S11A
Merged
20 µm
D - S11E
Merged
20 µm
FM4-64
GFP
FM4-64
GFP

Figure 2.28. Subcellular localization and distribution of GFP-EgSUSY1 fusion proteins in *Arabidopsis* leaf epidermal cells. (A) Confocal live cell images of leaf epidermal cells of *Arabidopsis* plants stably expressing EgSUSY1-GFP (A), GFP-EgSUSY1 (B), S11A (C) and S11E (D). All fusion lines showed varying degrees of colocalization (yellow pixels) of GFP-EgSUSY1 fusion proteins and FM4-64 membrane stain in merged images. There was evidence of cytosolic localization of the fusion protein found preferentially within the guard cells surrounding stomatal pores. All images are of single focal planes. Scale bars 20µm.

On closer examination of leaf epidermal guard cells it was found that GFP marker lines showed recordable levels of GFP fluorescence in both the nucleus and cytoplasm of guard cells (Figure 2.29 B, indicated by arrows). Contrary to this observation, it was observed that PIP2a and all GFP-EgSUSY1 lines had recordable levels of GFP fluorescence in the cytoplasm of guard cells but not the nucleus (Figure 2.29 C and Figure 2.30).

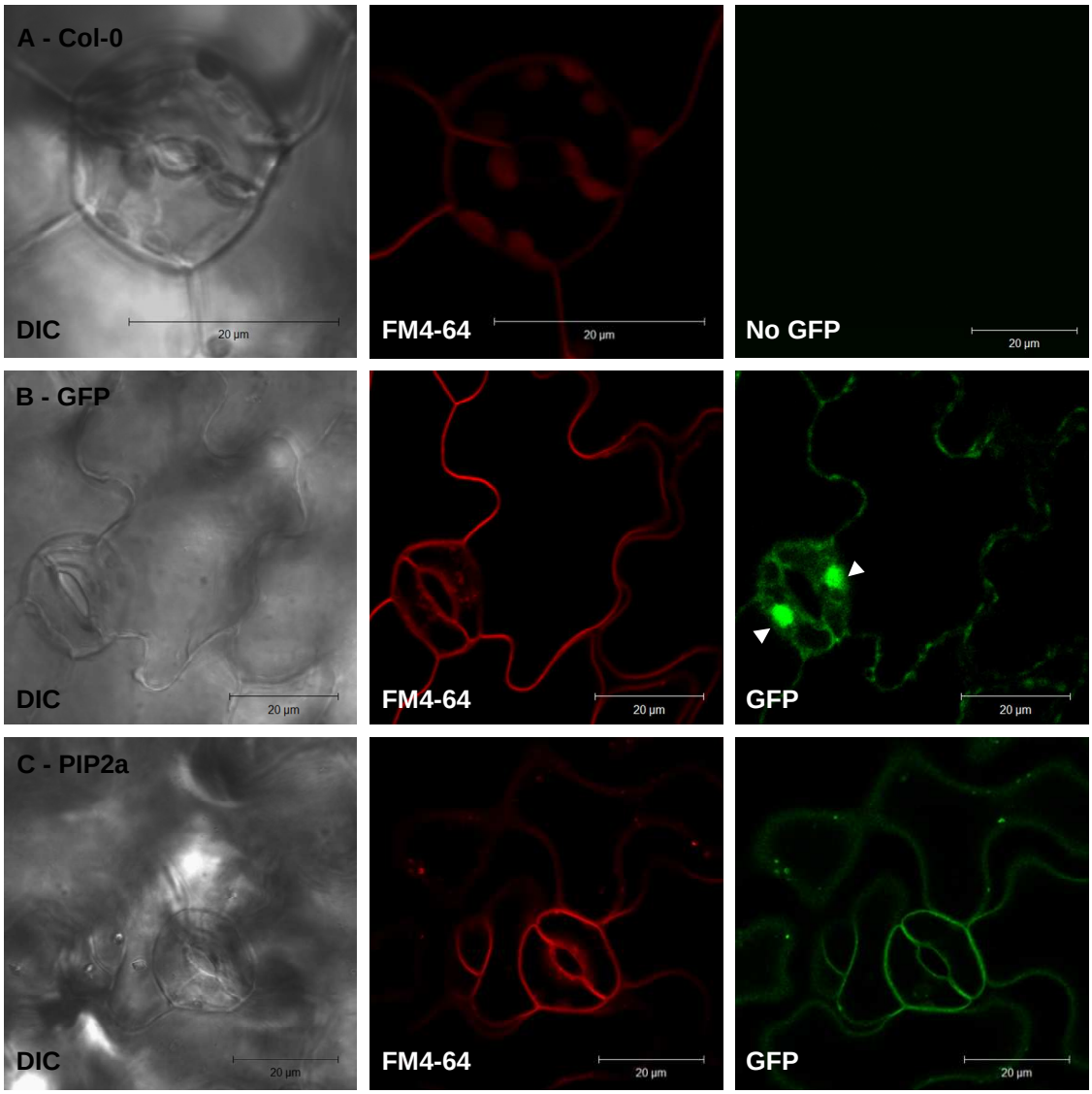

Figure 2.29. Live cell imaging of the cytosolic and plasma membrane specific subcellular markers in *Arabidopsis* leaf epidermal guard cells compared to untransformed cells. Confocal live cell images of leaf epidermal cells of untransformed *Arabidopsis* plants (A) and transformed marker lines stably expressing GFP (B) and PIP2a (C). GFP lines showed a cytosolic and nuclear distribution (indicated by arrows) typical of the localization of free GFP *in vivo*. Whereas Confocal live cell images of PIP2a plants showed the absence of fluorescence in the nucleus. Differential Interference Contrast (DIC) images give an indication of the morphology of Arabidopsis leaf epidermal cells in which the fluorescence signal was found. All images are single focal planes. Scale bars 20 µm.

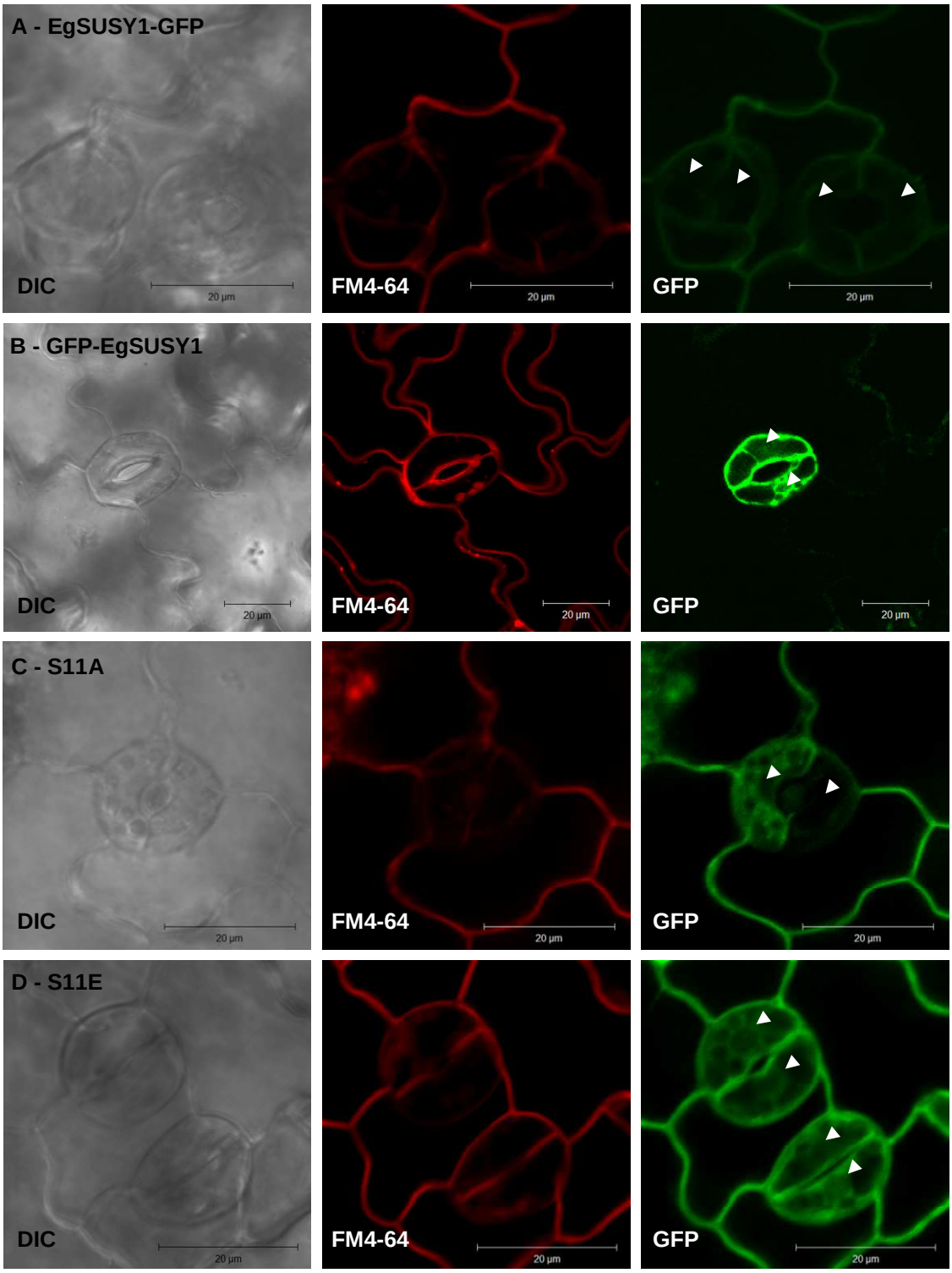

Figure 2.30. Subcellular localization and distribution of GFP-EgSUSY1 fusion proteins in *Arabidopsis* leaf epidermal guard cells. Confocal live cell images of leaf epidermal cells of *Arabidopsis* plants lines stably expressing EgSUSY1-GFP (A), GFP-EgSUSY1 (B), S11A (C) and S11E (D). All fusion lines showed varying degrees of cytoplasmic localization of GFP-EgSUSY1 fusion proteins especially within guard cells. There was no evidence of the nuclear localization of GFP-EgSUSY1 fusion proteins

supported by the lack of GFP fluorescence signal in the nuclear region of guard cells (indicated by arrows). This verifies that the fusion proteins are expressed in an intact form. Differential Interference Contrast (DIC) images give an indication of the morphology of Arabidopsis leaf epidermal cells in which the fluorescence signal was found. All images are single focal planes. Scale bars 20µm.

Co-localization of GFP-EgSUSY1 and FM4-64 in epidermal tissues of transgenic plants

Qualitative and quantitative colocalization analysis was performed to determine whether unmodified EgSUSY1 protein and modified EgSUSY1 proteins (S11A and S11E) showed any evidence of differential association with the plasma membrane. Qualitative colocalization was achieved through the sequential scanning of FM4-64 stained leaf epidermal cells with an Argon laser line and capturing a z-stack of GFP fluorescence and FM4-64 fluorescence. These image stacks were then passed through a Manders' Coefficients Plugin in the ImageJ public domain image processing software to create scatter plots illustrating the colocalization pattern present (Figure 2.31).

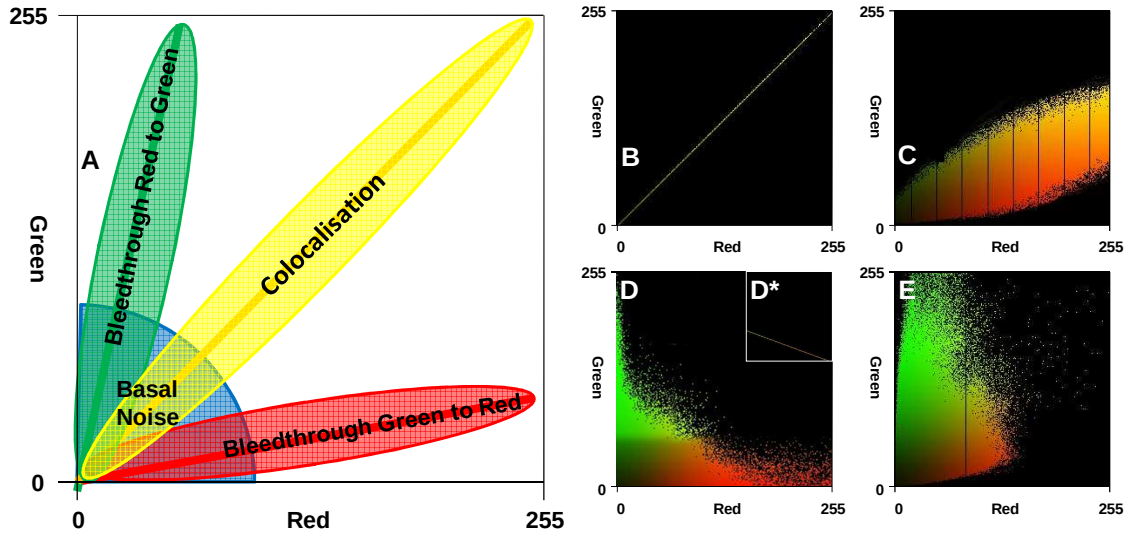

Figure 2.31. Scatter plots illustrating the various patterns indicative of the possible colocalization events in a biological sample. (A) Schematic Model of a scatter plot illustrating the regions in which colocalisation, channel bleedthrough and basal noise would be found. In the scatter plots, the first (red channel) image component is represented along the x-axis, whilst the second image (green channel) is represented along the y-axis. The x- and the y-coordinates of the scatter plot point is determined by the intensity of a given pixel in the first image (red channel) and the intensity of the corresponding pixel in the second image (green channel) respectively. (B) During a complete colocalization event under perfect conditions (i.e. no noise, bleedthrough and equal fluorophore intensities) it is expected that the pixels should be distributed along a straight line intersecting the axis at a 45° angle. (C) Biological samples are dynamic therefore the scatter plots generated usually appear as a cloud of pixels

surrounding this straight line due to noise corruption. (D) In the event that no colocalization of the two fluorophores is present, complete exclusion will be indicated by the distribution of the pixels remaining near the channel axis similar to the bleed through patterns illustrated in the schematic A. (D*) Complete exclusion under perfect conditions would result in the distribution of pixels along a straight line with a negative slope. (E) Partial colocalization is indicated by the distribution of the pixels in a fan like manner away from the axis. Biological samples often differ in intensity values for the two fluorescence channels resulting in the diversion of the straight line towards the axis of the channel with the highest intensity value. Scatter plots serve as a representation of each event and it should be noted that there is a measure of variability in observed patterns due to biological and experimental parameters. Schematic and scatter plots based on Bolte (2006)

To test the colocalization setup two marker lines were imaged concurrently. These included a GFP marker line to represent cytoplasmic compartmentation and a PIP2a marker line as a reference for plasma membrane localization. Colocalization images of the GFP marker line showed the absence of colocalized yellow pixels in merged confocal images and an exclusive localization pattern in the generated scatter plots (Figure 2.22 A). Colocalization images of the PIP2a marker line showed the presence of colocalized yellow pixels in merged confocal images and a partial colocalization pattern in the generated scatter plots (Figure 2.32 B).

Qualitative colocalization analysis of unmodified N-terminal (EgSUSY1-GFP) and C-terminal (GFP-EgSUSY1) EgSUSY1 fusion lines showed the presence of colocalized yellow pixels in merged confocal images and a partial colocalization pattern in the generated scatter plots (Figure 2.32 C and D). It was found that both modified EgSuSy1 proteins, S11A and S11E, showed similar colocalization patterns as observed for unmodified lines with the presence of colocalized yellow pixels in merged confocal images and a partial colocalization pattern in the generated scatter plots (Figure 2.33).

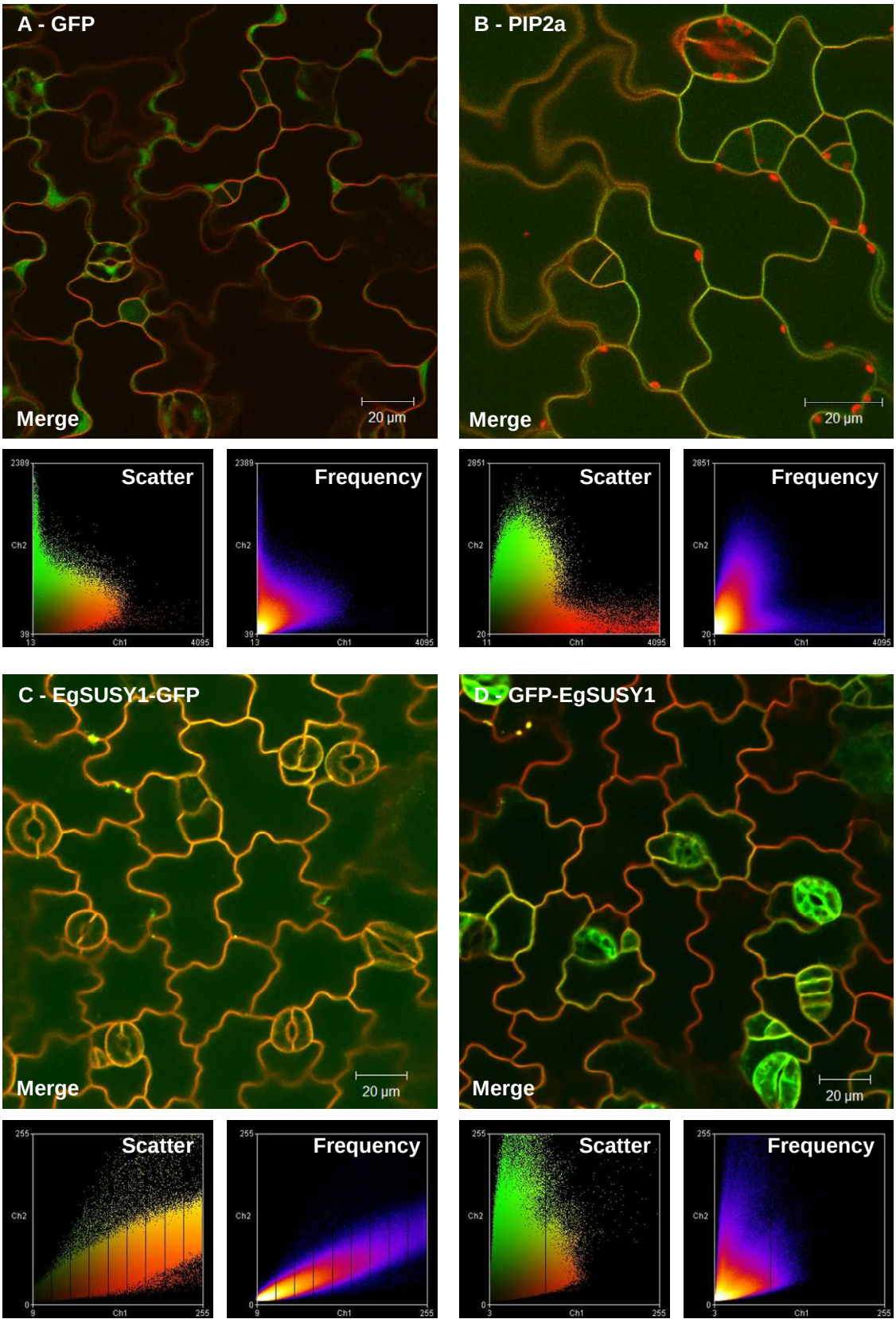
A - GFP
Merge
20 µm
B - PIP2a
Merge
20 µm
Scatter
Frequency
Ch2
Ch1
C - EgSUSY1-GFP
Merge
20 µm
D - GFP-EgSUSY1
Merge
20 µm

Figure 2.32. Qualitative colocalization analysis of subcellular marker references and unmodified GFP-EgSUSY1 *Arabidopsis* plant lines. Merged confocal images of leaf epidermal cells of *Arabidopsis* plants lines stably expressing GFP (A), PIP2a (B), EgSUSY1-GFP (C) and GFP-EgSUSY1 (D). Scatter plots correspond to the colocalization events as shown in merged confocal images. Green pixels indicate non-colocalized GFP signal and red pixels indicate non-colocalized FM4-64 stain signal. Qualitative colocalization is indicated by yellow pixels. Frequency scatter plots indicate high frequency signal events as hot colours (red) and low frequency signal events as cold colours (blue). Scatterplots were performed on no less than 10 slice thick z-stacks of leaf epidermal images. Three biological repeats were performed for each transgenic event of which only one is presented. Scale bars 20 µm.

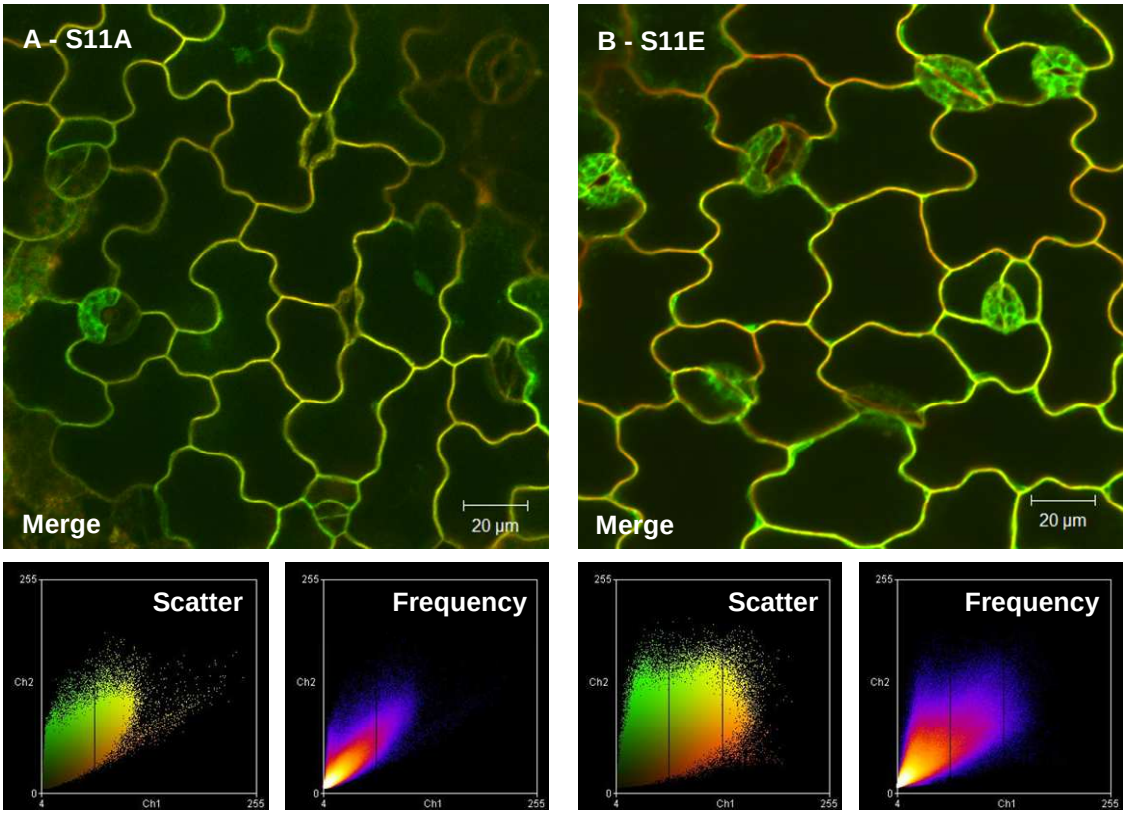

Figure 2.33. Qualitative colocalization analysis of modified GFP-EgSUSY1 *Arabidopsis* plant lines. Merged confocal images of leaf epidermal cells of *Arabidopsis* plants lines stably expressing S11A (A) and S11E (B). Scatter plots correspond to the colocalization events as shown in merged confocal images. Green pixels indicate non-colocalized GFP signal and red pixels indicate non-colocalized FM4-64 stain signal. Qualitative colocalization is indicated by yellow pixels. Frequency scatter plots indicate high frequency signal events as hot colours (red) and low frequency signal events as cold colours (blue). Scatterplots were performed on no less than 10 slice thick z-stacks of leaf epidermal images. Three biological repeats were performed for each transgenic event of which only one is presented. Scale bars 20µm.

Quantitative colocalization was assessed through the statistical analysis of scatter plots generated. Pearson correlation and Mander's overlap coefficients were calculated as a measure of the level of colocalization found in imaged *Arabidopsis* lines using the same Manders' Coefficients Plugin in ImageJ. The mean of three biological repeats was calculated for each transgenic event. It was found that the marker lines GFP and PIP2a generated uncharacteristic Pearson correlation (P) and Manders overlap (M) coefficients with the GFP coefficients (P mean = 0.675, M mean = 0.787) being higher than that of the PIP2a (P mean = 0.448, M mean = 0.621; Table 2.6). This suggests that there were more quantitative pixel colocalization events occurring in GFP lines than in PIP2a lines.

N-terminal EgSUSY1-GFP fusion line recorded high colocalization coefficients with a P mean of 0.915 and an M mean of 0.963 (Table 2.6). This suggests a high degree of colocalization and possible evidence of plasma membrane localization. It was found that C-terminal GFP-EgSUSY1 had a P mean of 0.621 and an M mean of 0.827 suggesting partial colocalization in this case (Table 2.6). Both modified S11A and S11E generated high Pearson's correlation and Mander's overlap coefficients above 0.8 suggesting a high level of colocalization and possible evidence of plasma membrane association of these fusion proteins (Table 2.6).

Table 2.6. Quantitative colocalization coefficients as determined using the Mander's coefficients Plugin in the ImageJ public domain image processing software. Two coefficients are shown the Pearson's correlation coefficient and the Mander's Overlap coefficient for triplicate biological repeats of each plant line. Coefficients were calculated for no less than 10 slice thick z-stacks of leaf epidermal images.

Plant line[a]	Image[b]	Channels[c]	Pearson's[d]	Mean[e]	Mander's[f]	Mean[g]
Col-0	Col-0 L7.lsm	Red : Green	0.199		0.568	
GFP	GFP6-1 LZ (5).lsm	Red : Green	0.923		0.958	
	GFP6-1 LZ (6).lsm	Red : Green	0.558	0.674	0.691	0.787
	GFP6-1 LZ (7).lsm	Red : Green	0.540		0.712	
GFP-EgSUSY1	P3-1 LZ (1).lsm	Red : Green	0.557		0.753	
	P3-1 LZ (2).lsm	Red : Green	0.792	0.621	0.895	0.827
	P3-1 LZ (3).lsm	Red : Green	0.515		0.832	
S11A	P5-5 LZ (1).lsm	Red : Green	0.883		0.935	
	P5-5 LZ (6).lsm	Red : Green	0.888	0.888	0.950	0.942
	P5-5 LZ (7).lsm	Red : Green	0.894		0.942	
S11E	P7-2 LZ (1).lsm	Red : Green	0.850		0.936	
	P7-2 LZ (7).lsm	Red : Green	0.850	0.834	0.904	0.908
	P7-2 LZ (10).lsm	Red : Green	0.803		0.883	
EgSUSY1-GFP	1-5.7 LZ (1).lsm	Red : Green	0.894		0.962	
	1-5.7 LZ (2).lsm	Red : Green	0.923	0.915	0.963	0.963
	1-5.7 LZ (3).lsm	Red : Green	0.929		0.965	
PIP2a	Q8-2 LZ (1).lsm	Red : Green	0.403		0.592	
	Q8-8 LZ (2).lsm	Red : Green	0.379	0.448	0.577	0.621
	Q8-2 LZ (6).lsm	Red : Green	0.562		0.694	

a. The identity of the plant line from which samples were prepared for quantitative colocalization analysis.

b. The identity of the image used to generate quantitative colocalization coefficients. The image name correlates with the raw image found within the image database on the supplemental DVD. Arabic numerals in brackets indicate the identity of the three biological repeats for each plant line. Each optical slice in the z-stack of no less than 10 slices acts as a technical repeat.

c.Two channels were considered during quantitative colocalization. The red channel was dedicated to FM-4-64 fluorescence readings and the green channel for GFP emissions.

d. The determined Pearson's correlations coefficient for each biological sample. The Pearson's correlation coefficient value can range from 1 to -1. Complete colocalization or a positive correlation between the two fluorophores is indicated by a value of 1. During complete exclusion or a negative correlation between the two fluorophores you would expect a value of -1. A value of zero would indicate that no correlation exists between the two fluorophore pixel distributions suggesting that there is partial colocalization (Bolte and Cordelieres, 2006).

e. The mean of the Pearson's correlation coefficient calculated for three biological samples per plant line.

f. The calculated Mander's overlap coefficient represents the fraction of overlap of the signal in the respective images. A value of 1 indicates 100% overlap and complete colocalization, whilst a value of

0 indicates the absence of signal overlap and therefore complete exclusion (Manders et al., 1993).

g. The mean of the Mander's overlap coefficient calculated for three biological samples per plant line.

Localization of GFP-EgSUSY1 in hypocotyl of transgenic plants

The third and final *Arabidopsis* tissue to be imaged was hypocotyl, which is characterised by large brick shaped palisade cells which have sparsely located chloroplasts on the cell periphery (**Figure 2.34** A). To investigate the subcellular localization of fusion proteins a z-stack of GFP fluorescence and chloroplast autofluorescence was captured over a number of optical slices. A y-projection was then generated using Zeiss LSM Image Browser version 4.2.0.121 software to create a three dimensional representation of the cellular architecture.

The GFP marker line showed an irregular hypocotyl surface topology indicative of cytoplasmic compartmentation (Figure 2.34 C and Supplemental Figure SP7). Contrastingly PIP2a marker line showed a solid cell surface topology of the EGFP-fusion protein indicative of plasma membrane association of the fusion protein (Figure 2.34 D and Supplemental Figure SP8). Unmodified EgSUSY1-GFP fusion proteins appeared to take on an irregular surface topology similar to that of GFP marker lines indicating that EgSUSY1-GFP fusion protein has a cytoplasmic component (Figure 2.34 B and Supplemental Figure SP9).

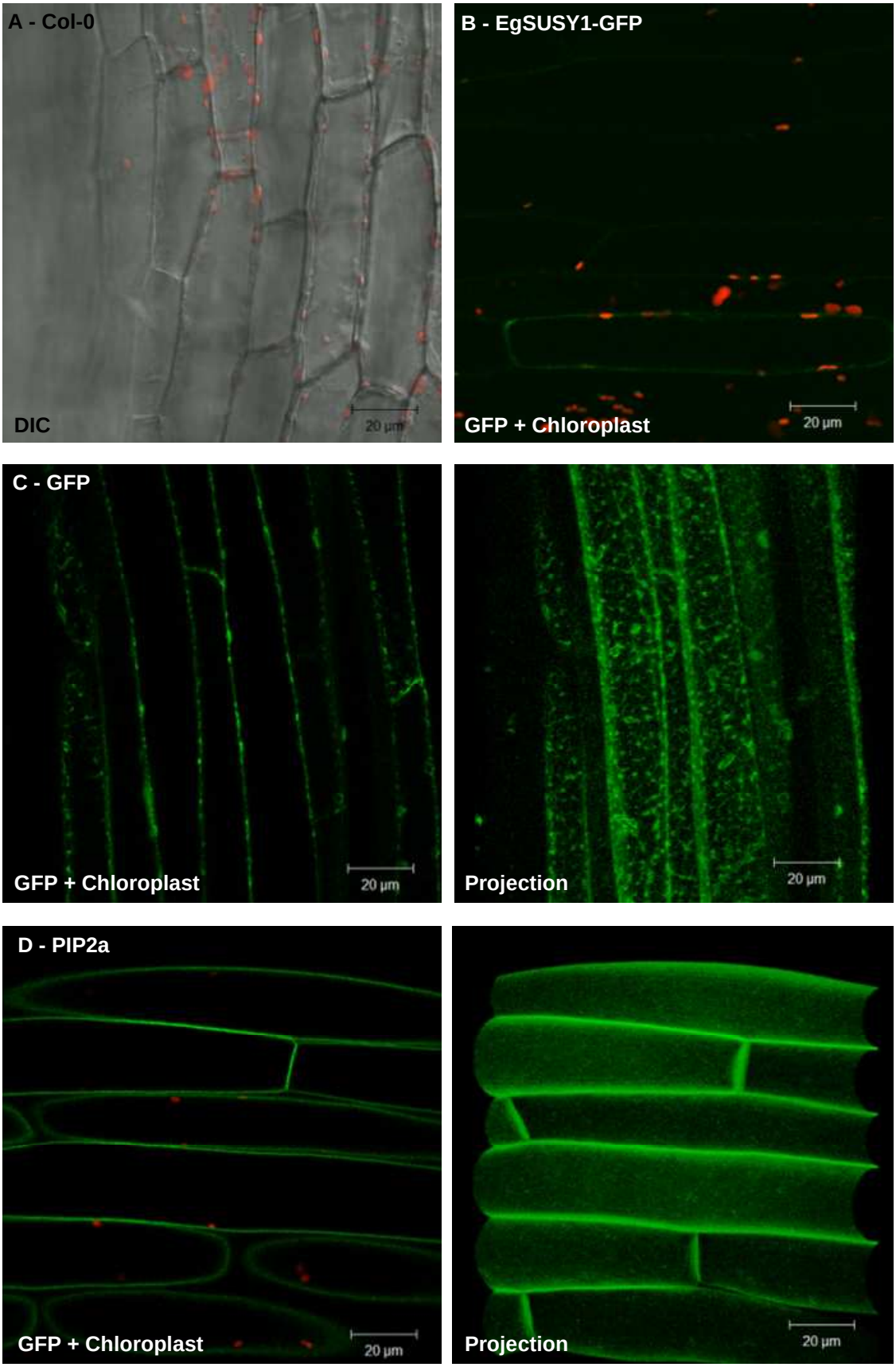
A - Col-0
DIC
20 µm
B - EgSUSY1-GFP
GFP + Chloroplast
20 µm
C - GFP
GFP + Chloroplast
20 µm
Projection
20 µm
D - PIP2a
GFP + Chloroplast
20 µm
Projection
20 µm

Figure 2.34. Live cell imaging of the subcellular localization and distribution of GFP-EgSUSY1 fusion proteins in *Arabidopsis* hypocotyl cells. (A) Differential Interference Contrast (DIC) images of untransformed Arabidopsis Col-0 plants give an indication of the morphology of hypocotyl cells in which the fluorescence signal was found. Confocal live cell images of hypocotyl tissues of *Arabidopsis* plant lines stably expressing EgSUSY1-GFP (B), GFP (C), and PIP2a (D). GFP plant lines showed a cytoplasmic distribution of GFP signal typical of free GFP. PIP2a plant lines had a smooth cell periphery localization of GFP signal indicative of the localization of the plasma-membrane. There was evidence that the EgSUSY1-GFP line has a cytoplasmic component due to the rough surface cell periphery morphology of GFP signal in this plant line. Single optical sections through hypocotyl tissues are indicated on the left and y-projections through z-stacks are indicated on the right. Chloroplast autofluorescence is indicated in the red channel. Scale bars 20µm.

Confocal live cell images of hypocotyl cells of *Arabidopsis* plants lines stably expressing GFP-EgSUSY1 (Figure 2.35 A), S11A (Figure 2.35 B, Supplemental Figure SP10 and SP11) and S11E (Figure 2.35 C and Supplemental Figure SP13) showed similar irregular peripheral morphologies of the GFP signal and the presence of budding vesicles and transvacuolar plasmic strands. This alludes to the cytoplasmic compartmentation of all GFP-EgSUSY1 fusion lines. Time series imaging of a single optical plane of S11A and S11E plant lines showed evidence of cytoplasmic streaming and vesicle budding characteristic of cytoplasmic association of the fusion proteins (Supplemental Figure SP12 and SP14 respectively.

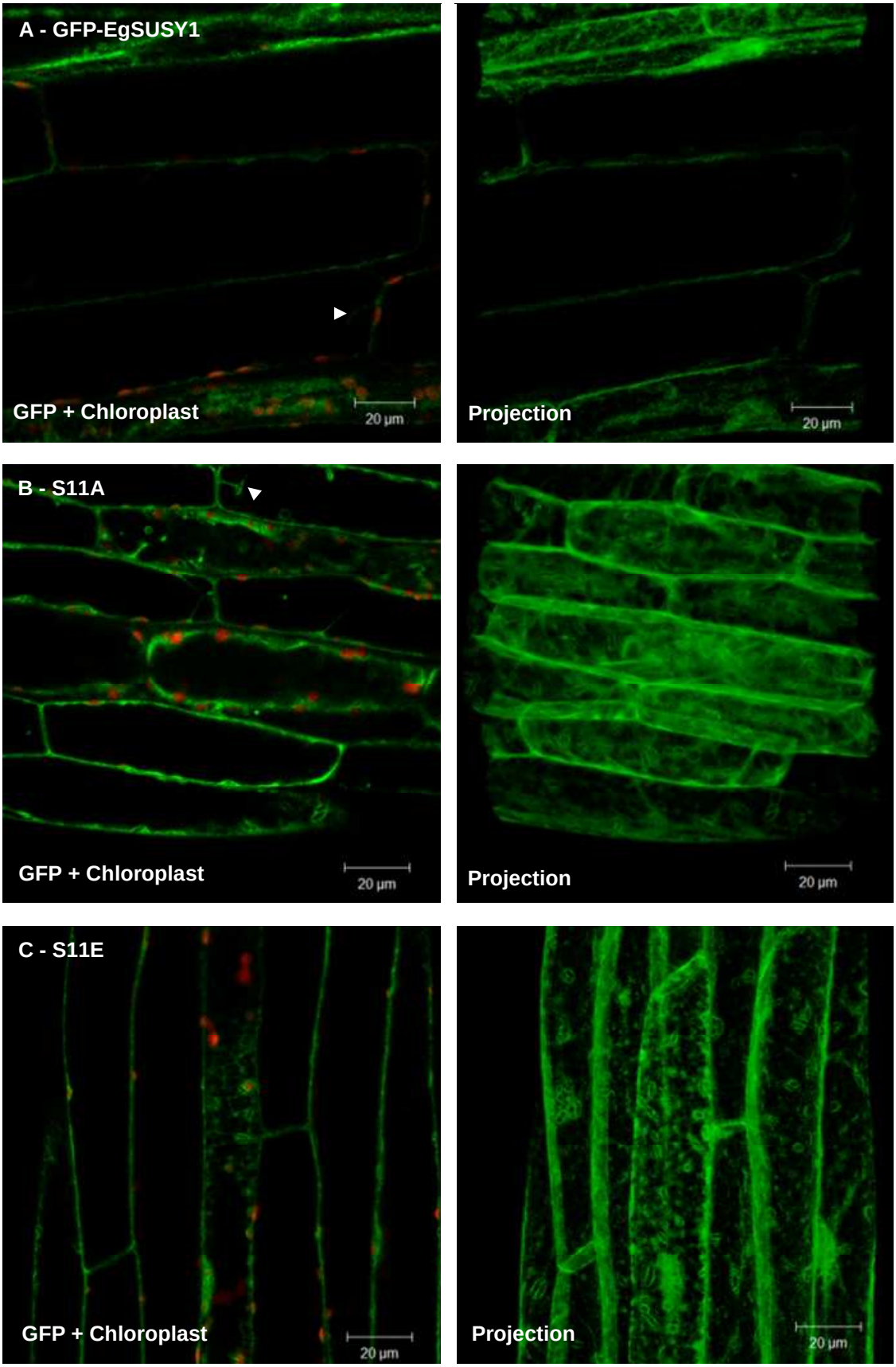
A - GFP-EgSUSY1
GFP + Chloroplast
20 µm
Projection
20 µm
B - S11A
GFP + Chloroplast
20 µm
Projection
20 µm
C - S11E
GFP + Chloroplast
20 µm
Projection
20 µm

Figure 2.35. Live cell imaging of the subcellular localization and distribution of GFP-EgSUSY1 fusion proteins in *Arabidopsis* hypocotyl cells. (Confocal live cell images of hypocotyl cells of *Arabidopsis* plants lines stably expressing GFP-EgSUSY1 (A), S11A (B) and S11E (C). The rough peripheral morphology of the GFP signal and the presence of transvacuolar plasmic strands is evidence that all GFP-EgSUSY1 fusion lines have a cytoplasmic component. Single optical sections through hypocotyl tissues are indicated on the left and y-projections through z-stacks are indicated on the right. Chloroplast autofluorescence is indicated in the red channel. Scale bars 20µm.

Effect of osmotic stress on the localization of GFP-EgSUSY1 in hypocotyl stems of transgenic plants

To ascertain if GFP-EgSUSY1 fusion proteins possess an extracellular component, hypocotyl tissues of marker and transgenic *Arabidopsis* lines were incubated in a 1M KNO_3 solution for 5 min. Hereafter a CLSM z-stack of GFP fluorescence and chloroplast autofluorescence was captured over a number of optical slices. A y-projection was then generated using Zeiss LSM Image Browser software to create a three dimensional representation of the cellular architecture.

Differential interference contrast images of *Arabidopsis* Col-0 hypocotyl tissues, after exposure to hypertonic potassium nitrate solution, indicated that cells were effectively plasmolysed and that the plasma membrane had retracted from the cell wall (Figure 2.36 B). Confocal images of plasmolysed GFP and PIP2a marker lines showed recordable levels of GFP associated with the retracted cell and the absence of GFP signal on the cell wall side of the membrane (Figure 2.36 B and C). PIP2a hypocotyl cells also showed the formation of hechtian strands composed of fibrillar plasma membrane structures attached to cell wall adhesion sites (Figure 2.36 C and Supplemental Figure SP15).

Examination of confocal images of plasmolysed GFP-EgSUSY1 hypocotyl tissues showed the absence of GFP signal associated with the extracellular matrix (Figure 2.36 D). Similarly modified S11A and S11E fusion proteins were also found to lack association with the

extracellular matrix, yet there was evidence of GFP signal associated with hechtian strands adhering to the cell wall (Figure 2.37).

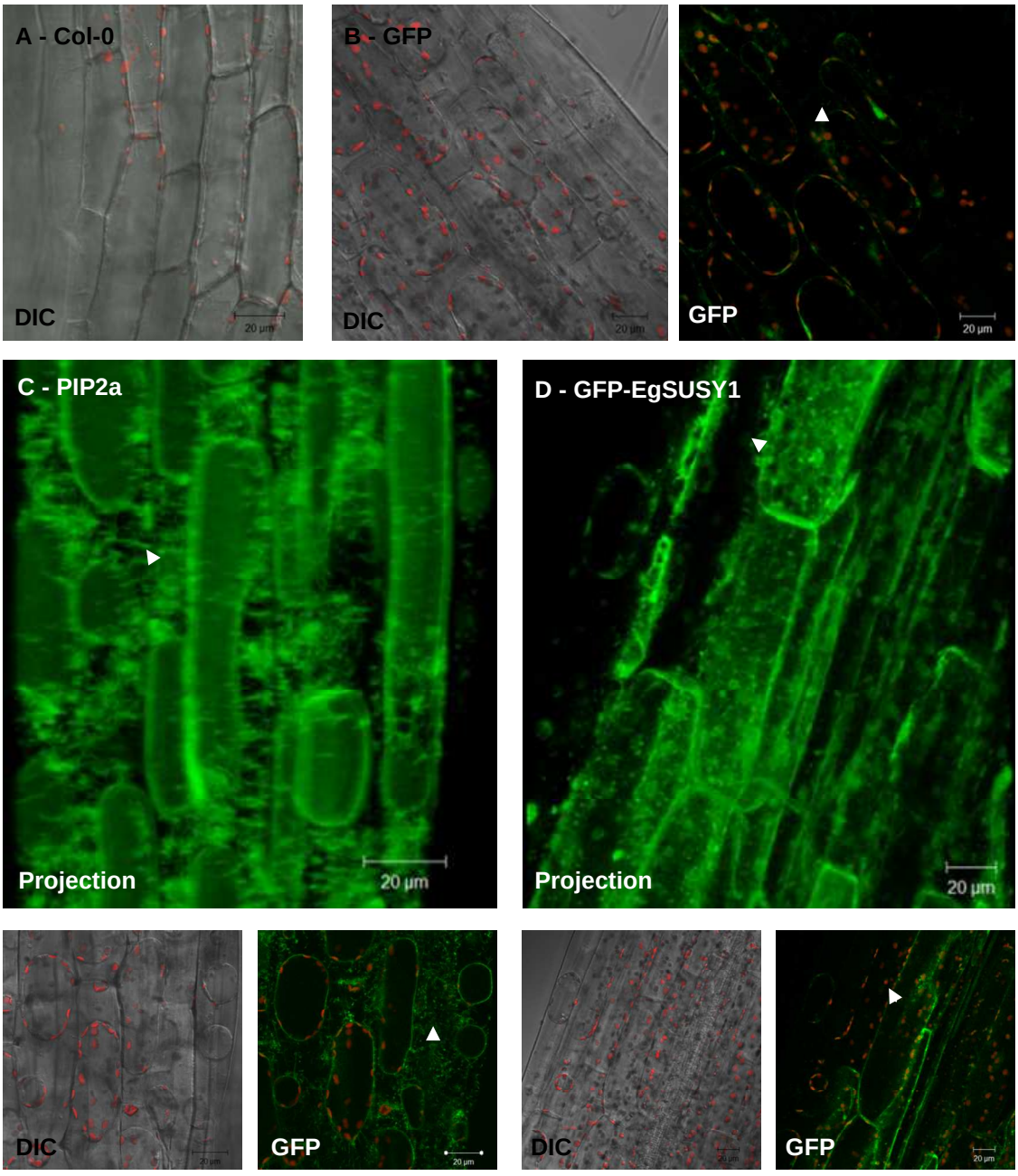

Figure 2.36. Live cell imaging of the subcellular localization and distribution of GFP-EgSUSY1 fusion proteins subcellular markers in plasmolysed *Arabidopsis* hypocotyl cells. (A) Differential Interference Contrast (DIC) images of normal Arabidopsis Col-0 plants before plasmolysis and plant lines after plasmolysis give an indication of the morphology of hypocotyl cells in which the fluorescence signal was found. Confocal live cell images of leaf epidermal cells of *Arabidopsis* plants lines stably

expressing GFP (B), PIP2a (C), and GFP-EgSUSY1 (D).Y-projections through the z-stacks and single focal plane images show no association of the GFP signal with the cell wall. Hechtian strands are indicated by arrows. Chloroplast autofluorescence is indicated in the red channel. Scale bars 20 µm.

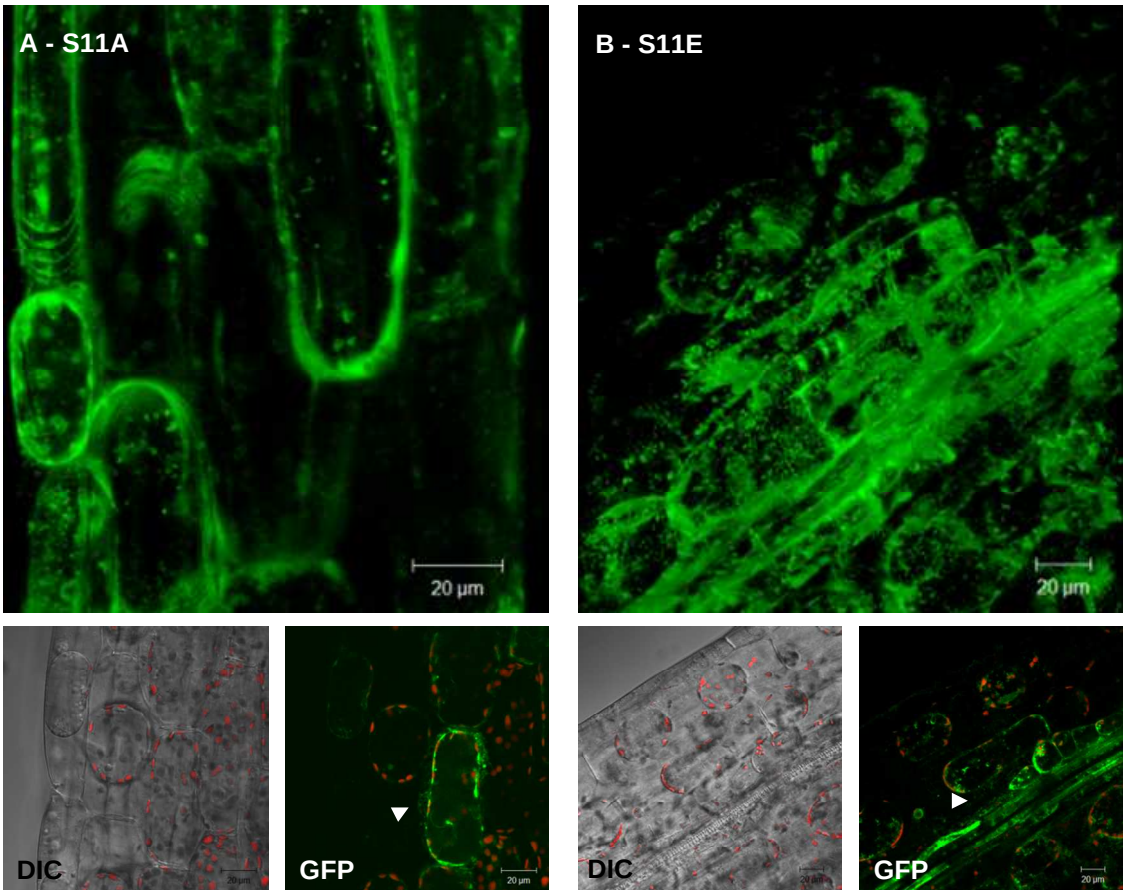

Figure 2.37. Live cell imaging of the subcellular localization and distribution of modified GFP-EgSUSY1 fusion proteins in plasmolysed *Arabidopsis* hypocotyl cells. Confocal live cell images of leaf epidermal cells of *Arabidopsis* plants lines stably expressing S11A (A) and S11E (B). Differential Interference Contrast (DIC) images of Arabidopsis plant lines after plasmolysis give an indication of the morphology of hypocotyl cells in which the fluorescence signal was found. Y-projections through the z-stacks and single focal plane images show no association of the GFP signal with the cell wall. Chloroplast autofluorescence is indicated in the red channel. Hechtian strands are indicated by arrows. Scale bars 20 µm

Computational prediction of the subcellular localization of EgSUSY1-GFP fusions based on amino acid sequence was determined by using YLoc an interpretable web server for predicting subcellular localization (www.multiloc.org/YLoc, (Briesemeister et al., 2010, 2010). Subcellular localization predictions for unmodified EgSUSY1 and modified S11A and S11E were determined based on protein sequences (Query ID:

1b5b124e7ca6d91b88025a9fc70c9e63, Query Date: 03/09/2010 08:26:48, Prediction based on model YLoc-HighRes Plants). These predictions were compared to the respective protein sequences without the induced basal mutations that occurred during cloning of EgSUSY1-GFP expression constructs.

It was predicted that all proteins would be located to the cytoplasm with high probability (between 0.9415 and 0.8654) and high confidence values (between 0.95 and 0.87). It was also noted that the cloning induced background mutations did not change the predicted locations, probability or confidence levels of unmodified and S11E modified EgSUSY1 sequence queries. Predicted values for the modified S11A EgSUSY1 sequence including background mutations dropped in probability from 0.9332 to 0.8654 and a confidence of 0.94 to 0.87 compared to mutation free S11A sequence query. These discrepancies', YLoc continued to predict a strong association of the S11A protein with the cytoplasm.

Table 2.7. Subcellular localization predictions of EgSUSY1-GFP fusions determined using YLoc an interpretable web server for predicting subcellular localization. Query sequences highlighted as +BM include the cloning induced background mutations prevelant in the final expression constructs. Query sequences without the subfix BM were obtained from GenBank (EgSuSy1, GenBank accession number DQ227993.1) and modified according at the eleventh serine residue.

Query Sequence[a]	Predicted Location[b]	Probability[c]	Confidence[d]
EgSUSY1	Cytoplasm	0.9014	strong (0.90)
EgSUSY1+BM	Cytoplasm	0.9014	strong (0.90)
EgSUSY1_S11A	Cytoplasm	0.9332	strong (0.94)
EgSUSY1_S11A+BM	Cytoplasm	0.8654	strong (0.87)
EgSUSY1_S11E	Cytoplasm	0.9415	very strong (0.95)
EgSUSY1_S11E+BM	Cytoplasm	0.9415	very strong (0.95)

a. Name of the sequence extracted from the given fasta format.
b. The most probable subcellular localization(s) predicted by YLoc.
c. The probability of the predicted subcellular localizations(s).
d. The confidence score that the predicted subcellular localizations(s) are correct. Proteins which are typical for YLoc can be predicted with a higher reliability and therefore are assigned with a higher confidence score.

2.4.3. Protein Extraction and Immunoblotting

Total proteins were successfully isolated from the eight transgenic plant lines and untransformed *Arabidopsis thaliana* Col-0 leaf tissue samples. Samples were resolved on a denaturing SDS-PAGE gel and stained using Coomassie Brilliant Blue to reveal protein profiles (Figure 2.38 A and C). Profiles were analysed for the presence of protein bands corresponding to the predicted size of heterologously expressed fusion proteins (Table 2.8). A distinguishable 29 kDa band was observed for the mammalian SF9 cell line corresponding to the size of free eGFP (Figure 2.38 Lane A1). Similar 27 kDa bands were observed for line GFP 6-1 (Figure 2.38 Lane A6) and GFP 7-1 (Figure 2.38 Lane A7) expressing free mGFP6. A single distinguishable 121 kDa band was found exclusively for line GFP-EgSUSY1-S11E 7-2 (Figure 2.38 Lane A5) corresponding to the expected size of an intact mGFP6-EgSUSY1 fusion. No distinguishable bands were visible for EgSUSY1-GFP line 1-5.7 (Lane 2), GFP-EgSUSY1 line 3-1 (Lane 3), GFP-EgSUSY1-S11A line 5-5 (Lane 4), GFP-PIP2a lines Q8-2 (Lane A8 and C7) and Q8-8 (Lane A9 and C8).

Replicas of the total protein SDS-PAGE gels were blotted onto a nitro-cellulose membrane and incubated with primary antibody targeting eGFP (Figure 2.38 B and D). Western Blot profiles revealed a single band approximately 27kDa in size for the mammalian SF9 cell line and GFP lines 6-1 and 7-1 (Figure 2.38 Lanes 1, 6 and B7). This band corresponds to the predicted size of free eGFP and mGFP6 proteins respectively. A single distinguishable 121 kDa band was found exclusively for samples GFP-EgSUSY1-S11A line 5-5 and GFP-EgSUSY1-S11E 7-2 (Figure 2.38 Lanes B4 and 5) corresponding to the expected size of an intact mGFP6-EgSUSY1 fusion. The GFP-PIP2a samples Q8-2 and Q8-8 both showed a multiple banding pattern in the region of 27kDa (Figure 2.38 Lanes B8, D7,

B9 and D8). No distinguishable bands were visible for samples EgSUSY1-GFP line 1-5.7 and GFP-EgSUSY1 line 3-1 (Figure 2.38 Lanes 2 and 3).

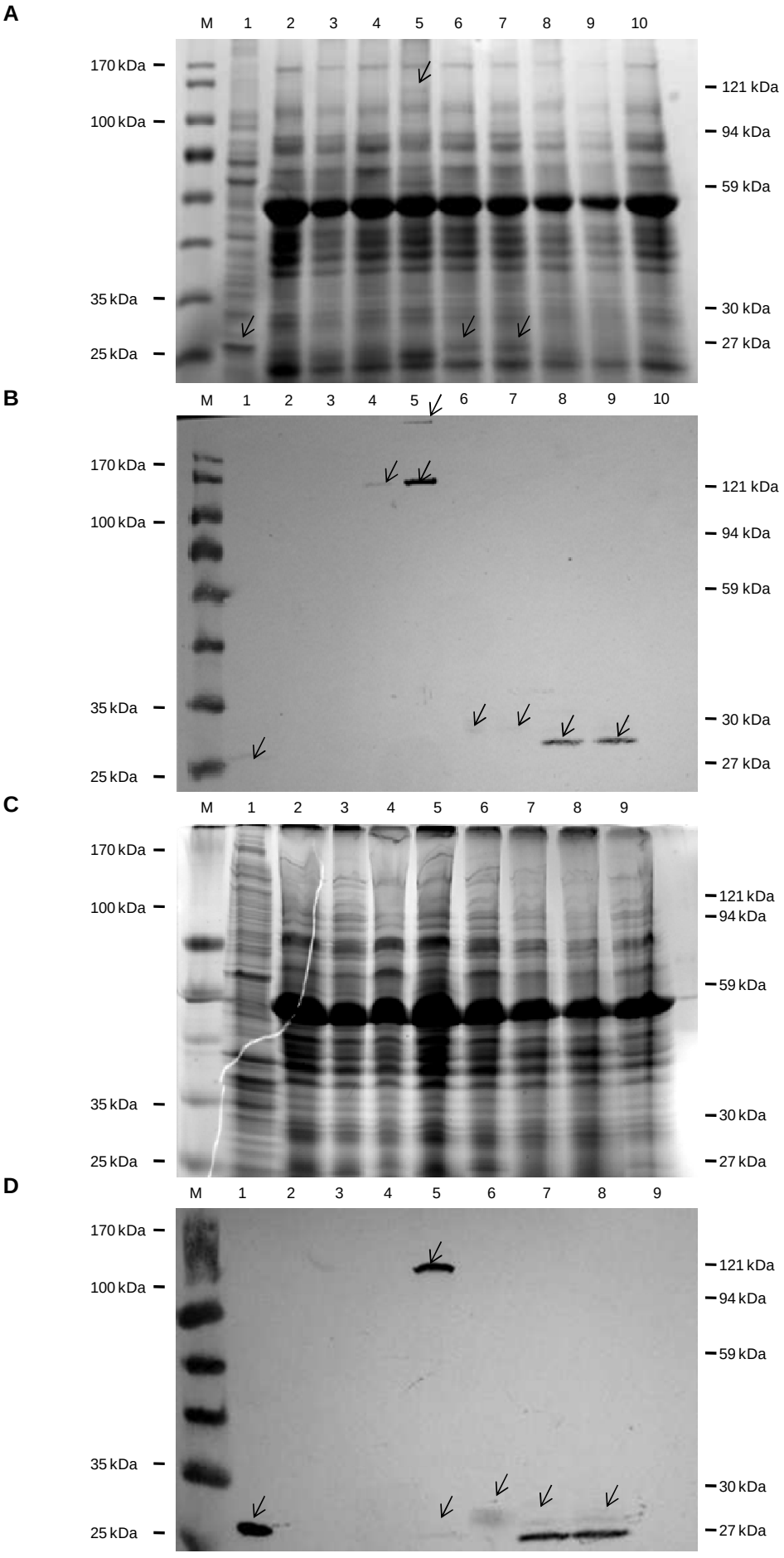
A
M 1 2 3 4 5 6 7 8 9 10
170 kDa
100 kDa
35 kDa
25 kDa
121 kDa
94 kDa
59 kDa
30 kDa
27 kDa
B
M 1 2 3 4 5 6 7 8 9 10
170 kDa
100 kDa
35 kDa
25 kDa
121 kDa
94 kDa
59 kDa
30 kDa
27 kDa
C
M 1 2 3 4 5 6 7 8 9
170 kDa
100 kDa
35 kDa
25 kDa
121 kDa
94 kDa
59 kDa
30 kDa
27 kDa
D
M 1 2 3 4 5 6 7 8 9
170 kDa
100 kDa
35 kDa
25 kDa
121 kDa
94 kDa
59 kDa
30 kDa
27 kDa

Figure 2.38. SDS-PAGE and Western Blot profiles of proteins extracted from wild-type (Col-0) and transgenic GFP fusion *Arabidopsis thaliana* plant lines. A and C, Coomassie Brilliant Blue-stained gels representing total proteins; the arrowheads indicate bands that seem to be exclusive to the transgenic GFP fusion lines. B and D, Western Blot detection of heterologously expressed GFP fusion proteins using an anti-eGFP primary antibody. Eight different samples representing the final positive transgenic plant lines are shown: EgSUSY1-GFP line 1-5.7 (Lane 2), GFP-EgSUSY1 line 3-1 (Lane 3), GFP-EgSUSY1-S11A line 5-5 (Lane 4) and GFP-EgSUSY1-S11E line 7-2 (Lane 5), GFP lines 6-1 (Lane 6) and 7-1 (Lane A/B7) and GFP-PIP2a lines Q8-2 (Lane A/B8 and C/D7) and Q8-8 (Lane A/B9 and C/D8) . Lane 1 is a protein sample from mammalian SF9 cell line expressing free eGFP used as a positive control for antibody detection. Lane A/B10 and C/D9 contains an untransformed Arabidopsis Col-0 control. Lane M is a prestained protein size standard (Fermentas).

Table 2.8. Summary of the predicted molecular weight, size and number of amino acids found within heterologously expressed proteins in transgenic *Arabidopsis thaliana* plants. Protein parameters were calculated using the ProtParam tool of the ExPASy Proteomics Server, Swiss Institute of Bioinformatics.

Protein[a]	Number of Amino Acids[b]	Molecular Weight g/mole[c]	Size (kDa)[d]
mGFP6	240	26952.3	27
eGFP	265	29256.0	29
EgSUSY1	805	92685.2	92
PiP2a	287	30474.2	30
mGFP6-EgSUSY1	1062	121491.7	121
EgSUSY1-mGFP6	1077	123413.9	123
eGFP-PIP2a	552	59712.2	59

a. The protein identity of the FASTA sequence queried using the ProtParam tool of the ExPASy Proteomics Server.
b. The determined number of amino acids found within the queried proteins.
c. The predicted molecular weight in grams per mole based on the amino acid sequence of the respective proteins.
d. The size of the protein in kiloDaltons used for the identification of protein bands on SDS-PAGE and western blots.

Total protein (C) samples were separated into soluble (S) and membrane (M) fractions to determine whether heterologously expressed proteins were soluble or membrane associated. Equal volumes of each fraction were resolved and analysed on a SDS-PAGE gel (Figure 2.39 A and C) followed by blotting on a nitrocellulose membrane and immunolabelling with an anti-eGFP primary antibody (Figure 2.39 B and D). A clear 29 kDa band was seen for control mammalian Sf9 cells expressing free eGFP in SDS-PAGE gels and immunoblots (Figure 2.39 Lane 1). GFP-PIP2a samples Q8-2 and Q8-8 were included as positive controls for membrane localization. Multiple bands were found in the soluble fractions in the region of 27 kDa and a single band of approximately 40 kDa was found in the membrane fraction (Figure 2.39 Lanes B2 and D7). GFP samples 6-1 and 7-1 were included as positive controls for cytoplasmic localization. A band approximately 27 kDa in size corresponding to the expected size of mGFP6 was found in the soluble fraction of sample 7-1 but was absent from membrane fractions (Figure 2.39 Lane B3). A 121 kDa band was found in the soluble fraction of GFP-EgSUSY1 line 3-1, but not in the membrane fraction (Figure 2.39 Lane B4). The GFP-EgSUSY1-S11E 7-2 had 121 kDa bands in both soluble and membrane fractions and an additional 27 kDa band in the soluble fraction (Figure 2.39 Lane B5 and D7). No bands were found for EgSUSY1-GFP line 1-5.7, GFP-EgSUSY1-S11A line 5-5 and GFP lines 6-1 (Figure 2.39).

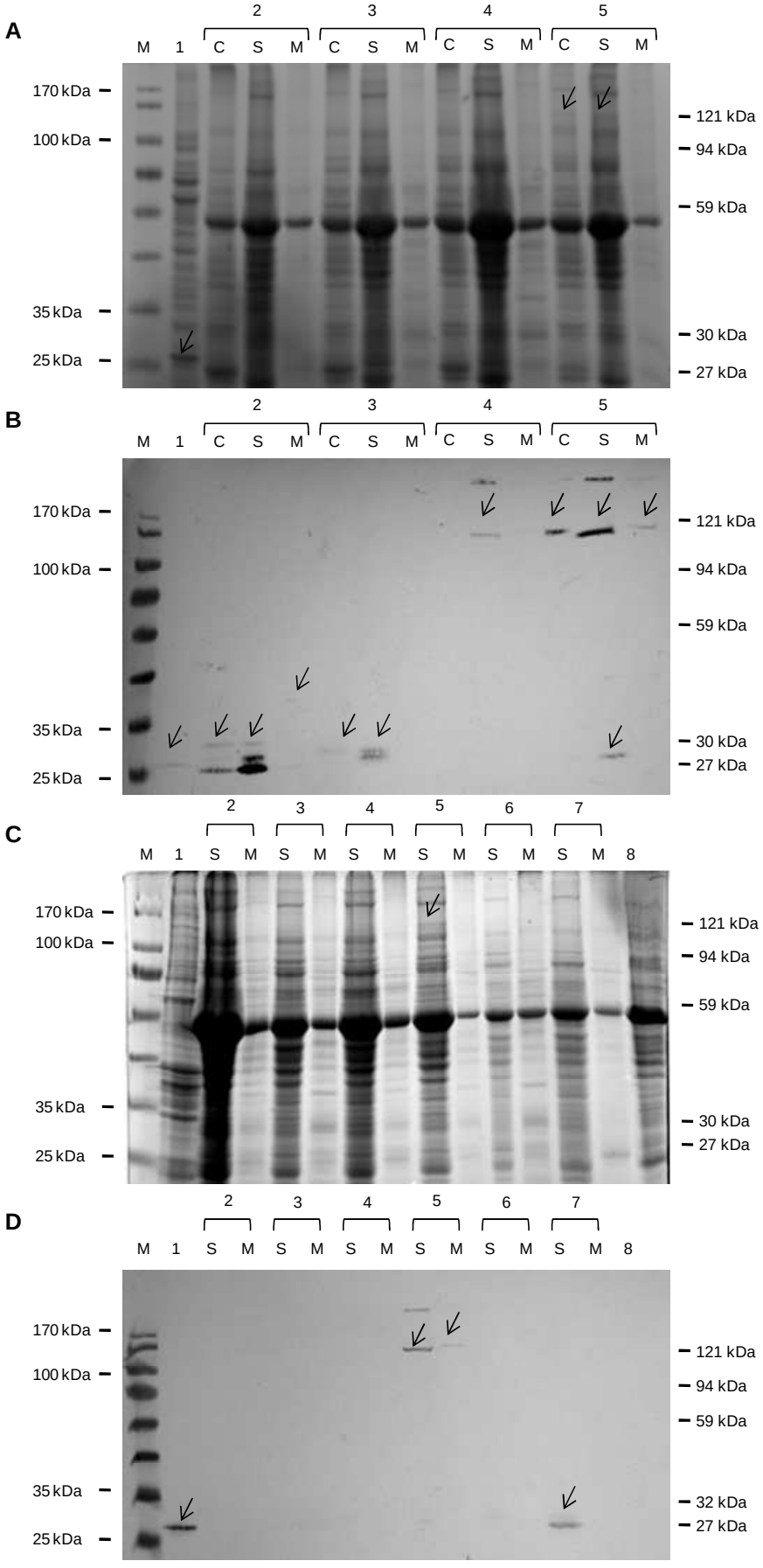
A
2
3
4
5
M 1 C S M C S M C S M C S M
170 kDa
100 kDa
35 kDa
25 kDa
121 kDa
94 kDa
59 kDa
30 kDa
27 kDa
B
2
3
4
5
M 1 C S M C S M C S M C S M
170 kDa
100 kDa
35 kDa
25 kDa
121 kDa
94 kDa
59 kDa
30 kDa
27 kDa
C
2
3
4
5
6
7
M 1 S M S M S M S M S M S M S M 8
170 kDa
100 kDa
35 kDa
25 kDa
121 kDa
94 kDa
59 kDa
30 kDa
27 kDa
D
2
3
4
5
6
7
M 1 S M S M S M S M S M S M S M 8
170 kDa
100 kDa
35 kDa
25 kDa
121 kDa
94 kDa
59 kDa
32 kDa
27 kDa

1

Figure 2.39. SDS-PAGE and Western blot profiles of soluble and membrane fractions separated by ultracentrifugation. A and C, Coomassie Brilliant Blue-stained gels representing total proteins; the arrowheads indicate bands that seem to be exclusive to the transgenic GFP fusion lines. B and D, Western Blot detection of heterologously expressed GFP fusion proteins using an anti-eGFP primary antibody. Eight different samples representing the final positive transgenic plant lines are shown: EgSUSY1-GFP line 1-5.7 (Lane C/D2), GFP-EgSUSY1 line 3-1 (Lane A/B4 and C/D3), GFP-EgSUSY1-S11A line 5-5 (Lane C/D4) and GFP-EgSUSY1-S11E line 7-2 (Lane 5), GFP lines 6-1 (Lane C/D6) and 7-1 (Lane A/B3) and GFP-PIP2a lines Q8-2 (Lane A/B2) and Q8-8 (Lane C/D7) . These samples were separated into two fractions (S) soluble fraction and (M) membrane fraction. Lanes indicated by (C) represent unfractionated crude protein extracts. Equal volumes of each fraction were loaded on SDS-PAGE gels. Lane 1 is a total cell lysate of mammalian SF9 cells expressing free eGFP used as a positive control for antibody detection. Lane 8 contains an untransformed *Arabidopsis* Col-0 control and Lane M is a prestained protein size standard (Fermentas).

2.5. Discussion

This study investigated the subcellular localization of unmodified and modified GFP-EgSUSY1 fusion proteins constitutively expressed in the dicot model plant *Arabidopsis thaliana*. Transgenic Col-0 plant lines heterologously expressing GFP-EgSUSY1 fusion proteins, were generated using Gateway cloning technology (Curtis and Grossniklaus, 2003) and *Agrobacterium* mediated plant transformation (Clough and Bent, 1998). The final transgenic plant lines were imaged using a Laser Scanning Confocal Microscope (CLSM) to determine the subcellular localization patterns of the GFP-EgSUSY1 fusion proteins in comparison with cytoplasmic and plasma membrane marker lines. Three plant tissues were imaged concurrently namely roots, leaf epidermis and hypocotyls. Single optical plane images, z-stack projections and time series confocal images were obtained to accurately deduce protein localization patterns. Hypocotyl tissues were also exposed to osmotic stress, and plasmolysed samples were imaged to determine whether GFP-EgSUSY1 fusions possessed an extracellular matrix associated component.

In addition to standard CLSM, quantitative and qualitative colocalization analysis was performed utilizing the Manders Coefficients Plugin (Manders et al., 1993) in the ImageJ public domain image processing software (http://rsbinfo.nih.gov.ij/). FM4-64 membrane

specific stain was used as a membrane marker with which colocalization of the GFP-fusions was established. To elucidate microscopy findings further, *in silico* prediction of the subcellular localization of GFP-EgSUSY1 fusions based on amino acid sequence was determined using YLoc (www.multiloc.org/YLoc, Briesemeister et al., 2010, 2010). Finally isolated GFP-EgSUSY1 proteins were resolved using SDS-PAGE and immediately imaged using Coomassie blue stain (Sambrook and Russel, 2001) or immunoblotted with Ant-GFP N-terminal primary antibody following membrane fractionation.

Two modified versions of the EgSUSY1 protein, EgSUSY1-S11A and EgSUSY1-S11E were analysed in parallel. It has been suggested in other plant species that a conserved N-terminal serine residue in sucrose synthase plays an integral role in the subcellular localization and thus functional regulation of sucrose synthase (Huber et al., 1996; Zhang and Chollet, 1997; Hardin et al., 2004). We hypothesised that the site directed modification of EgSUSY1 at this conserved eleventh serine residue to an alanine residue (EgSUSY1-S11A) or glutamate residue (EgSUSY1-S11E) would shift the subcellular localization of EgSUSY1 to the plasma membrane or cytoplasm, respectively. The functional ramifications of these modifications were investigated in a parallel M.Sc. study by Mr. M. M. Mphahlele (University of Pretoria, Pretoria) through the constitutive expression of the modified EgSUSY1 proteins in *Arabidopsis* plants, followed by chemical analysis and phenotypic characterisation.

Findings in this study (Table 2.9) point to the peripheral localization of modified and unmodified GFP-EgSUSY1 proteins with a prominent cytoplasmic component. No evidence was found for the localization of modified or unmodified GFP-EgSUSY1 proteins within the extracellular matrix. The current study did not establish nor negate plasma membrane association of any of the GFP-EgSUSY1 fusion proteins despite extensive microscopy

analysis and supporting SDS-PAGE, immunoblotting and *in silico* localization predictive methodologies.

Table **2.**9. Summary of the subcellular localization of GFP-EgSUSY1 proteins ectopically expressed in *Arabidopsis*.

Protein[a]	Subcellular localization[b]	Schematic representation[c]
GFP	Cytoplasmic distribution with a noticeable presence in the nucleus which was expected of free GFP. Colocalization analysis proved to be confounding as there was a high degree of colocalization with membrane marker FM4-64 and colocalization coefficients suggested membrane association.	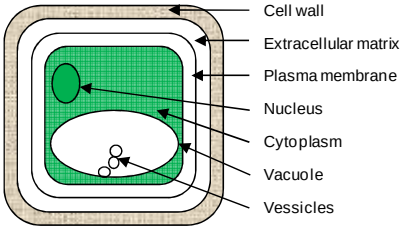
PIP2a	Confocal images showed a smooth surface topology typical of membrane association. Colocalization analysis proved to be contradicting as there was very little overlap with FM4-64 and colocalization coefficients suggested cytosol association. The presence of multiple bands in the soluble fractions of western blots also suggests that this fusion protein is degraded during plant protein isolations.	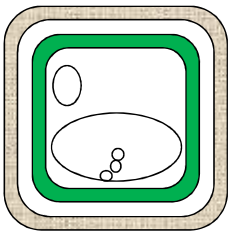
GFP-EgSUSY1	Confocal images supported a typical cytoplasmic distribution of the protein although there was a strong colocalized component suggesting that that the fusion protein is either directly or indirectly associated with the plasma membrane.	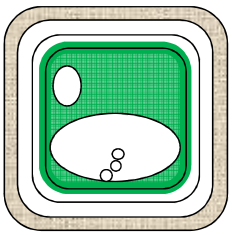
S11A	This fusion protein had very high observable levels of expression. The cellular distribution was similar to that of unmodified GFP-EgSUSY1 constructs with cytoplasmic distribution and a noticeable concentration of the signal at the plasma membrane. S11A was also found to be strongly associated with vesicles trafficking through the vacuolar space.	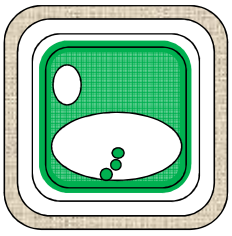

S11E	S11E had the highest observed expression of all of the fusion constructs studied. This protein was found to be associated with the cytoplasmic compartments of the cell. The scatterplot generated pointed to partial colocalization of the protein with the plasma membrane. Quantitative colocalization coefficients gave very high statistical support for association of this protein with the plasma membrane.	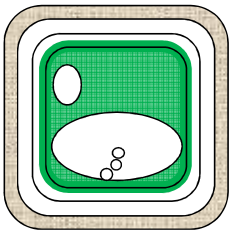
EgSUSY1-GFP	EgSUSY1-GFP had very low levels of expression which confounded further localization analysis. All lines of evidence pointed to a very weak association with the cytosol but a very strong association with the plasma membrane.	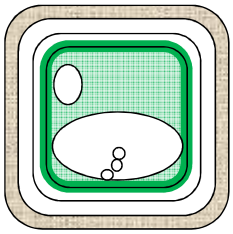

a. The fusion protein under investigation. Details of construct design can be found in Figure 2.23.

b. A brief description of the assumptive subcellular localization based on the cumulative findings in this study.

c. Schematic model of the subcellular localization of fusion proteins investigated.

2.2.1. Constitutive expression of EgSUSY1-GFP fusion proteins in *Arabidopsis thaliana*

Expression of GFP-EgSUSY1 fusion proteins was confirmed for all transgenic lines (EgSUSY1-GFP line 1-5.7, GFP-EgSUSY1 line 3-1, GFP-EgSUSY1-S11A line 5-5, GFP-EgSUSY1-S11E line 7-2, GFP lines 6-1 and 7-1, GFP-PIP2a lines Q8-2 and Q8-8 compared to untransformed *Arabidopsis* Col-0 plants as a negative control) at the transcriptional and translational level. Screening of transformants confirmed the incorporation of the transgenes into the genome of *Arabidopsis thaliana* plant lines (Figure 2.19) and the stable propagation of the transgenes in subsequent generations of the particular lines (Figure 2.20). RT-PCR analysis confirmed that the incorporated transgenes were fully transcribed into mRNA (Figure 2.21 and Figure 2.22). Translation of mRNA transcripts to protein was confirmed through CLSM imaging of recordable GFP emission levels in all transgenic lines (Figure 2.25) as

well as the presence of a 121 kDa band in Western blots (Figure 2.38 and Figure 2.39) corresponding to the predicted size of the GFP-EgSUSY1 chimeric proteins (Table 2.8).

Sequence analysis of the *GFP-EgSuSy1* transgenes (Supplemental Figure S6 and Figure S7) identified a number of background mutations other than the intended modification at the conserved eleventh serine residue. None of these were nonsense mutations which would have resulted in the truncation of the protein product (Supplemental Figure S7). Nonsynonymous mutations were analyzed for physiochemical differences compared to original amino acid (Supplemental Figure S8), conservation (Supplemental Figure S9 and S10) and effect on secondary structure predictions (Supplemental Figure S11 and Table S1) *in silico*.

It was found that a missense (L636P) mutation occurred in the conserved catalytic C-terminal region (amino acid 546 to 753) representing the glycosyltransferase active region (Supplemental Table S1,(Baud et al., 2004)). This PCR induced mutation was restricted to *EgSuSy1* Clone N22 which was used to create the N-terminal EgSUSY1-GFP plant line (P1-5.7). This line was used to determine whether there was any variation in the localization pattern induced by the terminal position of the GFP fusion protein. No PCR-induced background mutations were found in the conserved N-terminal non-catalytic phosphorylation domain (amino acid 8 to 17). It was also found that computational prediction of the subcellular localization of EgSUSY1-GFP fusions based on amino acid sequence using YLoc (www.multiloc.org/YLoc, (Briesemeister et al., 2010, 2010) was not altered by the incorporation of these background mutations (Table 2.7).

It was also found that the overexpression of identical (with the same PCR induced background mutations) unmodified *EgSuSy1* and modified EgSuSy1-S11A transgenes in *Arabidopsis* plants during a parallel M.Sc. study by Mr. M. M. Mphahlele (University of

Pretoria, Pretoria) showed increased growth and biomass of the transgenic plants compared to wild-type plants. This finding is consistent with the overexpression phenotype observed by Coleman, (2006) in transgenic tobacco lines overexpressing cotton SUSY, suggesting that the unmodified EgSuSy1 and the modified EgSuSy1-S11A proteins form functional sucrose synthase catalytic units despite the induced background mutations. Regardless of the above findings, the physiological effect of the mutations on the functionality and subcellular localization of EgSuSy1 is yet to be established.

Numerous positive transformants were generated yet only a single plant line, per transgenic event, showed recordable GFP expression levels (Figure 2.25). These findings are in accordance with a study by Cutler, (2000) who recorded an observed *Agrobacterium* mediated transformation rate of ~0.5–4% with only 0.1–1% of these transformed plants expressing GFP at recordable levels. Low emission intensities of the chosen intrinsically fluorescent protein, mGFP6, the imaging setup (Supplemental Figure SP4) enabled the localization of GFP fusions with no recordable cross talk between the GFP and FM4-64 emission spectra and low levels of observed photobleaching even during time series acquisitions of a single optical plane (Supplemental Figure SP12 and Figure SP14).

GFP is a 27 kDa protein which readily diffuses throughout the cytoplasm and into the nucleus of plant cells (Hanson and Köhler 2001). When fused to the 92 kDa EgSUSY1 protein, the resulting chimera is incapable of diffusing into the nucleus (Table 2.8). Therefore accumulation in the nucleus of fusion proteins can only occur through the active process of nuclear import. EgSUSY1 lacks nuclear import signalling peptides and therefore should not be found in the nucleus (Table 2.7). Only the cytoplasmic marker GFP line (P3-1) expressing free mGFP6 showed evidence of nuclear localization of the GFP signal (Figure 2.29). The remaining transgenic lines showed an absence of GFP signal in the vicinity of the nucleus

(Figure 2.29 and Figure 2.30). These findings suggest that all GFP-EgSUSY1 fusion lines as well as the PIP2a membrane marker line expressed intact fusion proteins.

Western blot analyses supported the expression of intact EgSUSY1-GFP fusions due to the presence of a 121kDa fragment (Figure 2.38and Figure 2.39). Indirect localization predictions based on these findings remained inconclusive as the membrane PIP2a control failed to be isolated without degradation resulting in the absence of an intact 59kDa control band in membrane fractions. There was however evidence of a 121kDa band in the membrane fractions of GFP-EgSUSY1-S11E (Figure 2.39).

2.2.2. EgSUSY1-GFP fusion proteins localize to the cell periphery with strong evidence of cytoplasmic association

To determine the subcellular localization and distribution of GFP-EgSUSY1 fusions; various transgenic and reference plant lines were imaged using a Laser Scanning Confocal Microscope. Confocal images of live plant tissues of modified and unmodified GFP-EgSUSY1 fusion lines all revealed a concentration of the GFP signal associated with the cell periphery (Figure 2.24, Figure 2.25, Figure 2.27 and Figure 2.28). On closer observation of hypocotyls cells it was found that this peripheral signal took on a unique topology typical of cytoplasmic localization (Figure 2.34 and Figure 2.35). This pattern was previously documented in a study by Cutler (2000) and is characterized by variations in cytoplasmic thickness, cytoplasmic invaginations, transvacuolar columns and a dynamic surface pattern (which often looks bubbly in nature) due to constant remodelling of the cytoplasm via cytoplasmic streaming. The temporal dynamics of this cytoplasmic streaming was also observed in time series animations of GFP-EgSUSY1 fusion plants (Supplemental Figure SP12. and Supplemental Figure SP14).

It was also observed that GFP-EgSUSY1-S11A plant lines showed high levels of fluorescence associated with trafficking vesicles in the cell vacuole. Novel vesicles found trafficking CESA subunits between the golgi and the cell periphery have been under much investigation (Wightman and Turner, 2010). These vesicles also known as compartments (SmaCCs; Gutierrez et al., 2009) or microtubule associated cellulose synthase compartments (MASCs; Crowell et al., 2009) function in the regulation of cellulose biosynthesis remains unknown. Should the vesicles GFP-EgSUSY1-S11A was found to associated with be these SmaCC's then the putative association of SuSy with CESA does not only occur at the plasma membrane as previously thought but occurs as early as the packaging of CESA's into vesicles at the golgi.

Cytoplasmic localization of GFP-EgSUSY1 chimeras was supported by *in silico* subcellular localization predictions based on amino acid sequence determined using YLoc (Table 2.7, www.multiloc.org/YLoc, (Briesemeister et al., 2010, 2010) These findings are consistent with a recent study by Baroja-Fernández (2009) who observed the cytoplasmic localization of sucrose synthase (SUS4) when constitutively expressed in *Solanum tuberosum* when fused to the N-terminus of GFP.

2.2.3. The investigation of the plasma membrane association of EgSUSY1

A number of independent studies have provided indirect evidence of the increase in the occurrence of sucrose synthase in the membrane fraction of plant tissues due to the inhibition of phosphorylation at the conserved N-terminal serine residue (Winter et al., 1997; Zhang et al., 1999; Anguenot et al., 2006). To date there has not been any direct evidence linking the phosphorylation status of sucrose synthase to its membrane affiliation (Hardin et al., 2004). To ascertain whether the modified EgSUSY1 fusion proteins, S11A and S11E, showed

differential association with the plasma membrane, quantitative and qualitative colocalization analyses were performed.

Qualitative colocalization was achieved through imaging FM4-64 stained leaf epidermal cells. Colocalized pixels were visualized as yellow pixels in merged confocal images and as a scatter plot indicating the generated pattern of colocalization. It was found that transgenic GFP-EgSUSY1 lines including the GFP line, which was used as a cytosolic marker line, showed varying degrees of colocalization with the membrane stain FM4-64 (Figure 2.31, Figure 2.33). Notably the N-terminal EgSUSY1-GFP line showed high levels of membrane colocalization. The inability to generate typical complete colocalization and exclusive localization patterns for the PIP2a membrane marker and GFP cytosolic marker respectively could be due to a number of technical and biological parameters.

The first parameter to consider is the unique architecture of plant cells, especially leaf epidermal cells, which contain a large vacuole that compresses the cytoplasm of the cell against the cell membrane (Figure 2.26). This coupled with the resolution limit of confocal microscopy, which can at best resolve molecules further than 200 nm apart, can result in proteins which are cytosolic in nature generating a pseudo membrane component in qualitative colocalization experiments (Lalonde et al., 2008). A review by Lalonde *et. al.* (2008) calculated that approximately 140 000 GFP molecules could fit into the resolution volume of conventional light microscopy. Therefore it is easy to assume that many different protein dynamics could result in the colocalization of confocal image pixels. Additional parameters that could have contributed to the unexpected and variable colocalization results include variability in FM-4-64 staining ((Jelínková et al., 2010)), fluorophore intensity variation, noise, and background chloroplast autofluorescence.

These findings were paralleled by quantitative colocalization which also observed unexpected high levels of colocalization in the cytosolic GFP marker line compared to that of the membrane PIP2a marker line (Table 2.6). An evaluation of the above results suggest that the determination of colocalization patterns of two fluorophores based on quantitative and qualitative colocalization can be ambiguous and therefore findings should be supported by alternative methodologies. This is especially true in the current scenario where cytosolic localization and mixed cytosolic-membrane localization are visually indistinguishable at the level of confocal imaging.

To conclude EgSUSY1 may be cytoplasmic and membrane associated, with the ratio dependent on cellular dynamics. EgSUSY1 may associate and move with the CESA rossetes, during which time it would be membrane bound, but then dynamically be disassociated and still have a peripheral localization.

2.2.4. EgSUSY1-GFP fusion proteins are excluded from the extracellular matrix during osmotic stress

To determine if GFP-EgSUSY1 chimeras possessed an extracellular matrix component, hypocotyl cells of all plant lines were plasmolysed by incubating seedlings in a hypertonic solution of potassium nitrate. During plasmolysis cells are exposed to a negative osmotic potential causing the loss of water from cells and therefore retraction of the plasma membrane from the cell wall. It was observed that all GFP-EgSUSY1 fusion lines showed the absence of GFP signal associated with the cell wall following plasmolysis (Figure 2.36 and Figure 2.37).

During plasmolysis the plasma membrane remains attached to the cell wall at adhesion sites causing the formation of fibrillar membrane structures called hechtian threads

or strands (Pringsheim, 1854; Nägeli, 1855). These strands, although mostly composed of plasma membrane, have been found to contain residual amounts of cytoplasm and therefore cannot be used as indicators of plasma membrane localization (Drake et al., 1978; Attree and Sheffield, 1985). Although this method was inconclusive in distinguishing between cytoplasmic and membrane localization the lack of GFP signal outside of plasmolysed cells, proves that the GFP-EgSUSY1 fusion constructs are not associated with the extracellular matrix or cell wall.

2.6. Conclusions

The subcellular localization of modified S11A and S11E GFP-EgSUSY1 fusions revealed that both proteins were localized to the cell periphery in various *Arabidopsis* tissues. In addition to cell peripheral localization it was established that modified GFP-EgSUSY1 fusions showed association with the cytoplasm, but were absent from the extracellular matrix and the cell wall. This observed cellular localization is typical of wildtype sucrose synthase (Baroja-Fernández et al., 2009). The current study did not establish nor negate plasma membrane association of any of the GFP-EgSUSY1 fusion proteins despite extensive microscopy analysis and supporting SDS-PAGE, immunoblotting and *in silico* localization predictive methodologies. There were also no distinguishable differences in the localization patterns of the modified GFP-EgSUSY1 fusions when compared to each other or unmodified GFP-EgSUSY1 chimeras.

This study does not provide support for the hypothesis that the site directed modification of EgSUSY1 at this conserved eleventh serine residue to an alanine residue (EgSUSY1-S11A) or glutamate residue (EgSUSY1-S11E) would shift the subcellular localization of EgSUSY1 to the plasma membrane and cytoplasm, respectively. However, it

does not provide support against the alternative hypothesis that regulation of EgSUSY1 cellular localization is governed by alternative physiological mechanisms that exclude phosphorylation at the conserved N-terminal serine residue.

Better understanding of sucrose synthase regulation will greatly benefit the agricultural industry as this enzyme plays a key role in the channelling of sugar monomers to several sink tissue associated polymers such as starch and cellulose. It is required that further *in planta* studies be performed to answer the underlying enigmas surrounding the regulation of EgSuSy1 and the channelling of UDP-glucose generated by sucrose synthase to various cellular processes. Questions that need to be addressed are: What is the underlying mechanism of membrane association of sucrose synthase? What is the nature of the association (direct or indirect) of sucrose synthase with the membrane and the cellulose synthase complex? And how could one manipulate the regulation of sucrose synthase through genetic engineering to shift sugar monomer channelling to a specific polymer biosynthesis such as cellulose biosynthesis? Hypotheses that could explain the observations made in this study and recommendations for future studies in this field are proposed in the Concluding Remarks section of this dissertation.

2.7. References

Amor Y, Haigler CH, Johnson S, Wainscott M, Delmar DP (1995) A membrane-associated form of sucrose synthase and its potential role in synthesis of cellulose and callose in plants. Plant Biology **92:** 9353-9357

Anguenot R, Nguyen-Quoc B, Yelle S, Michaud D (2006) Protein phosphorylation and membrane association of sucrose synthase in developing tomato fruit. Plant Physiology and Biochemistry **44:** 294–300

Anguenot R, Nguyen-Quoc, B., Yelle, S., and Michaud, D. (2006) Protein phosphorylation and membrane association of sucrose synthase in developing tomato fruit. Plant Physiology and Biochemistry **44:** 294-300

Attree SM, Sheffield E (1985) Plasmolysis of *Pteridium* protoplasts: a study using light and scanning-electron microscopy. Planta **165:** 151–157

Baroja-Fernández E, Muñoz FJ, Montero M, Etxeberria E, Sesma MT, Ovecka M, Bahaji A, Ezquer I, Li J, Prat S, Pozueta-Romero J (2009) Enhancing Sucrose Synthase Activity in Transgenic Potato (Solanum tuberosum L.) Tubers Results in Increased Levels of Starch, ADPglucose and UDPglucose and Total Yield. Plant Cell Physiology **50:** 1651–1662

Barratt DHP, Barber, L., Kruger, N.J., Smith, A.M., Wang, T.L., and Martin, C. (2001) Multiple, distinct isoforms of sucrose synthase in Pea. *Plant Physiology* **127:** 655-664

Baud S, Vaultier MN, Rochat C (2004) Structure and expression profile of sucrose synthase multigene family in Arabidopsis. Journal of Experimental Botany **55:** 396-409

Bernard P, Couturier M (1992) Cell killing by the F plasmid CcdB protein involves poisoning of DNA-topoisomerase II complexes. Journal of Molecular Biology **226:** 735-745

Bolte S, Cordelieres FP (2006) A guided tour into subcellular colocalization analysis in light microscopy. Journal of Microscopy **224:** 213–232

Briesemeister S, Rahnenführer J, Kohlbacher O (2010) Going from where to why - interpretable prediction of protein subcellular localization. Bioinformatics **26:** 1232-1238

Briesemeister S, Rahnenführer J, Kohlbacher O (2010) YLoc - an interpretable web server for predicting subcellular localization. Nucleic Acids Research **38:** W497-W502

Carlson SJ, Chourey PS, Helentjaris T, Datta R (2002) Gene expression studies on developing kernels of maize sucrose synthase (SUSY) mutants show evidence for a third SUSY gene. Plant Molecular Biology **49:** 15-29

Chourey PS, Taliercio, E.W., Carlson, S.J., and Ruan, Y.L. (1998) Genetic evidence that the two isoenzymes of sucrose synthase present in developing maize endosperm are critical, one for cell wall integrity and the other for starch biosynthesis Molecular and General Genetics **259:** 88-96

Clough SJ, Bent AF (1998) Floral Dip: a simplified method for Agrobacterium-mediated transformation of *Arabidopsis thaliana*. The Plant Journal **16:** 735-743

Coleman HD, Ellis DD, Gilbert M, Mansfield SD (2006) Up-regulation of sucrose synthase and UDP-glucose pyrophosphorylase impacts plant growth and metabolism. Plant Biotechnology Journal **4:** 87–101

Coleman HD, Yan J, Mansfield SD (2009) Sucrose synthase affects carbon partitioning to increase cellulose production and altered cell wall ultrastructure. Proceedings of the National Academy of Sciences **106:** 13118

Crowell EF, Bischoff V, Desprez T, Rolland A, Stierhof YD, Schumacher K, Gonneau M, Hofte H, Vernhettes S (2009) Pausing of Golgi bodies on microtubules regulates secretion of cellulose synthase complexes in Arabidopsis. Plant Cell **21:** 1141-1154

Curatti L, and Giarrocco, L.E., Cumino, A.C., and Salerno, G.L. (2008) Sucrose synthase is involved in the conversion of sucrose to polysaccharides in filamentous nitrogenifixing cyanobacteria. *Planta* **228:** 617-625

Curtis M, Grossniklaus U (2003) A Gateway Cloning Vector Set for High-Throughput Functional Analysis of Genes in Planta. Plant physiology **133:** 462–469

Cutler SR, Ehrhardt DW, Griffitts JS, Somerville CR (2000) Random GFP::cDNA fusions enable visualization of subcellular structures in cells of *Arabidopsis* at a high frequency. Proceedings of the National Academy of Sciences **97:** 3718–3723

De´jardin A, Rochat C, Wuille`m S, Boutin J-P (1997) Contribution of sucrose synthase, ADP-glucose pyrophosphorylase and starch synthase to starch synthesis in developing pea seeds. Plant Cell Environment **20:** 1421–1430

DeBlasio SL, Sylvester AW, Jackson D (2010) Illuminating plant biology: using fluorescent proteins for high-throughput analysis of protein localization and function in plants. Briefings in functional genomics **9:** 129-138

Drake G, Carr DJ, Anderson WP (1978) Plasmolysis, plasmodesmata, and the electrical coupling of oat coleoptile cells. Journal of Experimental Botany **29:** 1205–1214

Duncan KA, Huber SC (2007) Sucrose synthase oligomerization and F-actin association regulated by sucrose concentration and phosphorylation. Plant and Cell Physiology **48:** 1612-1623

Fu H, and Park, W.D. (1995) Sink- and vascular-associated sucrose synthase functions are encoded by different genes classes in potato. *The Plant Cell* **7:** 1369-1385

Gasteiger E, Hoogland C, Gattiker A, Duvaud S, Wilkins MR, Appel RD, Bairoch A (2005) Protein identification and analysis tools on the ExPASy server. *In* JM Walker, ed, The Proteomics Protocols Handbook. Humana Press, pp 571-607

Gutierrez R, Lindeboom JJ, Paredez AR, Emons AM, Ehrhardt DW (2009) *Arabidopsis* cortical microtubules position cellulose synthase delivery to the plasma membrane and interact with cellulose synthase trafficking compartments. Nature Cell Biology **11:** 797-806

Haigler CH, Ivanova-Datchev, M., Hogan, P.S., Salnikov, V.V., Hwang, S., Martin, K., and Delmer, D.P. (2001) Carbon partitioning to cellulose synthesis. *Plant Molecular Biology* **47:** 29-51

Hardin SC, Duncan KA, Huber SC (2006) Determination of structural requirements and probable regulatory effectors for membrane association of Maize sucrose synthase. Plant physiology **141:** 1106–1119

Hardin SC, Winter H, Huber SC (2004) Phosphorylation of the Amino Terminus of Maize Sucrose Synthase in Relation to Membrane Association and Enzyme Activity. Plant physiology **134:** 1427–1438

Haseloff J, Dormand EL, Brand AH (1999) Live imaging with green fluorescent protein. Methods in Molecular Biology **122:** 241–259

Huber SC (2007) Exploring the role of protein phosphorylation in plants: from signalling to metabolism. Biochemical Society Transactions **35:** 28-32

Huber SC, Huber, J.L., Liao, P-C., Gage, D.A., McMichael, Jr., R.W., Chourey, P.S., Hannah, L.C., and Koch, K. (1996) Phosphorylation of serine-15 of maize leaf sucrose synthase. *Plant Physiology* **112:** 793-802

Jelínková A, Malínská K, Simon S, Kleine-Vehn J, Parêzová M, Pejchar P, Kubeš M, Martinec J, Friml J, Zažímalová E, Petrášek J (2010) Probing plant membranes with FM dyes: tracking, dragging or blocking? The Plant Journal **61:** 883–892

Komatsu A, Moriguchi T, Koyama K, Omura M, Akihama T (2002) Analysis of sucrose synthase genes in Citrus suggest different roles and phylogenetic relationships. Journal of Experimental Botany **53:** 61-71

Konishi T, Nakia, T., Sakia, F., and Hayashi, T. (2001) Formation of callose from sucrose in cotton fiber microsomal membranes. Journal of Wood Science **47:** 331-335

Konishi T, Ohmiya, Y., and Hayashi, T. (2004) Evidence that sucrose loaded into phloem of a poplar leaf is used directly by sucrose synthase associated with various β-glucan synthases in the stem. Plant Physiology **134:** 1146-1152

Lalonde S, Ehrhardt DW, Loqué D, Chen J, Rhee SY, Frommer WB (2008) Molecular and cellular approaches for the detection of protein–protein interactions: latest techniques and current limitations. The Plant Journal **53:** 610–635

Lalonde S, Wipf D, Frommer WB (2004) Transport mechanisms for organic forms of carbon and nitrogen between source and sink. Annual Review of Plant Biology **55:** 341-372

Manders EMM, Verbeek FJ, Aten JA (1993) Measurement of co-localization of objects in dual-colour confocal images. Journal of Microscopy **169:** 375 - 382

Matic S, Akerlund, H-E, Everitt, E., and Widell, S. (2004) Sucrose synthase isoforms in cultured tobacco cells. Plant Physiology and Biochemistry **42:** 299-306

Nägeli C (1855) Pflanzenphysiologische Untersuchungen. Heft 1,Schulthess, Zu¨ rich**:** 1–35

Nakai T, Konishi, T., Zhang, X-Q., Chollet, Tonouchi, N., Tsuchida, T., Yoshinaga, F., Mori, H., Sakai, F., and Hayashi, T. (1998) An increase in apparent affinity for sucrose of Mung Bean sucrose synthase is caused by in vitro phosphorylation or directed mutagenesis of Ser11. Plant Cell Physiology **39:** 1337-1341

Nakai T, Tonouchi, N., Konishi, T., Kojima, Y., Tsuchida, T., Yoshinaga, F., Sakai, F., and Hayashi, T. (1999) Enhancement of cellulose production by expression of sucrose synthase in *Acetobacter xylinum*. PNAS USA **96:** 14-18

Plomion C, Leprovost, G., and Stokes, A. (2001) Wood formation in trees. *Plant Physiology* **127:** 1513-1523

Pringsheim N (1854) Untersuchungen u¨ ber den Bau und Bildung der Pflanzenzelle. Abt 1: Grundleinen einer Theorie der Pflanzanzelle Hershwald, Berlin**:** 12–13

Ross P, Mayer, R., and Benziman, M. (1991) Cellulose biosynthesis and function in bacteria. *MMBR* **55:** 35-58

Ruan Y-L, Chourey, P.S., Delmer, D.P., and Perez-Crau, L. (1997) The differential expression of sucrose synthase in relation to diverse patterns of carbon partitioning in developing Cotton seed. Plant Physiology **115:** 375-385

Salnikov VV, Grimson, M.J., Delmer, D.P., and Haigler, C.H. (2001) Sucrose synthase localizes to cellulose synthesis sites in tracheary elements. Phytochemistry **57:** 823-833

Salnikov VV, Grimson, M.J., Seagull, R.E., and Haigler, C.H. (2003) Localization of sucrose synthase and callose in freeze-substituted secondary-wall-stage cotton fiber. *Protoplasma* **221:** 175-184

Sambrook J, Russel DW (2001) Molecular cloning: A laboratory Manual, Ed Third. Cold Spring Harbor Laboratory Press, Cold Spring Harbor, NY

Speth EB, Imboden L, Hauck P, He SY (2009) Subcellular localization and functional analysis of the *Arabidopsis* GTPase *RabE1*. Plant Physiology **149:** 1824–1837

Tang GQ, Sturm A (1999) Antisense repression of sucrose synthase in carrot (*Daucus carota* L.) affects growth rather than sucrose partitioning. Plant Molecular Biology **41:** 465–479

Wightman R, Turner SR (2010) Trafficking of the plant cellulose synthase complex. Plant Physiology **153:** 427-432

Winter H, Huber JL, Huber SC (1997) Membrane association of sucrose synthase: changes during the graviresponse and possible control by protein phosphorylation. FEBS Letters **420:** 151-155

Winter H, Huber SC (2000) Sucrose metabolism and the actin cytoskeleton: SUSY as actin-binding protein. Kluwer Academic Publishe, The Netherlands

Xu R, Quinn Q (2008) Protocol: Streamline cloning of genes into binary vectors in *Agrobacterium* via the Gateway® TOPO vector system. Plant Methods **4**

Zhang X, Chollet R (1997) Seryl-phosphorylation of soybean nodule sucrose synthase (nodulin-100) by a Ca^{2+}-dependent protein kinase. FEBS Letters **410:** 126-130

Zhang X, Lund AA, Sarath G, Cerny RL, Roberts DM, Chollet R (1999) Soybean nodule sucrose synthase (Nodulin-100): further analysis of its phosphorylation using recombinant and authentic root-nodule enzymes. Archives of Biochemistry and Biophysics **371:** 70-82

Zhou H, Myburg AA, Berger DK (2005) Isolation and functional genetic analysis of *Eucalyptus* wood formation genes. University of Pretoria, Pretoria

Zrenner R, Salanoubat M, Willmitzer L, Sonnewald U (1995) Evidence of the crucial role of sucrose synthase for sink strength using transgenic potato plants (*Solanum tuberosum* L.). Plant Journal **7:** 97–107

SUPPLEMENTAL DATA

Appendix A: Supplemental figures and tables

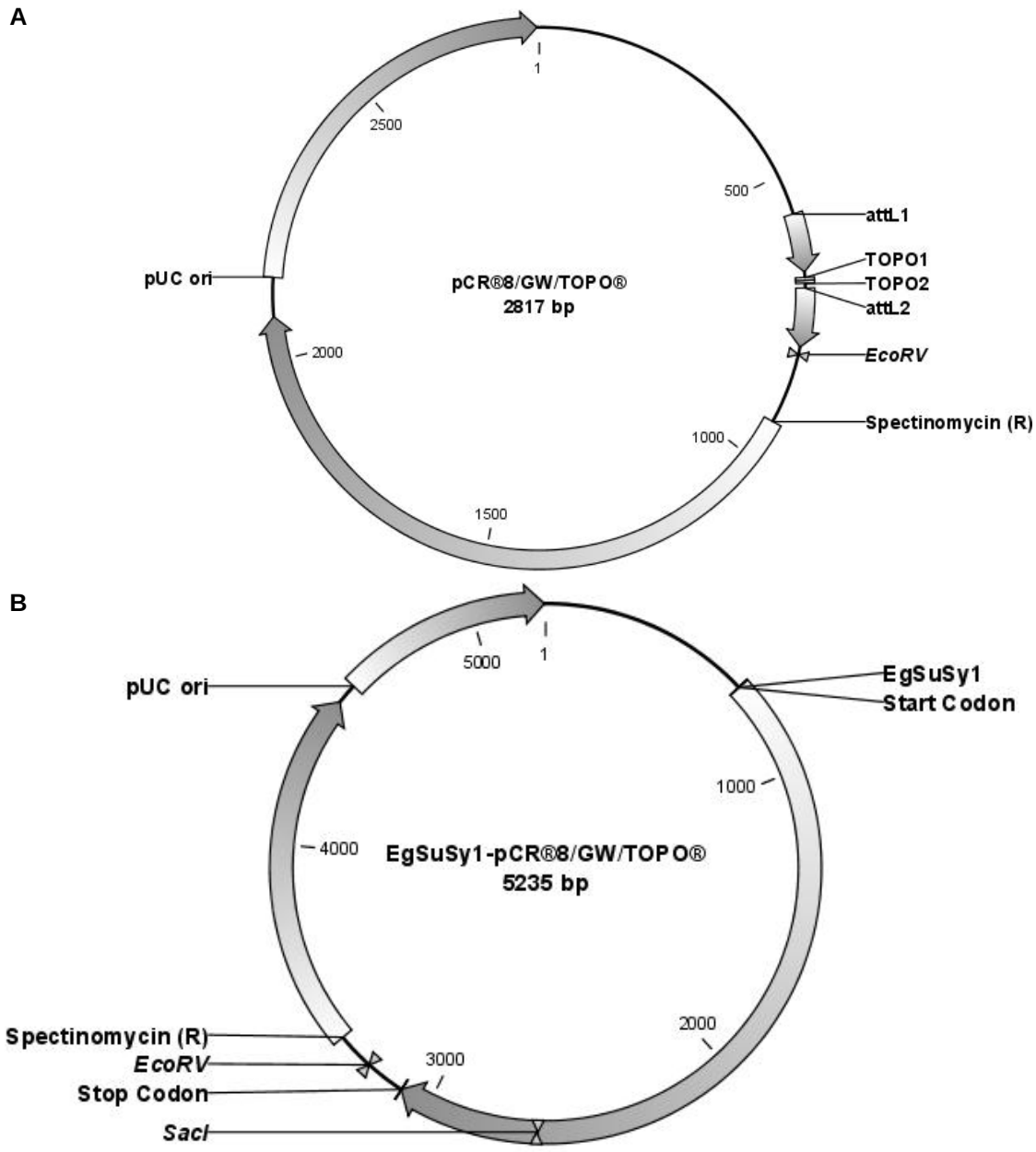

Figure S1. Vector plasmid maps of entry vector pCR®8/GW/TOPO® **(A)** and Recombinant entry vector *EgSuSy1*-pCR®8/GW/TOPO® (B) showing the restriction endonuclease sites of *EcoRV* and *SacI* used for screening putative positive recombinant colonies. pUC ori: Origin of replication for *E. coli.* attL: recombination sites . TOPO: Topoisomerase cloning sites. Vector map generated using CLC bio CLC Main Workbench 5.0.2.

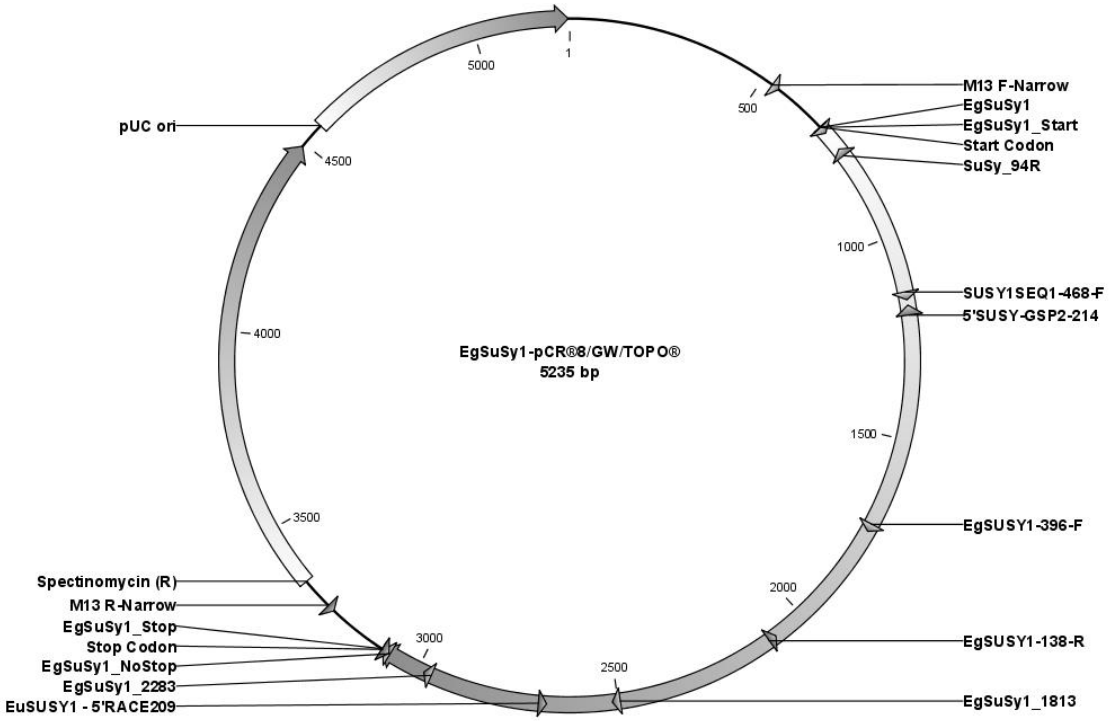

Figure S2. Vector plasmid map of Recombinant entry vector *EgSuSy1*-pCR®8/GW/TOPO® indicating primer binding sites used for cloning, screening and sequencing putative positive recombinants. pUC ori: Origin of replication for *E. coli*. Vector map generated using CLC bio CLC Main Workbench 5.0.2.

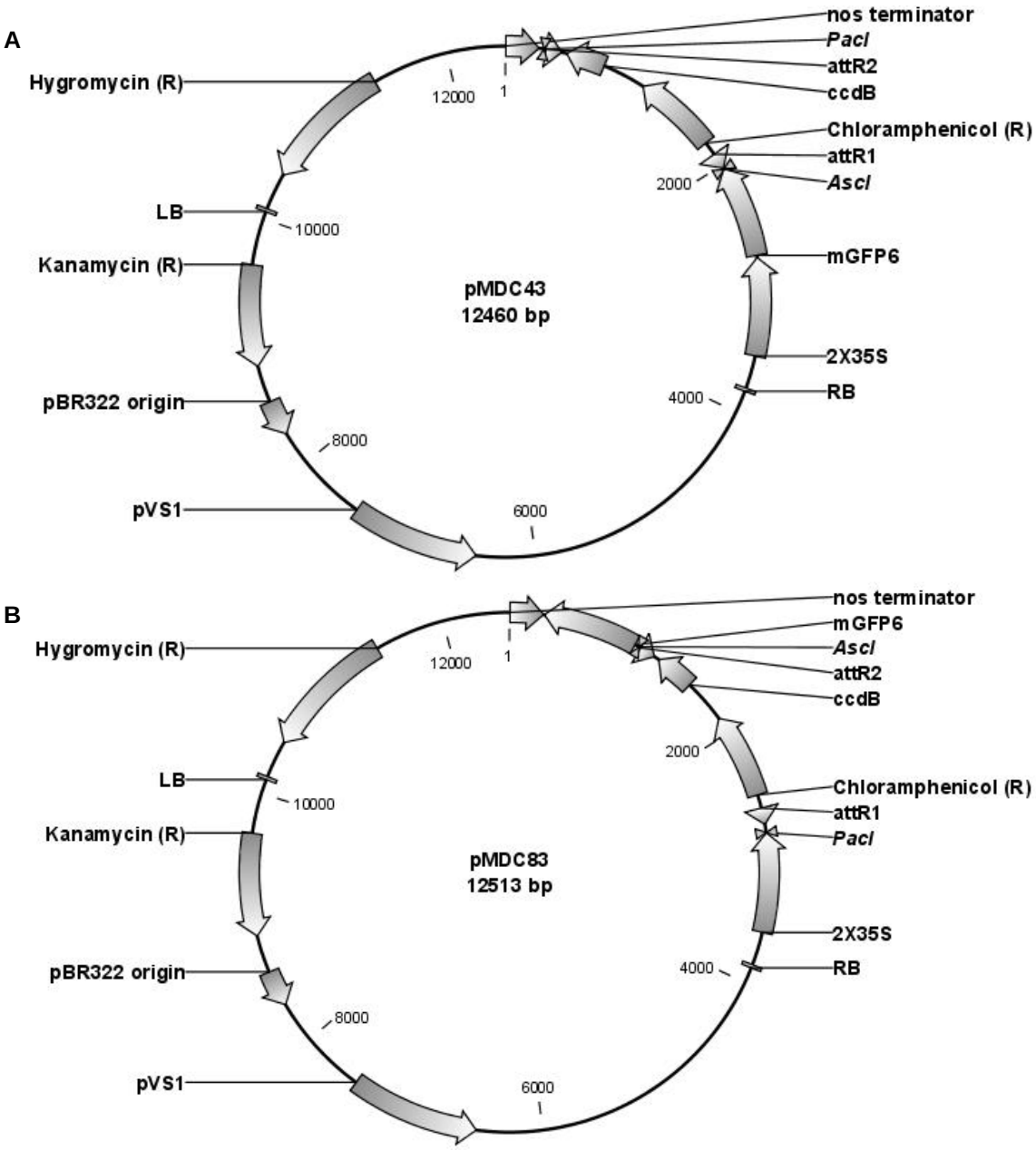

Figure S3. Vector plasmid maps of pMDC43 (A) and pMDC83 (B) showing *Pac*I restriction endonuclease sites. pBR322 ori: Origin of replication for *E. coli*. pVS1 ori: Origin of replication for *Agrobacteria*. ccdB: gene encodes a protein which interferes with *E. coli* DNA gyrase and inhibits growth of most *E. coli* strains, e.g. TOP10 and DH5α™. RB: T-DNA right border. LB: T-DNA left border. *att*R: recombination sites. 2X35S: Double Cauliflower mosaic virus promoter. Vector map generated using CLC bio CLC Main Workbench 5.0.2.

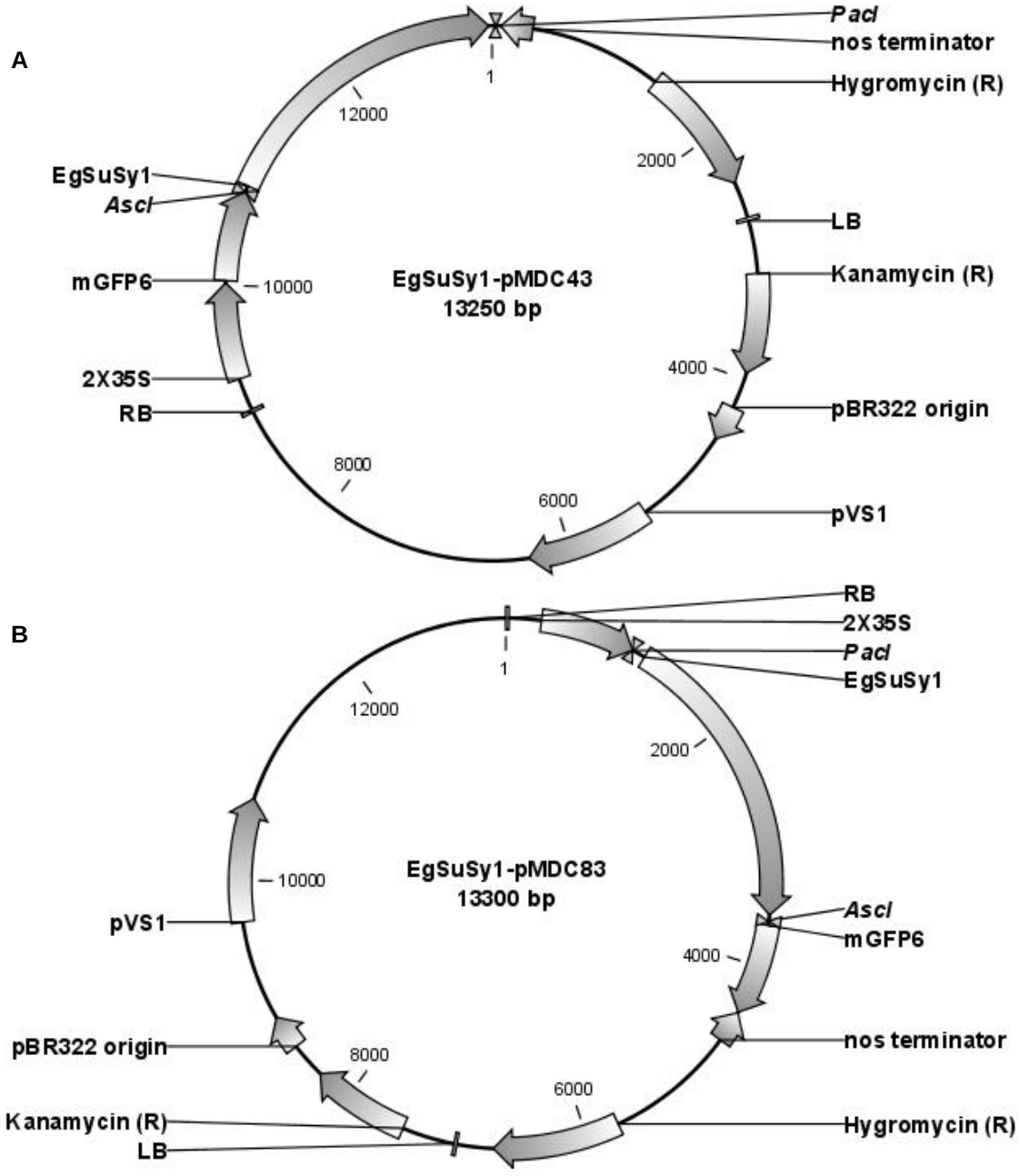

Figure S4. Vector plasmid maps of recombinant destination vectors *EgSuSy1*-pMDC43 and (A) *EgSuSy1*-pMDC83 (B) showing the restriction endonuclease sites of *Asc*I and *Pac*I used for screening putative positive recombinant colonies. pB322 ori: Origin of replication for *E. coli*. pVS1 ori: Origin of replication for *Agrobacterium*. RB: T-DNA right border. LB: T-DNA left border. 2X35S: Double Cauliflower mosaic virus promoter. Vector map generated using CLC bio CLC Main Workbench 5.0.2.

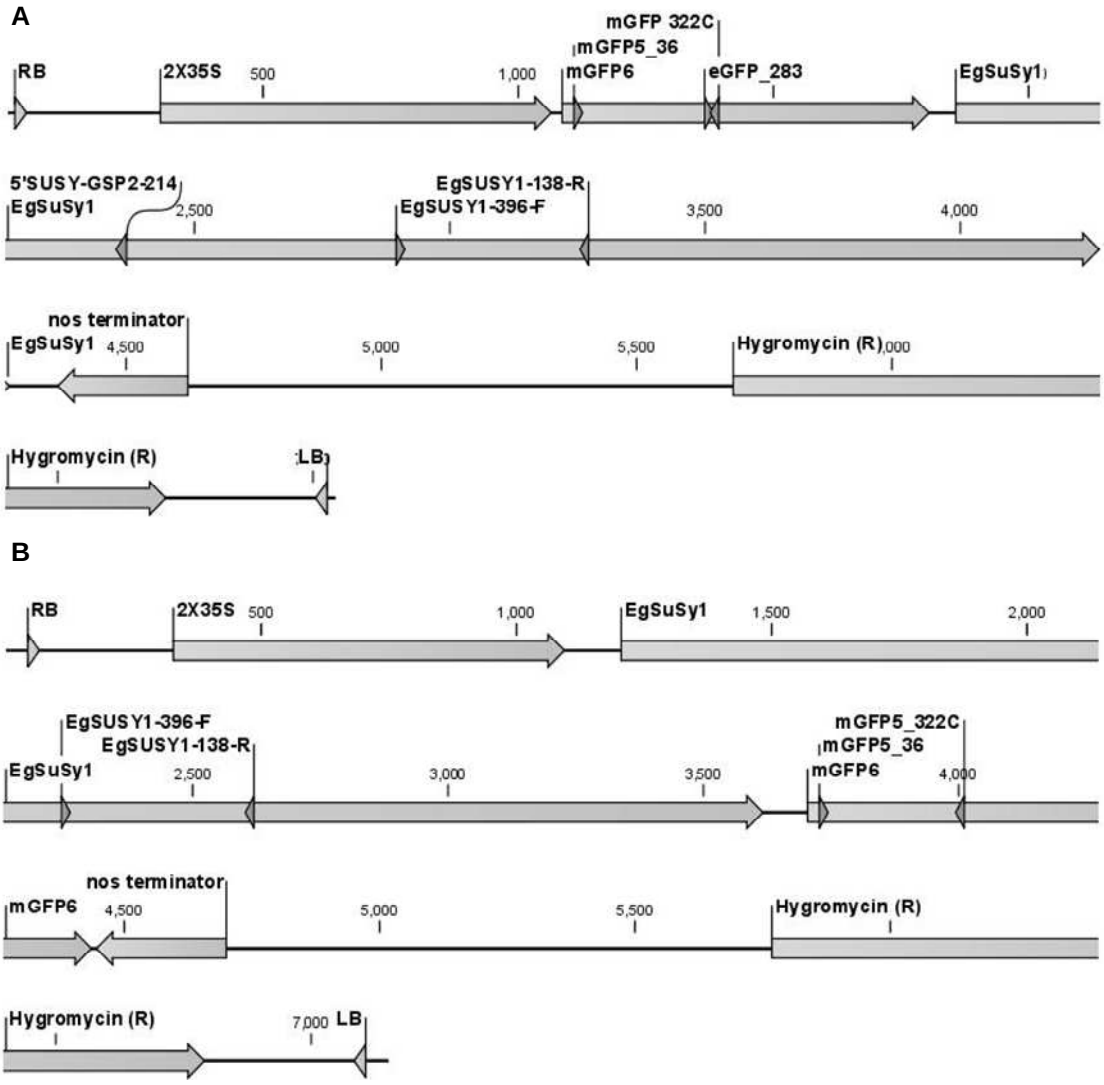

Figure S5. Vector plasmid maps of recombinant destination vectors *EgSuSy1*-pMDC43 and (A) *EgSuSy1*-pMDC83 (B) indicating primer binding sites used for cloning, screening and sequencing putative positive recombinants. RB: T-DNA right border. LB: T-DNA left border. 2X35S: Double Cauliflower mosaic virus promoter. Vector map generated using CLC bio CLC Main Workbench 5.0.2.

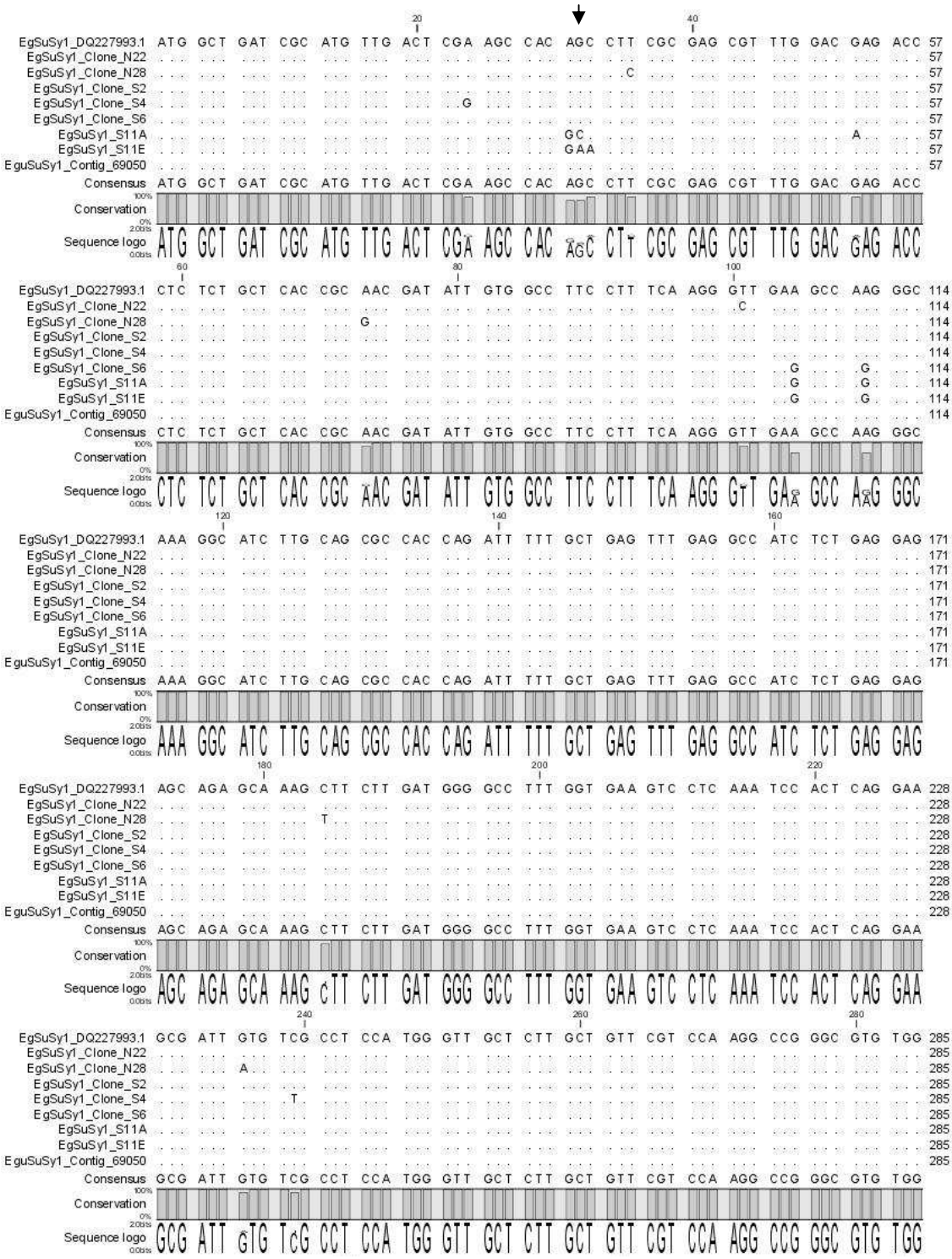
EgSuSy1_DQ227993.1
EgSuSy1_Clone_N22
EgSuSy1_Clone_N28
EgSuSy1_Clone_S2
EgSuSy1_Clone_S4
EgSuSy1_Clone_S6
EgSuSy1_S11A
EgSuSy1_S11E
EguSuSy1_Contig_69050
Consensus
Conservation
Sequence logo

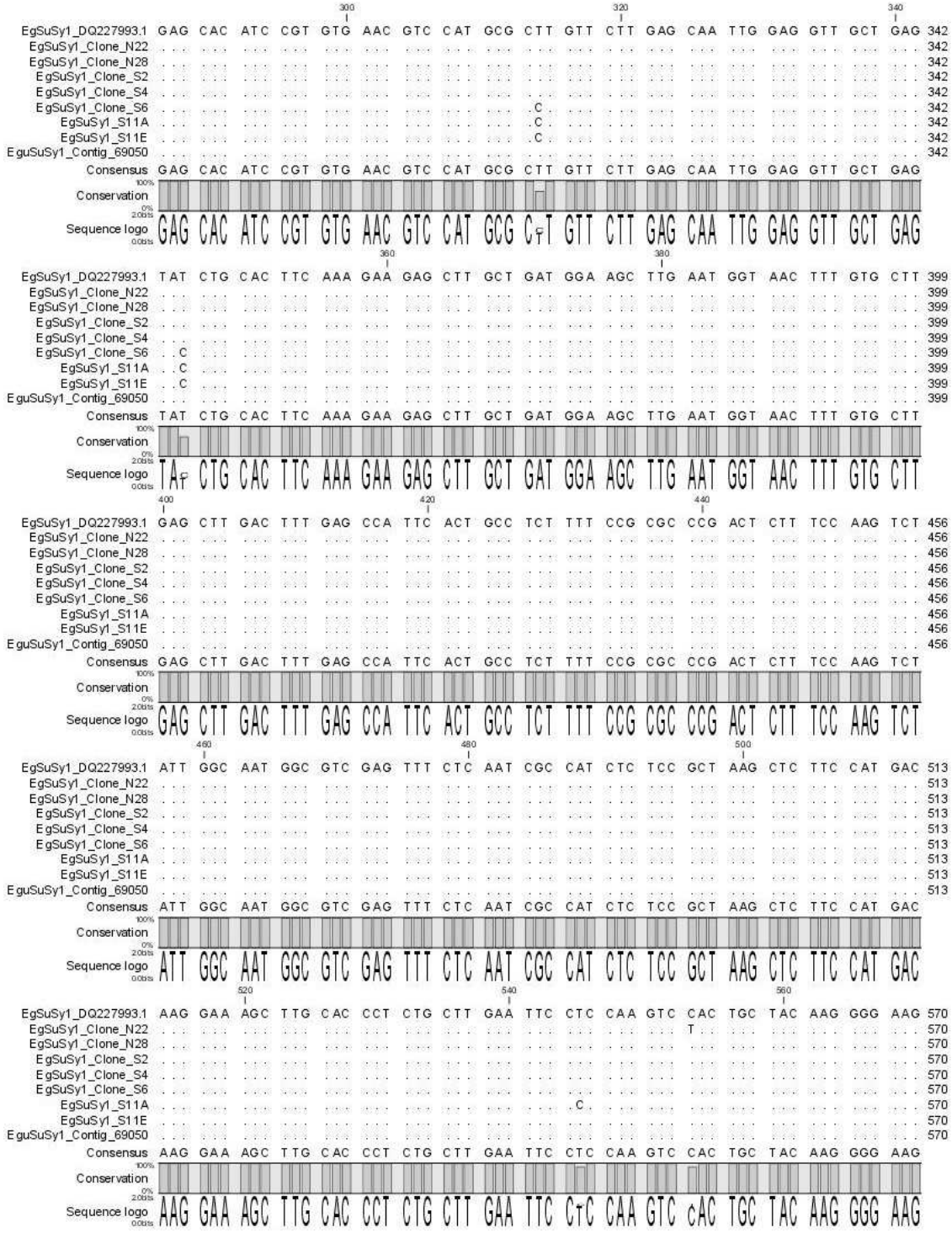
EgSuSy1_DQ227993.1 GAG CAC ATC CGT GTG AAC GTC CAT GCG CTT GTT CTT GAG CAA TTG GAG GTT GCT GAG 342
EgSuSy1_Clone_N22 342
EgSuSy1_Clone_N28 342
EgSuSy1_Clone_S2 342
EgSuSy1_Clone_S4 342
EgSuSy1_Clone_S6 342
EgSuSy1_S11A 342
EgSuSy1_S11E 342
EguSuSy1_Contig_69050 342
Consensus GAG CAC ATC CGT GTG AAC GTC CAT GCG CTT GTT CTT GAG CAA TTG GAG GTT GCT GAG
Conservation
Sequence logo
EgSuSy1_DQ227993.1 TAT CTG CAC TTC AAA GAA GAG CTT GCT GAT GGA AGC TTG AAT GGT AAC TTT GTG CTT 399
EgSuSy1_Clone_N22 399
EgSuSy1_Clone_N28 399
EgSuSy1_Clone_S2 399
EgSuSy1_Clone_S4 399
EgSuSy1_Clone_S6 399
EgSuSy1_S11A 399
EgSuSy1_S11E 399
EguSuSy1_Contig_69050 399
Consensus TAT CTG CAC TTC AAA GAA GAG CTT GCT GAT GGA AGC TTG AAT GGT AAC TTT GTG CTT
Conservation
Sequence logo
EgSuSy1_DQ227993.1 GAG CTT GAC TTT GAG CCA TTC ACT GCC TCT TTT CCG CGC CCG ACT CTT TCC AAG TCT 456
EgSuSy1_Clone_N22 456
EgSuSy1_Clone_N28 456
EgSuSy1_Clone_S2 456
EgSuSy1_Clone_S4 456
EgSuSy1_Clone_S6 456
EgSuSy1_S11A 456
EgSuSy1_S11E 456
EguSuSy1_Contig_69050 456
Consensus GAG CTT GAC TTT GAG CCA TTC ACT GCC TCT TTT CCG CGC CCG ACT CTT TCC AAG TCT
Conservation
Sequence logo
EgSuSy1_DQ227993.1 ATT GGC AAT GGC GTC GAG TTT CTC AAT CGC CAT CTC TCC GCT AAG CTC TTC CAT GAC 513
EgSuSy1_Clone_N22 513
EgSuSy1_Clone_N28 513
EgSuSy1_Clone_S2 513
EgSuSy1_Clone_S4 513
EgSuSy1_Clone_S6 513
EgSuSy1_S11A 513
EgSuSy1_S11E 513
EguSuSy1_Contig_69050 513
Consensus ATT GGC AAT GGC GTC GAG TTT CTC AAT CGC CAT CTC TCC GCT AAG CTC TTC CAT GAC
Conservation
Sequence logo
EgSuSy1_DQ227993.1 AAG GAA AGC TTG CAC CCT CTG CTT GAA TTC CTC CAA GTC CAC TGC TAC AAG GGG AAG 570
EgSuSy1_Clone_N22 570
EgSuSy1_Clone_N28 570
EgSuSy1_Clone_S2 570
EgSuSy1_Clone_S4 570
EgSuSy1_Clone_S6 570
EgSuSy1_S11A 570
EgSuSy1_S11E 570
EguSuSy1_Contig_69050 570
Consensus AAG GAA AGC TTG CAC CCT CTG CTT GAA TTC CTC CAA GTC CAC TGC TAC AAG GGG AAG
Conservation
Sequence logo

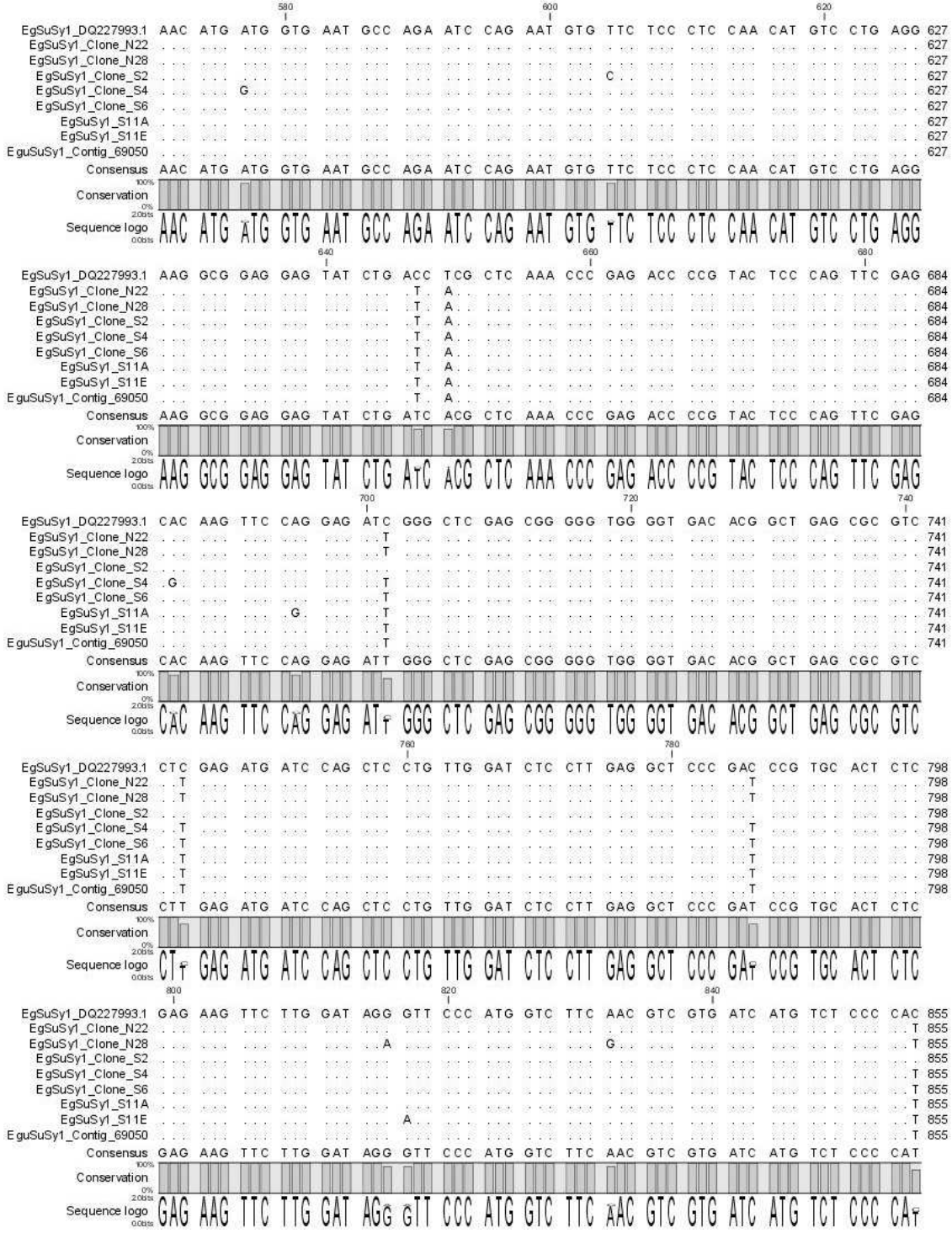
EgSuSy1_DQ227993.1
EgSuSy1_Clone_N22
EgSuSy1_Clone_N28
EgSuSy1_Clone_S2
EgSuSy1_Clone_S4
EgSuSy1_Clone_S6
EgSuSy1_S11A
EgSuSy1_S11E
EguSuSy1_Contig_69050
Consensus
Conservation
Sequence logo
AAC ATG ATG GTG AAT GCC AGA ATC CAG AAT GTG TTC TCC CTC CAA CAT GTC CTG AGG 627
AAG GCG GAG GAG TAT CTG ACC TCG CTC AAA CCC GAG ACC CCG TAC TCC CAG TTC GAG 684
CAC AAG TTC CAG GAG ATC GGG CTC GAG CGG GGG TGG GGT GAC ACG GCT GAG CGC GTC 741
CTC GAG ATG ATC CAG CTC CTG TTG GAT CTC CTT GAG GCT CCC GAC CCG TGC ACT CTC 798
GAG AAG TTC TTG GAT AGG GTT CCC ATG GTC TTC AAC GTC GTG ATC ATG TCT CCC CAC 855

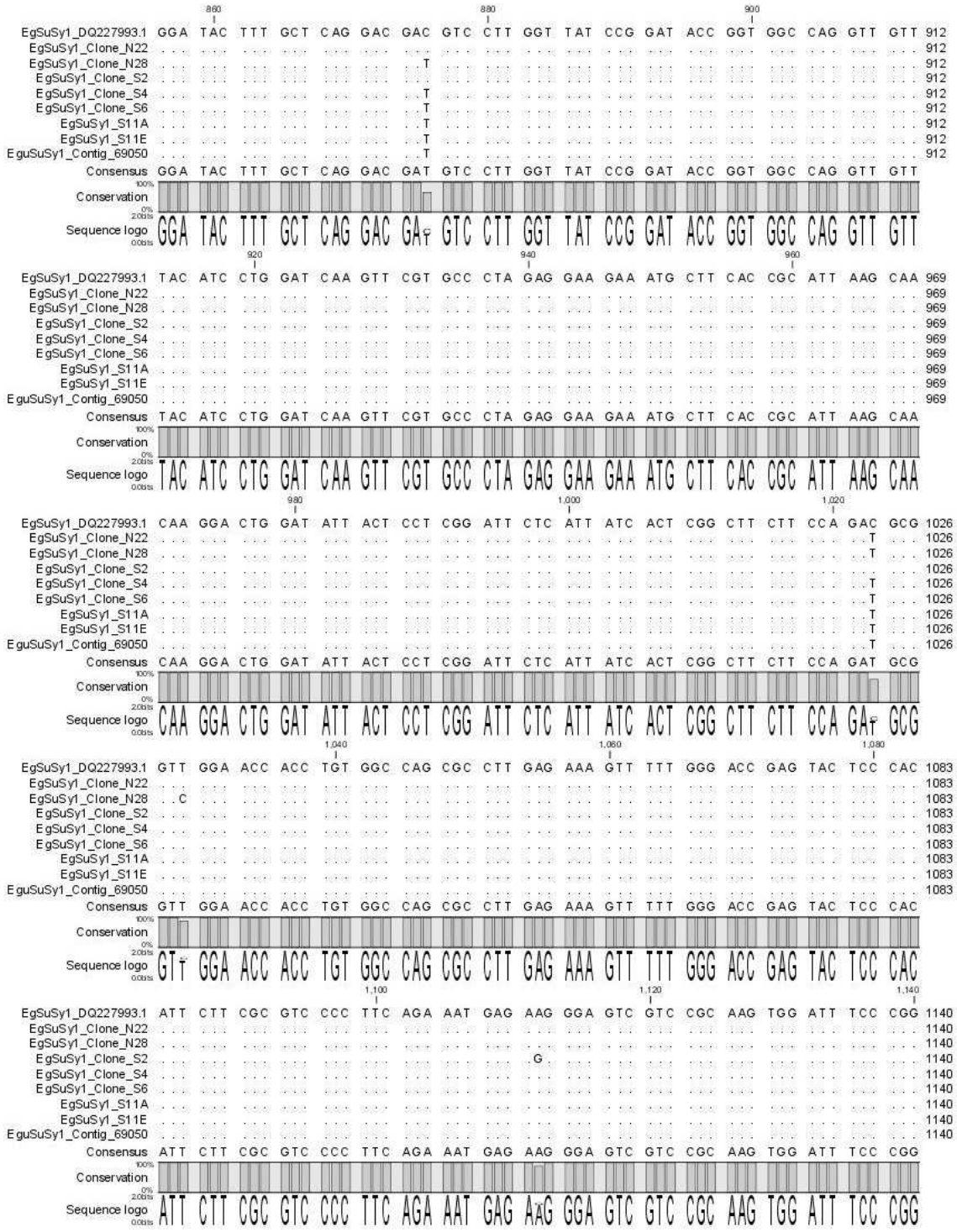
EgSuSy1_DQ227993.1
EgSuSy1_Clone_N22
EgSuSy1_Clone_N28
EgSuSy1_Clone_S2
EgSuSy1_Clone_S4
EgSuSy1_Clone_S6
EgSuSy1_S11A
EgSuSy1_S11E
EguSuSy1_Contig_69050
Consensus
Conservation
Sequence logo

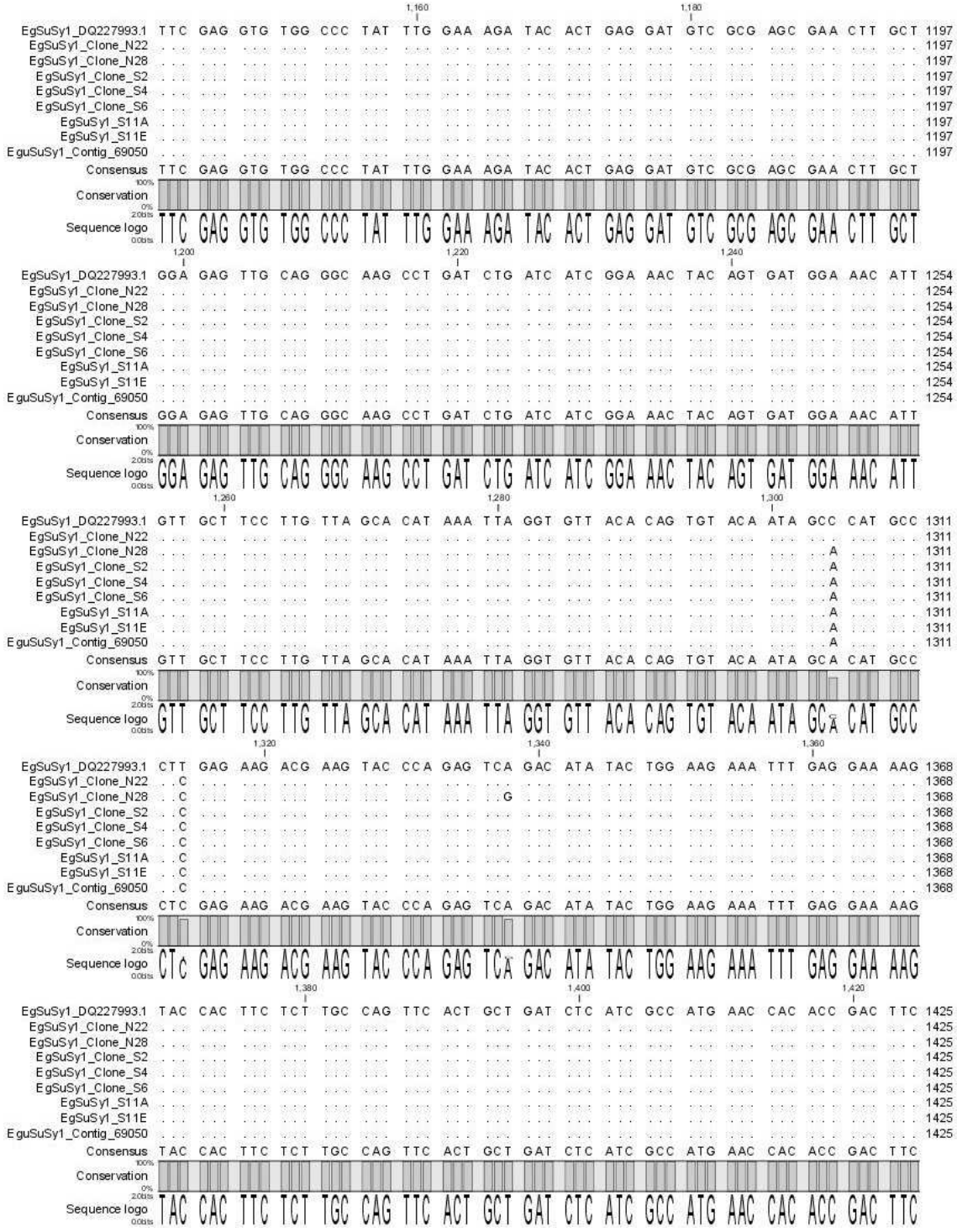
1,160
1,180
EgSuSy1_DQ227993.1 TTC GAG GTG TGG CCC TAT TTG GAA AGA TAC ACT GAG GAT GTC GCG AGC GAA CTT GCT 1197
EgSuSy1_Clone_N22 1197
EgSuSy1_Clone_N28 1197
EgSuSy1_Clone_S2 1197
EgSuSy1_Clone_S4 1197
EgSuSy1_Clone_S6 1197
EgSuSy1_S11A 1197
EgSuSy1_S11E 1197
EguSuSy1_Contig_69050 1197
Consensus TTC GAG GTG TGG CCC TAT TTG GAA AGA TAC ACT GAG GAT GTC GCG AGC GAA CTT GCT
Conservation
Sequence logo
1,200
1,220
1,240
EgSuSy1_DQ227993.1 GGA GAG TTG CAG GGC AAG CCT GAT CTG ATC ATC GGA AAC TAC AGT GAT GGA AAC ATT 1254
EgSuSy1_Clone_N22 1254
EgSuSy1_Clone_N28 1254
EgSuSy1_Clone_S2 1254
EgSuSy1_Clone_S4 1254
EgSuSy1_Clone_S6 1254
EgSuSy1_S11A 1254
EgSuSy1_S11E 1254
EguSuSy1_Contig_69050 1254
Consensus GGA GAG TTG CAG GGC AAG CCT GAT CTG ATC ATC GGA AAC TAC AGT GAT GGA AAC ATT
Conservation
Sequence logo
1,260
1,280
1,300
EgSuSy1_DQ227993.1 GTT GCT TCC TTG TTA GCA CAT AAA TTA GGT GTT ACA CAG TGT ACA ATA GCC CAT GCC 1311
EgSuSy1_Clone_N22 1311
EgSuSy1_Clone_N28 1311
EgSuSy1_Clone_S2 1311
EgSuSy1_Clone_S4 1311
EgSuSy1_Clone_S6 1311
EgSuSy1_S11A 1311
EgSuSy1_S11E 1311
EguSuSy1_Contig_69050 1311
Consensus GTT GCT TCC TTG TTA GCA CAT AAA TTA GGT GTT ACA CAG TGT ACA ATA GCA CAT GCC
Conservation
Sequence logo
1,320
1,340
1,360
EgSuSy1_DQ227993.1 CTT GAG AAG ACG AAG TAC CCA GAG TCA GAC ATA TAC TGG AAG AAA TTT GAG GAA AAG 1368
EgSuSy1_Clone_N22 1368
EgSuSy1_Clone_N28 1368
EgSuSy1_Clone_S2 1368
EgSuSy1_Clone_S4 1368
EgSuSy1_Clone_S6 1368
EgSuSy1_S11A 1368
EgSuSy1_S11E 1368
EguSuSy1_Contig_69050 1368
Consensus CTC GAG AAG ACG AAG TAC CCA GAG TCA GAC ATA TAC TGG AAG AAA TTT GAG GAA AAG
Conservation
Sequence logo
1,380
1,400
1,420
EgSuSy1_DQ227993.1 TAC CAC TTC TCT TGC CAG TTC ACT GCT GAT CTC ATC GCC ATG AAC CAC ACC GAC TTC 1425
EgSuSy1_Clone_N22 1425
EgSuSy1_Clone_N28 1425
EgSuSy1_Clone_S2 1425
EgSuSy1_Clone_S4 1425
EgSuSy1_Clone_S6 1425
EgSuSy1_S11A 1425
EgSuSy1_S11E 1425
EguSuSy1_Contig_69050 1425
Consensus TAC CAC TTC TCT TGC CAG TTC ACT GCT GAT CTC ATC GCC ATG AAC CAC ACC GAC TTC
Conservation
Sequence logo

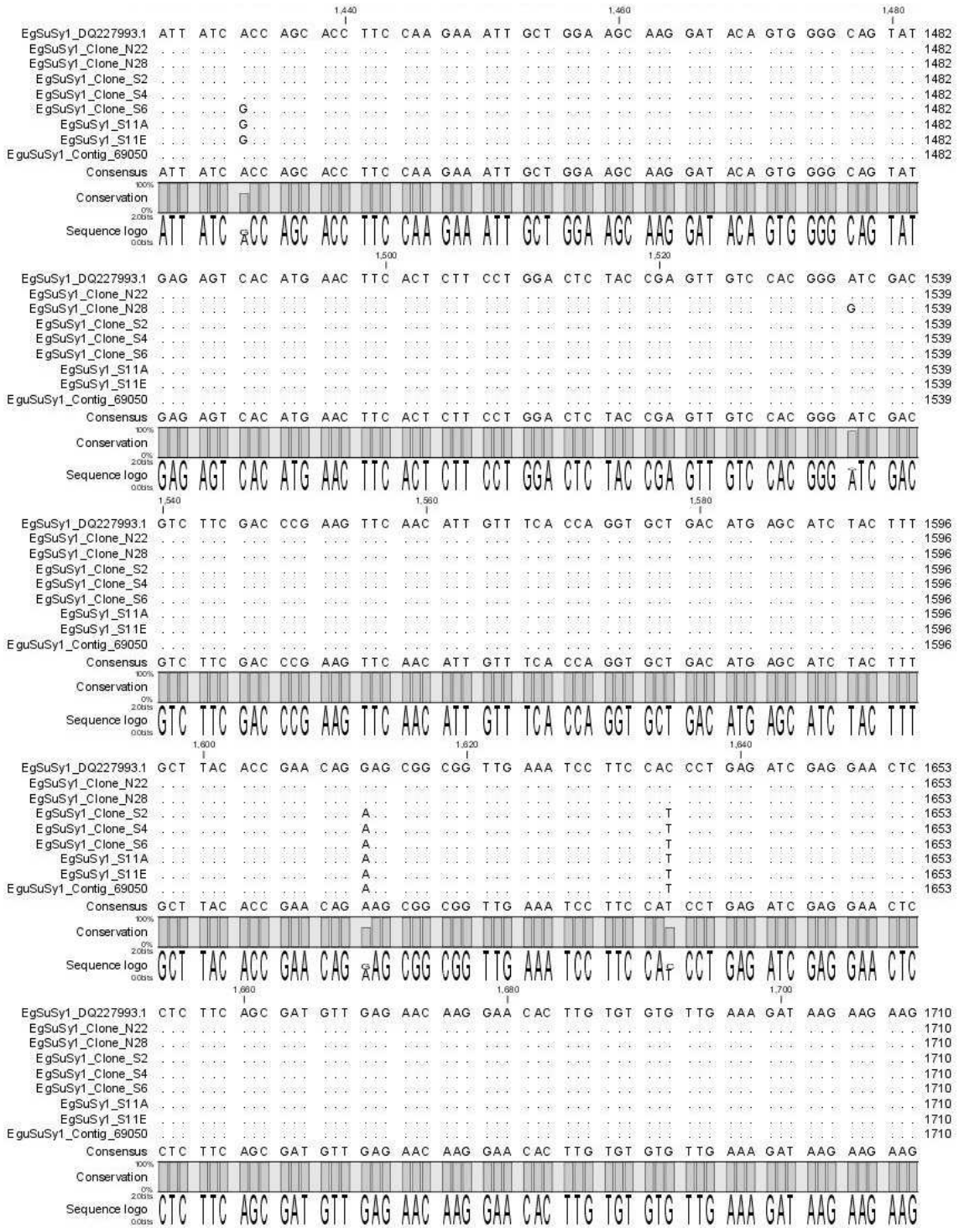
1,440
1,460
1,480
EgSuSy1_DQ227993.1 ATT ATC ACC AGC ACC TTC CAA GAA ATT GCT GGA AGC AAG GAT ACA GTG GGG CAG TAT 1482
EgSuSy1_Clone_N22 1482
EgSuSy1_Clone_N28 1482
EgSuSy1_Clone_S2 1482
EgSuSy1_Clone_S4 1482
EgSuSy1_Clone_S6 1482
EgSuSy1_S11A 1482
EgSuSy1_S11E 1482
EguSuSy1_Contig_69050 1482
Consensus ATT ATC ACC AGC ACC TTC CAA GAA ATT GCT GGA AGC AAG GAT ACA GTG GGG CAG TAT
Conservation
Sequence logo
1,500
1,520
EgSuSy1_DQ227993.1 GAG AGT CAC ATG AAC TTC ACT CTT CCT GGA CTC TAC CGA GTT GTC CAC GGG ATC GAC 1539
EgSuSy1_Clone_N22 1539
EgSuSy1_Clone_N28 1539
EgSuSy1_Clone_S2 1539
EgSuSy1_Clone_S4 1539
EgSuSy1_Clone_S6 1539
EgSuSy1_S11A 1539
EgSuSy1_S11E 1539
EguSuSy1_Contig_69050 1539
Consensus GAG AGT CAC ATG AAC TTC ACT CTT CCT GGA CTC TAC CGA GTT GTC CAC GGG ATC GAC
Conservation
Sequence logo
1,540
1,560
1,580
EgSuSy1_DQ227993.1 GTC TTC GAC CCG AAG TTC AAC ATT GTT TCA CCA GGT GCT GAC ATG AGC ATC TAC TTT 1596
EgSuSy1_Clone_N22 1596
EgSuSy1_Clone_N28 1596
EgSuSy1_Clone_S2 1596
EgSuSy1_Clone_S4 1596
EgSuSy1_Clone_S6 1596
EgSuSy1_S11A 1596
EgSuSy1_S11E 1596
EguSuSy1_Contig_69050 1596
Consensus GTC TTC GAC CCG AAG TTC AAC ATT GTT TCA CCA GGT GCT GAC ATG AGC ATC TAC TTT
Conservation
Sequence logo
1,600
1,620
1,640
EgSuSy1_DQ227993.1 GCT TAC ACC GAA CAG GAG CGG CGG TTG AAA TCC TTC CAC CCT GAG ATC GAG GAA CTC 1653
EgSuSy1_Clone_N22 1653
EgSuSy1_Clone_N28 1653
EgSuSy1_Clone_S2 1653
EgSuSy1_Clone_S4 1653
EgSuSy1_Clone_S6 1653
EgSuSy1_S11A 1653
EgSuSy1_S11E 1653
EguSuSy1_Contig_69050 1653
Consensus GCT TAC ACC GAA CAG AAG CGG CGG TTG AAA TCC TTC CAT CCT GAG ATC GAG GAA CTC
Conservation
Sequence logo
1,660
1,680
1,700
EgSuSy1_DQ227993.1 CTC TTC AGC GAT GTT GAG AAC AAG GAA CAC TTG TGT GTG TTG AAA GAT AAG AAG AAG 1710
EgSuSy1_Clone_N22 1710
EgSuSy1_Clone_N28 1710
EgSuSy1_Clone_S2 1710
EgSuSy1_Clone_S4 1710
EgSuSy1_Clone_S6 1710
EgSuSy1_S11A 1710
EgSuSy1_S11E 1710
EguSuSy1_Contig_69050 1710
Consensus CTC TTC AGC GAT GTT GAG AAC AAG GAA CAC TTG TGT GTG TTG AAA GAT AAG AAG AAG
Conservation
Sequence logo

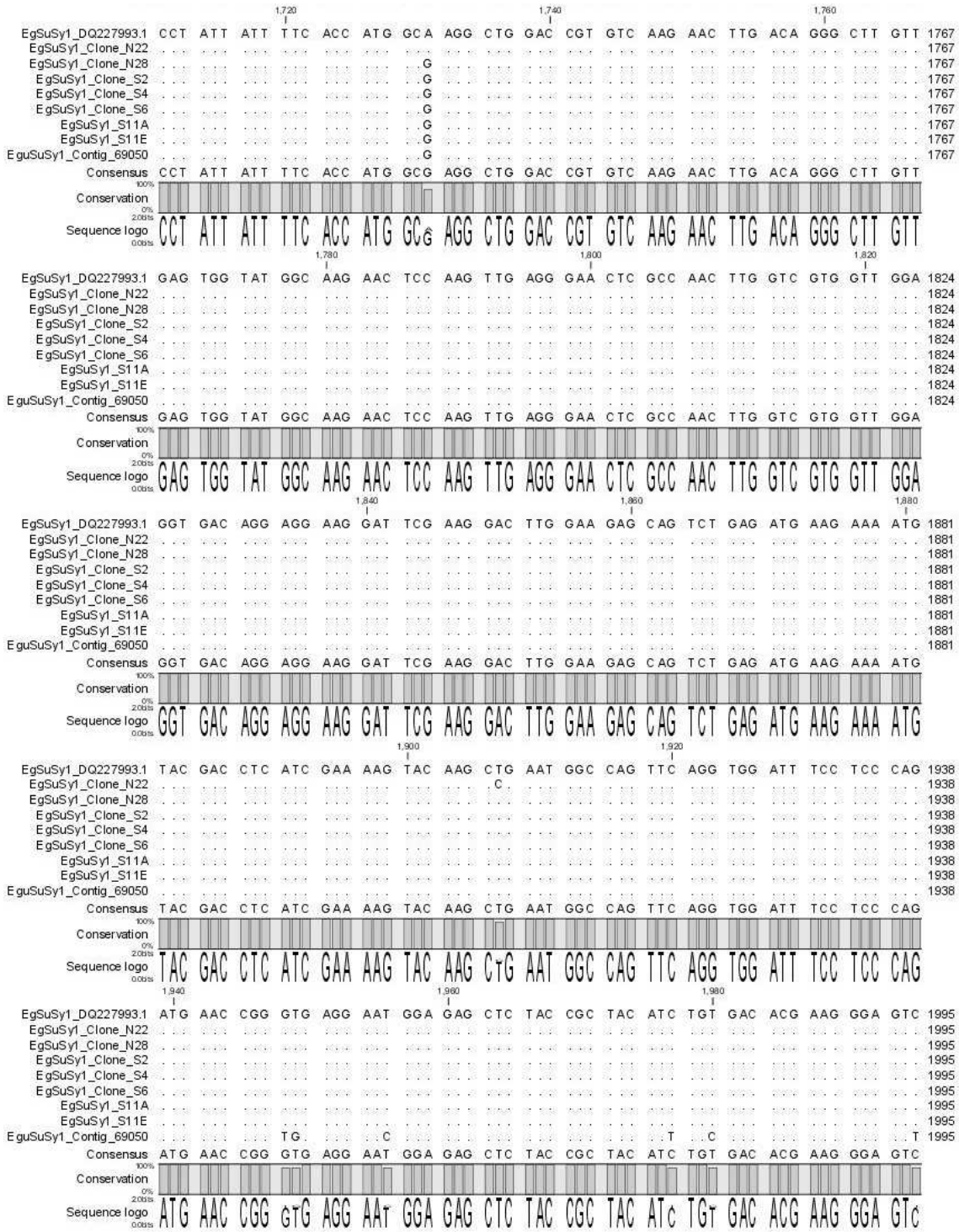
1,720
1,740
1,760
EgSuSy1_DQ227993.1 CCT ATT ATT TTC ACC ATG GCA AGG CTG GAC CGT GTC AAG AAC TTG ACA GGG CTT GTT 1767
EgSuSy1_Clone_N22 1767
EgSuSy1_Clone_N28 G 1767
EgSuSy1_Clone_S2 G 1767
EgSuSy1_Clone_S4 G 1767
EgSuSy1_Clone_S6 G 1767
EgSuSy1_S11A G 1767
EgSuSy1_S11E G 1767
EguSuSy1_Contig_69050 G 1767
Consensus CCT ATT ATT TTC ACC ATG GCG AGG CTG GAC CGT GTC AAG AAC TTG ACA GGG CTT GTT
Conservation
Sequence logo
1,780
1,800
1,820
EgSuSy1_DQ227993.1 GAG TGG TAT GGC AAG AAC TCC AAG TTG AGG GAA CTC GCC AAC TTG GTC GTG GTT GGA 1824
EgSuSy1_Clone_N22 1824
EgSuSy1_Clone_N28 1824
EgSuSy1_Clone_S2 1824
EgSuSy1_Clone_S4 1824
EgSuSy1_Clone_S6 1824
EgSuSy1_S11A 1824
EgSuSy1_S11E 1824
EguSuSy1_Contig_69050 1824
Consensus GAG TGG TAT GGC AAG AAC TCC AAG TTG AGG GAA CTC GCC AAC TTG GTC GTG GTT GGA
Conservation
Sequence logo
1,840
1,860
1,880
EgSuSy1_DQ227993.1 GGT GAC AGG AGG AAG GAT TCG AAG GAC TTG GAA GAG CAG TCT GAG ATG AAG AAA ATG 1881
EgSuSy1_Clone_N22 1881
EgSuSy1_Clone_N28 1881
EgSuSy1_Clone_S2 1881
EgSuSy1_Clone_S4 1881
EgSuSy1_Clone_S6 1881
EgSuSy1_S11A 1881
EgSuSy1_S11E 1881
EguSuSy1_Contig_69050 1881
Consensus GGT GAC AGG AGG AAG GAT TCG AAG GAC TTG GAA GAG CAG TCT GAG ATG AAG AAA ATG
Conservation
Sequence logo
1,900
1,920
EgSuSy1_DQ227993.1 TAC GAC CTC ATC GAA AAG TAC AAG CTG AAT GGC CAG TTC AGG TGG ATT TCC TCC CAG 1938
EgSuSy1_Clone_N22 C 1938
EgSuSy1_Clone_N28 1938
EgSuSy1_Clone_S2 1938
EgSuSy1_Clone_S4 1938
EgSuSy1_Clone_S6 1938
EgSuSy1_S11A 1938
EgSuSy1_S11E 1938
EguSuSy1_Contig_69050 1938
Consensus TAC GAC CTC ATC GAA AAG TAC AAG CTG AAT GGC CAG TTC AGG TGG ATT TCC TCC CAG
Conservation
Sequence logo
1,940
1,960
1,980
EgSuSy1_DQ227993.1 ATG AAC CGG GTG AGG AAT GGA GAG CTC TAC CGC TAC ATC TGT GAC ACG AAG GGA GTC 1995
EgSuSy1_Clone_N22 1995
EgSuSy1_Clone_N28 1995
EgSuSy1_Clone_S2 1995
EgSuSy1_Clone_S4 1995
EgSuSy1_Clone_S6 1995
EgSuSy1_S11A 1995
EgSuSy1_S11E 1995
EguSuSy1_Contig_69050 TG C T C T 1995
Consensus ATG AAC CGG GTG AGG AAT GGA GAG CTC TAC CGC TAC ATC TGT GAC ACG AAG GGA GTC
Conservation
Sequence logo

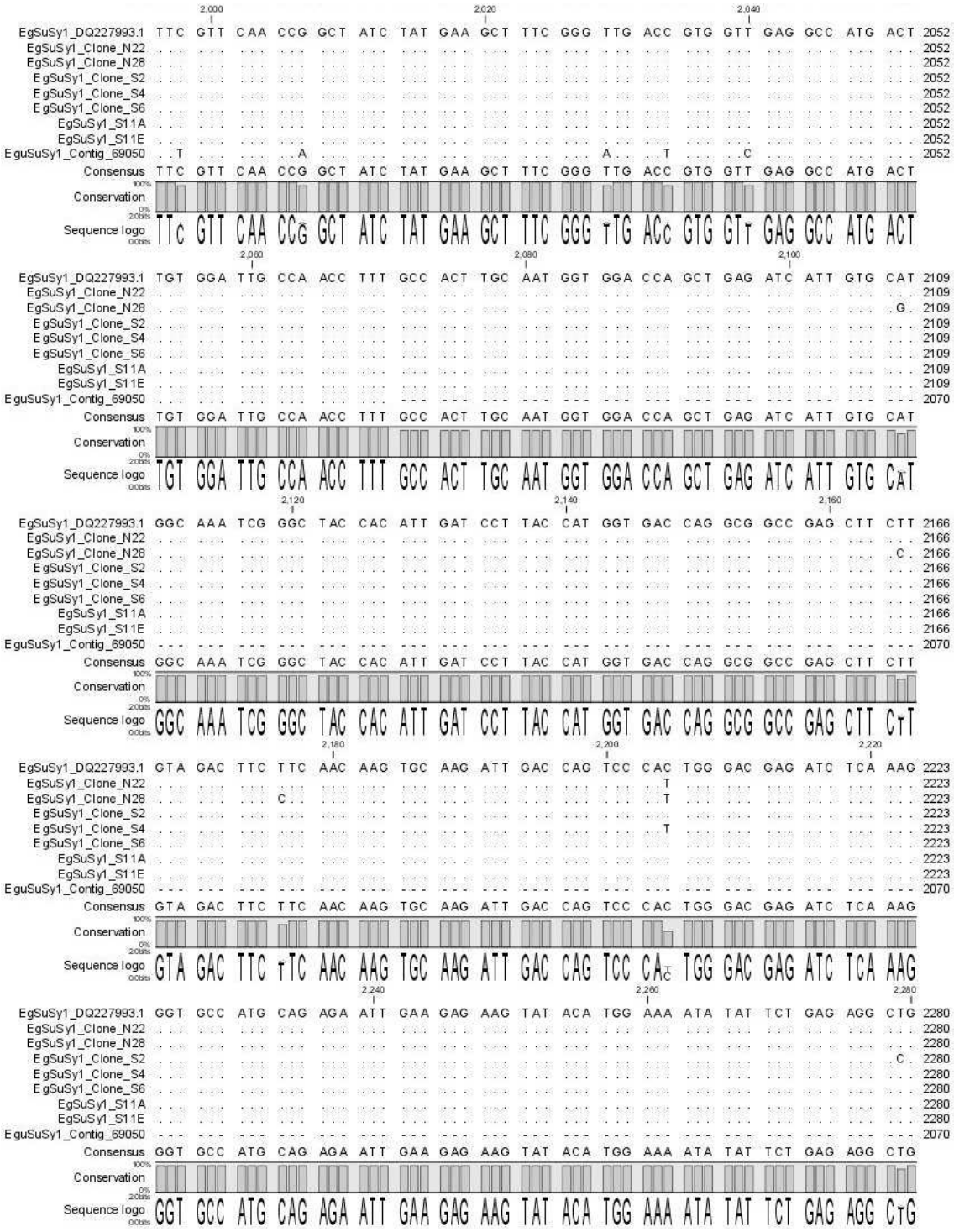
2,000
2,020
2,040
EgSuSy1_DQ227993.1 TTC GTT CAA CCG GCT ATC TAT GAA GCT TTC GGG TTG ACC GTG GTT GAG GCC ATG ACT 2052
EgSuSy1_Clone_N22 2052
EgSuSy1_Clone_N28 2052
EgSuSy1_Clone_S2 2052
EgSuSy1_Clone_S4 2052
EgSuSy1_Clone_S6 2052
EgSuSy1_S11A 2052
EgSuSy1_S11E 2052
EguSuSy1_Contig_69050 2052
Consensus TTC GTT CAA CCG GCT ATC TAT GAA GCT TTC GGG TTG ACC GTG GTT GAG GCC ATG ACT
Conservation
Sequence logo
2,060
2,080
2,100
EgSuSy1_DQ227993.1 TGT GGA TTG CCA ACC TTT GCC ACT TGC AAT GGT GGA CCA GCT GAG ATC ATT GTG CAT 2109
EgSuSy1_Clone_N22 2109
EgSuSy1_Clone_N28 2109
EgSuSy1_Clone_S2 2109
EgSuSy1_Clone_S4 2109
EgSuSy1_Clone_S6 2109
EgSuSy1_S11A 2109
EgSuSy1_S11E 2109
EguSuSy1_Contig_69050 2070
Consensus TGT GGA TTG CCA ACC TTT GCC ACT TGC AAT GGT GGA CCA GCT GAG ATC ATT GTG CAT
Conservation
Sequence logo
2,120
2,140
2,160
EgSuSy1_DQ227993.1 GGC AAA TCG GGC TAC CAC ATT GAT CCT TAC CAT GGT GAC CAG GCG GCC GAG CTT CTT 2166
EgSuSy1_Clone_N22 2166
EgSuSy1_Clone_N28 2166
EgSuSy1_Clone_S2 2166
EgSuSy1_Clone_S4 2166
EgSuSy1_Clone_S6 2166
EgSuSy1_S11A 2166
EgSuSy1_S11E 2166
EguSuSy1_Contig_69050 2070
Consensus GGC AAA TCG GGC TAC CAC ATT GAT CCT TAC CAT GGT GAC CAG GCG GCC GAG CTT CTT
Conservation
Sequence logo
2,180
2,200
2,220
EgSuSy1_DQ227993.1 GTA GAC TTC TTC AAC AAG TGC AAG ATT GAC CAG TCC CAC TGG GAC GAG ATC TCA AAG 2223
EgSuSy1_Clone_N22 2223
EgSuSy1_Clone_N28 2223
EgSuSy1_Clone_S2 2223
EgSuSy1_Clone_S4 2223
EgSuSy1_Clone_S6 2223
EgSuSy1_S11A 2223
EgSuSy1_S11E 2223
EguSuSy1_Contig_69050 2070
Consensus GTA GAC TTC TTC AAC AAG TGC AAG ATT GAC CAG TCC CAC TGG GAC GAG ATC TCA AAG
Conservation
Sequence logo
2,240
2,260
2,280
EgSuSy1_DQ227993.1 GGT GCC ATG CAG AGA ATT GAA GAG AAG TAT ACA TGG AAA ATA TAT TCT GAG AGG CTG 2280
EgSuSy1_Clone_N22 2280
EgSuSy1_Clone_N28 2280
EgSuSy1_Clone_S2 2280
EgSuSy1_Clone_S4 2280
EgSuSy1_Clone_S6 2280
EgSuSy1_S11A 2280
EgSuSy1_S11E 2280
EguSuSy1_Contig_69050 2070
Consensus GGT GCC ATG CAG AGA ATT GAA GAG AAG TAT ACA TGG AAA ATA TAT TCT GAG AGG CTG
Conservation
Sequence logo

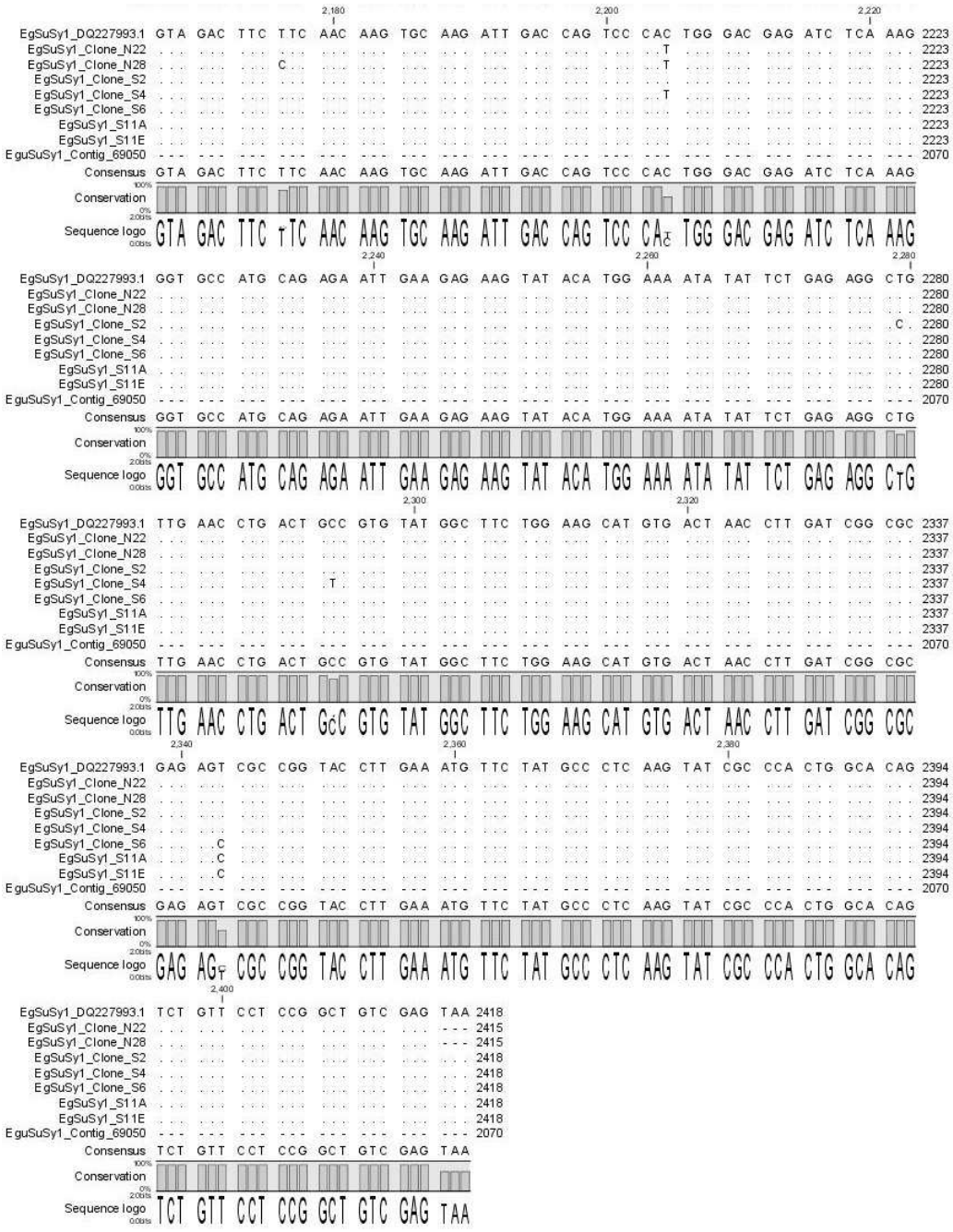

Figure S6. Nucleotide alignment of consensus sequences of the five sequenced *EgSuSy1*-pCR®8/GW/TOPO® clones showing the site directed modifications at the 11th serine residue (arrow). PCR induced background mutations were identified by comparing sequences to *EgSuSy1* sequence (GenBank accession DQ227993.1) and an *EguSuSy1* contig 69050 sourced from Eucspresso, a *Eucalyptus grandis x urophylla* transcriptome database (http://eucspresso.bi.up.ac.za) reference sequences. Nucleotide differences could be due to allelic differences between *Eucalyptus grandis* and *Eucalyptus grandis x urophylla* sequences. Nucleotide differences could also be attributed to PCR induced mutations which occurred when PCR cloning the original EgSuSy1 clone deposited in GenBank or the new clones used in the current study. (·) indicates identical amino acid and (–) a gap or the absence of a nucleotide at this site. Alignment generated using CLC bio CLC Main Workbench 5.0.2.

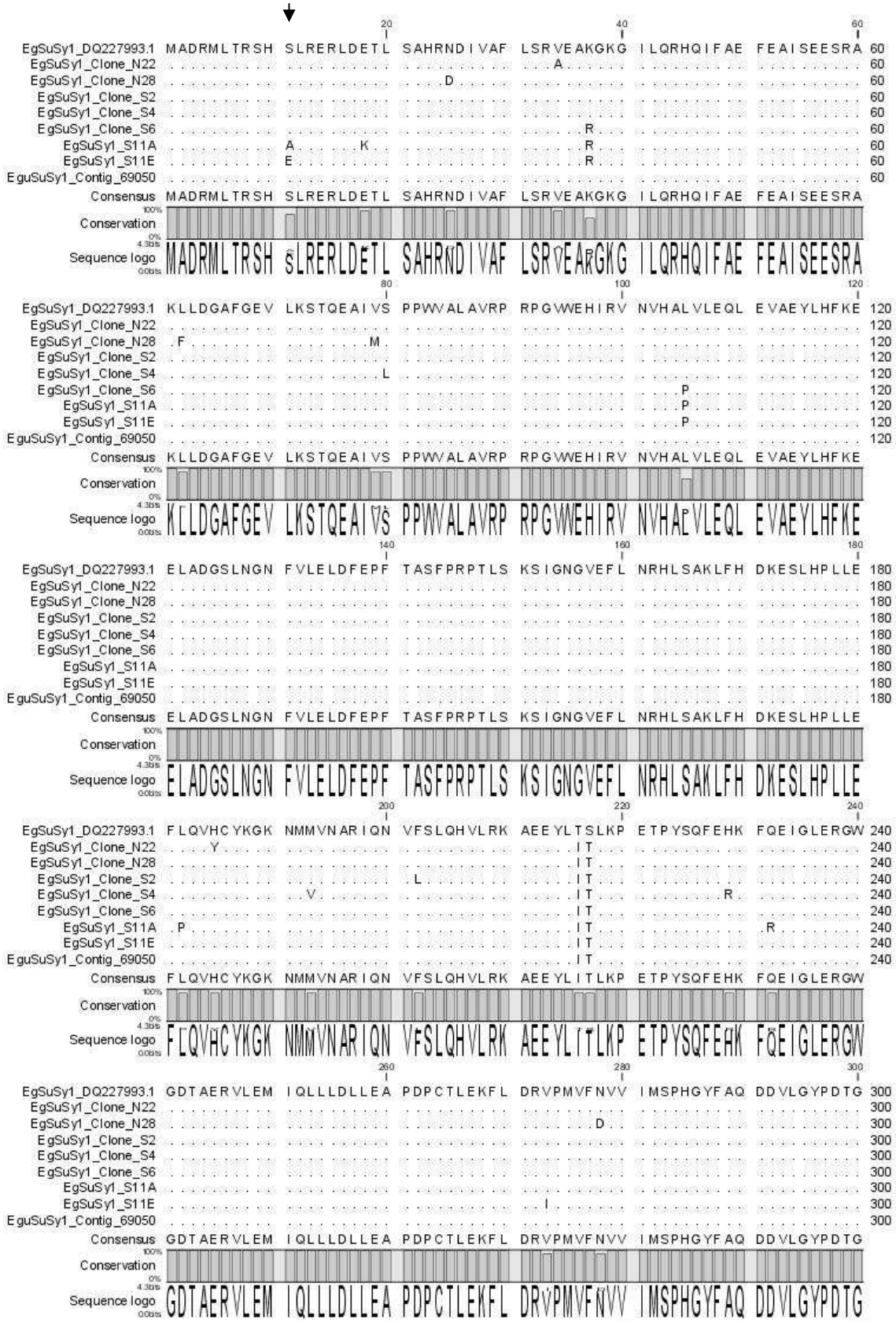
EgSuSy1_DQ227993.1
EgSuSy1_Clone_N22
EgSuSy1_Clone_N28
EgSuSy1_Clone_S2
EgSuSy1_Clone_S4
EgSuSy1_Clone_S6
EgSuSy1_S11A
EgSuSy1_S11E
EguSuSy1_Contig_69050
Consensus
Conservation
Sequence logo

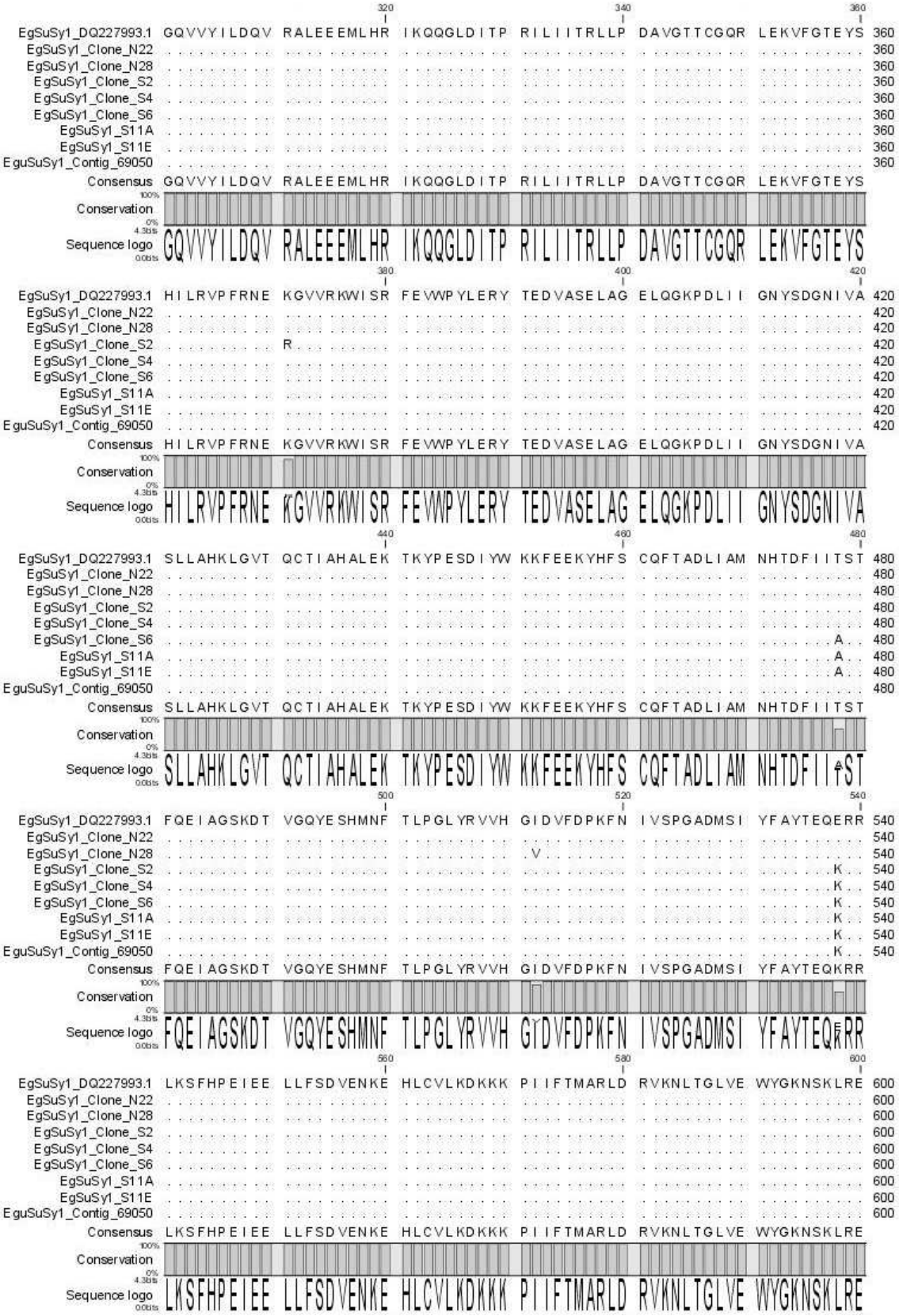
320 340 360
EgSuSy1_DQ227993.1 GQVVYILDQV RALEEEMLHR IKQQGLDITP RILIITRLLP DAVGTTCGQR LEKVFGTEYS 360
EgSuSy1_Clone_N22 360
EgSuSy1_Clone_N28 360
EgSuSy1_Clone_S2 360
EgSuSy1_Clone_S4 360
EgSuSy1_Clone_S6 360
EgSuSy1_S11A 360
EgSuSy1_S11E 360
EguSuSy1_Contig_69050 360
Consensus GQVVYILDQV RALEEEMLHR IKQQGLDITP RILIITRLLP DAVGTTCGQR LEKVFGTEYS
Conservation
Sequence logo
380 400 420
EgSuSy1_DQ227993.1 HILRVPFRNE KGVVRKWISR FEVWPYLERY TEDVASELAG ELQGKPDLII GNYSDGNIVA 420
EgSuSy1_Clone_N22 420
EgSuSy1_Clone_N28 420
EgSuSy1_Clone_S2 R 420
EgSuSy1_Clone_S4 420
EgSuSy1_Clone_S6 420
EgSuSy1_S11A 420
EgSuSy1_S11E 420
EguSuSy1_Contig_69050 420
Consensus HILRVPFRNE KGVVRKWISR FEVWPYLERY TEDVASELAG ELQGKPDLII GNYSDGNIVA
Conservation
Sequence logo
440 460 480
EgSuSy1_DQ227993.1 SLLAHKLGVT QCTIAHALEK TKYPESDIYW KKFEEKYHFS CQFTADLIAM NHTDFIITST 480
EgSuSy1_Clone_N22 480
EgSuSy1_Clone_N28 480
EgSuSy1_Clone_S2 480
EgSuSy1_Clone_S4 480
EgSuSy1_Clone_S6 A 480
EgSuSy1_S11A A 480
EgSuSy1_S11E A 480
EguSuSy1_Contig_69050 480
Consensus SLLAHKLGVT QCTIAHALEK TKYPESDIYW KKFEEKYHFS CQFTADLIAM NHTDFIITST
Conservation
Sequence logo
500 520 540
EgSuSy1_DQ227993.1 FQEIAGSKDT VGQYESHMNF TLPGLYRVVH GIDVFDPKFN IVSPGADMSI YFAYTEQERR 540
EgSuSy1_Clone_N22 540
EgSuSy1_Clone_N28 V 540
EgSuSy1_Clone_S2 K 540
EgSuSy1_Clone_S4 K 540
EgSuSy1_Clone_S6 K 540
EgSuSy1_S11A K 540
EgSuSy1_S11E K 540
EguSuSy1_Contig_69050 K 540
Consensus FQEIAGSKDT VGQYESHMNF TLPGLYRVVH GIDVFDPKFN IVSPGADMSI YFAYTEQKRR
Conservation
Sequence logo
560 580 600
EgSuSy1_DQ227993.1 LKSFHPEIEE LLFSDVENKE HLCVLKDKKK PIIFTMARLD RVKNLTGLVE WYGKNSKLRE 600
EgSuSy1_Clone_N22 600
EgSuSy1_Clone_N28 600
EgSuSy1_Clone_S2 600
EgSuSy1_Clone_S4 600
EgSuSy1_Clone_S6 600
EgSuSy1_S11A 600
EgSuSy1_S11E 600
EguSuSy1_Contig_69050 600
Consensus LKSFHPEIEE LLFSDVENKE HLCVLKDKKK PIIFTMARLD RVKNLTGLVE WYGKNSKLRE
Conservation
Sequence logo

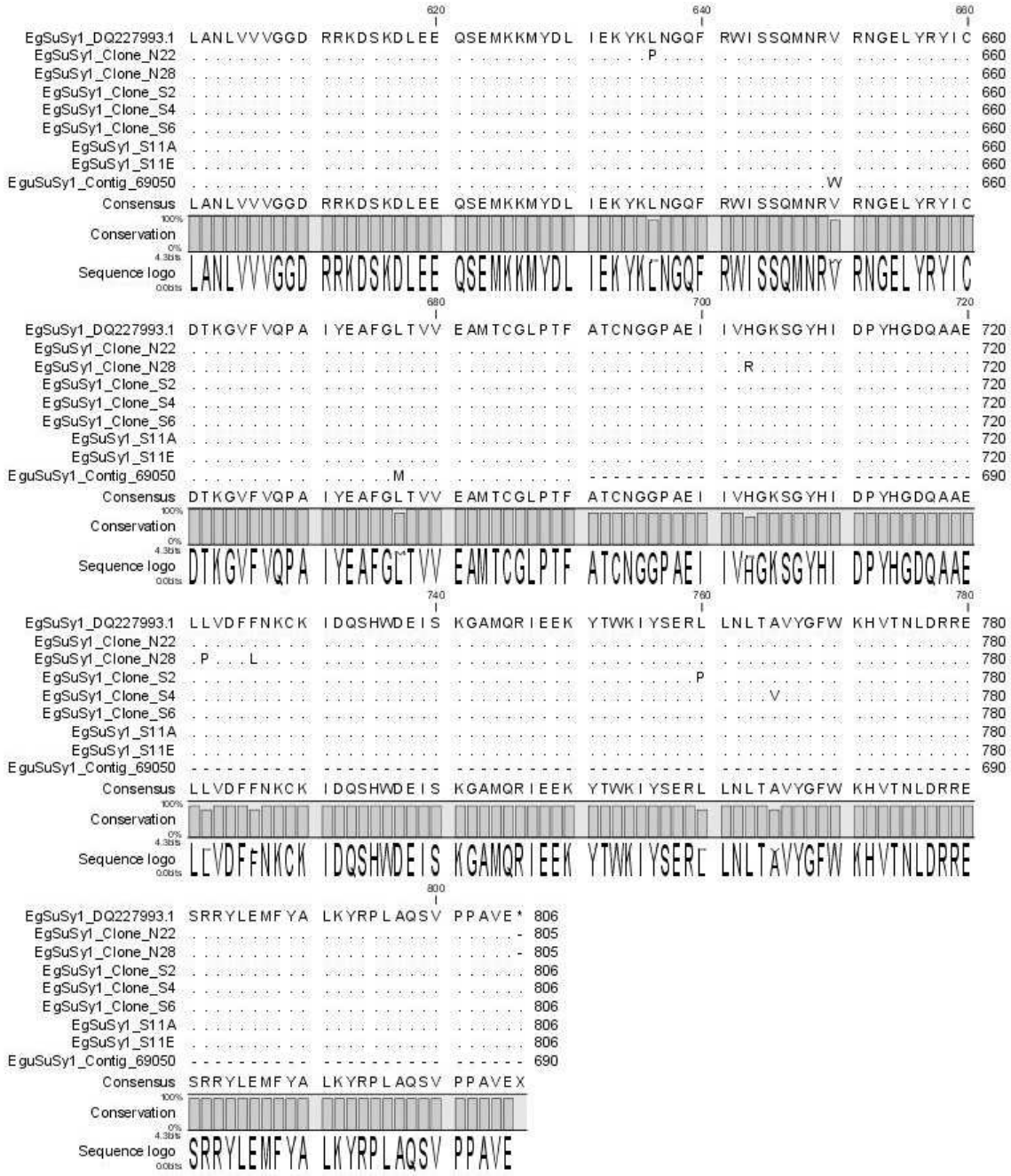

Figure S7. Amino acid alignment of the predicted amino acid sequences of entry clones showing the site directed modifications at the 11th serine residue (arrow) within the phosphorylation domain LTRVHSLRERL (Amor et al., 1995; Huber et al., 1996; Zhang et al., 1999; Komatsu et al., 2002). The C-terminal catalytic domain representing the glucosyltransferase region is found from amino acid 564 to 753 (Baud et al., 2004). PCR induced background mutations were identified by comparing sequences to EgSUSY1 sequence (GenBank accession DQ227993.1) and an EguSuSy1 contig 69050 sourced from Eucspresso a *Eucalyptus grandis x urophylla* transcriptome database (http://eucspresso.bi.up.ac.za) reference sequences. (·) indicates identical amino acid and (–) a gap or the absence of an amino acid at this site. Alignment generated using CLC bio CLC Main Workbench 5.0.2.

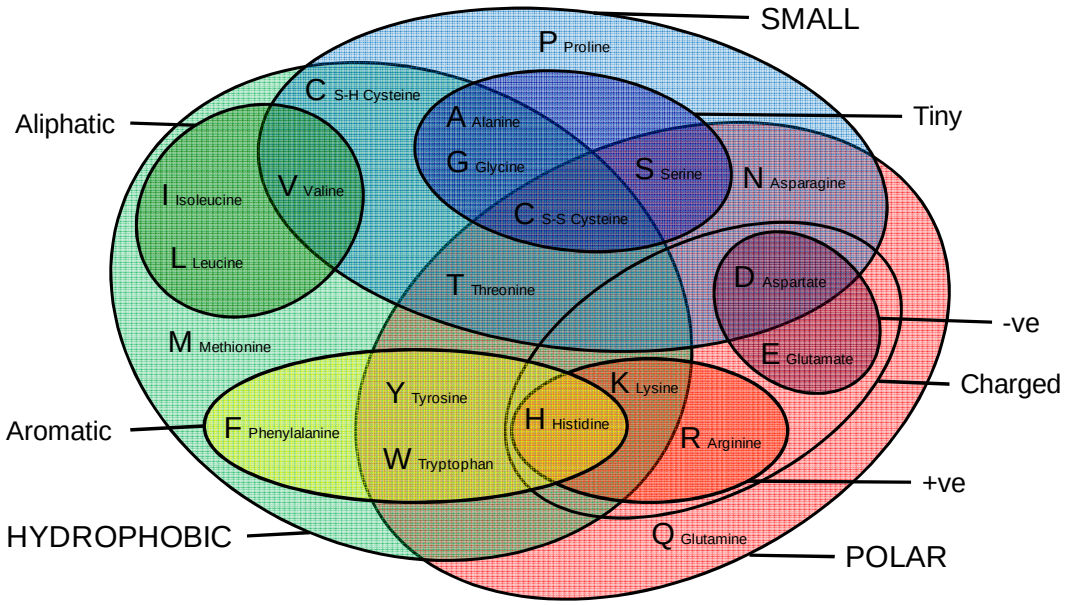

Figure S8. Schematic representation of the physicochemical groupings of amino acids based on Livingstone and Barton (1993)

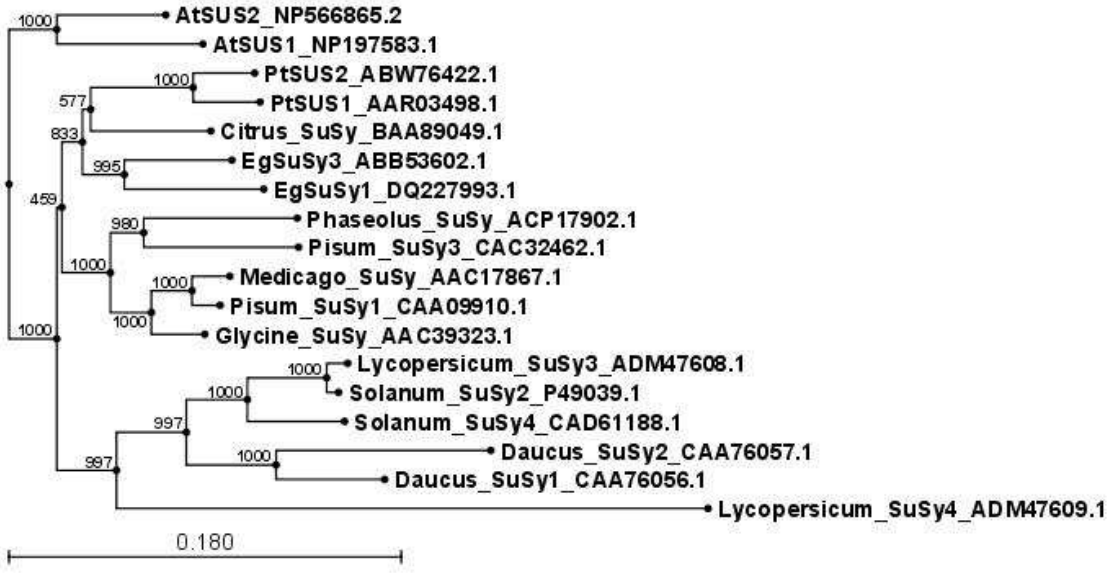

Figure S9. Neighbour joining tree showing the relationship between Dicot SUSA sucrose synthases based on amino acid conservation. The tree was constructed using CLC bio CLC Main Workbench Version 5.0.2 and 1000 bootstrap permutations.

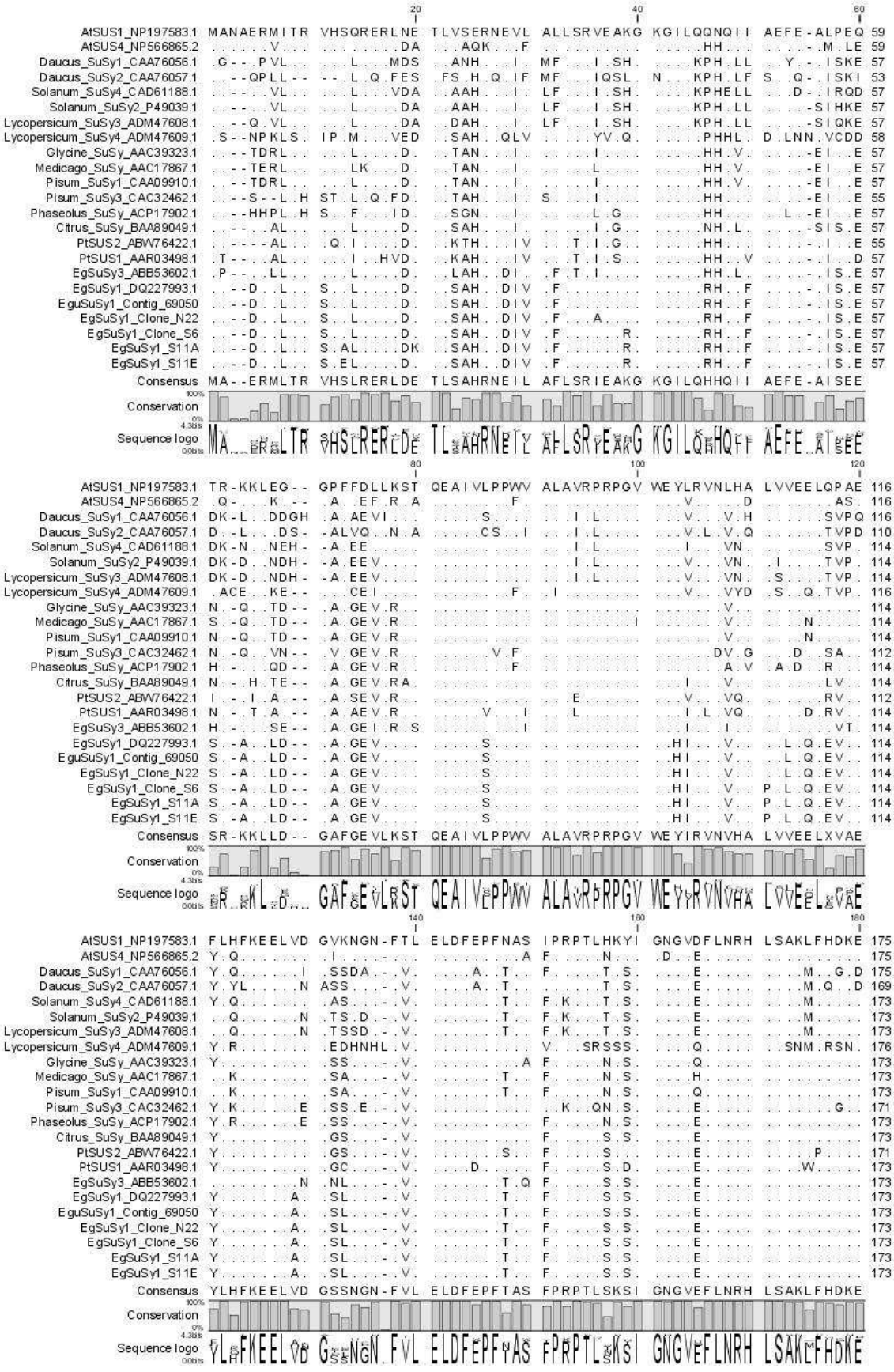
AtSUS1_NP197583.1
AtSUS4_NP566865.2
Daucus_SuSy1_CAA76056.1
Daucus_SuSy2_CAA76057.1
Solanum_SuSy4_CAD61188.1
Solanum_SuSy2_P49039.1
Lycopersicum_SuSy3_ADM47608.1
Lycopersicum_SuSy4_ADM47609.1
Glycine_SuSy_AAC39323.1
Medicago_SuSy_AAC17867.1
Pisum_SuSy1_CAA09910.1
Pisum_SuSy3_CAC32462.1
Phaseolus_SuSy_ACP17902.1
Citrus_SuSy_BAA89049.1
PtSUS2_ABW76422.1
PtSUS1_AAR03498.1
EgSuSy3_ABB53602.1
EgSuSy1_DQ227993.1
EguSuSy1_Contig_69050
EgSuSy1_Clone_N22
EgSuSy1_Clone_S6
EgSuSy1_S11A
EgSuSy1_S11E
Consensus
Conservation
Sequence logo

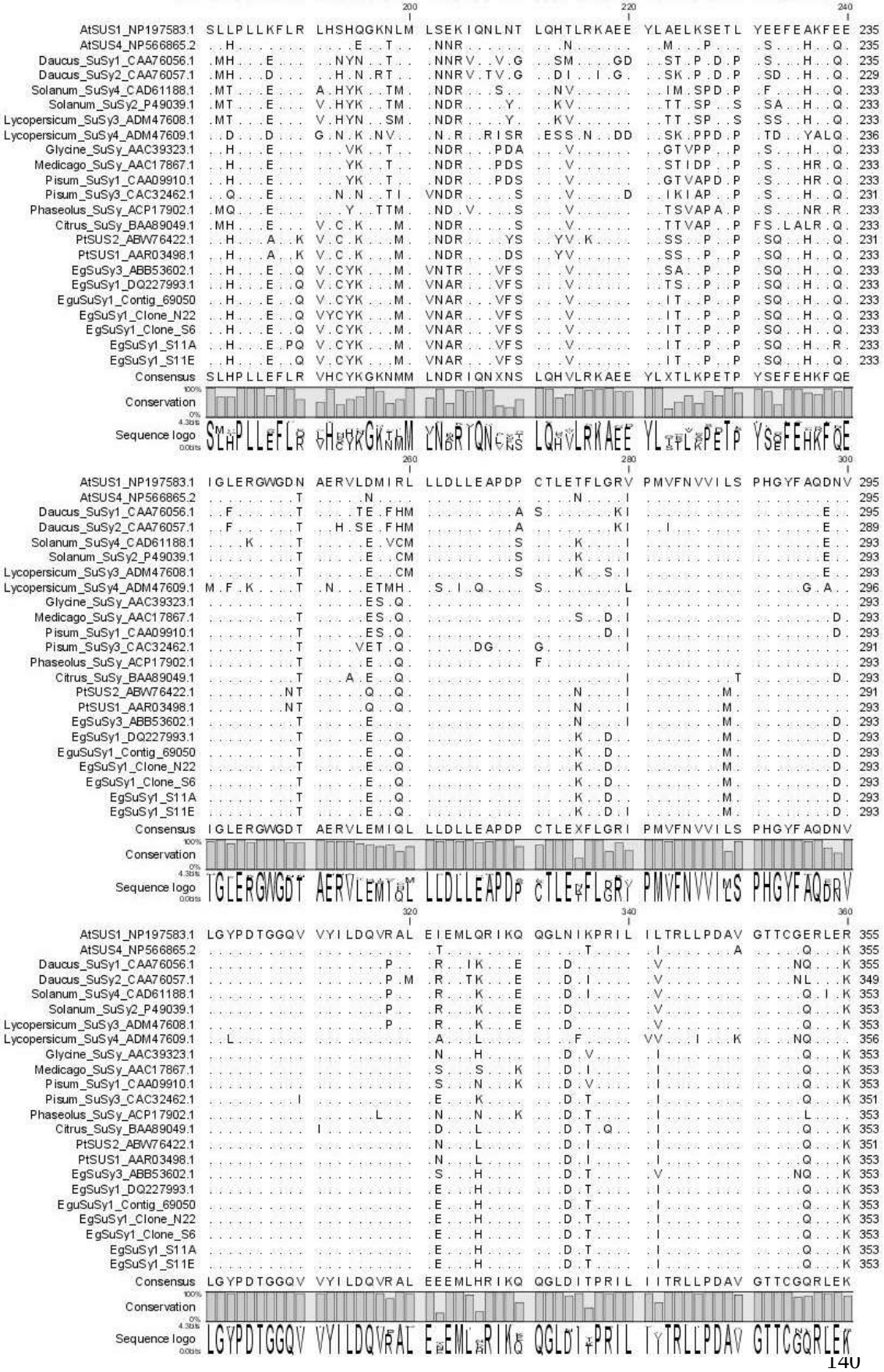
200
220
240
AtSUS1_NP197583.1 SLLPLLKFLR LHSHQGKNLM LSEKIQNLNT LQHTLRKAEE YLAELKSETL YEEFEAKFEE 235
AtSUS4_NP566865.2 .H.....E..T.. .NNR..... ...N..... ..M...P.... .S...H..Q. 235
Daucus_SuSy1_CAA76056.1 .MH...E.... ..NYN..T.. .NNRV..V.G ..SM....GD ..ST.P.D.P .S...H..Q. 235
Daucus_SuSy2_CAA76057.1 .MH...D.... ..H.N.RT.. .NNRV.TV.G ..DI...I.G. ..SK.P.D.P .SD..H..Q. 229
Solanum_SuSy4_CAD61188.1 .MT...E.... A.HYK..TM. .NDR...S.. ..NV..... ..IM.SPD.P .F...H..Q. 233
Solanum_SuSy2_P49039.1 .MT...E.... V.HYK..TM. .NDR....Y. ..KV..... ..TT.SP..S .SA..H..Q. 233
Lycopersicum_SuSy3_ADM47608.1 .MT...E.... V.HYN..SM. .NDR....Y. ..KV..... ..TT.SP..S .SS..H..Q. 233
Lycopersicum_SuSy4_ADM47609.1 ..D...D.... G.N.K.NV.. .N.R.RISR .ESS.N..DD ..SK.PPD.P .TD..YALQ. 236
Glycine_SuSy_AAC39323.1 ..H...E.... ...VK..T.. .NDR...PDA ...V..... ..GTVPP..P .S...H..Q. 233
Medicago_SuSy_AAC17867.1 ..H...E.... ...YK..T.. .NDR...PDS ...V..... ..STIDP..P .S...HR.Q. 233
Pisum_SuSy1_CAA09910.1 ..H...E.... ...YK..T.. .NDR...PDS ...V..... ..GTVAPD.P .S...HR.Q. 233
Pisum_SuSy3_CAC32462.1 ..Q...E.... ..N.N..TI. VNDR.....S ...V.....D ..IKIAP..P .S...H..Q. 231
Phaseolus_SuSy_ACP17902.1 .MQ...E.... ...Y..TTM. .ND.V....S ...V..... ..TSVAPA.P .S...NR.R. 233
Citrus_SuSy_BAA89049.1 .MH...E.... V.C.K...M. .NDR.....S ...V..... ..TTVAP..P FS.LALR.Q. 233
PtSUS2_ABW76422.1 ..H...A..K V.C.K...M. .NDR....YS ..YV.K.... ..SS..P..P .SQ..H..Q. 231
PtSUS1_AAR03498.1 ..H...A..K V.C.K...M. .NDR....DS ..YV..... ..SS..P..P .SQ..H..Q. 233
EgSuSy3_ABB53602.1 ..H...E..Q V.CYK...M. .VNTR...VFS ...V..... ..SA..P..P .SQ..H..Q. 233
EgSuSy1_DQ227993.1 ..H...E..Q V.CYK...M. .VNAR...VFS ...V..... ..TS..P..P .SQ..H..Q. 233
EguSuSy1_Contig_69050 ..H...E..Q V.CYK...M. .VNAR...VFS ...V..... ..IT..P..P .SQ..H..Q. 233
EgSuSy1_Clone_N22 ..H...E..Q VYCYK...M. .VNAR...VFS ...V..... ..IT..P..P .SQ..H..Q. 233
EgSuSy1_Clone_S6 ..H...E..Q V.CYK...M. .VNAR...VFS ...V..... ..IT..P..P .SQ..H..Q. 233
EgSuSy1_S11A ..H...E.PQ V.CYK...M. .VNAR...VFS ...V..... ..IT..P..P .SQ..H..R. 233
EgSuSy1_S11E ..H...E..Q V.CYK...M. .VNAR...VFS ...V..... ..IT..P..P .SQ..H..Q. 233
Consensus SLHPLLEFLR VHCYKGKNMM LNDRIQNXNS LQHVLRKAEE YLXTLKPETP YSEFEHKFQE
100%
Conservation
0%
4.38bits
Sequence logo
0.00bits
260
280
300
AtSUS1_NP197583.1 IGLERGWGDN AERVLDMIRL LLDLLEAPDP CTLETFLGRV PMVFNVVILS PHGYFAQDNV 295
AtSUS4_NP566865.2 ....T .....N..... .....I..... .....I..... .....I..... .....I..... 295
Daucus_SuSy1_CAA76056.1 ..F.....T. ....TE.FHM .....A.... S.....KI. .....I..... .....E... 295
Daucus_SuSy2_CAA76057.1 ..F.....T. ...H.SE.FHM .....A.... .....KI.. ..I..I..... .....E... 289
Solanum_SuSy4_CAD61188.1 ....K....T ....E.VCM .....S.... ...K....I. .....I..... .....E... 293
Solanum_SuSy2_P49039.1 ....T ....E..CM .....S.... ...K....I. .....I..... .....E... 293
Lycopersicum_SuSy3_ADM47608.1 ....T ....E..CM .....S.... ...K..S.I. .....I..... .....E... 293
Lycopersicum_SuSy4_ADM47609.1 M.F.K...T. .N...ETMH. .S.I.Q.... S.....L... .....I..... .....G.A.. 296
Glycine_SuSy_AAC39323.1 ....ES.Q.. .....I..... .....I..... .....I..... .....I..... 293
Medicago_SuSy_AAC17867.1 ....T ....ES.Q.. .....I..... ....S..D.I .....I..... .....D... 293
Pisum_SuSy1_CAA09910.1 ....T ....ES.Q.. .....I..... .....D.I. .....I..... .....D... 293
Pisum_SuSy3_CAC32462.1 ....T ...VET.Q.. .....DG... G.....I... .....I..... .....I..... 291
Phaseolus_SuSy_ACP17902.1 ....T ....E..Q.. .....I..... F.....I... .....I..... .....I..... 293
Citrus_SuSy_BAA89049.1 ....T ...A.E..Q. .....I..... .....I..... .....T..... .....D... 293
PtSUS2_ABW76422.1 ....NT. ....Q..Q.. .....I..... ...N....I. .....I..... .....M..... 291
PtSUS1_AAR03498.1 ....NT. ....Q..Q.. .....I..... ...N....I. .....I..... .....M..... 293
EgSuSy3_ABB53602.1 ....T ....E..... .....I..... ...N....I. .....I..... .....M..... 293
EgSuSy1_DQ227993.1 ....T ....E..Q.. .....I..... ...K..D... .....I..... .....M..... 293
EguSuSy1_Contig_69050 ....T ....E..Q.. .....I..... ...K..D... .....I..... .....M..... 293
EgSuSy1_Clone_N22 ....T ....E..Q.. .....I..... ...K..D... .....I..... .....M..... 293
EgSuSy1_Clone_S6 ....T ....E..Q.. .....I..... ...K..D... .....I..... .....M..... 293
EgSuSy1_S11A ....T ....E..Q.. .....I..... ...K..D... .....I..... .....M..... 293
EgSuSy1_S11E ....T ....E..Q.. .....I..... ...K..D.I. .....I..... .....M..... 293
Consensus IGLERGWGDT AERVLEMIQL LLDLLEAPDP CTLEXFLGRI PMVFNVVILS PHGYFAQDNV
100%
Conservation
0%
4.38bits
Sequence logo
0.00bits
320
340
360
AtSUS1_NP197583.1 LGYPDTGGQV VYILDQVRAL EIEMLQRIKQ QGLNIKPRIL ILTRLLPDAV GTTCGERLER 355
AtSUS4_NP566865.2 .... .T........ .....T.... .I.....A.. .....Q...K 355
Daucus_SuSy1_CAA76056.1 ....P.... .R..IK...E ...D..... .V..... ....NQ...K 355
Daucus_SuSy2_CAA76057.1 ....P..M. .R..TK...E ...D.I.... .V..... ....NL...K 349
Solanum_SuSy4_CAD61188.1 ....P.... .R...K...E ...D.I.... .V..... .....Q.I.K 353
Solanum_SuSy2_P49039.1 ....P.... .R...K...E ...D..... .V..... .....Q...K 353
Lycopersicum_SuSy3_ADM47608.1 ....P.... .R...K...E ...D..... .V..... .....Q...K 353
Lycopersicum_SuSy4_ADM47609.1 .L........ .... .A...L.... ....F..... VV...I...K ....NQ.... 356
Glycine_SuSy_AAC39323.1 .... .N...H.... ...D.V.... .I..... .....Q...K 353
Medicago_SuSy_AAC17867.1 .... .S...S...K ...D.I.... .I..... .....Q...K 353
Pisum_SuSy1_CAA09910.1 .... .S...N...K ...D.V.... .I..... .....Q...K 353
Pisum_SuSy3_CAC32462.1 ....I .... .E...K.... ...D.T.... .I..... .....Q...K 351
Phaseolus_SuSy_ACP17902.1 ....L.. .... .N...N...K ...D.T.... .I..... .....L.... 353
Citrus_SuSy_BAA89049.1 .... I......... .... .D...L.... ...D.T.Q.. .I..... .....Q...K 353
PtSUS2_ABW76422.1 .... .N...L.... ...D.I.... .I..... .....Q...K 351
PtSUS1_AAR03498.1 .... .N...L.... ...D.I.... .I..... .....Q...K 353
EgSuSy3_ABB53602.1 .... .S...H.... ...D.T.... .V..... ....NQ...K 353
EgSuSy1_DQ227993.1 .... .E...H.... ...D.T.... .I..... .....Q...K 353
EguSuSy1_Contig_69050 .... .E...H.... ...D.T.... .I..... .....Q...K 353
EgSuSy1_Clone_N22 .... .E...H.... ...D.T.... .I..... .....Q...K 353
EgSuSy1_Clone_S6 .... .E...H.... ...D.T.... .I..... .....Q...K 353
EgSuSy1_S11A .... .E...H.... ...D.T.... .I..... .....Q...K 353
EgSuSy1_S11E .... .E...H.... ...D.T.... .I..... .....Q...K 353
Consensus LGYPDTGGQV VYILDQVRAL EEEMLHRIKQ QGLDITPRIL IITRLLPDAV GTTCGQRLEK
100%
Conservation
0%
4.38bits
Sequence logo
0.00bits

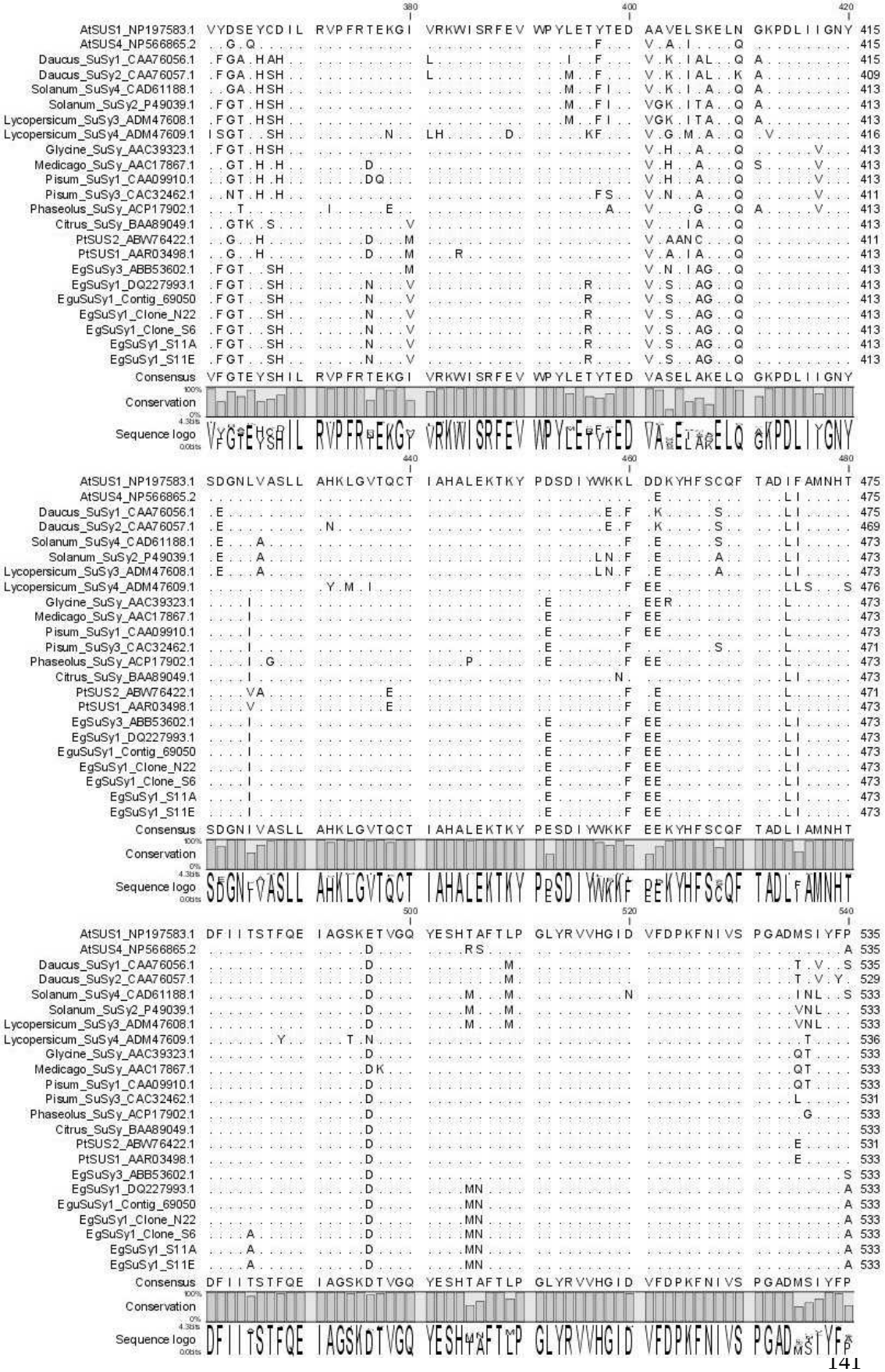
380
400
420
AtSUS1_NP197583.1 VYDSEYCDIL RVPFRTEKGI VRKWISRFEV WPYLETYTED AAVELSKELN GKPDLIIGNY 415
AtSUS4_NP566865.2 ..G.Q..... ....F. V.A.I...Q. 415
Daucus_SuSy1_CAA76056.1 .FGA.HAH.. .....L.....I..F... V.K.IAL..Q A..... 415
Daucus_SuSy2_CAA76057.1 .FGA.HSH.. .....L.....M..F... V.K.IAL..K A..... 409
Solanum_SuSy4_CAD61188.1 ..GA.HSH.. .....M..FI.. V.K.I.A..Q A..... 413
Solanum_SuSy2_P49039.1 .FGT.HSH.. .....M..FI.. VGK.ITA..Q A..... 413
Lycopersicum_SuSy3_ADM47608.1 .FGT.HSH.. .....M..FI.. VGK.ITA..Q A..... 413
Lycopersicum_SuSy4_ADM47609.1 ISGT..SH.. .....N..LH.....D.....KF... V.G.M.A..Q .V..... 416
Glycine_SuSy_AAC39323.1 .FGT.HSH.. .....V.... V.H..A..Q.....V... 413
Medicago_SuSy_AAC17867.1 ..GT.H.H..D..... V.H..A..QS.....V... 413
Pisum_SuSy1_CAA09910.1 ..GT.H.H..DQ..... V.H..A..Q.....V... 413
Pisum_SuSy3_CAC32462.1 ..NT.H.H..... V.N..A..Q.....V... 411
Phaseolus_SuSy_ACP17902.1 ...T.....I.....E..... .....A.. V....G..Q A.....V... 413
Citrus_SuSy_BAA89049.1 ..GTK.S.....V..... V...IA..Q 413
PtSUS2_ABW76422.1 ..G..H.....D...M..... V.AANC..Q 411
PtSUS1_AAR03498.1 ..G..H.....D...M...R..... V.A.IA..Q 413
EgSuSy3_ABB53602.1 .FGT..SH.....M..... V.N.IAG..Q 413
EgSuSy1_DQ227993.1 .FGT..SH.....N...V..... .....R.... V.S..AG..Q 413
EguSuSy1_Contig_69050 .FGT..SH.....N...V..... .....R.... V.S..AG..Q 413
EgSuSy1_Clone_N22 .FGT..SH.....N...V..... .....R.... V.S..AG..Q 413
EgSuSy1_Clone_S6 .FGT..SH.....N...V..... .....R.... V.S..AG..Q 413
EgSuSy1_S11A .FGT..SH.....N...V..... .....R.... V.S..AG..Q 413
EgSuSy1_S11E .FGT..SH.....N...V..... .....R.... V.S..AG..Q 413
Consensus VFGTEYSHIL RVPFRTEKGI VRKWISRFEV WPYLETYTED VASELAKELQ GKPDLIIGNY
100%
Conservation
0%
4.38 bits
Sequence logo
0.00 bits
440
460
480
AtSUS1_NP197583.1 SDGNLVASLL AHKLGVTQCT IAHALEKTKY PDSDIYWKKL DDKYHFSCQF TADIFAMNHT 475
AtSUS4_NP566865.2 .....E.....LI..... 475
Daucus_SuSy1_CAA76056.1 .E.....E.F .K....S...LI..... 475
Daucus_SuSy2_CAA76057.1 .E.....N..... .....E.F .K....S...LI..... 469
Solanum_SuSy4_CAD61188.1 .E...A.....F .E....S...LI..... 473
Solanum_SuSy2_P49039.1 .E...A.....LN.F .E....A...LI..... 473
Lycopersicum_SuSy3_ADM47608.1 .E...A.....LN.F .E....A...LI..... 473
Lycopersicum_SuSy4_ADM47609.1 .....Y.M.I.....F EE.....LLS...S 476
Glycine_SuSy_AAC39323.1 ....I.....E..... EER.....L..... 473
Medicago_SuSy_AAC17867.1 ....I.....F EE.....L..... 473
Pisum_SuSy1_CAA09910.1 ....I.....E.....F EE.....L..... 473
Pisum_SuSy3_CAC32462.1 ....I.....E.....F.....S...L..... 471
Phaseolus_SuSy_ACP17902.1 ....I.G.....P.....E.....F EE.....L..... 473
Citrus_SuSy_BAA89049.1 ....I.....N..... .....LI..... 473
PtSUS2_ABW76422.1 ....VA.....E..... .....F .E.....L..... 471
PtSUS1_AAR03498.1 ....V.....E..... .....F .E.....L..... 473
EgSuSy3_ABB53602.1 ....I.....E.....F EE.....LI..... 473
EgSuSy1_DQ227993.1 ....I.....E.....F EE.....LI..... 473
EguSuSy1_Contig_69050 ....I.....E.....F EE.....LI..... 473
EgSuSy1_Clone_N22 ....I.....E.....F EE.....LI..... 473
EgSuSy1_Clone_S6 ....I.....E.....F EE.....LI..... 473
EgSuSy1_S11A ....I.....E.....F EE.....LI..... 473
EgSuSy1_S11E ....I.....E.....F EE.....LI..... 473
Consensus SDGNIVASLL AHKLGVTQCT IAHALEKTKY PESDIYWKKF EEKYHFSCQF TADLIAMNHT
100%
Conservation
0%
4.38 bits
Sequence logo
0.00 bits
500
520
540
AtSUS1_NP197583.1 DFIITSTFQE IAGSKETVGQ YESHTAFTLP GLYRVVHGID VFDPKFNIVS PGADMSIYFP 535
AtSUS4_NP566865.2 .....D.....RS..... .....A 535
Daucus_SuSy1_CAA76056.1 .....D.....M..... .....T.V..S 535
Daucus_SuSy2_CAA76057.1 .....D.....M..... .....T.V.Y. 529
Solanum_SuSy4_CAD61188.1 .....D.....M..M.....N..... .....INL..S 533
Solanum_SuSy2_P49039.1 .....D.....M..M..... .....VNL... 533
Lycopersicum_SuSy3_ADM47608.1 .....D.....M..M..... .....VNL... 533
Lycopersicum_SuSy4_ADM47609.1 .....Y....T.N..... .....T.... 536
Glycine_SuSy_AAC39323.1 .....D..... .....QT.... 533
Medicago_SuSy_AAC17867.1 .....DK..... .....QT.... 533
Pisum_SuSy1_CAA09910.1 .....D..... .....QT.... 533
Pisum_SuSy3_CAC32462.1 .....D..... .....L..... 531
Phaseolus_SuSy_ACP17902.1 .....D..... .....G.... 533
Citrus_SuSy_BAA89049.1 .....D..... 533
PtSUS2_ABW76422.1 .....D..... .....E..... 531
PtSUS1_AAR03498.1 .....D..... .....E..... 533
EgSuSy3_ABB53602.1 .....D..... .....S 533
EgSuSy1_DQ227993.1 .....D.....MN..... .....A 533
EguSuSy1_Contig_69050 .....D.....MN..... .....A 533
EgSuSy1_Clone_N22 .....D.....MN..... .....A 533
EgSuSy1_Clone_S6 ....A.....D.....MN..... .....A 533
EgSuSy1_S11A ....A.....D.....MN..... .....A 533
EgSuSy1_S11E ....A.....D.....MN..... .....A 533
Consensus DFIITSTFQE IAGSKDTVGQ YESHTAFTLP GLYRVVHGID VFDPKFNIVS PGADMSIYFP
100%
Conservation
0%
4.38 bits
Sequence logo
0.00 bits

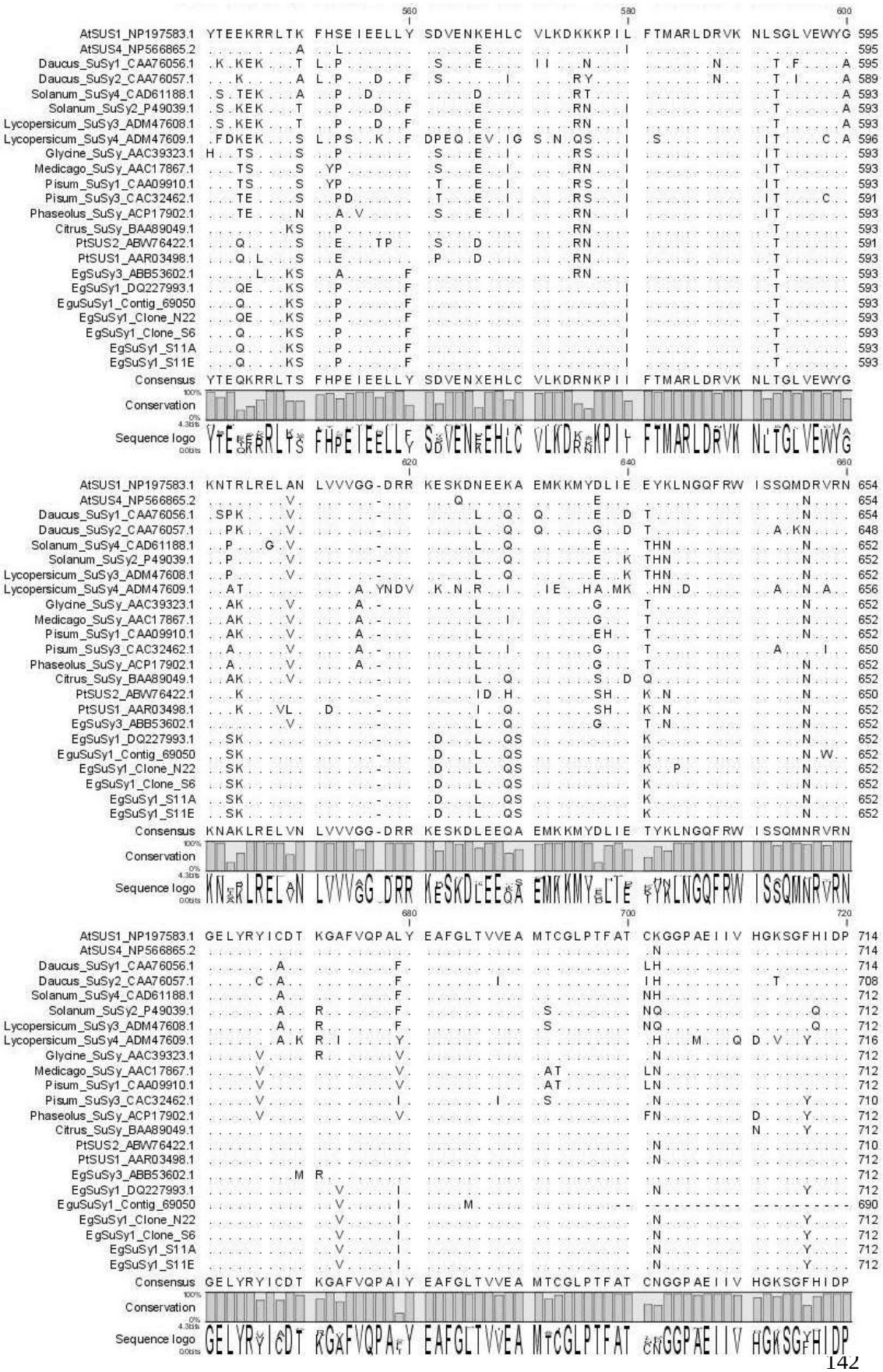
AtSUS1_NP197583.1
AtSUS4_NP566865.2
Daucus_SuSy1_CAA76056.1
Daucus_SuSy2_CAA76057.1
Solanum_SuSy4_CAD61188.1
Solanum_SuSy2_P49039.1
Lycopersicum_SuSy3_ADM47608.1
Lycopersicum_SuSy4_ADM47609.1
Glycine_SuSy_AAC39323.1
Medicago_SuSy_AAC17867.1
Pisum_SuSy1_CAA09910.1
Pisum_SuSy3_CAC32462.1
Phaseolus_SuSy_ACP17902.1
Citrus_SuSy_BAA89049.1
PtSUS2_ABW76422.1
PtSUS1_AAR03498.1
EgSuSy3_ABB53602.1
EgSuSy1_DQ227993.1
EguSuSy1_Contig_69050
EgSuSy1_Clone_N22
EgSuSy1_Clone_S6
EgSuSy1_S11A
EgSuSy1_S11E
Consensus
Conservation
Sequence logo

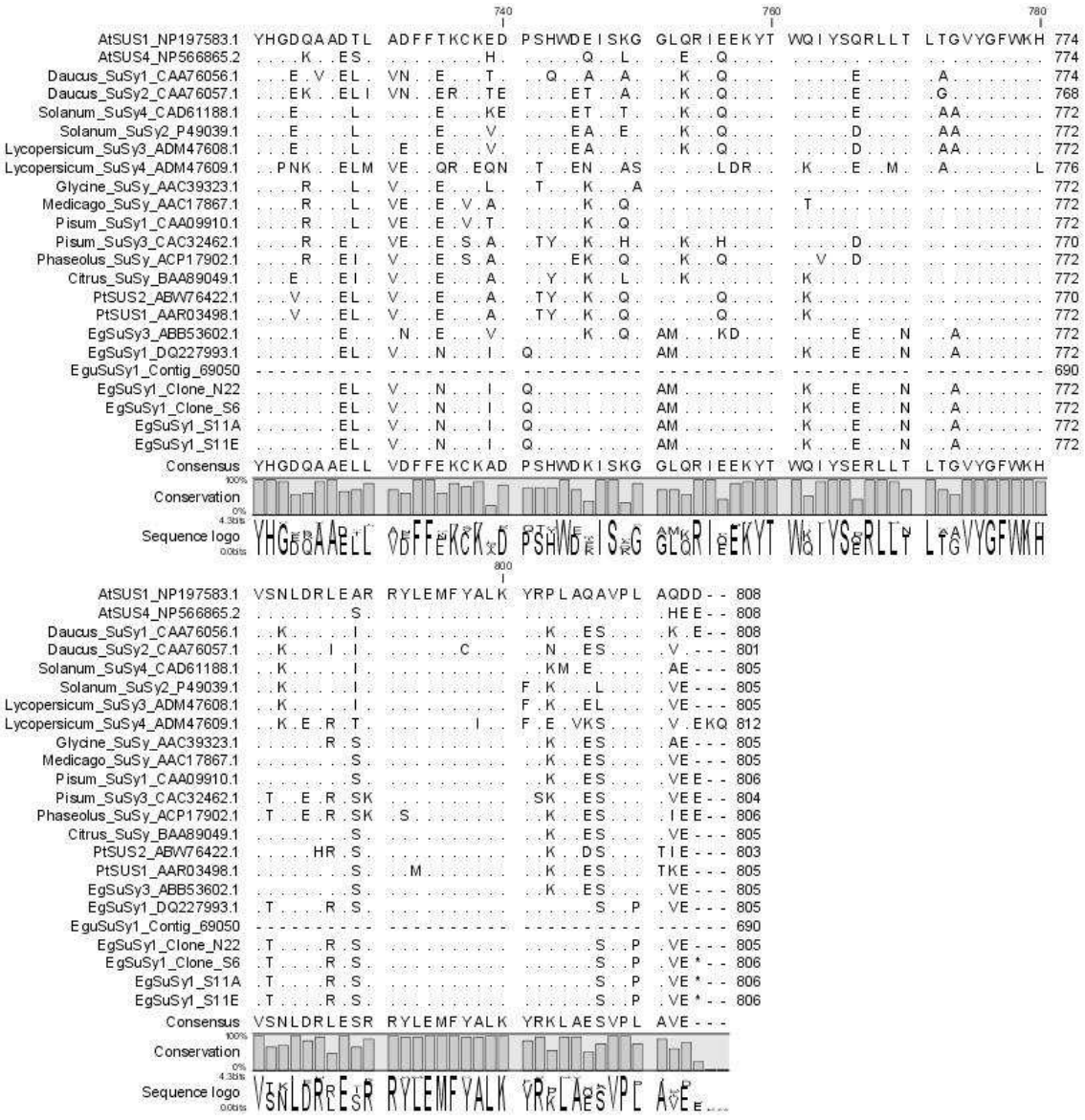

Figure S10. Amino acid alignment of 16 Dicot SUSA Sucrose synthases coding sequences indicating regions of amino acid conservation. (· indicates identical amino acid and – a gap or the absence of an amino acid at this site). The alignment was generated using CLC bio CLC Main Workbench Version 5.0.2.

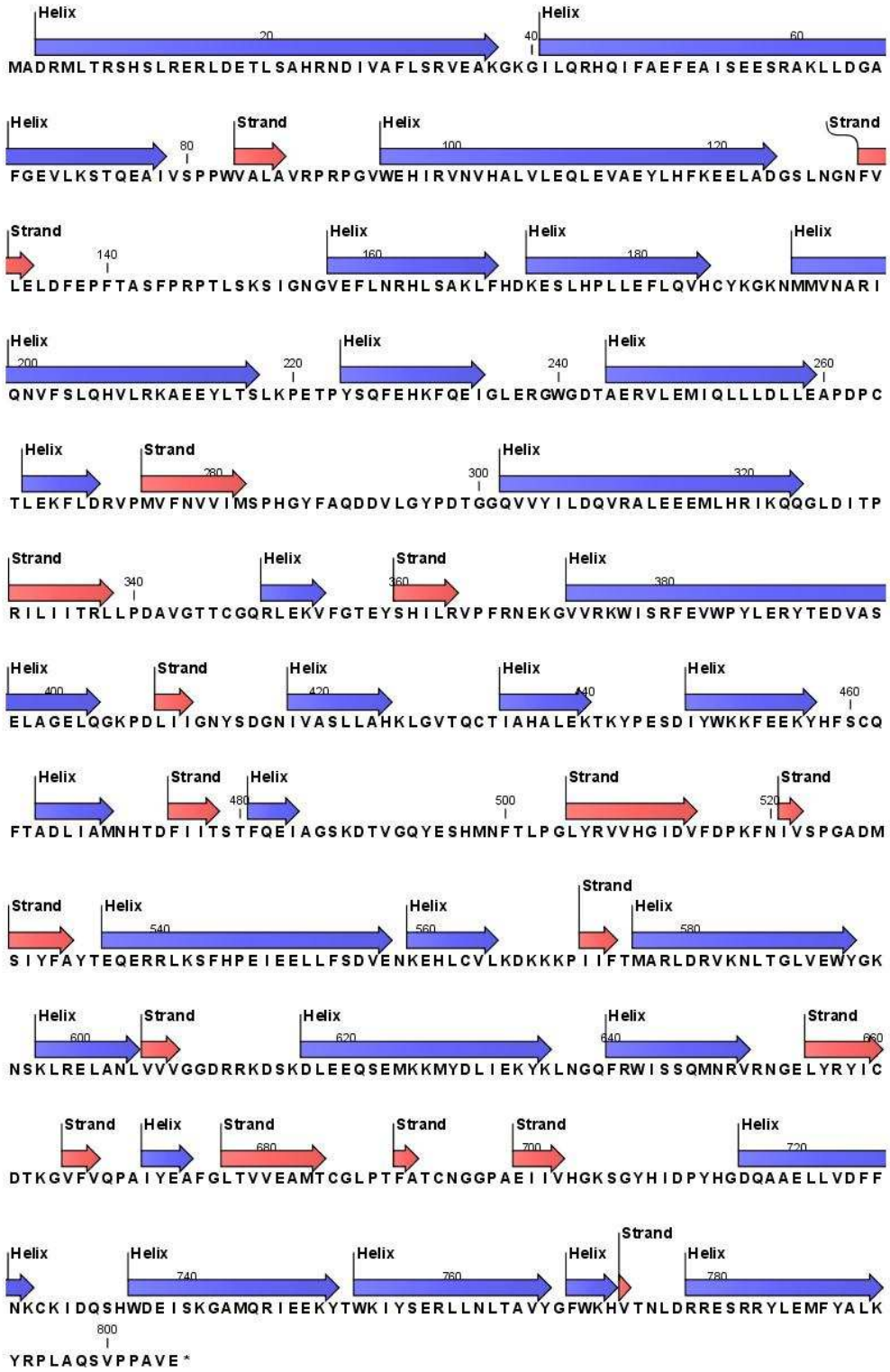

Figure S11. Secondary structure of EgSUSY1 (GenBank accession number DQ227993.1) as predicted using CLC bio CLC Main Workbench Version 5.0.2. α-Helixes and β-Strands are shown as arrows superimposed on the 805 amino acid sucrose synthase proteins.

Table S1. Secondary structure predictions of the predicted amino acid sequences of sequenced clones compared to EgSUSY1 sequence (GenBank accession DQ227993.1) and an EguSuSy1 contig 69050 sourced from Eucspresso a Eucalyptus grandis x urophylla transcriptome database (http://eucspresso.bi.up.ac.za). Secondary structures were generated using CLC bio CLC Main Workbench Version 5.0.2. (- Indicates the absence of a predicted secondary structure in the designated region.)

EgSuSY1_DQ227993.1			EgSuSy1_Clone_N22			EgSuSy1_Clone_S6			EgSuSy1_S11A			EgSuSy1_S11E			EguSuSy1_Contig_69050		
Start	End	Region name	Start	End	Region name	Start	End	Region name	Start	End	Region name	Start	End	Region name	Start	End	Region name
3	37	alpha helix	3	37	alpha helix	4	37	alpha helix	3	37	alpha helix	3	37	alpha helix	3	37	alpha helix
41	78	alpha helix	41	78	alpha helix	40	78	alpha helix	40	78	alpha helix	40	78	alpha helix	41	78	alpha helix
84	87	beta strand	84	87	beta strand	84	87	beta strand	84	87	beta strand	84	87	beta strand	84	87	beta strand
95	124	alpha helix	95	124	alpha helix	95	101	beta strand	95	101	beta strand	95	101	beta strand	95	124	alpha helix
		-			-	106	124	alpha helix	106	124	alpha helix	106	124	alpha helix			-
131	134	beta strand	131	134	beta strand	131	135	beta strand	131	135	beta strand	131	135	beta strand	131	134	beta strand
157	169	alpha helix	157	169	alpha helix	157	169	alpha helix	157	169	alpha helix	157	169	alpha helix	157	169	alpha helix
172	185	alpha helix	172	186	alpha helix	172	185	alpha helix	172	175	alpha helix	172	185	alpha helix	172	185	alpha helix
		-			-			-	177	179	alpha helix			-			-
		-			-			-	184	185	beta strand			-			-
192	217	alpha helix	192	218	alpha helix	192	218	alpha helix	192	218	alpha helix	192	218	alpha helix	192	218	alpha helix
224	234	alpha helix	224	234	alpha helix	224	234	alpha helix	224	234	alpha helix	224	234	alpha helix	224	234	alpha helix
244	259	alpha helix	244	259	alpha helix	244	259	alpha helix	244	259	alpha helix	244	259	alpha helix	244	259	alpha helix
266	271	alpha helix	266	271	alpha helix	266	271	alpha helix	266	271	alpha helix	266	272	alpha helix	266	271	alpha helix
275	282	beta strand	275	282	beta strand	275	282	beta strand	275	282	beta strand	276	282	beta strand	275	282	beta strand
302	324	alpha helix	302	324	alpha helix	302	324	alpha helix	302	324	alpha helix	302	324	alpha helix	302	324	alpha helix
331	338	beta strand	331	338	beta strand	331	338	beta strand	331	338	beta strand	331	338	beta strand	331	338	beta strand
350	354	alpha helix	350	354	alpha helix	350	354	alpha helix	350	354	alpha helix	350	354	alpha helix	350	354	alpha helix
360	364	beta strand	360	364	beta strand	360	364	beta strand	360	364	beta strand	360	364	beta strand	360	364	beta strand
373	403	alpha helix	373	403	alpha helix	373	403	alpha helix	373	403	alpha helix	373	403	alpha helix	373	403	alpha helix
408	410	beta strand	408	410	beta strand	408	410	beta strand	408	410	beta strand	408	410	beta strand	408	410	beta strand
418	425	alpha helix	418	425	alpha helix	418	425	alpha helix	418	425	alpha helix	418	425	alpha helix	418	425	alpha helix
434	440	alpha helix	434	440	alpha helix	434	440	alpha helix	434	440	alpha helix	434	440	alpha helix	434	440	alpha helix
448	457	alpha helix	448	457	alpha helix	448	457	alpha helix	448	457	alpha helix	448	457	alpha helix	448	457	alpha helix
465	470	alpha helix	465	470	alpha helix	465	470	alpha helix	465	470	alpha helix	465	470	alpha helix	465	470	alpha helix
475	478	beta strand	475	478	beta strand	475	478	beta strand	475	478	beta strand	475	478	beta strand	475	478	beta strand
481	484	alpha helix	481	484	alpha helix	481	485	alpha helix	481	485	alpha helix	481	485	alpha helix	481	484	alpha helix
		-			-	493	495	alpha helix	493	495	alpha helix	493	495	alpha helix			-
505	514	beta strand	505	514	beta strand	505	514	beta strand	505	514	beta strand	505	514	beta strand	505	514	beta strand
521	522	beta strand	521	522	beta strand	521	522	beta strand	521	522	beta strand	521	522	beta strand	521	522	beta strand
529	533	beta strand	529	533	beta strand	529	532	beta strand	529	532	beta strand	529	532	beta strand	529	532	beta strand
536	557	alpha helix	536	557	alpha helix	533	557	alpha helix	533	557	alpha helix	533	557	alpha helix	533	557	alpha helix
559	565	alpha helix	559	565	alpha helix	559	565	alpha helix	559	565	alpha helix	559	565	alpha helix	559	565	alpha helix
572	574	beta strand	572	574	beta strand	572	574	beta strand	572	574	beta strand	572	574	beta strand	572	574	beta strand
576	592	alpha helix	576	592	alpha helix	576	592	alpha helix	576	592	alpha helix	576	592	alpha helix	576	592	alpha helix
597	604	alpha helix	597	604	alpha helix	597	604	alpha helix	597	604	alpha helix	597	604	alpha helix	597	604	alpha helix
605	607	beta strand	605	607	beta strand	605	607	beta strand	605	607	beta strand	605	607	beta strand	605	607	beta strand
617	635	alpha helix	617	634	alpha helix	617	635	alpha helix	617	635	alpha helix	617	635	alpha helix	617	635	alpha helix
640	650	alpha helix	640	643	beta strand	640	650	alpha helix	640	650	alpha helix	640	650	alpha helix	640	650	alpha helix
		-	644	647	alpha helix			-			-			-			-
655	660	beta strand	655	660	beta strand	655	660	beta strand	655	660	beta strand	655	660	beta strand	655	660	beta strand
665	667	beta strand	665	667	beta strand	665	667	beta strand	665	667	beta strand	665	667	beta strand	665	667	beta strand
671	674	alpha helix	671	671	beta strand	671	674	alpha helix	671	674	alpha helix	671	674	alpha helix	670	674	alpha helix
		-	672	674	alpha helix			-			-			-			-
677	684	beta strand	677	684	beta strand	677	684	beta strand	677	684	beta strand	677	684	beta strand	678	683	beta strand
690	691	beta strand	690	691	beta strand	690	691	beta strand	690	691	beta strand	690	691	beta strand			
699	702	beta strand	699	702	beta strand	699	702	beta strand	699	702	beta strand	699	702	beta strand			
716	728	alpha helix	716	728	alpha helix	716	728	alpha helix	716	728	alpha helix	716	728	alpha helix			
736	751	alpha helix	736	751	alpha helix	736	751	alpha helix	736	751	alpha helix	736	751	alpha helix			
753	767	alpha helix	753	767	alpha helix	753	767	alpha helix	753	767	alpha helix	753	767	alpha helix			
769	772	alpha helix	769	772	alpha helix	769	772	alpha helix	769	772	alpha helix	769	772	alpha helix			
773	773	beta strand	773	773	beta strand	773	773	beta strand	773	773	beta strand	773	773	beta strand			
778	792	alpha helix	778	792	alpha helix	778	792	alpha helix	778	792	alpha helix	778	792	alpha helix			

Table S2. Summary of the background mutations identified in the amino acid alignment, their amino acid conservation and their impact on secondary structure predictions of EgSUSY1 entry clones N22

and S6 and site directed modified clones EgSUSY1-S11A and EgSUSY1-S11E compared to EgSUSY1.

Amino Acid Site[a]	EgSuSy1 DQ227993.1[b]	EgSuSy1 Clone N22[c]	EgSuSy1 Clone S6[d]	EgSuSy1 S11A[e]	EgSuSy1 S11E[f]	EguSuSy1 Contig 69050[g]	Conservation[h]	Secondary Structure[i]
11	S	S	S	A	E	S	Y	N
18	E	E	E	K	E	E	N	N
34	V	A	V	V	V	V	N	N
37	K	K	R	R	R	K	N	Y
105	L	L	P	P	P	L	Y	Y
182	L	L	L	P	L	L	Y	Y
185	H	Y	H	H	H	H	Y	N
216	T	I	I	I	I	I	N	Y
217	S	T	T	T	T	T	N	Y
232	Q	Q	Q	R	Q	Q	N	N
273	V	V	V	V	I	V	N	N
478	T	T	A	A	A	T	Y	Y
538	E	K	K	K	K	K	N	Y
636	L	P	L	L	L	L	Y	Y

a. The amino acid site at which the missense mutations were identified.

b. The *Eucalyptus grandis* EgSUSY1 protein sequence as determined by Zhou et al. (2005) and deposited in GenBank (accession DQ227993.1)

c. EgSuSy1 Clone N22 protein sequence used to construct N-terminal GFP-EgSUSY1 fusion constructs. This transgene lacks the stop codon (N = NoStop) to accommodate for the translational fusion to GFP.

d. EgSuSy1 Clone S6 protein sequence used to construct C-terminal EgSUSY1-GFP fusion constructs. This transgene consists of the full-length EgSUSY1 CDS including the stop codon (S = Stop).

e. EgSUSY1-S11A clone where the 11th Serine residue of EgSUSY1 was modified via site directed mutagenesis to give rise to an Alanine residue.

f. EgSUSY1-S11E clone where the 11th Serine residue of EgSUSY1 was modified via site directed mutagenesis to give rise to an Glutamate residue.

g. EguSuSy1 contig 69050 sourced from Eucspresso a *Eucalyptus grandis x urophylla* transcriptome database (http://eucspresso.bi.up.ac.za)

h. Conservation of respective amino acid sites. A site was described as conserved (Y = Yes) if there were no amino acid variations based on the amino acid alignment of Dicot SUSYs (Supplemental Figure S10). If any variations were found the site was described as not conserved (N = No).

i. Summary of the effect of the missense mutations on the secondary structure as predicted by CLC bio (Figure S11). A Y (Yes) indicates that the mutation altered the predicted secondary structure while N (No) indicates that the mutation had no impact on the secondary structure predictions.

Appendix B: Supplemental DVD directory

Powerpoint Presentation

- Instructions to Examiners
  - Playing of animations
  - Accessing hyperlinks to additional resources
  - File naming convention
- Introduction
  - **Figure SP1.** The two modifications made to the conserved 11th Serine residue of EgSUSY1(Campbell and Farrel, 2003).
  - **Figure SP2.** *Arabidopsis* tissues viewed using Laser scanning confocal microscopy.
  - **Figure SP3**. *Arabidopsis* autofluorescence present in 6 day old seedlings.
  - **Figure SP4.** Confocal laser scanning imaging setup used to image subcellular localization and distribution of GFP-EgSUSY1 fusion proteins.
  - **Figure SP5.** Z-stack animation of a longitudinal section of a S11A *Arabidopsis* root.
  - **Figure SP6.** Z-stack animation of a longitudinal section of a S11A Arabidopsis root.
- Localization of GFP-EgSUSY1 in hypocotyl of transgenic plants
  - **Figure SP7.** Z-stack animation of a longitudinal section of *Arabidopsis* hypocotyl stably expressing GFP.
  - **Figure SP8.** Z-stack animation of a longitudinal section of *Arabidopsis* hypocotyls stably expressing GFP-PIP2a expression constructs.
  - **Figure SP9.** Z-stack animation of a longitudinal section of *Arabidopsis* hypocotyls stably expressing GFP-EgSUSY1 expression constructs.
  - **Figure SP10.** Z-stack animation of a longitudinal section of *Arabidopsis* hypocotyls stably expressing GFP-S11A fusion constructs.
  - **Figure SP11.** Orthogonal section through a z-stack of hypocotyl cells of S11A *Arabidopsis* plant line.
  - **Figure SP12.** Time series of a single longitudinal optical plane of hypocotyl S11A *Arabidopsis* plant cells.
  - **Figure SP13.** Z-stack animation of a longitudinal section of *Arabidopsis* hypocotyls stably expressing S11E fusion constructs.
  - **Figure SP14.** Time series of a single longitudinal optical plane of hypocotyl S11E *Arabidopsis* plant cells.
- Effect of Osmotic stress on the localization of GFP-EgSUSY1 in Hypocotyl of transgenic plants
  - **Figure SP15.** Z-stack animation of PIP2a hypocotyl cells following plasmolysis.
- Additional Resources
  - Dissertation
  - Microscopy Image Database
  - Zeiss LSM Image Browser
- References

References:

Amor Y, Haigler CH, Johnson S, Wainscott M, Delmar DP (1995) A membrane-associated form of sucrose synthase and its potential role in synthesis of cellulose and callose in plants. Plant Biology **92:** 9353-9357

Baud S, Vaultier MN, Rochat C (2004) Structure and expression profile of sucrose synthase multigene family in Arabidopsis. Journal of Experimental Botany **55:** 396-409

Campbell MK, Farrel SO (2003) Biochemistry, Ed 4. Thomson Learning

Huber SC, Huber JL, Liao P-C, Gage DA, McMichael JRW, Chourey PS, Hannah LC (1996) Phosphorylation of Serine-15 of maize leaf sucrose synthase. Plant physiology **112:** 793-802

Komatsu A, Moriguchi T, Koyama K, Omura M, Akihama T (2002) Analysis of sucrose synthase genes in Citrus suggest different roles and phylogenetic relationships. Journal of Experimental Botany **53:** 61-71

Livingstone CD, Barton GJ (1993) Protein sequence alignments: a strategy for the hierarchical analysis of residue conservation. Computer Applications in the Biosciences **9:** 745-756

Zhang X, Lund AA, Sarath G, Cerny RL, Roberts DM, Chollet R (1999) Soybean nodule sucrose synthase (Nodulin-100): further analysis of its phosphorylation using recombinant and authentic root-nodule enzymes. Archives of Biochemistry and Biophysics **371:** 70-82

Zhou H, Myburg AA, Berger DK (2005) Isolation and functional genetic analysis of *Eucalyptus* wood formation genes. University of Pretoria, Pretoria

CHAPTER 3

Concluding Remarks

This MSc study successfully produced *Arabidopsis* plant lines heterologously expressing modified and unmodified GFP-EgSUSY1 protein fusions. Observation of the subcellular localization of GFP-EgSUSY1 proteins *in planta* provided evidence for the peripheral localization of fusions with a prominent cytosolic component. Plasma membrane association was not confirmed nor negated and the current study failed to identify any significant differences in the subcellular localizations of the two modified GFP-EgSUSY1 fusions (S11A and S11E). To address these inconclusive findings and the limitations encountered during the current study a number of hypotheses explaining the reported observations will be outlined below.

The first scenario to explain the observations is that the PCR induced background mutations resulted in the alteration of the enzyme properties. The effects of the mutations could range from complete loss of enzyme functionality to the targeting of the enzyme to a different subcellular localization. Evidence in the parallel study by Mr. M. M. Mphahlele (University of Pretoria, Pretoria) showing increased growth and biomass of the transgenic plants compared to wild-type plants consistent with the overexpression phenotype observed in a similar study by Coleman, (2006). Extensive *in silico* analysis of the effect of the mutations on the physiochemical properties and localization affinities of the proteins, the true nature of the impact of the induced mutations is yet to be established. Functionality of the sucrose synthase enzyme can be determined through the functional complementation of the transgene in a double mutant (*sus1*/*sus4*) background as described in Bieniawska et al.(2007).

The second hypothesis to explain the observed results is the intrinsic limitations of the current methodology. As stipulated previously, LSCM can only resolve molecules that are further than 200 nm apart (Lalonde et al., 1999). This lack in resolution suggests that any association that falls under this resolution limit will remain ambiguous as was prevalent in the

current study. A number of alternative methodologies can be explored to address this issue. These methodologies include direct observations of subcellular localization through modified confocal methodologies described in Serna (2005), super resolution microscopy, such as PALM (Photoactivated Localization Microscopy) and STORM (Stochastic Optical Reconstruction Microscopy Huang et al., 2009), and immunogold labelling of sucrose synthase followed by electron microscopy (Gregory et al., 2002). Other methodologies such as FRET (Fluorescence Resonance Energy Transfer, (Lalonde et al., 2008) and BiFC (Bimolecular Fluorescence Complementation, Zamyatnin et al., 2006) could be used to determine whether sucrose synthase directly associates with the cellulose synthase complex.

Proteins are known to frequently associate with other proteins to form protein complexes (Alberts, 1998; Grigoriev, 2003; Kerrien et al., 2007). The oligomerization of proteins in complexes can serve a plethora of functions such as regulating enzyme functionality and targeting an enzyme to a specific cellular compartment. It is common understanding that sucrose synthase exists as a functional tetramer, yet a recent study by Duncan and Huber (2007), suggests that SUS1 in maize exists as both dimers and trimers. The study goes on to speculate that the membrane association of the SUS1 protein is dependent on the oligomerization status of the protein.

The third and final explanation for the current observations is that *Arabidopsis thaliana* is not a good model for the functional analysis of EgSUSY1 regulation and activity as it may lack the cellular machinery to promote the oligomerization of EgSUSY1. This issue can be addressed through the ectopic expression of EgSUSY1 in a woody plant species such as *Populus*. Optimally, functional studies of EgSUSY1 should be carried out in the *Eucalyptus* native environment under the action of the respective promoter. Future research will establish

which of these scenarios successfully characterizes the regulation of EgSUSY1 through subcellular localization.

The third hypothesis is supported by two studies performed by Coleman and colleagues. In a 2006 study Coleman and colleagues evaluated the physiological effect of ectopically expressing cotton (*Gossypium hirsutum*) SuSy in tobacco (*Nicotiana tabacum* cv. Xanthi). They found that transformants presented with an increase in plant biomass yet no increase in the allocation of carbon to starch or cellulose was observed. In a subsequent study the same cotton SuSy was overexpressed in the tree poplar (*Populus alba-grandidentata*). Contrary to previous findings transformants were found to have a 2% to 6% increase in their cellulose content per dry weight (Coleman et al., 2009). These findings suggest that the physiological background especially the sink strength of the model organism chosen is vital to correctly elucidate the function and regulation of SuSy especially with regard to cell wall formation.

References

Alberts B (1998) The cell as a collection of protein machines: preparing the next generation of molecular biologists. Cell **92:** 291–294

Bieniawska Z, Barratt DHP, Garlick AP, Thole V, Kruger NJ, Martin C, Zrenner R, Smith AM (2007) Analysis of the sucrose synthase gene family in *Arabidopsis*. The Plant Journal **49:** 810–828

Coleman HD, Ellis DD, Gilbert M, Mansfield SD (2006) Up-regulation of sucrose synthase and UDP-glucose pyrophosphorylase impacts plant growth and metabolism. Plant Biotechnology Journal **4:** 87–101

Coleman HD, Ellis, D.D., Gilbert, M., and Mansfield, S.D. (2006) Up-regulation of sucrose synthase and UDP-glucose pyrophosphorylation impacts plant growth and metabolism. *Plant Biotechnology Journal* **4:** 87-101

Coleman HD, Yan J, Mansfield SD (2009) Sucrose synthase affects carbon partitioning to increase cellulose production and altered cell wall ultrastructure. Proceedings of the National Academy of Sciences **106:** 13118

Duncan KA, Huber SC (2007) Sucrose synthase oligomerization and F-actin association regulated by sucrose concentration and phosphorylation. Plant and Cell Physiology **48:** 1612-1623

Gregory ACE, Smith C, Kerry ME, Wheatley ER, Bolwella GP (2002) Comparative subcellular immunolocation of polypeptides associated with xylan and callose synthases in French bean (*Phaseolus vulgaris*) during secondary wall formation. Phytochemistry **59:** 249–259

Grigoriev A (2003) On the number of protein–protein interactions in the yeast proteome. Nucleic Acids Research **31:** 4157–4161

Huang B, Bates M, Zhuang X (2009) Super resolution fluorescence microscopy. Annual Review of Biochemistry **78:** 993–1016

Kerrien S, Alam-Faruque Y, Aranda B, Bancarz I (2007) IntAct – open source resource for molecular interaction data. Nucleic Acids Research **35:** D561–565

Lalonde S, Boles E, Hellmann H, Barker L, Patrick JW, Frommer WB (1999) The dual function of sugar carriers: transport and sugar sensing. Plant Cell **11:** 707–726

Lalonde S, Ehrhardt DW, Loqué D, Chen J, Rhee SY, Frommer WB (2008) Molecular and cellular approaches for the detection of protein–protein interactions: latest techniques and current limitations. The Plant Journal **53:** 610–635

Serna L (2005) A simple method for discriminating between cell membrane and cytosolic proteins. New Phytologist **165:** 947-952

Zamyatnin Jr AA, Solovyev AE, Bozhkov PV, Valkonen JPT, Yu S, Savenkov M, Savenkov EI (2006) Assessment of the integral membrane protein topology in living cells. The Plant Journal **46:** 145–154